The University Of Sheffield.

Tribbles: the tumour microenvironment and their involvement in cancer

Swapna Santosh Satam

Registration No: 170276050

A thesis submitted in partial fulfilment of the requirements for the degree of
Doctor of Philosophy

The University of Sheffield
Faculty of Medicine, Dentistry & Health
Department of Infection, Immunity & Cardiovascular Disease

October 2020

This thesis is dedicated to my parents

Thank you for your constant love and support

Thesis format

Each chapter of this thesis is structured individually and consists of:

1. A general introduction, providing a background to each results chapter (Chapter 1);

2. General materials and methods, describing all the techniques, procedures and assay used in this work (Chapter 2);

3. First results chapter, structured as a traditional thesis chapter but intended to be published (Chapter 3);

4. Second results chapter, structured as a traditional thesis chapter (Chapter 4);

5. Third results chapter, structured as a traditional thesis chapter but intended to be published (Chapter 5);

6. A conclusive chapter, summarizing the major findings (Chapter 6);

List of contents, figures and tables is also provided at the beginning of the thesis.

Declaration

All the work presented in this thesis is my own unless otherwise stated; I have performed over 90% of the experiments, with minor support for genotyping from our technical staff (Elke Pultz) and some help from kind colleagues from the Institute of Diabetes and Cancer (IDC) and TRAIN consortium. Data supplied by others (Adam Lindford and Laura Martinez Campesino) is stated in each of the relevant sections. I confirm that the Thesis is my own work. This work has not been previously presented for an award at this, or any other, university.

Acknowledgments

First of all, I would like to thank my supervisors Natalia Pellegata and Endre Kiss-Toth for their constant support, patience and motivation throughout my project. They have always supported my ideas and allowed me to grow as a researcher. This PhD would not have been possible without the TRAIN consortium and I am immensely grateful for the funding provided by Marie Sklodowska Curie ITN. I want to thank Stefan Herzig, Marcel Scheideler and Tobias Schafmeier for selecting me for this position and providing me with this great opportunity to work at Institute of Diabetes and Cancer (IDC) at Helmholtz centre Munich. Moreover, also providing me with the opportunity to continue my research as a Post-doc.

I want to thank all the members of the TRAIN consortium, especially Graham Hughes, who did an amazing job along with Endre Kiss-Toth in managing the TRAIN programme. It was a wonderful experience being part of such a great consortium and working with immensely talented scientists. My sincere appreciation goes to Chiara Niespolo and Laura Martinez Campesino for always being readily available for their help and endless PebblePad support and to Dominika Grzesik who has been really supportive throughout the PhD.

In the IDC, I would like to thank all my colleagues. I would like to thank Tobias Wiedemann for helping me with the mouse work in the beginning. I sincerely thank Elke Pultz for helping me with the genotyping and always making time for it. I greatly appreciate the help from my dear friend Valeria Lopez Salazar, for all my adipose related queries and teaching me how to make great Empanadas! I am very grateful to Miriam Guhl for making all bureaucratic work so easy and being always available with a smile. I would like to thank the lab members, Eva-Maria Bogner, Nina Minaskan and Amy Rose Fumo, for their help and pleasant working experience. Lastly, I would like to thank Sebastian Gulde for all his help in the lab, especially when I was away for TRAIN workshops and holidays and thanks being such a patient housemate and being motivated to cook for hours even after long days of work.

Finally, a huge thanks to my family, my parents and my sister, I have come a long way entirely because of your constant love, motivation and support. I will be forever grateful for all the things you have done so far and keep doing. I hope you will enjoy reading my work (Yes, I am finally finishing the PhD!).

Table of Contents

List of Figures

List of Tables

List of Abbreviations

ECIS European Cancer Information System	INS Insulin
2D 2 dimentional	ITN Initial training network
3D 3 dimentional	JNK-STAT Janus kinase-signal transducer and activator of transcription
ACC Acetyl-CoA carboxylase	KD Knockdown
ACTH Adrenocorticotropic hormone	KO Knock out
Adipoq-CreER	LDL Low-density lipoprotein
AKT Protein Kinase B	LGC Laboratory of the Government Chemist
AML Acute myeloid leukaemia	LH Luteinizing hormone
ANOVA Analysis of variance	MAPK Mitogen-activated protein kinase
ATC Anaplastic thyroid cancer	MEK Mitogen-activated protein kinase
ATCC American Type Culture Collection	MEN Multiple endocrine neoplasia
ATP Adenosine Triphosphate	MMP Matrixmetalloproteins
BAT Brown adipose tissue	MTC Medullary thyroid cancer
BMI Body mass index	mTOR mammalian target of rapamycin
BPH Benign prostatic hyperplasia	NAMPT Nicotinamide phosphoribosyltransferase
BSA Bovine serum albumin	NF-κB nuclear factor kappa B
C/EBP CCAAT-enhancer-binding proteins	NFκB Nuclear factor-κB
CAA Cancer associated adipocytes	OE overexpression
CCL Chemokine C-C motif ligand	OPN Osteopontin
CCL Chemokine-C motif ligand	PBS Phosphate buffer saline
CCR Chemokine-C motif receptor	PCa Prostate cancer
CM Conditioned media	PDK1 3-phosphoinositide-dependent kinase-1
COP1 Constitutive photomorphogenic 1	PI3K Phosphoinositide 3-kinases
Cre cyclization recombination	PIN Prostatic intraepithelial neoplasia

CreER cyclization recombination estrogenreceptor	PIP2 Phosphatidylinositol-4,5-bisphosphate
CXCL Chemokine X-C motif ligand	PIP3 Phosphatidylinositol (3,4,5)-trisphosphate
DAPI 4’,6-diamidino-2-phenylindole	PLCγ phospholipase C-γ
DDB1 Damage Specific DNA Binding Protein 1	PPAR Peroxisome proliferator activated receptor
DET1 De-etiolated 1	PPAT Periprostatic adipose tissue
DEX Dexamethasone	PSA Prostate-specific antige
DHEA Dehydroepiandrosterone	PSMA Prostate membrane antigen
DHT Dihydrotestosterone	PTC Papillary thyroid cancer
DMSO Dimethyl sulfoxide	PTEN phosphatase and tensin homolog
ECL Enhanced chemiluminescent	RAS Rat sarcoma
ECM extracellular matrix	RBP Retinol-binding protein
EGFR Epidermal growth factor recepto	RET REarranged during Transfection
EMT Epithelial–mesenchymal transition	RIPA Radioimmunoprecipitation assay buffer
ERK Extracellular-signal-regulated kinase	SFRP secreted Frizzled-related proteins
ESR Early stage researcher	SNP Single nucleotide polymorphisms
FAK Focal adhesion kinase	subWAT Subcutaneous white adipose tissue
FBS Foetal Bovine Serum	SVF Stromal vascular fraction
FISH Fluorescence in situ hybridization	T3 Triiodothyronine
FMTC Familial medullary thyroid cancer	T4 Thyroxine
FTC Follicular thyroid cancer	TG Triglycerides
GDNF Glial cell-derived neurotrophic factor	TNF Tumour necrosis factor
GFP Green fluorescent protein	TNF-α tumour necrosis factor-α
GPI glycosylphosphatidylinositol	TRAIN Tribbles Research Innovation Network
HDF High fat diet	TRIBs Tribbles
HDL High-density lipoprotein	TRIBs Tribbles family of proteins

HNF4A Hepatocyte Nuclear Factor 4 Alpha	UCP1 Uncoupling protein 1
IBMX 1-Methyl-3-Isobutylxanthine	ULA ultra low attachment
IGF Insulin-like growth factor	VGRF Vascular endothelial growth factor receptor
IgG Immunoglobulin G	visWAT Visceral white adipose tissue
IHC Immunohistochemistry	WAT White adipose tissue
IL Interleukin	WT Wildtype

Abstract

Cancer is the leading cause of death worldwide and the tumour microenvironment plays an active role in cancer progression. Tumour cells recruit numerous cell types in the stroma and build a favourable microenvironment for tumour growth and metastasis. Adipose tissue contributes to a major part of prostate cancer microenvironment and several studies have reported its association with poor prognosis. However, limited data is available underlying the molecular mechanism responsible for this effect. Understanding the molecular mechanisms underlying adipose tissue associated prostate cancer aggressiveness can help develop new therapeutic strategies for patient treatment in the future. Tribbles proteins (TRIB1/2/3) belong to the family of pseudo-kinases involved in the development of various cancers including leukaemia, colorectal, breast and prostate. In this thesis, we focus on the Tribbles-mediated cross-talk between adipose cells and prostate cancer cells. Here we show that adipocytes secrete chemokines that modulate TRIB1 and TRIB3 expression in prostate cancer cells, Du145 and PC3. Furthermore, we observed that knockdown of *TRIB3* expression in prostate cancer cells inhibited tumour growth and progression *in vitro*. This effect was more prominent with the use of conditioned media from adipocytes. Thus suggesting, *TRIB3* acts as an oncogene in prostate cancer cells *in vitro* and can have a worse outcome under the influence of secretory factors from adipocytes. The second aim of this study was investigating the biological role of *TRIB2* in medullary thyroid cancer; we observed that *TRIB2* acts as a tumour suppressor *in vitro* by inhibiting cell viability, proliferation, migration and invasion. We also report that *TRIB2* overexpression decreases cell viability to Cabozantinib treatment compared to control in MZ-CRC-1 cells carrying an aggressive RET mutation, associated with poor prognosis. Overall, this thesis shows the diverse role of Tribbles, either as a tumour suppressor or an oncogene depending on the cellular context. Moreover, we found a novel role of *TRIB3* contributing to prostate cancer aggressiveness, while *TRIB2* inhibiting medullary thyroid cancer progression *in vitro*.

Chapter 1 : Introduction

1.1 Hallmarks of cancer

Despite recent medical advances, cancer remains the major cause of death in the European Union. The European Cancer Information System (ECIS) published this year alone, there were 2.7 million new cases detected and 1.3 million deaths (ECIS 2020). In the UK, it is estimated that every 1 in 2 people will develop cancer in their lifetime (Cancer Research UK). It has been previously observed that ageing contributes to increased incidences of cancers. Increased DNA mutations, telomere instability and dysfunctional epigenetic regulation are some of the factors involved in ageing (DePinho 2000). Figure 1.1.1 shows the most commonly occurring cancers in Europe and their age-wise distribution. Prostate cancer remains the most commonly detected cancer in males and breast cancer in females. Thyroid cancer cases have significantly increased in recent years and now account for 10.06% of the total cancer cases detected from age 0-44 (ECIS 2020).

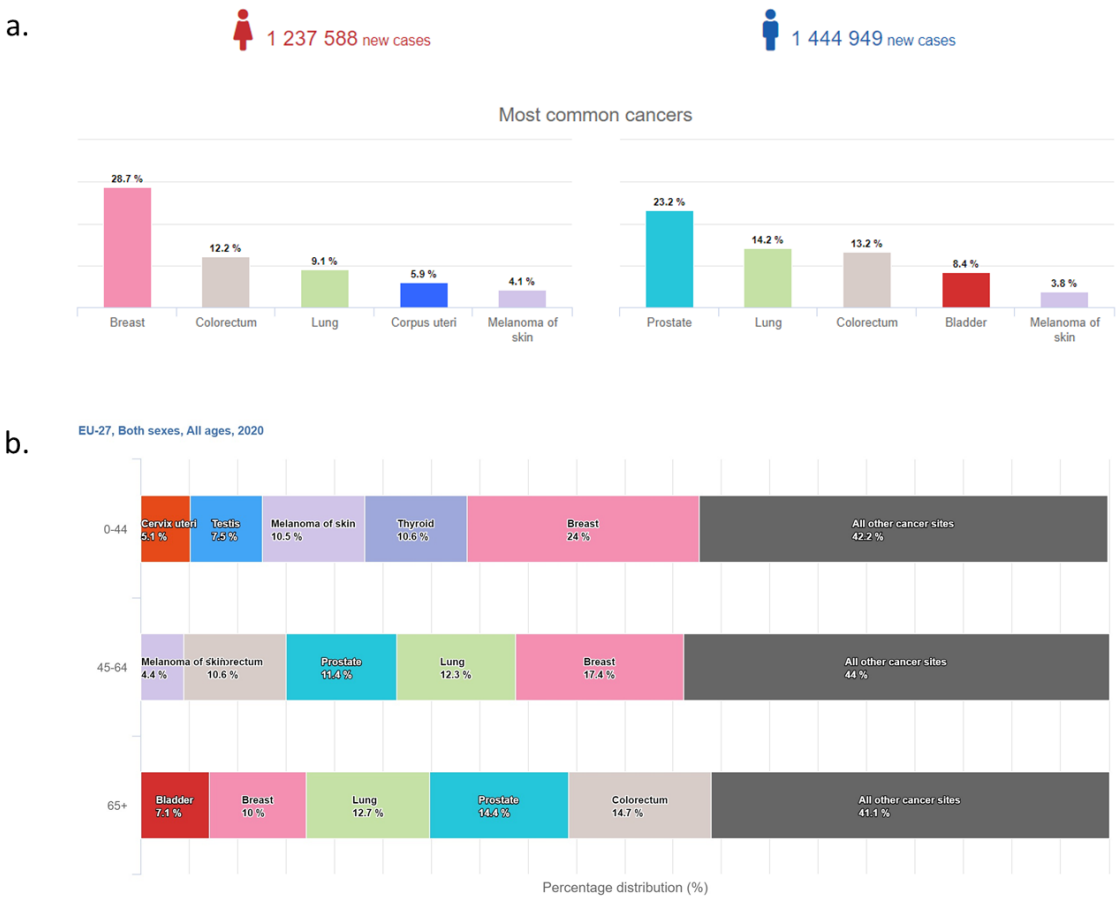

Figure 1.1.1: Cancer incidences in Europe.
(a) In 2020, the number of new cancer cases in Europe has reached 2.7 million and contributes to 1.3 million deaths. (b) Bar graph showing percentage distribution of various cancers according to age. ECIS - European Cancer Information System from https://ecis.jrc.ec.europa.eu, accessed on 15.10.2020 © European Union, 2020

In 2000, Hanahan and Weinberg published a review on the hallmarks of cancer, describing in detail the six mechanisms that lead to cancer progression (Hanahan and Weinberg 2000). Almost a decade later, they published an updated review describing the rapid advances in the field shown in Figure 1.1.2. In the initial review, six factors were described that affect the fate of cancer cells including independent functioning of growth signalling and altered response to antigrowth signals, inhibition of apoptosis and uncontrolled proliferation potential and angiogenesis, thus finally leading to tissue invasion and metastasis. Metastasis to distant organs is responsible for 90% of the cancer-associated deaths (Hanahan and Weinberg 2000). In the subsequent review, Hanahan and Weinberg they describe the essential role of tumour microenvironment in tumour progression and metastasis (Hanahan and Weinberg 2011).

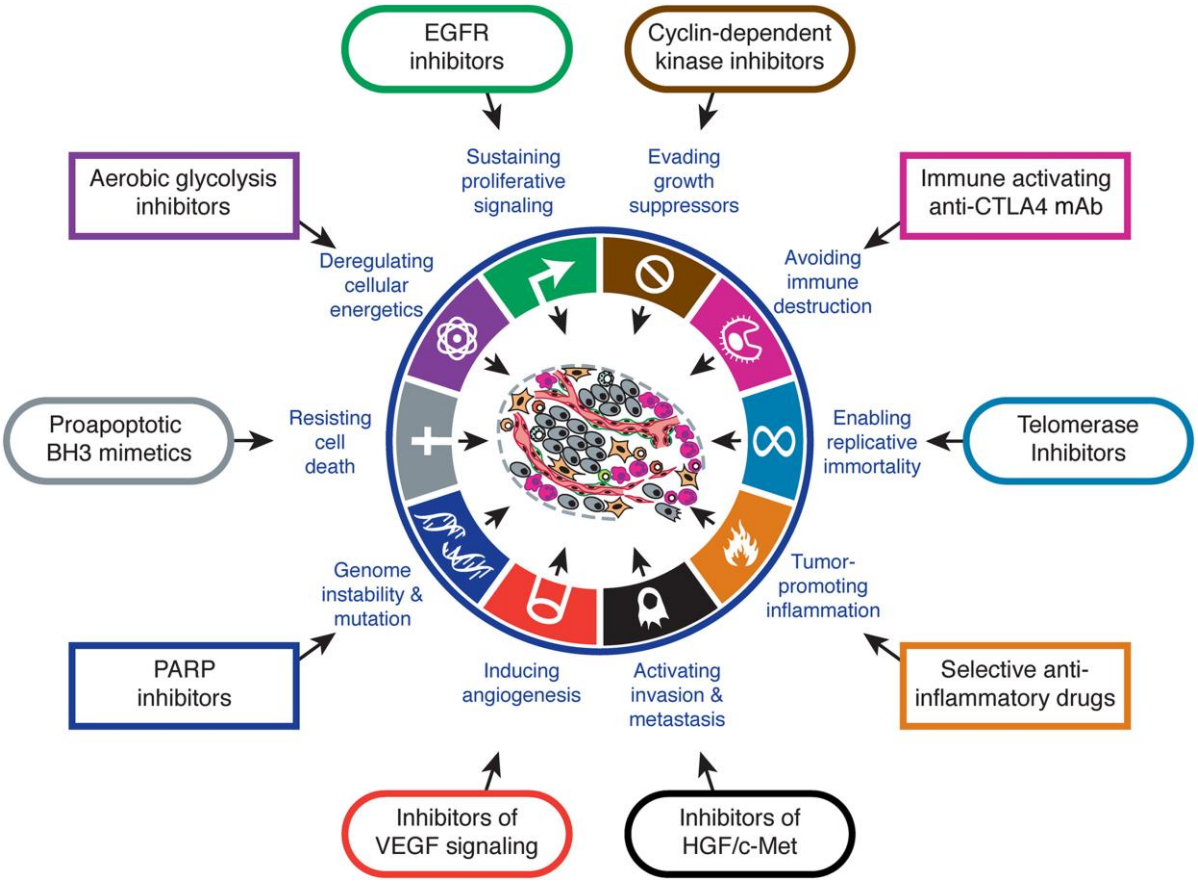

Figure 1.1.2 The hallmarks of cancer and designed targeted therapies
Schematic representations of the ten hallmarks of cancer and some of the approved drugs for inhibition of tumour growth and progression and others still under clinical trial. (Reprinted from the Hallmarks of Cancer: The Next Generation, Hanahan and Weinberg, 2011 with permission from Elsevier)

Recent studies have described the tumour microenvironment as a pathologically active site that controls tumour cell behaviour. The tumour microenvironment comprises an extracellular matrix (ECM), immune and inflammatory cells, adipose cells, fibroblasts, myofibroblasts, neuroendocrine cells, and lymphatic networks (Wang, Zhao et al. 2017). *In vitro* and *in vivo* results suggest that adipocytes are modulated in the proximity of cancer cells and they become cancer-associated adipocytes (CAA) (Dirat, Bochet et al. 2010). In 2013, Nieman *et al.* reported that tumours which are in close proximity to adipose tissue (breast, colon, prostate, renal, melanoma, gastric and ovarian cancers), support the formation of CAA and thus contribute to tumour growth and metastasis as shown in Figure 1.1.3 (Nieman, Romero et al. 2013). Increased adipose mass leads to obesity, which has been directly correlated to cancer development and increased mortalities in cancer patients (Nieman, Romero et al. 2013).

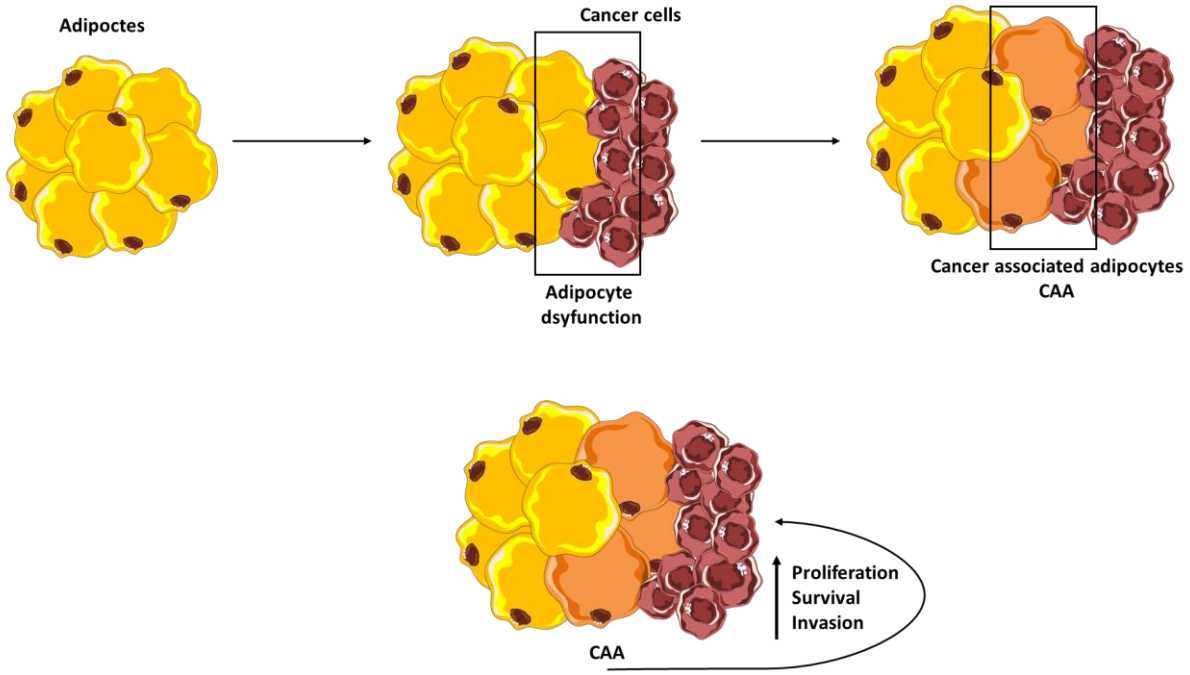

Figure 1.1.3: Schematic representation of the development of cancer-associated adipocytes
When adipocytes are in close contact with cancer cells, the latter can cause adipose cell dysfunction and adipocytes can switch into cancer-associated adipocytes (CAA). CAA secrete cytokines/adipokines that promote aggressiveness by enhancing cell proliferation, invasion and survival.

1.2 3D models for cancer research

Cancer research relies on the use of isolation of primary tumours from mice or human patients, paraffin-embedded tissue sections, cell lines derived from xenografts of human tumours and transgenic mice (Vargo-Gogola and Rosen 2007, van Staveren, Solís et al. 2009, Louzada, Adega et al. 2012). Cell lines are widely used as a routine experimental model (van Staveren, Solís et al. 2009) and are cultured *in vitro* to perform cell behavioural studies that include cell differentiation, growth, migration and invasion that can reflect the *in vivo* conditions (Huh, Hamilton et al. 2011). Cells are mostly cultured on flat surfaces and grow as monolayers. Unfortunately, this does not reflect the *in vivo* situation due to lack of a cell-to-cell contract, absence of cellular heterogeneity and lack of internal structure (Costa, Moreira et al. 2016). Recently, labs are adopting 3D culture systems as an alternative to 2D monolayers. Several studies have compared cancer cells in 2D and 3D cultures and have concluded that the 3D culture systems can precisely mimic the 3D structure *in vivo* and also the cancer microenvironment (Fischbach, Kong et al. 2009, Pickl and Ries 2009, Dolznig, Rupp et al. 2011, Costa, Moreira et al. 2016). Furthermore, results from gene expression profiles and response to drug treatment of 3D cultures show a close resemblance to *in vivo* conditions (Desoize and Jardillier 2000, Takagi, Watanabe et al. 2007).

There are various methods to generate 3D spheroids *in vitro*, the most common method is using an anchorage-independent system by seeding the cells in ultra-low attachment (ULA) plates (Langhans 2018). The cells tend to self-aggregate themselves and establish physiological characteristics seen *in vivo* by providing a cell-to-cell contact and synthesising their own ECM (Cukierman, Pankov et al. 2001, Ekert, Johnson et al. 2014). Härmä *et al*. performed a comprehensive characterisation of PCa cell lines, including Du145 and PC3, in 3D cultures to study the morphology, growth and invasiveness of the cells. They reported that PCa cell lines grown in 3D cultures are a better model to perform tumour behavioural assays when compared to the traditional 2D culture (Härmä, Virtanen et al. 2010). Thus, based on the available literature, we tried to adopt 3D culture assays for our experiments whenever possible. Due to commercially available assays for measuring cell viability and invasion, we adopted these methods for our experiments. For cell proliferation and migration assays, we used 2D cultures since there are not many studies using these assays in the 3D system and

lack of data on their reproducibility. Lastly, for studying tumour microenvironment, it is essential to maintain the 3D structure *in vitro* in order to mimic the *in vivo* conditions observed in humans.

1.3 Obesity and Adipose tissue

Extensive research has shown that obesity is rapidly increasing worldwide, to the extent that has reached a pandemic level. Being a high-risk factor for several diseases including type 2 diabetes, cardiovascular diseases and cancer amongst a few, obesity also has a significant impact on socio-economic productivity and contributes to an economic burden in the world (Blüher 2019). Obesity can be defined as the increased accumulation of lipids in the adipose tissue and other organs, such as the liver and skeletal muscle, due to excess caloric intake (Hopkins, Goncalves et al. 2016). According to the WHO, obesity can be measured by calculating the body mass index (BMI); BMI is calculated by dividing weight in kilograms by the height in meters squared. BMI ranging from 18.5 to 24.9 is considered healthy. BMI above 25 is classified as overweight and BMI over 30 is considered obese (Taylor, Lo et al. 2015).

Adipose tissue is a metabolically active organ and one of the major components of the body. It consists of pre-adipocytes, mature adipocytes, immune cells, stem cells, fibroblasts, endothelial cells and pericytes. Adipose tissue is mainly composed of mature adipocytes that constitute about 14-24% of the total cell population (Duong, Geneste et al. 2017). In adipose tissue, increased adipose mass during obesity is due to enlargement of the size of adipocytes (hypertrophy) and increase in the number of adipocytes (hyperplasia) as shown in Figure 1.3.1a (Zhou, Tardivel et al. 2010). Hypertrophy is a condition characterised by increased lipid accumulation in adipocytes that become dysfunctional and causes cell death. Thus triggering innate immune responses and pathogenesis. Due to the increased expansion of adipose cells, their cell membrane is ruptured and all the cellular contents are exposed into the microenvironment, these mainly consist of lipids, cytokines and damaged molecular elements such as ATP, nucleic acids and reactive oxygen species (Zhou, Tardivel et al. 2010, Vandanmagsar, Youm et al. 2011, Youm, Kanneganti et al. 2012). Thus leading to increased production of cytokines, for instance, IL-6, TNF, IFNγ and IL-1β that are released in the bloodstream (Brestoff and Artis 2015) and accumulation of phagocytic macrophages

(Weisberg, McCann et al. 2003). These phagocytic macrophages encircle the ruptured adipocytes forming crown-like structures, cellular debris, foam cells and scavenge lipids (Haka, Barbosa-Lorenzi et al. 2016). Thus triggering downstream signalling through inflammation. Formation of crown-like structures by macrophages is one of the biomarkers of adipose tissue inflammation (Quail and Dannenberg 2019). Moreover, it has been reported that in malignancies like cancer, crown-like structures are associated with poor prognosis (Quail and Dannenberg 2019). Hyperplasia constitutes a healthy expansion from pre-adipocytes to mature adipocytes through a process called adipogenesis (Lefterova, Zhang et al. 2008, Fuster, Ouchi et al. 2016). Peroxisome proliferator-activated receptor γ (PPARγ), is a well-studied member of the nuclear receptor family that functions as a critical regulator of adipogenesis (Rosen, Walkey et al. 2000). Adipocytes produce a large number of secretory factors such as hormones, chemokines and growth factors called adipokines (Fasshauer and Blüher 2015).

Adipocytes produce more than 50 different adipokines that can contribute to tumorigenesis. Leptin and Adiponectin are the most studied adipokines (Lengyel, Makowski et al. 2018). It has been reported that Leptin levels are increased, while Adiponectin levels are reduced in obesity (Hopkins, Goncalves et al. 2016). Leptin is a pro-tumorigenic adipokine, which is involved in regulating energy balance and controls appetite. It also activates numerous signalling cascades such as PI3K, MAPK, JAK/STAT pathway that promote cell proliferation, invasiveness and angiogenesis as shown in Figure 1.3.1b (Hopkins, Goncalves et al. 2016, Wang, Zhu et al. 2019). Several studies have shown that high levels of Leptin in the blood increase cancer progression in breast, ovarian, prostate and renal cell cancer (Hopkins, Goncalves et al. 2016). On the contrary, Adiponectin acts as an anti-tumorigenic adipokine by suppressing the effects of Leptin. It activates AMP kinase that regulates cellular metabolism and inhibition of mTOR signalling pathway (Hopkins, Goncalves et al. 2016). Adipokines have various roles in regulating body homeostasis, as shown in Table 1.

Adipokine	Primary source(s)	Binding partner	Function	References
Adiponectin	Adipocytes	Adiponectin receptors 1 and 2, T-cadherin, calreticulin–CD91	Insulin sensitizer, anti-inflammatory	(Lago, Dieguez et al. 2007, Lago, Gómez et al. 2009)
ANGPTL2	Adipocytes, other cells	Unknown	Local and vascular inflammation	(Kadomatsu, Tabata et al. 2011)
CCL2	Adipocytes, stromal vascular fraction cells		Monocyte recruitment	(Juge-Aubry, Henrichot et al. 2005, Cancello and Clément 2006)
CXCL5	Stromal vascular fraction cells (macrophages)	CXCR2	Antagonism of insulin signalling through the JAK–STAT pathway	(Chavey, Lazennec et al. 2009)
IL-18	Stromal vascular fraction cells	CCR2	Broad-spectrum inflammation	(Trøseid, Seljeflot et al. 2010)
IL-6	Adipocytes, stromal vascular fraction cells, liver, muscle	IL-6 receptor	Changes with source and target tissue	(Juge-Aubry, Henrichot et al. 2005, Cancello and Clément 2006)
Leptin	Adipocytes	Leptin receptor	Appetite control through the central nervous system	(Lago, Dieguez et al. 2007, Lago,

				Gómez et al. 2009)
Lipocalin 2	Adipocytes, macrophages	Unknown	Promotes insulin resistance and inflammation through TNF secretion from adipocytes	(Esteve, Ricart et al. 2009)
NAMPT	Adipocytes, macrophages, other cells	Unknown	Monocyte chemotactic activity	(Audrito, Messana et al. 2020)
RBP4	Liver, adipocytes, macrophages	Retinol (vitamin A), transthyretin	Implicated in systemic insulin resistance	(Esteve, Ricart et al. 2009)
Resistin	Peripheral blood mononuclear cells and adipocytes	TLR4	Promotes insulin resistance and inflammation through IL-6 and TNF secretion from macrophages	(Lago, Dieguez et al. 2007, Lago, Gómez et al. 2009)
SFRP5	Adipocytes	WNT5a	Suppression of pro-inflammatory WNT signalling	(Ouchi, Higuchi et al. 2010)
TNF	Stromal vascular fraction cells, adipocytes	TNF receptor	Inflammation, antagonism of insulin signalling	(Cawthorn and Sethi 2008)

Table 1: List of the commonly secreted adipokines and their functions

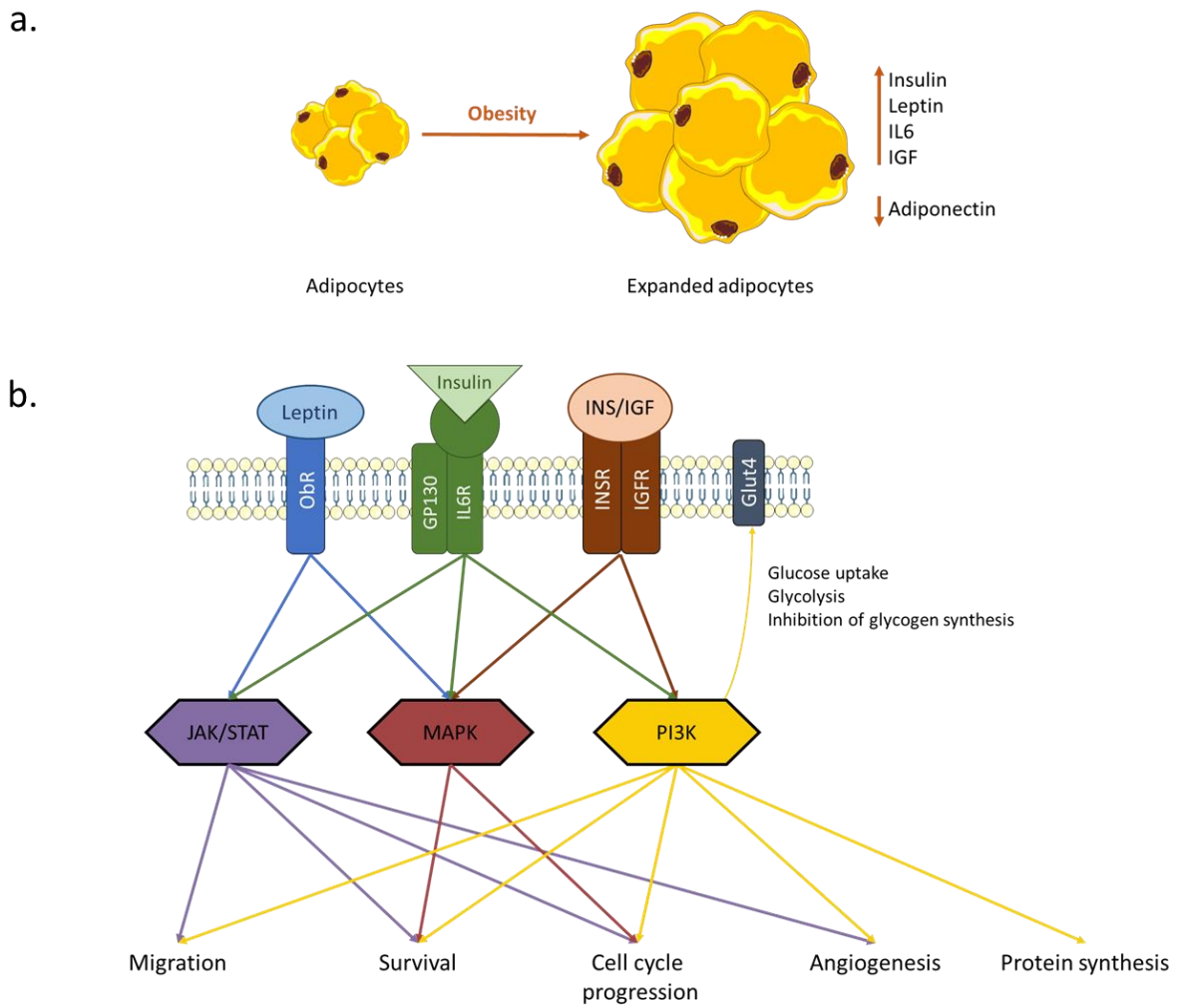

Figure 1.3.1: Effect of obesity on adipose tissue and associated intracellular signalling
(a) In obesity, there is adipocyte expansion in the WAT, resulting in increased lipid accumulation. Expanded adipocytes secrete higher levels of insulin (INS), Leptin, interleukin-6 (IL6 a), insulin-like growth factor (IGF) and inhibit the secretion of adiponectin. (b) Leptin, Insulin, IGF activate cell surface receptors and promote intracellular signalling pathways such Janus kinase phosphatidylinositol 3-kinase (PI3K), (JAK)/signal transducers and activators of transcription (STAT) and mitogen-activated protein kinase (MAPK). Thus promoting increased cell survival, migration and inhibiting apoptosis, leading to poor prognosis in cancer patients. Glucose transporter type 4 (Glut4), Glycoprotein 130 (GP130), Insulin-like growth factor receptor (IGFR), Interleukin 6 receptor (IL6R), Insulin receptor (INSR), Leptin receptor (ObR).

Depending on its function, adipose tissue is categorized into two major subtypes: white adipose tissue (WAT) and brown adipose tissue (BAT) (Poulos, Dodson et al. 2010). WAT is the most abundant adipose tissue in the body whereas BAT is present neonatally, during early childhood and in adults it is located beneath the clavicle (Fuster, Ouchi et al. 2016, Wang, Zhu et al. 2019). WAT is further classified as visceral white adipose tissue (visWAT) and subcutaneous white adipose tissue (scWAT). Approximately 80% of adipose depots in the body is subcutaneous. In men, visWAT constitutes for 10-20% of the total fat whereas in women it is 5-8%. With age, the visWAT content increases for both men and women (Ibrahim 2010). visWAT surrounds organs providing a protective layer and scWAT is found under the skin that provides heat insulation (Wang, Zhu et al. 2019). Additionally, adipocytes are present in tissues and organs that include heart, liver and bone marrow, as shown in Figure 1.3.2. Adipose deposits are correlated with ageing and obesity (Fuster, Ouchi et al. 2016).

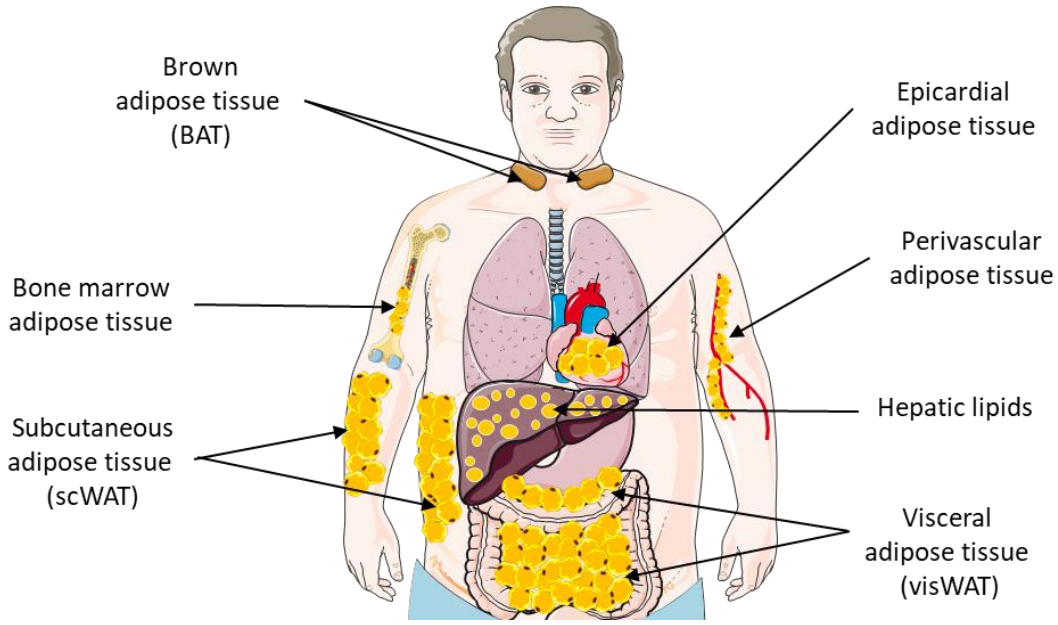

Figure 1.3.2: Distribution of adipose tissue in the body
Brown fat (BAT) regulates body temperature and is present in the supraclavicular and paraspinal regions. In contrast, white adipose tissue (WAT) is distributed throughout the body and constitute 15-20% body weight. Subcutaneous adipose tissue (scWAT) is mainly located in abdomen, thighs and buttocks. Whereas visceral adipose tissue is found surrounding organs such as omentum, bowel, and perineal areas. Additionally, fat deposits can be located in perivascular and pericardial regions, bone marrow and liver.

White adipocytes consist of a large lipid droplet with nucleus and cytoplasm pushed toward the cell membrane. The primary function of WAT is to store energy and it is essential for bodyweight management (Poulos, Dodson et al. 2010). Brown adipocytes comprise a nucleus in the centre and number of small lipid droplets (Lafontan 2012). BAT regulates thermogenesis in response to food intake and cold (Poulos, Dodson et al. 2010) and produce heat by oxidizing fatty acids via UCP1. Upon thermogenic signals though activated adipocyte receptors like PPARγ, WAT can undergo browning, and white adipocytes transform into brown adipocytes (Wang, Zhu et al. 2019). The third subtype of adipose tissue is called Beige adipose tissue. This is similar to WAT, having very low levels of UCP1 (Wang, Zhu et al. 2019).

The size of the adipocytes depends on their location and lipid content; subcutaneous adipocytes are usually larger than adipocytes in visceral depots. The visWAT is metabolically active, and therefore their adipokine secretion pattern is different from that of the subcutaneous deposits. For instance, visWAT shows a higher secretion of IL6 (200%) and vascular endothelial growth factor (400%) than subcutaneous fat (Toren and Venkateswaran 2014).

In recent years, there has been an increasing interest in understanding adipose tissue homeostasis controlled by immune cells. In adipose tissue, abundant expression of immune cells regulates systemic metabolism by influencing the adipose tissue to adapt while changing environmental conditions and food intake (Kane and Lynch 2019). Macrophages are the most abundant cell type in the immune cell population of adipose tissue. In lean condition, they constitute up to 10% of leukocytes, however, in obesity there are more than 50% of the leukocytes (Weisberg, McCann et al. 2003, Bapat, Myoung Suh et al. 2015, Catrysse and van Loo 2018). Adipose tissue macrophages in obese condition, promote insulin resistance by secreting inflammatory cytokines such as TNFα, IL-6, IL-1 and nitric oxide (Lumeng, Deyoung et al. 2007, Boutens, Hooiveld et al. 2018). Granulocytes such as Eosinophils and Neutrophils regulate glucose homeostasis and promote inflammatory response by secretion of TNFα and MCP-1 (Dam, Sikder et al. 2016, Silva, Báfica et al. 2019). Another cell population that is altered during obesity are T regulatory cells (Tregs); in humans, the Tregs cells are abundant in the visWAT, while their number is significantly lowered in obesity. Most of the studies focusing on Tregs biology are on mice (Cipolletta 2014, Becker, Levings et al. 2017). Eller *et al.*

reported Tregs depletion in db/db mice, established model of murine type 2 diabetes, enhanced insulin resistance by increasing fasting blood glucose level (Eller, Kirsch et al. 2011). Overall, in addition to removal of hypertrophic adipocytes, immune cells contribute to adipogenesis, angiogenesis, ECM, and controlling insulin sensitivity in lean conditions.

In addition to the immune responses that can alter adipose tissue microenvironment, recent studies have also shown the impact of adipocytes on tumour cells. Several studies have reported the cross-talk between adipose tissue and cancer (Quail and Dannenberg 2019). When adipocytes are in direct contact with tumours, for instance, breast, prostate, ovarian, colon there are several inflammatory signals in the adipose tissue and in the ECM of tumour cells that initiate cancer progression (Lengyel, Makowski et al. 2018). Novakovic *et al.* histologically stained prostatectomy specimens from benign, low and high-grade prostate tumours to determine their adipocyte phenotype. They found that adipocytes from PPAT were unable to infiltrate the prostatic capsule in normal prostate or BPH tissues (Novakovic, Fitchev et al. 2012). However, they observed that the infiltration of adipocytes corelated with tumour grade. The low-grade tumour had 20% infiltration whereas high-grade tumours had up to 90% infiltration of adipoctes (Novakovic, Fitchev et al. 2012). Therefore suggesting that tumour cell promote infiltration of adipocytes into the prostatic capsule.

Adipocytes supply fatty acids and inflammatory cytokines to the cancer cells, thus promoting proliferation and growth of tumour cells (Wang, Zhu et al. 2019). The direct contact between the tumour cells and the adipose tissue results in invasion through the adipose tissue. Previous studies have reported the invasion of breast tumours into the mammary adipose tissue, ovarian tumours through the ovarian adipose tissue and prostate tumour through the adjacent periprostatic tissue (Lengyel, Makowski et al. 2018). Moreover, Nieman *et al.* showed that cancer cells could promote the lipolysis in adipocytes, thus releasing fatty acids. These fatty acids were taken up by cancer cells to promote their growth (Nieman, Romero et al. 2013). It has been well described that adipose tissue can influence normal body homeostasis by influencing the secretion of adipokines (Ouchi, Parker et al. 2011). Furthermore, it has been shown that co-culturing of adipocytes with breast cancer cells resulted in altered gene expression in the latter (Strong, Strong et al. 2013, Lee Isla Crake, Phillips et al. 2019). A recent study on breast cancer showed the role of cancer-associated

adipocytes in modulating protein expression in cancer cells. After performing pathway analysis, reported that the proteins upregulated in tumour cells are mainly involved in metabolism, purine synthesis and ubiquitination (Lee Isla Crake, Phillips et al. 2019). Overall, these studies suggest the alteration of gene expression in cancer cells upon contact with adipocytes; this effect might be limited to the cancer cells since the non-cancer cells are not directly exposed to adipocytes. Further studies are required to understand the underlying mechanisms in adipocyte dysfunction to preventing and/or treating obesity related diseases.

1.4 Prostate cancer

In the UK, Prostate cancer (PCa) is the most common cancer in men (Cancer Research UK). More than 500,000 cases are diagnosed annually in Europe and North America. Although a considerable amount of research has been done, PCa still has a high mortality rate due to inadequate therapies for metastatic cancer (Wang, Zhao et al. 2018). Age, race and family history are the most critical factors contributing to the development of PCa (Sathianathen, Konety et al. 2018). PCa incidences are recorded in older men >65 years of age. Although recent data report cases in middle-aged men, the mortality rates are directly correlated to increasing age (Templeton 2007).

The prostate is a walnut-sized gland which is found below the bladder. In an adult male, it weighs about 18g. The prostate gland is comprised of 3 zones: the peripheral, central and transitional zones (Templeton 2007). Development of the Prostatic Intraepithelial Neoplasia (PIN) is known to be a primary precursor for the development of some PCas (Montironi, Mazzucchelli et al. 2011). As shown in Figure 1.4.1, the normal prostate epithelium consists of luminal cells that develop into PIN. The PIN is classified as low grade or high grade, depending on the number of cells involved (Montironi, Mazzucchelli et al. 2011). The PIN is detected by histopathological staining that shows a reduction in basal cell number, enlargement of nuclei and nucleoli, luminal epithelial hyperplasia, cytoplasmic hyperchromasia and nuclear atypia (Shen and Abate-Shen 2010). Bostwick *et al.* proposed a three-grade system (Grade 1, 2 and 3) to distinguish PIN based on histological characteristics (Bostwick and Brawer 1987). Later in 1989, the PIN was classified into two grades: PIN1 which is low-grade and PIN2 and PIN3 that are grouped as high-grade (Bostwick, Montironi et al. 2000). In some patients, PIN might progressively develop into PCa; abnormalities that are found in the normal epithelium can become low grade PIN followed by high-grade PIN and that finally metastasize to other organs (De Marzo, Haffner et al. 2016). Figure 1.4.2 shows distinct histological staining from low grade PIN to invasive carcinoma.

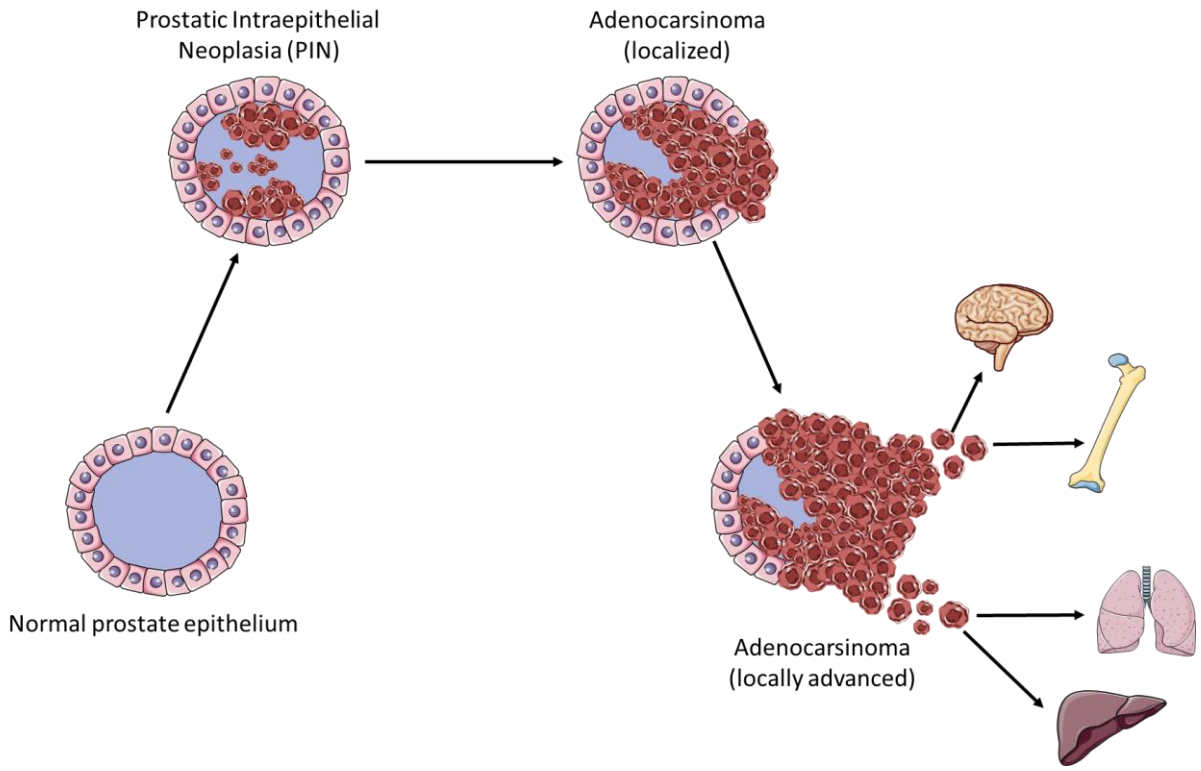

Figure 1.4.1: Progression of PCa: from PIN to locally advanced PCa
The normal prostate epithelium consists of luminal cells that can develop abnormalities and progress into Prostatic Intraepithelial Neoplasia (PIN). PIN can further develop into localised adenocarcinoma that might be invasive by degrading the basal membrane. Invasive PCa first metathesized to lymph nodes followed by distinct organs such as bones, liver, lungs and brain.

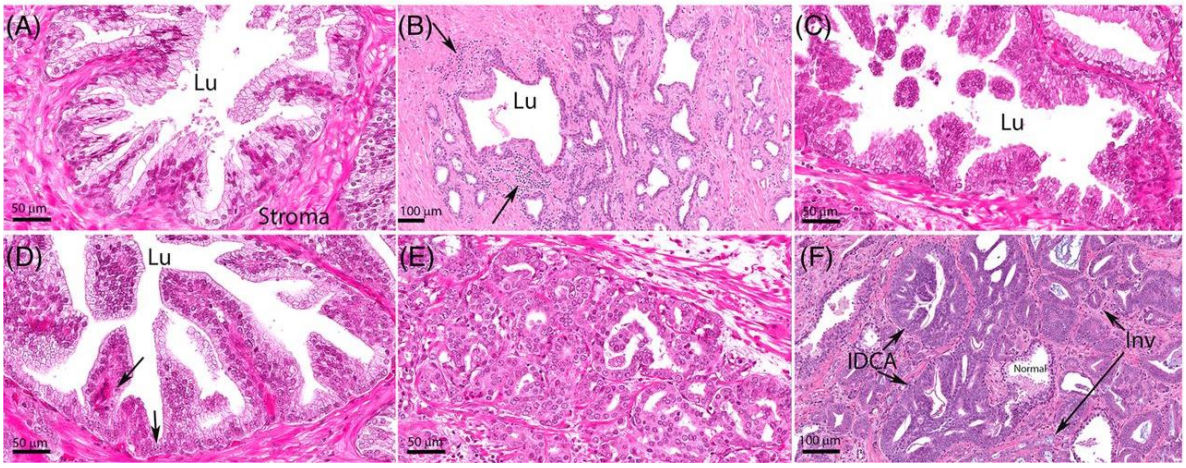

Figure 1.4.2: H&E staining of different types of prostate tissue
(A) normal prostate epithelium, (B) focal atrophy with inflammation, (C) low-grade PIN, (D) high-grade PIN, (E) invasive adenocarcinoma (Gleason score 3+4=7) and (F) intraductal carcinoma and adjacent invasive adenocarcinoma. Lu, lumens of glands. (Reprinted from De Marzo, Haffner *et al*., 2016 with permission from AACR publication)

1.4.1 Signalling pathways dysregulated in PCa

Androgen receptor signalling

It has been well established that androgens play a vital role in the prostate gland's development and function throughout the lifetime. In normal and PCa conditions, circulating androgens bind to androgen receptors and activate the downstream androgen signalling (Labrie, Dupont et al. 1983, Labrie, Dupont et al. 1985, Tombal and van Soest 2017). Androgens derived from testes contribute to about 80% of the circulating androgens (Attard, Richards et al. 2011). In 1941, Huggins *et al.* observed that decreasing the circulating androgens by surgery or chemotherapy could lead to better prognosis in advanced PCa patients (Huggins and Hodges 1941), thus suggesting that PCa is androgen-sensitive, at least in the early stages. Therefore, PCa patients receive androgen deprivation therapy such as surgical castration and they are provided with luteinizing hormone-releasing hormone analogues (Taplin and Balk 2004, Arai, Akaza et al. 2008). This method inhibits the androgens derived from testes; however, for complete inhibition of androgens, receptor antagonist is required. Initially, the patient responds well to the suggested therapies; however, most PCa becomes resistant to androgen deprivation therapy and become castration-resistant PCa (Shen and Abate-Shen 2010). The mortality rate for castration-resistant PCa exceeds 50%. Therefore, novel therapeutic strategies to prolong the survival of advanced PCa patients are required.

Androgen receptors are present in the cytoplasm in an inactive state bound to heat shock proteins as shown in Figure 1.4.3 (Shafi, Yen et al. 2013). They have a ligand and DNA binding domain and several phosphorylation sites. Upon ligand binding, the ligand-binding domain undergoes a conformation change that leads to detachment of heat shock protein. The receptor becomes dimerized with another androgen receptor and then translocated to the nucleus, thus activating cell proliferation, differentiation and anti-apoptotic pathways (Maughan and Antonarakis 2015). In PCa, there is an aberrant activation of cell proliferation and reduced activation in anti-apoptotic pathways (Maughan and Antonarakis 2015). Dihydrotestosterone (DHT), an androgen receptor binding ligand is formed from testosterone by 5α-reductase activity. DHT contributes to a majority of androgen receptor binding (Roy, Lavrovsky et al. 1999, Feldman and Feldman 2001, Brinkmann 2011). As shown in Figure 1.4.3 aberrant androgen receptor activations occur by: androgen receptor amplification (I), that

allows continuous activation of androgen receptor even in the presence of low androgen levels (Liu, Xie et al. 2008, Taylor, Schultz et al. 2010), signalling pathways such as AKT and MAPK pathways (II) contribute to activation of androgen receptor (Wang, Li et al. 2009, Shtivelman, Beer et al. 2014) and lastly, point mutations in androgen receptors (III) which leads to activation even with non-steroidal ligands (Thompson, Saatcioglu et al. 2001, Hara, Kouno et al. 2005). Further studies describe aberrant activation via splice variants (Hu, Dunn et al. 2009, Dehm and Tindall 2011) that are not covered in this thesis. Identifying the molecular mechanisms that lead to aberrant activation of androgen signalling is crucial for developing therapies for castration-resistant PCa.

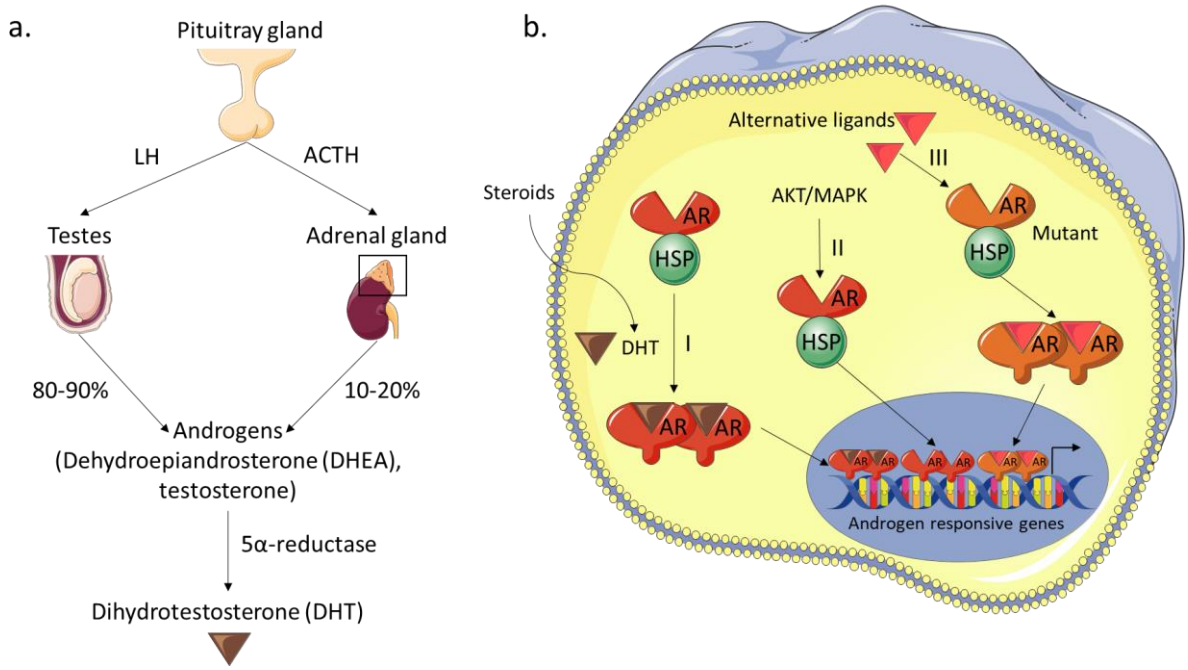

Figure 1.4.3: Generation of DHT and androgen receptor activation
Androgen receptor activation. (a) The hypothalamus-pituitary-axis controls the productions of androgens via testes and adrenal gland. Testicular androgens are produced by releasing Luteinizing hormone (LH), while adrenal androgens are produced by secreting ACTH from the anterior pituitary. Androgens such as dehydroepiandrosterone (DHEA) and testosterone are reduced to dihydrotestosterone (DHT) by 5α-reductase. (b) Androgen receptor activation occurs via various mechanisms, (I) Steroids such as DHT bind to androgen receptor leading to conformational change thereby leading to the removal of heat shock proteins, (II) by signalling pathways such as AKT and MAPK and (III) point mutations in androgen receptor leads to its activation by non-steroidal ligands, therefore, increased activation. The activated androgen receptor is transported to the nucleus and binds to the DNA and binds to androgen-responsive genes to modulate gene transcription.

PI3K/PTEN pathway signalling

Phosphoinositide 3-kinases (PI3Ks) are part of lipid kinases family regulating critical signal transduction that mediates cell cycle progression, cell survival, differentiation, proliferation, adhesion, migration, metabolism and transcription (Fruman 2003). Uncontrolled activation of signalling pathways through PI3K is observed in various cancer, including PCa (Taylor, Schultz et al. 2010). Around 70% of PCa with metastasis have aberrant activation of PI3K pathway (Taylor, Schultz et al. 2010, Carver, Chapinski et al. 2011). PI3Ks phosphorylate the 3'-hydroxyl group of phosphoinositides on the plasma membrane, for instance, lipid phosphatidylinositol-4,5-bisphosphate (PIP_2) is converted to phosphatidylinositol-3,4,5-trisphosphate (PIP_3) (Cantley 2002). As shown in Figure 1.4.4 phosphatase and tensin homolog (PTEN) is a negative regulator of PIP_3 by dephosphorylating it back to PIP_2 and controlling cellular proliferation and survival (Cantley 2002). Aberrant activation PIP_3 in cancer promotes activation of downstream signalling pathways such as AKT (Gonzalez and McGraw 2009). AKT is activated by phosphorylation of two serine (Ser) or threonine (Thr) residues, the threonine residue (Thr308) is phosphorylated by phosphoinositide-dependent kinase 1 (PDK1), a master regulator of AGC protein kinase family while the serine residue (Ser473) is phosphorylated by the mammalian target of rapamycin complex 2 (mTORC2) (Alessi, James et al. 1997, Sarbassov, Guertin et al. 2005). Activated AKT promotes activation and inhibition of various downstream targets thus leading to nutrient metabolism, cell survival, proliferation, migration and angiogenesis (Yan and Huang 2019).

PTEN is a tumour suppressor located on chromosome 10. Mutations in *PTEN* are found in samples derived from prostate, breast, kidney, lung, colon, endometrium and glioblastoma cancer (Leslie and Foti 2011). Transgenic mice with *PTEN* deletion are studied to assess its tumour suppressor function *in vivo*. It has been previously reported that the homozygous deletion of *PTEN* is responsible for embryonic lethality in mice (Suzuki, de la Pompa et al. 1998). Several studies have performed *PTEN* deletion specifically in mouse prostate to characterise its role in PCa progression. Heterozygous deletion of *PTEN* in mouse prostate results in PIN development in all mice (Trotman, Niki et al. 2003). In comparison, homozygous deletion of *PTEN* depicts the process of human PCa progression from the development of PIN to adenocarcinoma and in some cases, metastasis (Trotman, Niki et al. 2003, Wang, Gao et al. 2003). Therefore, these transgenic prostate cancer-specific mice are often crossed with

other mutant mice to study the role of various target gene on PCa progression *in vivo* (Yan and Huang 2019). In PCa patients, the levels of PTEN are assessed by performing fluorescence in situ hybridisation (FISH) and IHC (Leslie and Foti 2011). PTEN levels are often correlated with higher Gleason score and poor prognosis (Suzuki, de la Pompa et al. 1998).

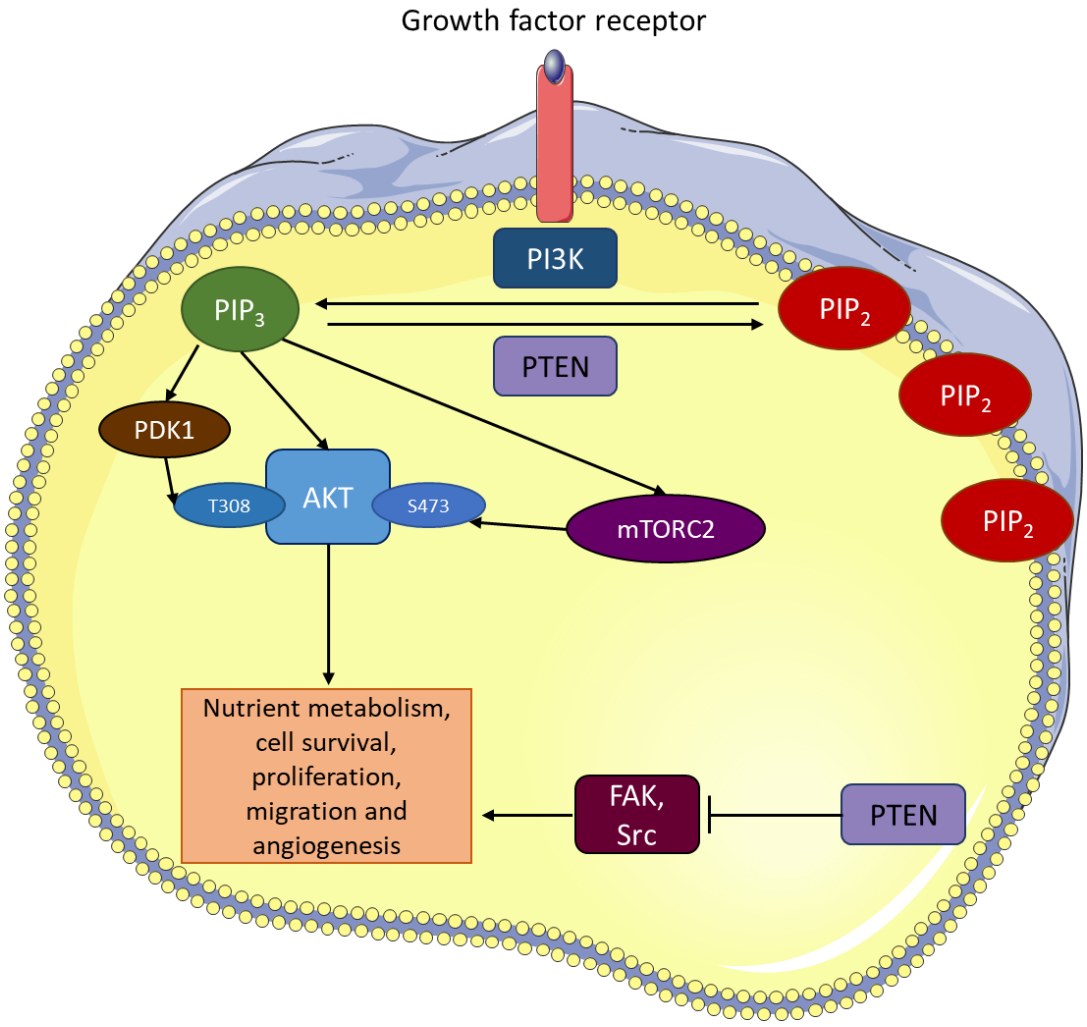

Figure 1.4.4: Activation and regulation of the PI3K/AKT
Growth factor receptors regulate the PI3K/ATK pathway via PI3K signalling. PI3K coverts phosphatidylinositol 4,5-bisphosphate (PIP2) into phosphatidylinositol 3,4,5-trisphosphate (PIP3). Activated PIP3 promotes activation of phosphoinositide-dependent kinase 1 (PDK1) and mammalian target of rapamycin complex 2 (mTORC2), thereby activating AKT at its serine 473 (ser473) and threonine (Thr308) residues. AKT activates an array of proteins that lead to cellular growth, proliferation and survival. Phosphatase and tensin homologue (PTEN) acts as lipid phosphatase by converting PIP3 to PIP2. PTEN acts as a tumour suppressor by blocking PI3K signalling and additionally inhibits focal adhesion kinase 1 (FAK) and proto-oncogene tyrosine-protein kinase Src. Loss of PTEN function occur in up to 60% of PCa patients that promotes over-activation of AKT and leading to uncontrolled cell proliferation, enhanced angiogenesis and decreased apoptosis.

1.4.2 Grading and treatment of PCa

In PCa, the early stages of tumour development are asymptomatic. Later, the symptoms include bladder dysfunction, blood in urine and seminal fluid. And finally in the metastatic stage, the symptoms include organ and muscle pain (Templeton 2007). Prostate-specific antigen (PSA) is a serine protease that is involved in liquefying the seminal fluid. In normal prostate tissue, PSA secretion is tightly regulated and its secretion in the bloodstream is rare. However, in PCa high levels of circulating PSA are detected. This also occurs in benign prostate diseases (Lilja, Ulmert et al. 2008). Presence of PCa is often assessed by biopsies after finding elevated levels of PSA in blood. This is followed by histopathological staining of prostate tissue and scoring accordingly (Shen and Abate-Shen 2010). Prostate-specific membrane antigen (PSMA) is a membrane protein, which is found abundantly on the cell membrane in PCa. There are several studies that indicate high PSMA levels in PCa tissue correlates with high Gleason score and it is used for diagnosis (Ferraro, Rüschoff et al. 2020). The most common classification for PCa is the Gleason scoring. Over decades the scoring system has been modified as compared to the original description by Gleason and Mellinger in 1974 (Pierorazio, Walsh et al. 2013). The Gleason score is dependent on the glandular arrangement of the cells and can be categorised into the following subtypes: ≤6; 3 + 4 = 7; 4 + 3 = 7; 8; and 9–10. The score determines the prognostic grading groups (Table 2) based on which treatment is suggested (Pierorazio, Walsh et al. 2013). For better prognosis, the Gleason score is considered for the management of PCa (Sathianathen, Konety et al. 2018). Staging of tumours is based on tumour–node–metastasis (TNM) system that classify tumours based on localised in organs to fully invasive (T1–4), with or without lymph node detection (N0 or 1), and on the extent of distant metastases (M0 and 1a–c) (Ohori, Wheeler et al. 1994). For localised PCa, treatment options include active monitoring, radical prostatectomy or radical radiotherapy. In advance condition, hormone therapy is suggested (Templeton 2007).

Gleason scores (1-10)	Prognostic Grade Groups	Characteristics
Gleason score ≤6	Prognostic Grade Group I	Only individual discrete well-formed glands
Gleason score 3 + 4 = 7	Prognostic Grade Group II	Predominantly well-formed glands with lesser component of poorly-formed/fused/cribriform glands
Gleason score 4 + 3 = 7	Prognostic Grade Group III	Predominantly poorly formed glands with lesser component of well-formed glands
Gleason score 8	Prognostic Grade Group IV	Predominantly well-formed glands and lesser component lacking glands
Gleason score 9-10	Prognostic Grade Group V	Lacks gland formation (or with necrosis) with or w/o poorly formed/fused/cribriform glands

Table 2: Reporting Gleason score based on Prognostic Grading groups.
Gleason score ranges from Prognostic Grade Group I (most favourable) to Prognostic Grade Group V (least favourable) (Pierorazio, Walsh et al. 2013).

1.4.3 Obesity and PCa

The prostate gland is surrounded by adipose tissue in the form of a capsular structure known as periprostatic adipose tissue (PPAT) (Ribeiro, Monteiro et al. 2012). During the development of cancer, the tumour arises from the peripheral zone and infiltrates the capsule, positioning tumour cells in the immediate proximity of adipose tissue (Templeton 2007, Ribeiro, Monteiro et al. 2012). PPAT secretes some soluble factors in addition to ECM components that modulate the malignant behaviour of the tumour cells. These cells further metastasise through lymph nodes and blood vessels to other lymph nodes and muscles (Ribeiro, Monteiro et al. 2012).

Obesity is correlated with increased prostatic volume (Chughtai, Forde et al. 2016). Several studies have reported that the thickness of PPAT directly corresponds to PCa aggressiveness (Taylor, Lo et al. 2015). Thus, patients having thicker PPAT tend to have a poorer prognosis (Venkatasubramanian, Brendler et al. 2014, Tan, Lin et al. 2016). As previously described, adipocytes secrete several cytokines and hormones known as adipokines. During obesity, there is an elevated production of cytokines IL6, MCP-1, leptin and a decrease in adiponectin production (Hopkins, Goncalves et al. 2016). There have been plenty of studies that link IL6 with several cancers including, breast, lung, ovarian, and prostate (Toren and Venkateswaran 2014). Thus suggesting that high levels of IL6 create a favourable microenvironment for PCa (Toren and Venkateswaran 2014). It has been shown that the conditioned media from PPAT from PCa patients secrete some cytokines and growth factors such as IL6 that are responsible for high-grade tumour (Sacca, Creydt et al. 2012). The levels of IL6 are much higher in the PPAT from PCa patients as compared to BPH (Sacca, Creydt et al. 2012). Recent studies supported these results by analysing the thickness of PPAT and their involvement in the production of IL6, contributing to PCa progression (Ribeiro, Monteiro et al. 2012).

Increased adipose tissue mass contributes to increased fatty acid metabolism in PPAT (Taylor, Lo et al. 2015). In obese conditions, the levels of lipolysis are elevated; meaning the breakdown of triglycerides to produce free fatty acids is increased. Previously, it has been reported that the fatty acid oxidation is higher in PCa cells (PC3, LNCap, VCap) when compared to normal prostate epithelial cells (BPH-1 and WPMY-1) (Taylor, Lo et al. 2015). This suggests that fatty acid oxidation is enhanced during tumorigenesis, as shown in Figure 1.4.5.

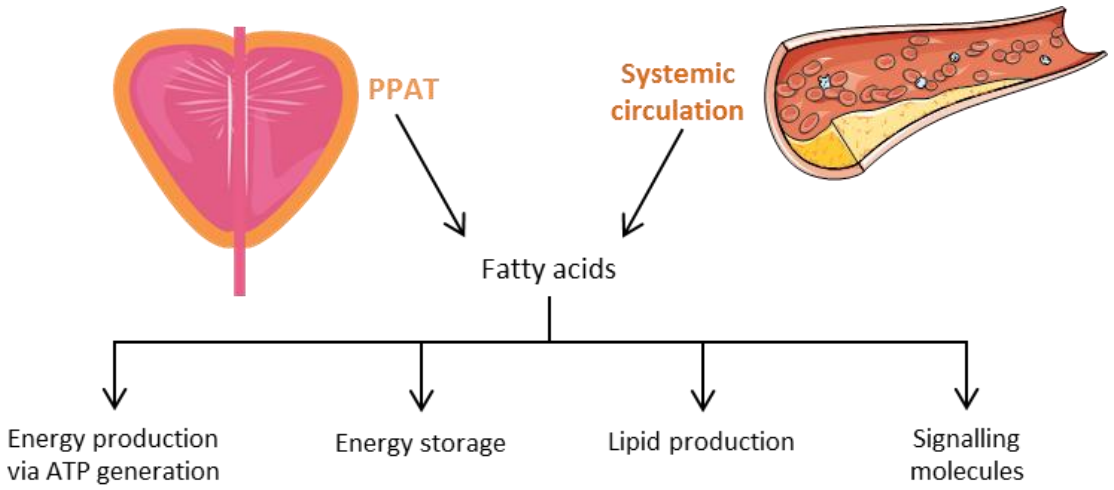

Figure 1.4.5: Schematic representation of fatty acid metabolism in prostate
Fatty acids are transported from PPAT and systemic circulation into the prostate epithelial cell. Here they are subjected to various processes that include (1) oxidation in mitochondria for energy production; (2) energy storage in the form of triglycerides; (3) lipid production by conversion into phospholipids and sterol; (4) conversion into signalling molecules (Taylor, Lo et al. 2015).

There have been increasing studies on the effect of adipocytes on tumour progression: when tumour cells are adjacent to adipocytes, the latter undergo phenotypic changes and behave as cancer cells. These are termed as cancer associated-adipocytes (CAAs).

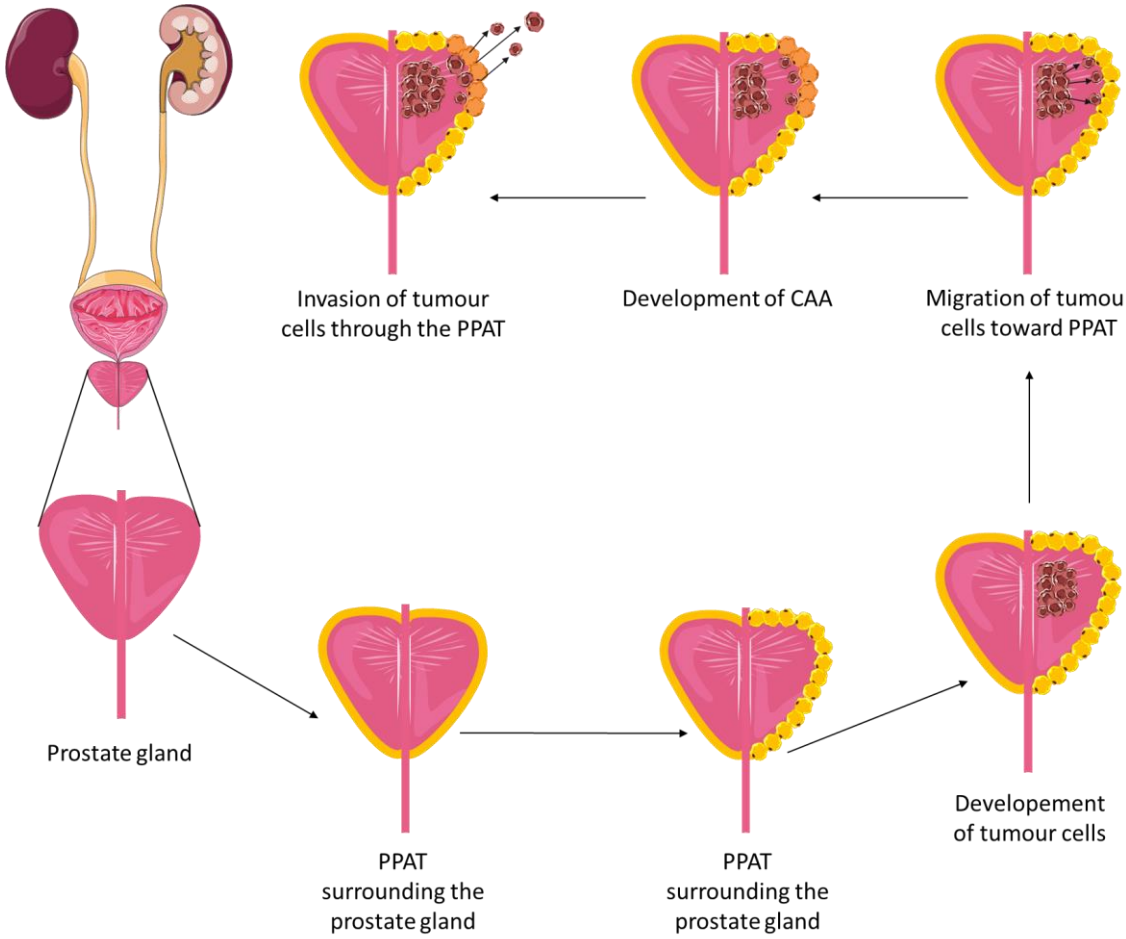

Figure 1.4.6: Development of cancer-associated adipocytes.
The prostate gland is surrounded by a covering called PPAT (yellow covering). This PPAT is composed of adipocytes and other cells (yellow cells). During the development of PCa, the cancer cells within the capsule metastasize to the edge of the capsule, thus interacting with the adipose cells to become Cancer-Associated adipocytes. These are adipose cells that behave like cancer cells and promote their to metastasis to other organs.

The CAAs can modulate the activity of cancer cells by promoting their proliferation and invasion potentials by secretion of adipokines (Laurent, Guerard et al. 2016). Laurent *et al.* demonstrated that adipokines secreted from mature adipocytes promote the migration of PCa cells outside the PPAT capsule, as shown in Figure 1.4.6. This was further enhanced by increased expression of IL6 and matrix metalloproteases secreted by surrounding PPAT, which creates a favourable microenvironment for the migration and invasion of cancer cells (Laurent, Guerard et al. 2016). Furthermore, the authors showed that in PPAT, mature adipocytes secrete CCL7, which diffuses through the periprostatic capsule, reaching the

peripheral region of the prostate. The CCR3 receptor is present on the cancer cells and interacts with the CCL7 ligand, resulting in an increased cell migration (Laurent, Guerard et al. 2016). This CCL7-CCR3 interaction promotes cell migration both *in vivo* and *in vitro.*

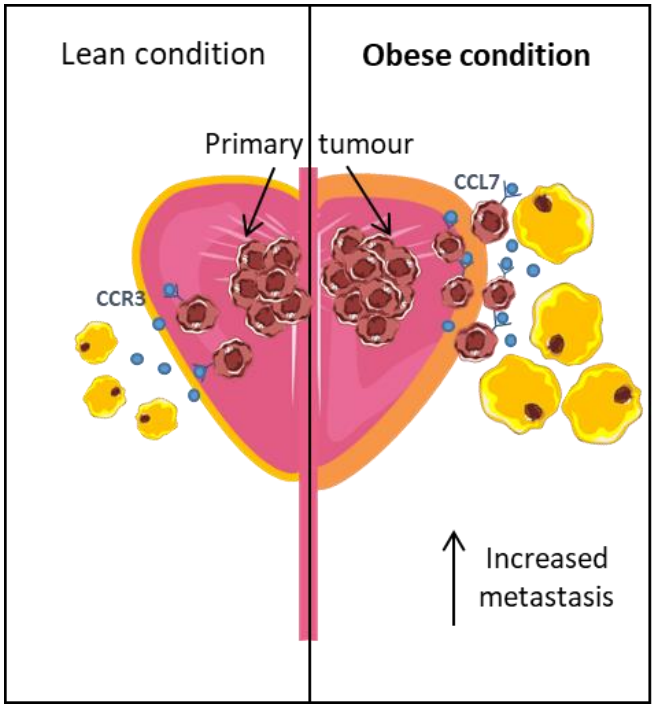

Figure 1.4.7: Schematic summary of the role of PPAT in PCa progression in lean and obese metabolic condition.
Mature adipocytes in obese condition have enhanced production of the CCL7 ligand that interacts with CCR3 receptor on the prostate cells. This interaction promotes the invasion and migration of cancer cells outside the periprostatic capsule (Laurent, Guerard et al. 2016).

A similar study was performed to characterise the influence of cancer cells on adipose tissue and the results showed that PCa cells increase the metabolic activity of adipocytes by creating an ideal tumour microenvironment for invasion and metastasis (Ribeiro, Monteiro et al. 2012). Ribeiro *et al.* showed that the conditioned media obtained from PPAT promotes cell proliferation and migration by modulating metalloproteinases (MMPs) activity. MMP2 and MMP9 regulate cell mechanisms and increase progression and metastasis in PCa (Ribeiro, Monteiro et al. 2012). Together, these studies indicate that PPAT enhances the secretion of adipokines (TNF, IL6 and OPN) when exposed to PCa conditioned media *in vitro*. Thus suggesting that in locally advanced PCa patients, the levels of adipokine secretion are modulated in PPAT by the cancer cells, therefore resulting in a more aggressive phenotype (Ribeiro, Monteiro et al. 2012).

1.5 Thyroid cancer

In the past few decades, thyroid cancer incidence increased worldwide. In Europe, as shown in section 1.1, the number of thyroid cancer cases account for 10.09% of the total cancer cases detected in the age group 0-44. The thyroid gland, as indicated in Figure 1.5.1, is located between larynx and the trachea and is responsible for organ development and secretion of various hormones (Nilsson and Fagman 2017). The thyroid gland is mainly composed of follicular cells that secrete the thyroid hormones triiodothyronine (T3) and thyroxine (T4). Another cell population within the thyroid gland is represented by the Para-follicular C cells. C cells are neuroendocrine cells that secrete calcitonin and carcinoembryonic antigen (Nilsson and Fagman 2017). They are located in the upper one-third of the thyroid lobes bilaterally and due to their low number, are generally difficult to observe in H&E staining (Chernock and Hagemann 2015). Additionally, there are capillary cells present between the thyroid follicles that secrete hormones (Nilsson and Fagman 2017).

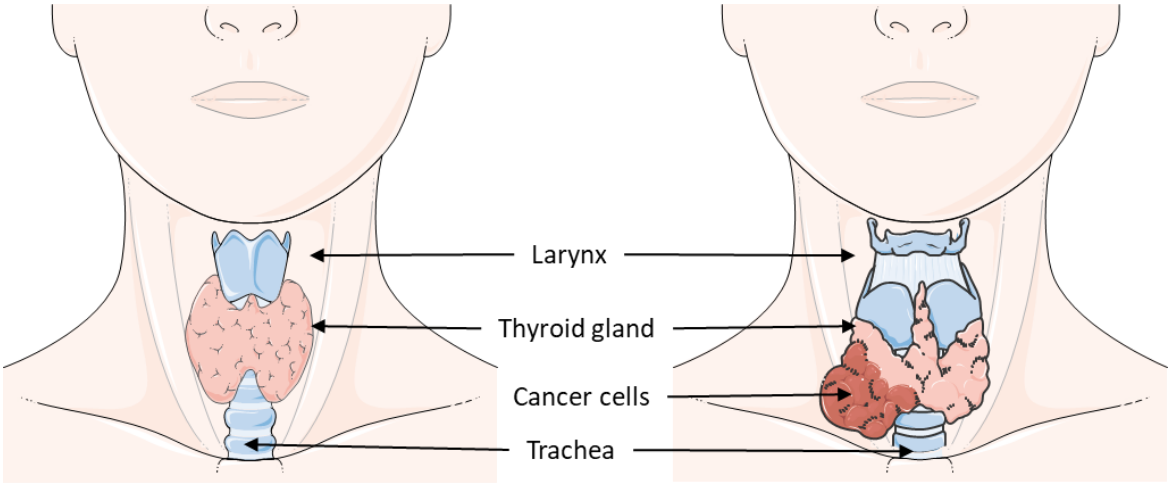

Figure 1.5.1: Location of the thyroid gland.
The thyroid gland is located in front of the neck surrounding the trachea. It has two lobes and a connecting branch called the isthmus. Collectively the cells in the thyroid gland secrete thyroid hormones such as T3, T4 and calcitonin. Tumour cells in the thyroid gland can first develop as thyroid nodules and progress to cancer formation.

Depending on the cell type origin, thyroid cancer can be classified into three types as illustrated in Figure 1.5.2: differentiated thyroid cancer, undifferentiated thyroid cancer and thyroid cancer from C-cells (Cabanillas, McFadden et al. 2016). Differentiated thyroid cancer arising from the follicular cells is the most common type of thyroid cancer that contribute to more than 95% of the cases. Follicular cells can cause papillary thyroid cancer, follicular

thyroid cancer, and Hurthle cell thyroid cancer. Papillary thyroid cancer is well-differentiated and the metastasis is confined to lymph nodes, making the overall prognosis much better than the other subtypes. Follicular and Hurthle cell thyroid cancer is more aggressive, poorly differentiated and can usually metathesize to distinct organs like lungs and bones (Cabanillas, McFadden et al. 2016). Anaplastic thyroid cancer develops rapidly into a tumour mass, which aids in detection. However, the tumour often metathesizes primarily to lungs, followed by bones and brain. This leads to poor prognosis even with early detection (Cabanillas, McFadden et al. 2016).

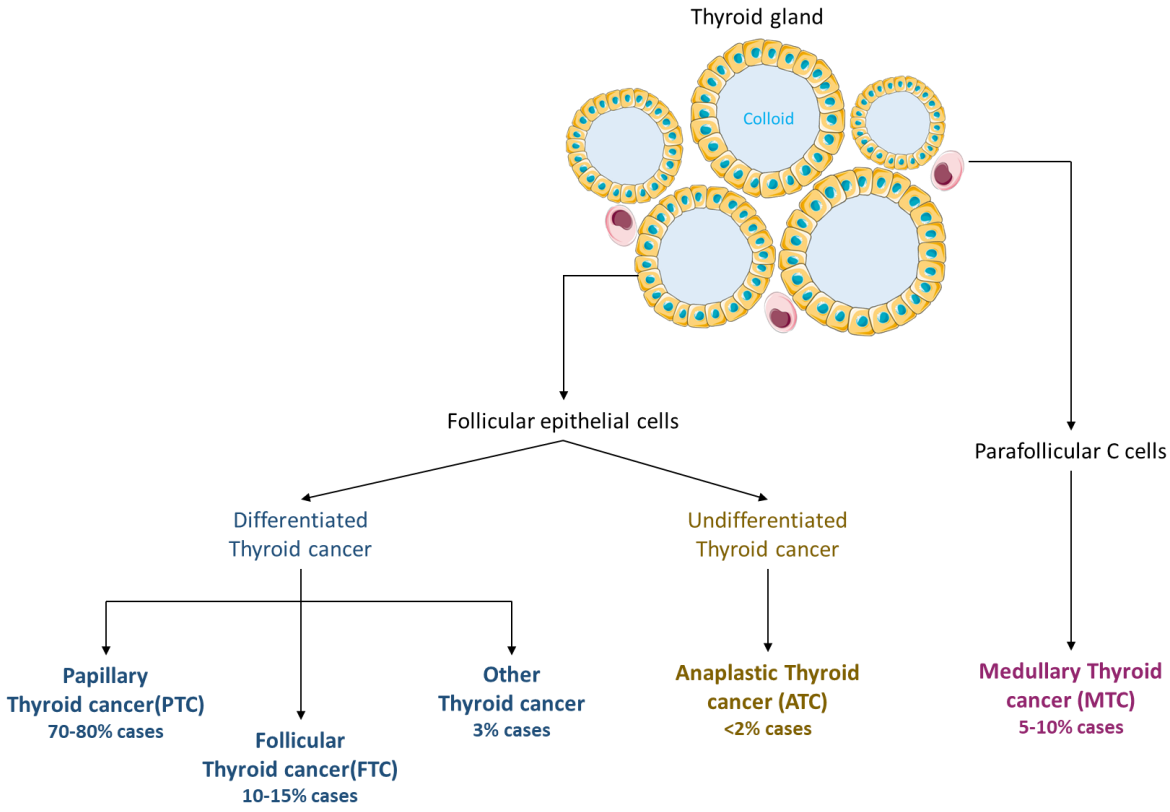

Figure 1.5.2: Types of Thyroid Cancer
Thyroid cancer can be classified into two major subtypes based on the cell type of origin, which can be follicular epithelial cells or parafollicular cells. The follicular cells can further develop into differentiated or undifferentiated thyroid cancer. The differentiated thyroid cancer is the most common subtype and is classified majorly as papillary thyroid cancer and follicular thyroid cancer. Anaplastic thyroid cancer, which arises from undifferentiated thyroid cells, is rare. Medullary thyroid cancer arises from Para-follicular C cells and accounts for 5-10% of cases. MTC has poor prognosis when diagnosed at a late stage.

Medullary thyroid cancer (MTC) occurs in 5%-10% of total thyroid cancer cases and arise from Para-follicular C cells (Cabanillas, Hu et al. 2014). Most of the MTC cases carry a (REarranged during Transfection) RET mutation, while few cases are due to sporadic RAS mutations (Cabanillas, McFadden et al. 2016). Early detection of MTC has overall good prognosis. In patients with localised MTC, the 10-year survival rate is 96%. However, patients with distant metastasis have only a 3-year survival rate (Cabanillas, Hu et al. 2014). One of the first stages of MTC is C-cell hyperplasia (McGregor, McCune et al. 1999) and it occurs in both somatic and familial cases (Chernock and Hagemann 2015). Hyperplastic C-cells are enlarged in size and number and form an aggregate (McGregor, McCune et al. 1999, Chernock and Hagemann 2015). Calcitonin immunohistochemistry is used to identify the C-cell hyperplasia (Chernock and Hagemann 2015).

1.5.1 Signalling pathways activated in MTCs

It has been well described that continuous activation of tyrosine kinase receptors is responsible for cancer progression. Para-follicular C cells in thyroid gland regulate various cellular processes such proliferation, differentiation, migration and apoptosis through activation of RET, RAS/MAPK, PI3K, VEGF, c-MET and mTOR pathways (Ceolin, Duval et al. 2019). Takahashi *et al.* first identified RET oncogene on chromosome 10q11.2 containing 21 exons (Takahashi, Ritz et al. 1985). RET mutations have been well described in the development of various diseases, as shown in Table 3. RET has a tyrosine kinase receptor for neurotrophic factors of the glial cell line-derived neurotrophic factor (GDNF) family: GDNF, neurturin, artemin and persephin which promotes cell growth, migration and apoptosis. GDNF family receptors (GFRα1-4) bind and activate of RET (Airaksinen and Saarma 2002). The RET receptor is constituted by three functional domains: an extracellular, a transmembrane, and an intracellular domain, as shown in Figure 1.5.3 (Arighi, Borrello et al. 2005). The extracellular domain provides conformational changes needed for ligand binding, the intracellular domain has two tyrosine kinase domains (TK1 and TK2), that are phosphorylated during receptor activation and initiate downstream signalling.

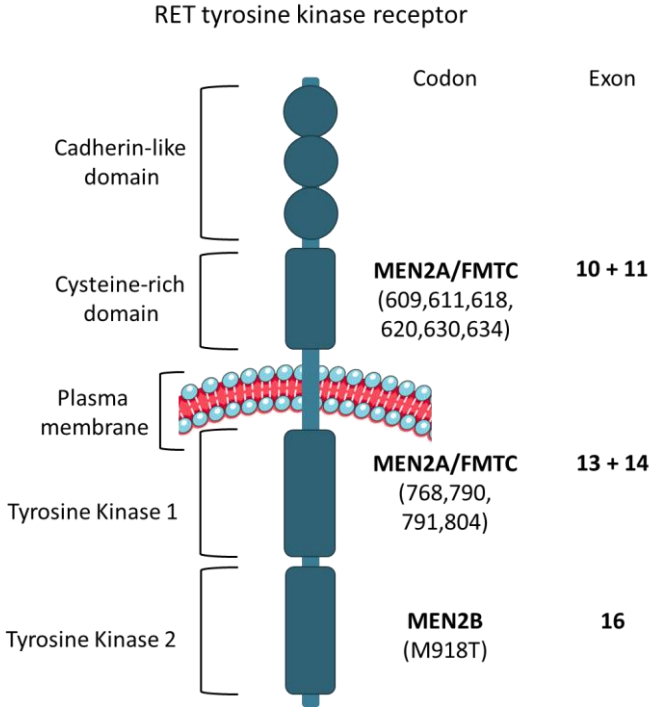

Figure 1.5.3: Structure of RET

RET is a tyrosine kinase receptor with a large extracellular domain containing a series of Cadherin-like domains and a cysteine-rich domain, followed by a transmembrane domain and an intracellular tyrosine kinase domain. RET mutation responsible for MEN 2A or FMTC is majorly found in the cysteine-rich domain on exon 10 and exon 11. Mutations in exon 13 and exon 14 are present in tyrosine kinase domain 1. For MEN 2B patients, 95% of the cases have mutations in exon 16 tyrosine kinase domain 2.

In normal tissues, such as the central and peripheral nervous systems and excretory system, RET is an essential regulator of differentiation and maturation (Castellone and Melillo 2018, Ceolin, Duval et al. 2019). In the absence of ligand binding, RET exists in a steady, non-phosphorylated state. Upon ligand binding, RET receptor is trans-phosphorylated and stimulates activation of downstream signalling pathways such as RAS/extracellular signal-regulated protein kinase 1 and 2 (ERK1/2), the phosphatidylinositol 3-kinase (PI3K)/AKT, c-Jun amino-terminal kinase (JNK), p38 mitogen-activated protein kinase (p38MAPK), signal transducer and activator of transcription 1/3 (STAT1/3) and phospholipase C-γ (PLCγ) (Castellone and Melillo 2018). RET is activated upon binding with four co-receptors belonging to the GDNF receptor α1-4 family of glycosylphosphatidylinositol (GPI) linked proteins (Castellone and Melillo 2018). In MTC, up to 68% of RET-negative MTC cases have RAS mutations (Ceolin, Duval et al. 2019).

Type of RET mutation	Disease	Reference
Loss-of-function mutations		
RET mutations all over the gene and in regulatory sequences	Hirschsprung disease	(Edery, Lyonnet et al. 1994), (Romeo, Ronchetto et al. 1994)
RET point mutations in the intracellular domain	Congenital anomalies of the kidney or lower urinary tract	(Davis, Hoshi et al. 2014)
Gain-of-function mutations		
RET point mutations	Familial and sporadic medullary thyroid carcinoma (MTC), Anaplastic thyroid carcinoma (ATC), Sporadic paraganglioma Urothelial carcinoma	(Mulligan, Kwok et al. 1993, Eng, Smith et al. 1994, Hofstra, Landsvater et al. 1994) (Kunstman, Juhlin et al. 2015) (Krawczyk, Hasse-Lazar et al. 2010) (Kato, Subbiah et al. 2017)
RET fusions	Papillary thyroid carcinoma (PTC), Lung adenocarcinoma, Colon carcinoma, Myeloproliferative disorders	(Grieco, Santoro et al. 1990) (Kohno, Ichikawa et al. 2012, Lipson, Capelletti et al. 2012) (Ballerini, Struski et al. 2012)
RET amplifications	Fallopian tube adenocarcinoma, Uterine carcinosarcoma, Duodenal adenocarcinoma	(Kato, Subbiah et al. 2017)

RET aberrant expression	Breast cancer, Pancreatic adenocarcinoma	(Amit, Na'ara et al. 2017) (Esseghir, Todd et al. 2007)

Table 3: RET alternations associated with human diseases

1.5.2 Occurrences

The majority of thyroid cancers are sporadic due to somatic mutations (Guilmette and Nosé 2018). Sporadic cases account for 75–80% of MTC cases, whereas familial MTC cases represent about 20–25% (Ceolin, Duval et al. 2019). More than 50% of sporadic MTCs have somatic RET M918T mutations (Roskoski and Sadeghi-Nejad 2018). Some studies have also described partial deletion in the RET gene and mutations in codons 618, 603, 634, 768, 804, and 883 (Ceolin, Duval et al. 2019). Some studies have also shown RAS mutations for MTC patients. Sporadic MTCs usually occur in the fifth or sixth decade of life (Chernock and Hagemann 2015).

Familial thyroid cancer arises from follicular cells due to inherited mutations and it is called familial follicular thyroid cancer (FFTC). Familial C cell tumours belong to the multiple endocrine neoplasia 2 (MEN2) syndrome and named as familial medullary thyroid cancer (FMTC) (Nilsson and Fagman 2017). MEN syndrome is further classified as multiple endocrine neoplasia type 2A (MEN 2A) and multiple endocrine neoplasia type 2B (MEN 2B) depending on the organs involved (Ceolin, Duval et al. 2019). The MEN 2A is the most common subtype and occurs in approximately 70–80% of all MEN 2 cases and is usually diagnosed in the second or the third decades of life (Roskoski and Sadeghi-Nejad 2018, Ceolin, Duval et al. 2019). MEN 2A is further divided into four types: classical MEN 2A, MEN 2A is associated with cutaneous lichen amyloidosis (CLA), MEN 2A and Hirschsprung's disease, and FMTC (Ceolin, Duval et al. 2019). MEN 2A are associated with MTC (95%), pheochromocytoma (30-50%) and occurrences of hyperparathyroidism (10-20%) (Ceolin, Duval et al. 2019). 98% of MEN 2A cases have RET mutations in the cysteine residues of the cysteine rich extracellular domain. Out of which 80% of the cases have a mutation in codon 634 of exon 11 (Nilsson and Fagman 2017). Other less common mutations are found in exons 10 and 11, where codons 609, 611, 618, 620, 630, 790 and 791 mutations. These mutations lead to constitutive dimerization without ligand binding and constant activation of kinases (Castellone and Melillo 2018). Previous studies have also documented less frequent RET mutations in exon 8, 13, 14, and 15

(Ceolin, Duval et al. 2019).

Although the MEN 2B syndrome only contributes to 5% of the overall MEN 2 cases, it has been reported to be more aggressive than MEN 2A. The 10-year survival rate for MEN 2B patients is just 75.5% when compared with MEN 2A patients having 97.4% survival rate (Castinetti, Moley et al. 2018). MEN 2B is diagnosed at a young age within the first years of life and it is associated with a poor prognosis (Nilsson and Fagman 2017). MEN 2B is associated with MTC (90%), ganglioneuromatosis (100%), Marfanoid habitus (65%) and pheochromocytoma (30-50%) (Roskoski and Sadeghi-Nejad 2018, Ceolin, Duval et al. 2019). In MEN 2B, more than 95% of the MTC cases have mutations in RET in codon 918 of exon 16 (Chernock and Hagemann 2015).

1.5.3 Diagnostic markers

A palpable thyroid nodule in the thyroid gland is a primary indication of an abnormality. Calcitonin and carcinoembryonic antigen screening are standard tests for MTC (Guilmette and Nosé 2018). High levels of serum calcitonin levels are an important MTC marker. In MTC patients, serum calcitonin levels are proportional to tumour size and lymph node metastasis (Castellone and Melillo 2018). Figure 1.5.4 shows the immunohistochemical staining of different stages of MTC. As shown in the figure, the calcitonin staining gradually increases from normal thyroid tissue to metastatic MTC. In 1999, McGregor *et al.* published the changes in trk family of neurotrophin receptors, trkA, trkB, and trkC in various MTC stages that can contribute to the progression of the disease (McGregor, McCune et al. 1999).

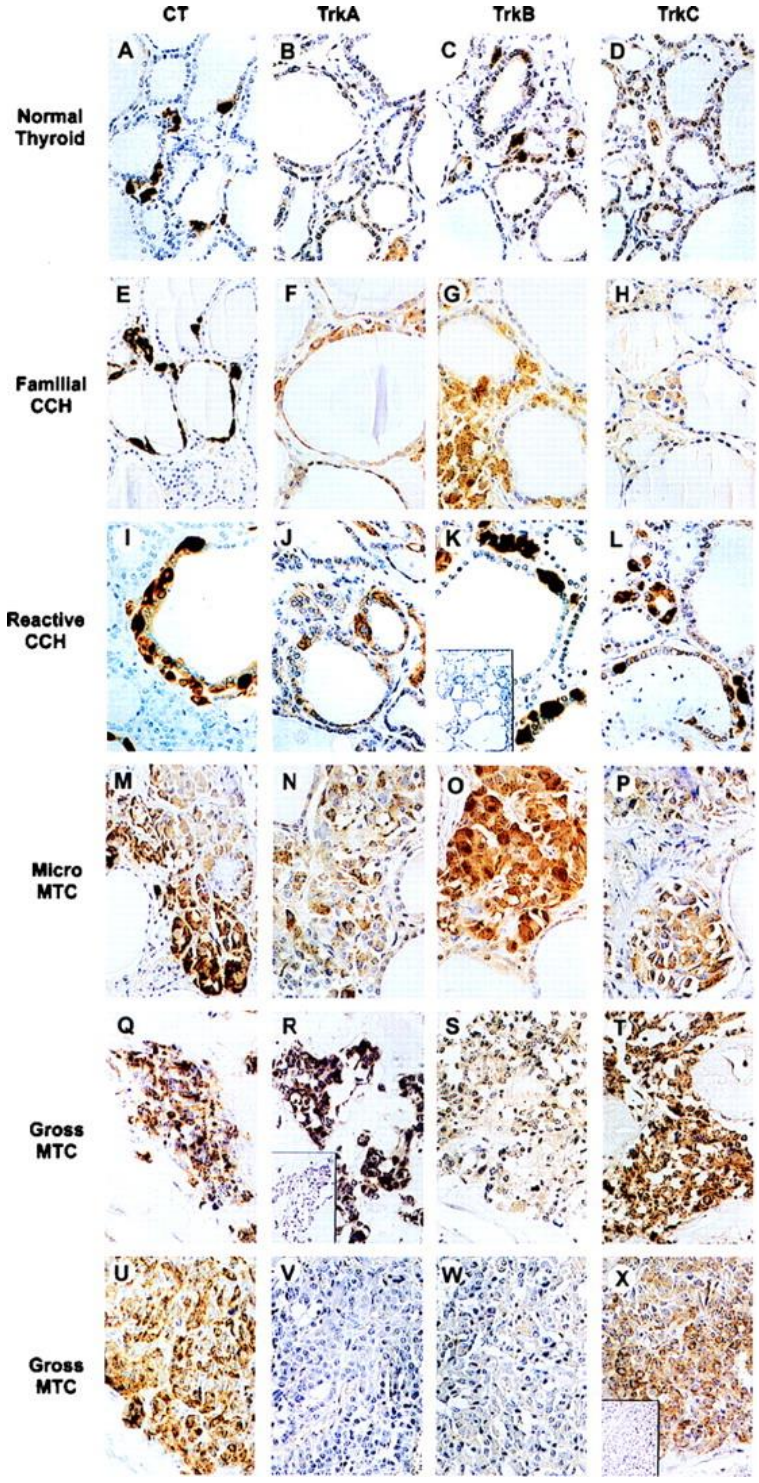

Figure 1.5.4: Immunohistochemistry staining of calcitonin (CT), and tyrosine kinase family of receptor (TrkA, TrkB, TrkC).

Figures A-D show normal thyroid with C cells stained for calcitonin. Figures E-H represents C cell hyperplasia (CCH) from MEN 2A patient. Figures I-L are samples from reactive C cell hyperplasia with PTC. Figures M-P show localised microscopic MTC. Figures Q-T and U-X show staining for two metastatic MTC patients. (Reprinted from McGregor, McCune *et al*., 1999 with permission from PNAS, Copyright (1999) National Academy of Sciences, U.S.A))

1.5.4 Treatment of MTC

Surgery still remains the only curative treatment for MTC patients (Cabanillas, McFadden et al. 2016, Ceolin, Duval et al. 2019). In MTC patients, depending on the serum calcitonin levels, a complete thyroidectomy with central lymph node dissection is suggested (Ceolin, Duval et al. 2019). For the treatment of MTC, several multikinase inhibitors have been tested; these include motesanib, sorafenib, sunitinib, axitinib, imatinib, pazopanib, anlotinib, lenvatinib, vandetanib and cabozantinib. These tyrosine kinase inhibitors can inhibit one or several tyrosine kinases. Out of these drugs, only Vandetanib and Cabozantinib are approved for the treatment of advanced MTC (Ceolin, Duval et al. 2019). Vandetanib was approved in 2011 for advanced MTC. It is a tyrosine kinase inhibitor for RET, VEGFR2 and -3, and EGFR (Cabanillas, Hu et al. 2014). Cabozantinib was approved in 2012 for advanced MTC. It is a tyrosine kinase inhibitor for VEGFR2, RET, and c-MET as shown in Figure 1.5.5 (Cabanillas, Hu et al. 2014). Over time, patients develop severe side effects as a consequence of tyrosine kinase inhibitors administration. Moreover, these drugs eventually have acquired drug resistance in patients due to the development of secondary mutations (Ceolin, Duval et al. 2019). Studies show that neither of the drugs are curative and prolonged use leads to diminished quality of life. Therefore, alternative therapies are required (Cabanillas, Hu et al. 2014). Recently, next-generation small-molecule inhibitors were developed specifically against RET variants. BLU-667 and LOXO-292 were currently under clinical trial. BLU-667 is a RET inhibitor, *in vivo* results against thyroid cancer xenografts with RET were promising as well as phase II clinical trial (Castellone and Melillo 2018). LOXO-292, an active RET inhibitor, was approved by the FDA this year in May against thyroid and non-small-cell lung cancers with RET mutations.

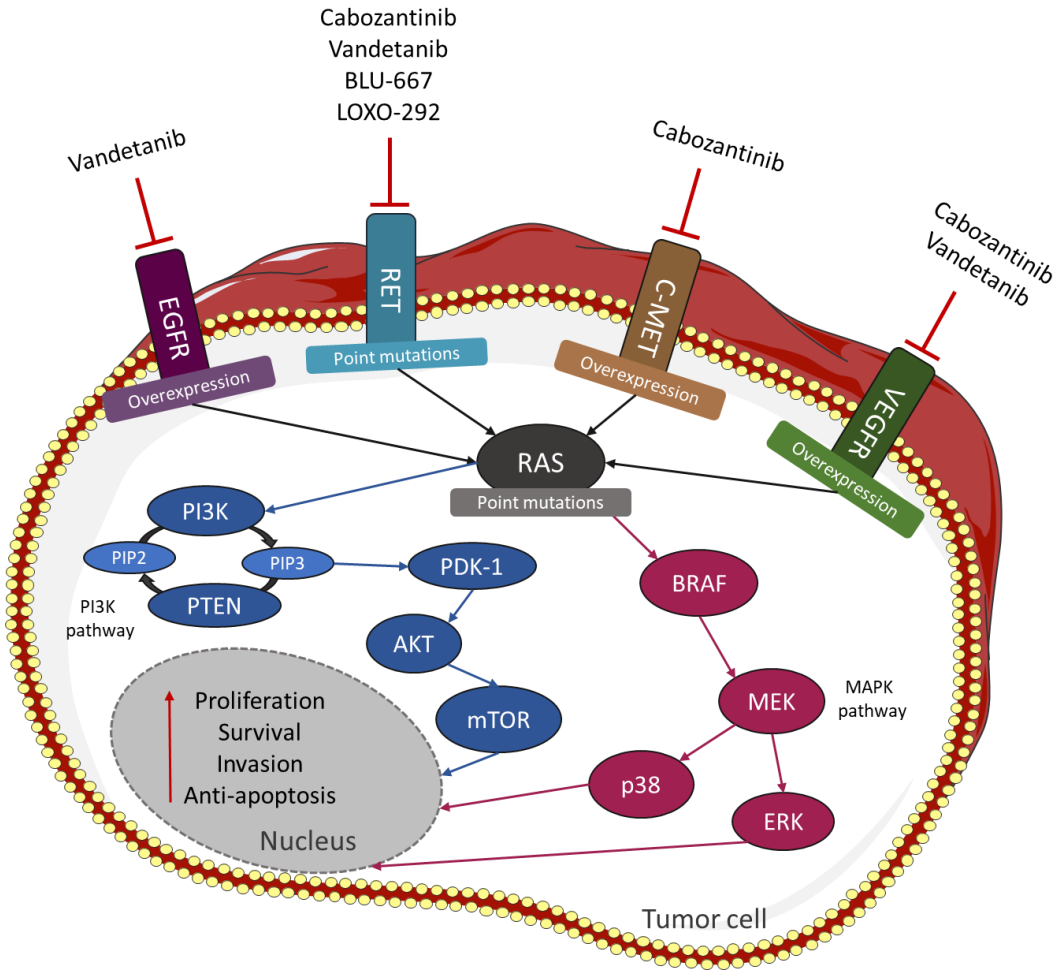

Figure 1.5.5: Schematic representation of activated pathways in MTC and molecular targeted tyrosine kinase inhibitors.
Point mutations in RET result in constant phosphorylation of tyrosine kinases and continuous activation of intracellular signalling pathways such as PI3K and MAPK pathway. Cabozantinib, Vandetanib, BLU-667 and LOXO-292 are tyrosine kinase inhibitors that act of different receptors and block the continuous activation of signalling pathways.
(AKT, v-akt murine thymoma viral oncogene homolog; BRAF, serine/threonine-protein kinase B-Raf; c-Kit, tyrosine-protein kinase Kit; c-MET, hepatocyte growth factor; EGFR, epidermal growth factor receptor; ERK, extracellular signal-regulated kinase; MEK,mitogen-activated protein kinase; mTOR, mammalian target of rapamycin; P38, mitogen-activated protein kinase; PDK-1, pyruvate dehydrogenase kinase isozyme 1; PI3K, phosphatidylinositol-3 kinase; PIP2, phosphatidylinositol (4,5) biphosphate; PIP3, phosphatidylinositol 3,4,5-triphosphate; PTEN, phosphatase and tensin homolog; RAS, rat sarcoma viral oncogene homolog; RET, rearranged during transfection; VEGFR, vascular endothelial growth factor receptor.)

MTC, which occurs in 5-10% of the total thyroid cancer cases, has a good prognosis when detected at an early stage. However, even with recent advances with tyrosine kinase inhibitors, the survival rate is low. Alternative biomarkers and therapies are therefore required for a better prognosis, especially for patients with metastatic disease.

Our group has a MENX rat model with a germline mutation in *Cdkn1b* and therefore develop multiple neuroendocrine tumours including MTCs (Fritz, Walch et al. 2002). The tumours from MENX rat resemble human tumours when the morphology and serum calcitonin are compared (Molatore, Kügler et al. 2018). A recent study from our group compared the medullary thyroid tumours from MENX rat model with tumours with aggressive RET-M918T mutations from MTC patients. They found 26 genes to be dysregulated and TRIB2 was one of the genes that was significantly upregulated (Molatore, Kügler et al. 2018) . MENX rat model and the associated tumours are further described in section 5.3.

1.6 Tribbles family of proteins

The role of protein kinases in regulating eukaryotic processes is well described. However, they are commonly dysregulated in cancer. The primary function of protein kinases is to activate the protein substrate by phosphorylation (Kung and Jura 2016). The class of pseudoenzymes comprises protein pseudokinases, pseudophosphatases and pseudoproteases. Protein pseudokinases are well-studied members of the family that, as the name suggests, lack canonical phosphotransferase activity (Kwon, Scott et al. 2019). However, pseudokinases can regulate signal transduction and protein degradation by ubiquitination (Durzynska, Xu et al. 2017). Tribbles pseudokinases (TRIBs) include three members: Tribbles 1 (TRIB1), Tribbles 2 (TRIB2) and Tribbles 3 (TRIB3). TRIBs were first identified in Drosophila and were later shown to be involved in cell division and migration (Mata, Curado et al. 2000, Lohan and Keeshan 2013). Interestingly, both the mammalian TRIBs and mouse TRIBs have highly conserved amino acid sequences between human and mouse (TRIB1, 97.5%; TRIB2, 99.2%; TRIB3, 81.2%) (Yokoyama and Nakamura 2011). Figure 1.6.1 illustrates TRIBs have an N-terminal domain, central kinase-like domain, and C-terminal protein-binding domain. It has previously been observed that although TRIBs possess a kinase domain, they lack kinase activity (Richmond and Keeshan 2019).

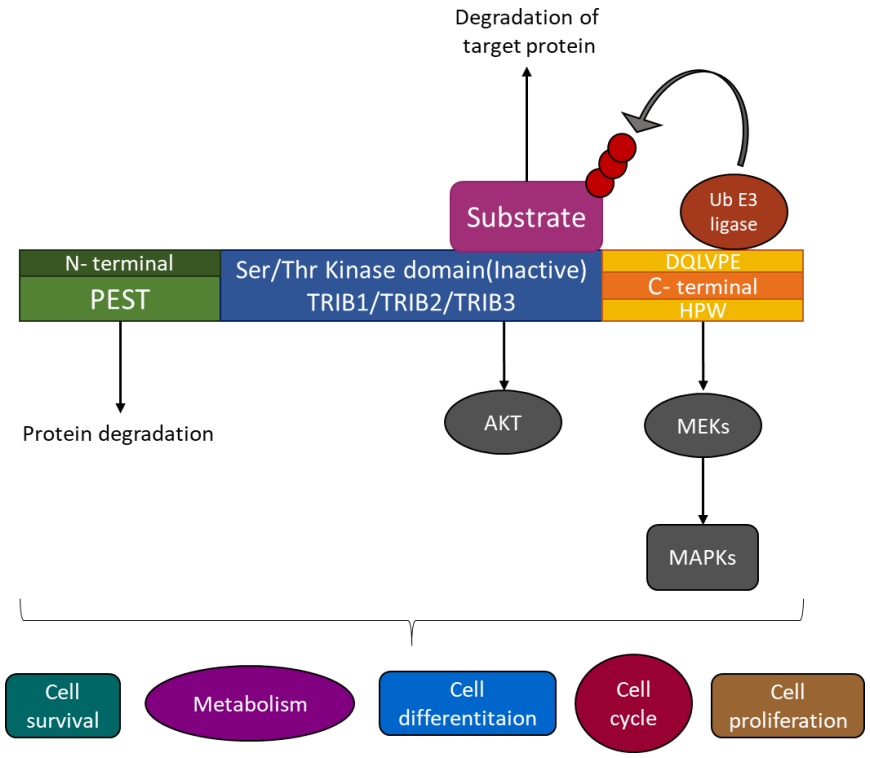

Figure 1.6.1: Structure of Tribbles and their role in signalling.
TRIBs have three distinct regions that have variable roles. The PEST domain regulates protein degradation. The kinase domain lacks kinase activity but is a scaffolding region for substrate proteins. The C-terminal region has a HPW motif that interacts with MAPKK/MEK family members that regulate the MAPK pathway. TRIBs are also involved in modulating AKT signalling. Together, these factors indicate that TRIBs-regulated signalling pathways support cellular differentiation, proliferation, survival, metabolism and cell cycle.

TRIBs are commonly associated with a variety of diseases, which include diabetes, cancer, lipid disorders, cardiovascular disease and neurological disorders (Kiss-Toth 2011). Several studies highlight their role in multiple cellular processes, including glucose and lipid metabolism, inflammation, cellular stress, survival, apoptosis, and tumorigenesis (Cunard 2013). Some of the diverse functions of TRIBs are described in Table 4.

TRIBs	Biological function	Model used	Reference
TRIB1	Involved in hepatic lipid metabolism	various models	(Bauer, Sasaki et al. 2015, Bauer, Yenilmez et al. 2015, Soubeyrand, Martinuk et al. 2016)
TRIB1	Regulation of liver metabolism through HNF4A	HepG2 and HEK293T cells	(Soubeyrand, Martinuk et al. 2017)
TRIB1	Regulation of cell cycle and survival mediated via the modulation of NFκB signalling	MDA-MB-231, SUM149PT, MDA-MB-436, MDA-MB-468 cell	(Gendelman, Xing et al. 2017)
TRIB1	Controls the production of immunoglobulins especially IgG1 in murine B cells	Knock-in mouse model with B-cell-specific overexpression of Trib1	(Mack, Stein et al. 2019)
TRIB2	Maintaining self-renewal and pluripotency in embryonic stem cells	Mouse embryonic stem cells	(Do, Park et al. 2017)
TRIB2	Regulation of thermogenic genes in subcutaneous adipose tissues in cold environments	Human subcutaneous adipose tissue (SAT) and visceral adipose tissue (VAT) samples	(Nakayama and Iwamoto 2017)
TRIB3	Negatively regulates adipogenesis by block the activity of a critical adipogenic transcription factor C/EBPβ	3T3-L1 adipocyte cells	(Bezy, Vernochet et al. 2007)
TRIB3	Promoted acetyl–coenzyme A carboxylase ubiquitination through COP1 and regulates lipid metabolism	3T3-L1 preadipocytes cell line, Transgenic mice expressing TRB3 in adipose tissue from diet-induced obesity	(Qi, Heredia et al. 2006)
TRIB3	Promotes glucose output from liver under fasting conditions through Akt phosphorylation	HEK 293, C57BL6 mice	(Du, Herzig et al. 2003)
TRIB3	Induces apoptosis and autophagy in amyloid-β-induced neuronal death	Cortical neurons from E18-day embryonic rat brains	(Saleem and Biswas 2017)

TRIB3	Regulates cell division via cycle 25 A protein	293, HeLa and A375 cells	(Sakai, Ohoka et al. 2010)
TRIB1 &TRIB3	Regulation of Haematopoiesis	various models	(Satoh, Kidoya et al. 2013, Johnston, Basatvat et al. 2015, Stein, Mack et al. 2015, Salomé, Hopcroft et al. 2018, Mack, Stein et al. 2019)

Table 4: Biological role of TRIBs

1.6.1 Structure of TRIBs

a) N-terminal segment

The N-terminal region of TRIBs usually includes 60-80 residues and has high proline (7-24%) and serine (6-23%) content. Due to the high abundance of these amino acids, this segment is referred to as the PEST region, which controls the half-life of the protein (Hegedus, Czibula et al. 2007). Each of the TRIBs proteins has unique sequences in this region (Eyers, Keeshan et al. 2017).

b) Kinase domain

The kinase domain is further sub-grouped in 12 distinct subdomains. The first four subdomains (I-IV) are located at the N-terminal region and this region acts as an ATP binding site. Subdomains (VA-XI) are responsible for the binding of a phosphate acceptor peptide substrate. Lastly, subdomain V serves as a catalytic region (Hegedus, Czibula et al. 2007). The ATP-binding property of TRIBs is controversial and debated. Structural studies on TRIB1 confirm that it lacks the ATP binding ability while TRIB2 might have low affinity for ATP binding (Bailey, Byrne et al. 2015, Murphy, Nakatani et al. 2015). The kinase domain also promotes proteasomal degradation with E3 ubiquitin ligase by anchoring the protein next to the E3 ligase. Several studies have described COP1 degradation by C/EBPα through TRIBs (Keeshan, He et al. 2006, Uljon, Xu et al. 2016).

c) C-terminal segment

The C-terminal region is usually 35-45 residues long and enriched with charged amino acids (Hegedus, Czibula et al. 2007). Furthermore, this region has two unique sequences: the HPW[F/L] and DQXVP[D/E]. The HPW[F/L] region acts as a binding site for MEK1 and other

MAPKK. Therefore, TRIBs are involved in regulating the MAPK signalling pathway by increased ERK phosphorylation (Yokoyama, Kanno et al. 2010). The DQXVP[D/E] sequence is responsible for COP1 binding in all the TRIBs members and for directing target proteins to proteasomal degradation (Dobens and Bouyain 2012).

1.6.2 Tribbles family members

1.6.2.1 Tribbles 1 (TRIB1, C8FW, SKIP-1)

TRIB1 was first identified by Wilkin *et al.* in 1997 (Wilkin, Suarez-Huerta et al. 1997). The endogenous location of TRIBs family is still unknown. However, the overexpression of a TRIB1-GFP fusion protein in HeLa cells suggests that TRIB1 is a nuclear protein (Hegedus, Czibula et al. 2007). TRIB1 is expressed in liver, kidney, heart, brain, skin, small intestine, bone marrow, peripheral blood leukocytes, mainly monocytes, macrophages and B cells, thyroid gland, WAT, and pancreas (Cunard 2013).

TRIB1 and cancer:

Amplification of chromosome 8q24 commonly occurs in acute myeloid leukaemia (AML), colorectal cancer, PCa, gastric cancer, malignant mesothelioma, oesophageal carcinoma and ovarian cancer (Wang, Wu et al. 2017). During the development of AML, a region of chromosome 8q24 is amplified, including the MYC gene. TRIB1 is also located on chromosome 8q24, which is just 1.5 Mb from c-MYC. Previous studies have shown that usually TRIB1 is amplified instead of the MYC gene. This suggests that TRIB1 but not c-MYC has a role in AML development (Dugas, Kiss-Toth et al. 2012). TRIB1 is also amplified in follicular and ovarian cancer and hepatocellular cancer (Dugas, Kiss-Toth et al. 2012, Ye, Wang et al. 2017). In colorectal cancer, TRIB1 promotes cell migration and invasion by increasing the activity of matrix metalloprotease- 2 through activation of FAK/Src and ERK pathway (Wang, Wu et al. 2017). However, in oesophageal cancer, the TRIB1 protein was not shown to be upregulated and also the gene was not amplified (Dugas, Kiss-Toth et al. 2012). Therefore, it can be speculated that TRIB1 overexpression in malignancies is confined to specific cancer types.

In 2004, Kiss-Toth *et al.* demonstrated that TRIB1-3 interacts with MEK1, MKK4 or MKK7 in HeLa cells and that the overexpression of TRIB1 enhances the phosphorylation of ERK (Kiss-

Toth, Bagstaff et al. 2004). TRIB1 has shown to interact with MEK-1 through the HPW domain on the C-terminal (Figure 1.6.1). This interaction is necessary for activating the ERK pathway and in turn, promotes AML progression (Dugas, Kiss-Toth et al. 2012). Another study reported the involvement of TRIB1 in cell invasion by activation of ERK signalling in ovarian cancer (Puiffe, Le Page et al. 2007). Overall, these studies suggest that TRIB1 is majorly involved in activating various cancers through ERK signalling.

In 2015, Miyajima *et al.* showed a correlation between TRIB1 and p53 activity. p53 is a tumour suppressor which regulates several genes involved in cell cycle arrest and apoptosis to prevent tumour growth (Miyajima, Inoue et al. 2015). When TRIB1 was downregulated in breast cancer cell line MCF-7, this increased the transcriptional activity of p53, thus resulting in decreased cell survival. This preliminary study suggests that TRIB1 acts as a negative regulator of p53 in breast cancer cells by promoting cell proliferation in tumour cells (Miyajima, Inoue et al. 2015). A recent study has identified TRIB1 as a target of miR-23a in hepatocellular carcinoma (Ye, Wang et al. 2017). They reported that downregulation of p53 and TRIB1 promoted cell migration and invasion via epithelial-mesenchymal transition pathway. This lead to increased activity of c-myc and matrix metalloprotease-7.

TRIB1 and lipid metabolism:

Increased lipid concentration contributes to the development of coronary artery diseases (CAD) and atherosclerosis. Kathiresan *et al*. in 2008 carried out genome-wide associated studies to identify novel chromosomal loci that are associated with LDL cholesterol, HDL cholesterol, and triglycerides (Kathiresan, Melander et al. 2008). A SNP on chromosome 8q24 (SNP rs17321515) was significantly associated with triglycerides levels, total cholesterol, low-density lipoprotein cholesterol and high-density cholesterol (Iwamoto, Boonvisut et al. 2015). Previous studies have shown that Trib1 deficiency in mice leads to increases in plasma cholesterol and TG levels (Iwamoto, Boonvisut et al. 2015). A recent study has shown the beneficial effect of Trib1 in atherosclerosis, in a myeloid-specific knock out (KO) model of *Trib1,* OLR1 RNA and protein expression and oxLDL is elevated, thus reducing reduces early atheroma formation (Johnston, Angyal et al. 2019).

Bauer *et al.* reported that Trib1 deletion in hepatocytes upregulated genes that are involved in the fatty acid synthesis and lipogenesis (Bauer, Sasaki et al. 2015). Furthermore, there was an increase in C/EBPα protein levels that upregulated lipogenesis. C/EBPα is a transcription factor that regulated lipogenesis in adipose tissue and liver (Bauer, Sasaki et al. 2015). Deletion of C/EBPα in the liver of Trib1 deficient mice decreased the levels of the gene that regulates lipogenesis and was comparable to WT mice. Thus, they showed that Trib1 mediates the activity of C/EBPα *in vivo* and this might control hepatic lipogenesis in humans (Bauer, Sasaki et al. 2015). Moreover, overexpression of C/EBPα in WT mice increases the transcription of Trib1 (Bauer, Sasaki et al. 2015).

1.6.2.2 Tribbles 2 (TRIB2, c5fw, SKIP2)

TRIB2 was first identified by Wilkin *et al.* in 1996 in dog thyroid in response to mitogens. TRIB2 is located on chromosome 2p24.3 and shows distinct cytoplasmic localisation using fusion proteins (Hegedus, Czibula et al. 2006). TRIB2 is detected in thymus, heart, brain, kidney, lung, skin, spleen, T and B lymphocytes, and WAT (Cunard 2013).

TRIB2 and cancer:

The oncogenic role of TRIB2 is suggested in liver cancer, where TRIB2 overexpression negatively regulates WNT signalling thus affecting cell proliferation (Wang, Park et al. 2013, Eyers, Keeshan et al. 2017). Furthermore, downregulation of TRIB2 in HepG2 cells resulted in decreased cell survival and proliferation (Wang, Park et al. 2013). Additionally, TRIB2 acts as an oncogene in lung cancer by controlling the activity of C/EBPα by transcriptional inactivation and protein degradation (Grandinetti, Stevens et al. 2011). A recent study by Hill *et al.* showed that TRIB2 promotes the activity for AKT signalling in cancer cells (Hill, Madureira et al. 2017). Additionally, they used patient tumour samples from melanoma, pancreatic and colon cancer before undergoing treatment and found that the TRIB2 levels were higher at RNA and protein levels when compared to healthy tissue. Furthermore, the protein levels of pSer473-AKT1 and pSer253-FOXO3a were significantly higher as TRIB2 (Hill, Madureira et al. 2017). Increase in the TRIB2 expression level correlated with poor prognosis in melanoma and colon cancer patients. Their study suggests that TRIB2 inhibitors can be used as potential therapeutic

targets for targeting the PI3K/AKT pathway (Hill, Madureira et al. 2017). Salome *et al.* showed TRIB2 acts as a tumour suppressor in myeloid leukaemia by interacting with p38 and inducing stress signalling, including cell cycle progression and mitosis (Salome, Magee et al. 2018).

TRIB2 and lipid metabolism:

In 2007, Hegedus *et al.* reported an interaction between TRIB2 and AKT. TRIB2 has been shown to regulate adipocyte differentiation by inhibiting the AKT and C/EBPβ activity (Cunard 2013).

1.6.2.3 Tribbles 3 (TRIB3, NIPK, SINK)

TRIB3 was first identified by Mayumi *et al.* in 1999 (McGregor, McCune et al. 1999). TRIB3 is located on chromosome 20p13-p12.2, and it is a nuclear protein (Hegedus, Czibula et al. 2006). TRIB3 is the most studied isoform amongst the TRIBs family (Cunard 2013). TRIB3 has been shown to be expressed in liver, spleen, thymus, prostate, heart, kidney, lung, skin, small intestine, WAT, neurons, skeletal muscle, and stomach (Cunard 2013).

TRIB3 and cancer:

TRIB3 is implicated in various cancers including breast, colon, lung and prostate (Yokoyama and Nakamura 2011). TRIB3 has been found to interact with SMAD3, a transcription factor that regulates TGF- β signalling, and thus increasing the cell invasion and migration of tumour cells (Hua, Mu et al. 2011). Dong *et al.* reported the oncogenic role of TRIB3 in gastric cancer by staining 191 patient tissues from stages I to IV. TRIB3 levels were highly expressed in all the TNM stage (T stage, N stage, and tumours with distant metastasis) as compared to adjacent healthy tissue. Furthermore, elevated TRIB3 levels showed a poor prognosis in gastric cancer patients (Dong, Xia et al. 2016). In breast cancer, high TRIB3 levels were correlated with poor prognosis (Wennemers, Bussink et al. 2011, Yu, Sun et al. 2019). Contrarily, it was reported that the TRIB3 protein levels were associated with better prognosis since TRIB3 was shown to be involved in hypoxia tolerance. Breast tumours that had elevated levels of TRIB3 were more sensitive to hypoxia as compared to the TRIB3 hypoxia-tolerant tumours (Wennemers, Bussink et al. 2011). In summary, there is a lot of discrepancies and no

consensus view between tumour suppressive or oncogenic role of TRIB3 in breast cancer prognosis. For patients with non-small cell lung cancer, the levels of TRIB3 were increased in the tissues. TRIB3 knockdown in A549 lung cancer cell line showed a significant reduction in cell invasion, migration, and proliferation. They also identified a positive correlation between TRIB3 and Notch1 in A539 cells. Since Notch signalling regulates cancer progression and metastasis, this suggests a role for TRIB3 in lung cancer progression (Zhou, Luo et al. 2013). Very little is currently known about the role of TRIB3 in PCa. When the PCa cell line C4-2B was subjected to a drug combination treatment, TRIB3 expression significantly increased, thus, elevating caspase-3 activity and apoptosis in cells (Mathur, Abd Elmageed et al. 2014).

TRIB3 and lipid metabolism:

It has been previously reported that during fasting condition, TRIB3 expression is upregulated and associated with insulin resistance by inhibition of AKT phosphorylation in the liver (Du, Herzig et al. 2003, Koo, Satoh et al. 2004). Further studies have reported that TRIB3 mutations contribute to insulin resistance in humans and can predict clinical outcomes (Prudente, Hribal et al. 2005). Qi *et al.* reported the beneficial role of *Trib3*, which promotes lipid metabolism during fasting condition (Qi, Heredia et al. 2006). Fasted *Trib3* transgenic mice have higher food consumption without gaining weight compared to WT mice suggesting that *Trib3* mice had increased fat metabolism. Histological staining's also revealed the decreased adipocyte size in adipose tissue compared to WT mice (Qi, Heredia et al. 2006). Their group further conducted mass spectroscopy experiments to identify the interacting proteins in 3T3-L1 cells upon *Trib3* overexpression. The proteins that were significantly upregulated were related to ubiquitination. These included COP1, de-etiolated-1 (DET1), DNA damage binding protein 1 (DDB1), components of cullin 4A ubiquitin ligase family. Immunoblotting confirmed that Trib3 promotes degradation acetyl–coenzyme carboxylase (ACC), a rate-limiting enzyme in fatty acid synthesis, by ubiquitination with COP1. This effect was mediated by the interaction between Trib3 and COP1 since COP1 alone in the cells is not involved in ubiquitination of ACC (Qi, Heredia et al. 2006). Overall, this study suggests that *Trib3* might have a beneficial role by protecting against diet-induced obesity by promoting lipid metabolism through COP1 mediated degradation of ACC. Several lines of evidence suggest that *TRIB3* plays an essential role in lipid metabolism, which is further discussed in section 3.3 (Angyal and Kiss-Toth 2012).

1.6.3 Factors modulating TRIBs expression

TRIBs expression in the body is variable and often cell-type and tissue-specific (Sung, Francis et al. 2006, Dobens and Bouyain 2012) and various factors can affect their expression in cell and tissues. miRNAs are negative regulators of gene activity. TRIB1 expression was downregulated by miR-23a and miR-224-5p in hepatocellular and PCa (Lin, Huang et al. 2014, Ye, Wang et al. 2017). A recent publication from TRAIN consortium releveled that miR-101-3p and miR-132-3p regulate TRIB1 expression in macrophages and promote the secretion of IL-8, pro-inflammatory chemokine (Niespolo, Johnston et al. 2020). Moreover, it has been reported that expression of TRIBs in cumulus cells is altered upon treatment with fatty acid oxidation inhibitor etomoxir (Brisard, Chesnel et al. 2014). Cumulus cells surround the oocyte and are involved in oocyte maturation and fertilization (Brisard, Chesnel et al. 2014). Brisard *et al.* showed all the three TRIBs are differentially expressed during oocyte maturation and the expression is altered by various factors. Fatty acid oxidation is necessary for oocyte maturation due to extensive energy requirement maturation (Paczkowski, Schoolcraft et al. 2014). Cumulus cells around *in vivo* mature oocytes showed higher TRIB1 expression compared to immature oocytes (Brisard, Chesnel et al. 2014). Therefore suggesting the involvement of lipids in modulating TRIB1 expression. Another study shows altered TRIB2 expression in monocytes upon contact with acetylated LDL, a modified form of LDL. Increased TRIB2 expression promotes IL-8 production in LPS-stimulated monocyte cells (Eder, Guan et al. 2008).

A considerable amount of research has been carried out on understanding molecular mechanisms regulating TRIBs in various diseases (Eyers, Keeshan et al. 2017, Richmond and Keeshan 2019). TRIBs have been associated with the development and progression of various cancers and can be involved in drug resistance (Hill, Madureira et al. 2017, O'Connor, Yalla et al. 2018). Therefore, the factors affecting TRIBs expression can play an important role in early detection of some cancers and improve treatment options.

1.6.4 Tribbles Research and Innovation Network (TRAIN)

My PhD project is a part of Tribbles Research and Innovation Network (TRAIN) (http://train-itn.eu/), a project funded by the European Union's Horizon 2020 research and innovation programme that started in 2017, under the Marie Sklodowska Curie ITN Project Grant No 721532. TRAIN consortium consists of fifteen interdisciplinary PhD projects in ten different institutions or universities across Europe. All the projects within the TRAIN consortium are interconnected with an aim to understand the mechanisms that govern Tribbles-mediated control of immune-metabolism and their role in PCa aggressiveness. All the PhD projects were divided into six different work packages that are specialized in each field that includes cancer, metabolism, immunity, and system biology. My PhD project contributes to work package three (Adipocyte Cell Biology) and four (Obesity Regulated Disease – Prostate Cancer). I have worked on two main projects during the PhD; the first project focuses on *Trib1* and *Trib3* modulation in adipose tissue and its impact on PCa progression, while the latter was to investigate the cross-talk between the adipocytes and Tribbles-mediated control of PCa. Therefore, the focus of this PhD was to understand the role of Tribbles in both adipose and tumour cell population that mediate PCa progression. However, additionally, based on some previous work in our group, this thesis would also give some insights into the role of TRIB2 in thyroid cancer.

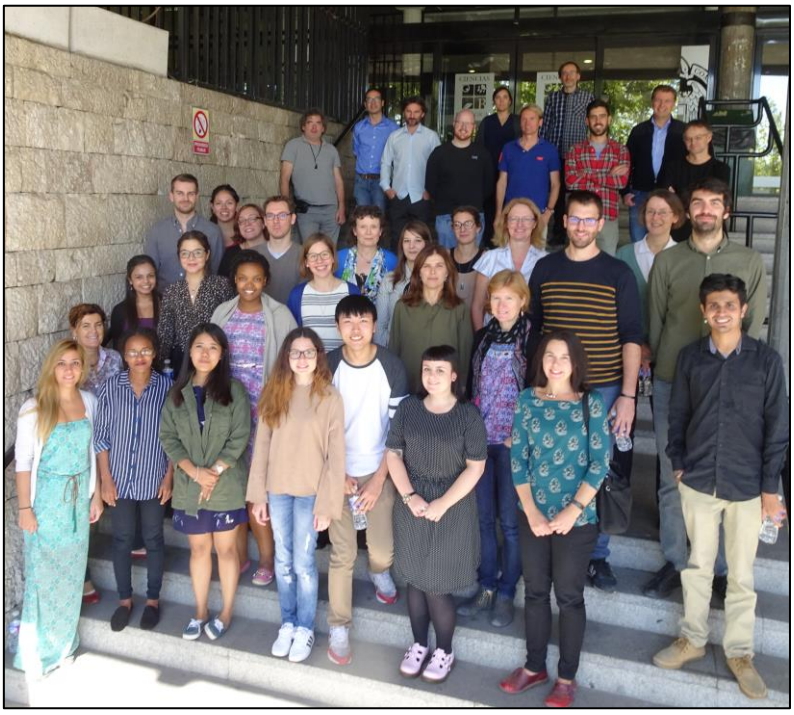

1.7 Summary

The above literature review clearly indicates the critical role of adipose tissue microenvironment on prostate cancer (PCa) aggressiveness. It has been previously described that adipocytes modulate gene expression in breast cancer cells in a co-culture system. The altered gene expression upon exposure to adipocytes could also be the case in PCa cells since both breast and PCa have similar adipose tissue microenvironment.

The cross-talk between adipocytes and PCa cells leads to poor prognosis in PCa cancer patients. Previous studies have reported the role of *Trib1* and *Trib3* in adipose tissue dysfunction. It has been reported that during obesity, adipose tissue becomes dysfunctional and have altered cytokine secretion that promotes pro-inflammatory signalling in cancer cells. However, there have not been many studies trying to understand the underlying mechanism of the cross-talk between adipocytes and PCa cells.

Medullary thyroid cancer (MTC) is considered to be more aggressive than the cancers arising from the follicular cells in the thyroid gland due to its early metastasis and late-stage diagnosis. The previous study in our group compared tumours from MENX rat model that develops medullary thyroid tumours that are similar to human MTC patients. *Trib2* was one of the genes that were found to be differentially expressed in transcriptomic profiling.

1.8 Hypothesis

Based on current knowledge, I hypothesise that

- *TRIBs* play a critical role in the cross-talk between adipocytes and PCa cells, thus contributing to an adverse tumour microenvironment. Adipokines secreted by adipocytes influence *TRIBs* expression in PCa cells, thereby contributing to PCa aggressiveness
- On the other hand, *Trib1* and *Trib3* in adipocytes promote PCa tumorigenesis by altered secretome
- Based on previous work from our group, *TRIB2* might be involved in MTC progression

1.9 Aims

To address these hypothesises, this thesis aims to:

1. Determine whether the cross-talk between the adipocytes and cancer cells can modulate TRIBs levels in PCa cells
2. Identify the secretory factors from adipocytes that influence TRIBs modulations in PCa cells
3. Investigate the role of TRIBs in PCa aggressiveness under the influence of adipose tissue microenvironment
4. Investigate the effect of *Trib1* and *Trib3* modulation in adipose tissue of mice and their impact on PCa cell behaviour
5. Lastly, to determine whether TRIB2 acts as an oncogene in MTC

Chapter 2 : General materials and methods

In this chapter, the general techniques used for all studies are described. Methods used for specific experiments are mentioned at the beginning of each chapter.

2.1 Animals Experiments

2.1.1 Licensing

All animal experiments were performed in accordance with guidelines approved by the Government of Upper Bavaria, Germany. Licence number ROB-55.2-2532.Vet_02-17-125 was used when Trib1 STOP Adipoq-CreER^{T2} mice were injected with Tamoxifen. In order to perform animal experiments in German Mouse Facility in Munich, I had undertaken internal training courses offered by the Helmholtz Zentrum München and additionally, I have a FELASA B certificate to work with mice.

2.1.2 Husbandry

Mice were kept in the animal facility at a controlled environment with 12 hours light and dark cycle at 22°C. Littermates were housed together (maximum of four mice per cage) and identified by ear punches. All the mice were fed with a standard chow diet unless otherwise stated.

2.1.3 Development of *Trib1* transgenic mice

Inducible adipose-specific *Trib1* KO mouse strain was generated by crossing *Trib1*$^{fl/fl}$ mice with Tamoxifen inducible Adipoq-CreER^{T2} similar to previous studies (Seo, Riopel et al. 2019). This line encountered several problems while breeding and thus the line could not be sustained. The adipose-specific Trib1 overexpression mouse strain was generated by crossing Rosa26-STOP$^{fl/fl}$-*Trib1* and Tamoxifen inducible Adipoq-CreER^{T2} similar to previous studies (Sassmann, Offermanns et al. 2010) as shown in Figure 2.1.1. Tamoxifen injections were carried out on 10-week old mice by injecting 100 mg/kg tamoxifen per day for five days per week.

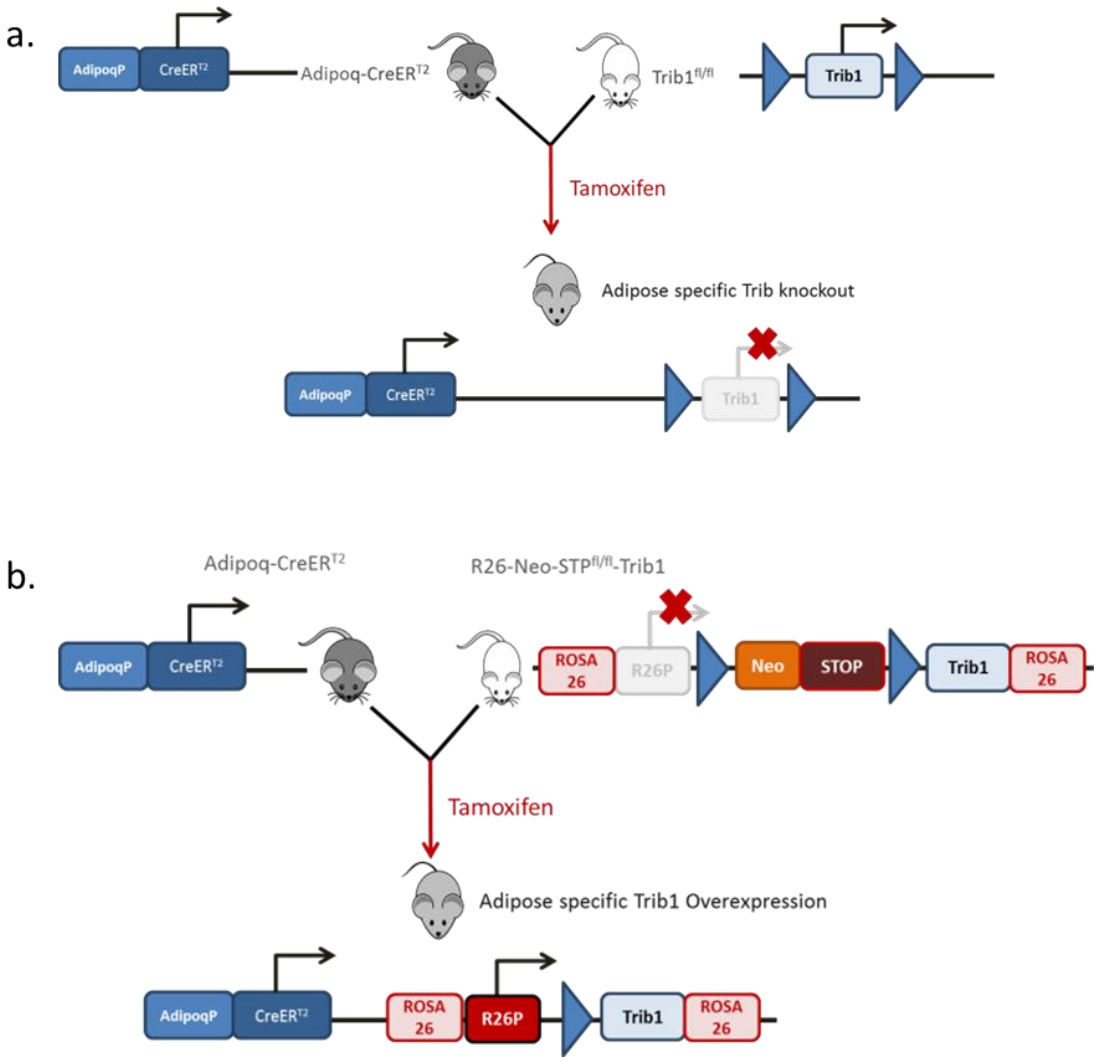

Figure 2.1.1: Schematic representation of the generation of *Trib1* adipose-specific KO mice and *Trib1* adipose-specific OE mice

(a) *Trib1* adipose-specific KO mice were generated using the Cre-Lox system, the *Trib1* transgene between the loxP sites was excised after using Tamoxifen. (b) *Trib1* adipose-specific OE mice were generated using Cre-Lox system, after Tamoxifen injections, Cre is expressed, thereby removing the STOP codon and promoting *Trib1* expression.

Genotyping of *Trib1* mice

Genomic DNA isolated from mouse ear clips and was amplified by end-point PCR by using mTrib1 WT, OE/KO and Cre primers as shown in Table 5.

Gene	Forward primer	Reverse primer	Band size (bp)
Cre	GGAAATGGTTTCCCGCAGAAC	ACGGAAATCCATCGCTCGACC	~450
mTrib1 WT	GTGATCTGCAACTCCAGTCTTTCTAG	CGCGACACTGTAATTTCATACTGTAG	~350
mTrib1 OE	GTGATCTGCAACTCCAGTCTTTCTAG	CCTTCTTGACGAGTTCTTCTGAGG	~260
mTrib1 WT	AAGTTCACATTTGAACTGATGGC	AGCTGGTTTCAGGGGAAGAC	~356
mTrib1 KO	AAGTTCACATTTGAACTGATGGC	ACCTTGATCTGCAGTCCTAGG	~450

Table 5: Mouse Trib1 primer sequences used for genotyping

GoTAq Colourless Master Mix (Promega, Mannheim, Germany) was used, with a final concentration of 25µl for each reaction. 12 µl of Master Mix, 0.1 µM of forward and reverse primers (Sigma-Aldrich, Steinheim Germany; Table 6), and 2 µl of DNA template was used. The reaction mixture was placed into an Eppendorf® Mastercycler X50i (Eppendorf, Hamburg, Germany) with the following functions:

PCR step	Temperature	Time	Cycle number
Initial denaturation	95°C	3 minutes	1
Denaturation	95°C	30 seconds	35
Annealing	58°C	1 minute	
Extension	72°C	1 minute	
Final Extension	72°C	5 minutes	1
Hold	4°C	∞	

Table 6: Endpoint PCR settings for *Trib3* KO mice genotyping

Samples obtained from end-point PCR were loaded on the QIAxcel Advanced System using the QIAxcel High Resolution Kit (Qiagen, Hilden, Germany) with 100 bp ladder. Figure 2.1.2 shows an example of the genotyping result generated by QIAxcel imaging, this data was kindly provided by Adam Lindford (ESR 5).

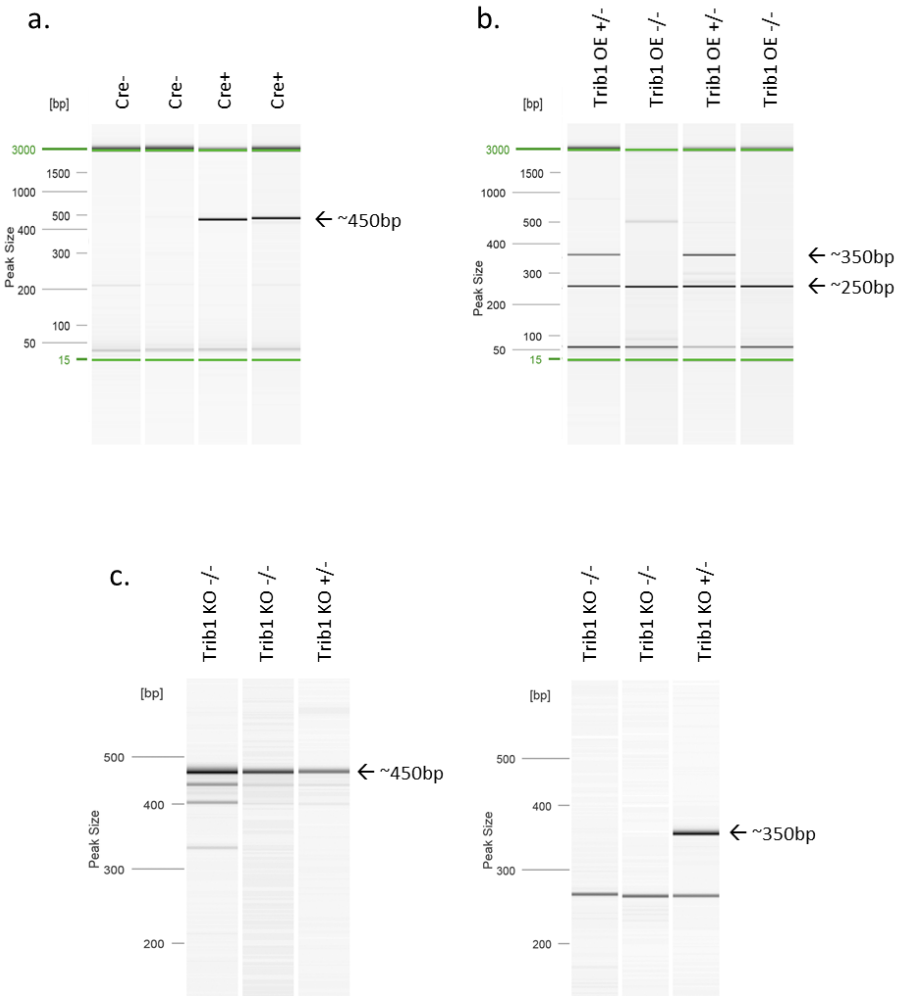

Figure 2.1.2: Genotyping results from *Trib1* OE mice
(a) The band observed at 450bp represents Cre+ mice. (b) The 350bp band represents the WT allele, and the 250bp band represents the mutant allele. Heterozygosity is indicated by the presence of bands both at 350 and 250bp. (c) The 450bp band represents the mutant allele, while the band at 350bp represents the WT allele. Heterozygosity is indicated by the presence of both bands at 450 and 350bp.

2.1.4 *Trib3* whole-body KO mice

Previously published full-body *Trib3* knock out (KO) 129S5_BL/6J mice (Trib3$^{-/-}$) mice were used in this study (Salazar, Lorente et al. 2015). Briefly, *Trib3* heterozygous mice were obtained from European Mouse Mutant Archive, Munich, Germany and were backcrossed for ten generations with C57/BL6. Later these mice were inter-crossed to obtain homozygous knock out (KO) embryos. For generating transgenic KO mice, gene trap vector was used on an ES cell line from gene trap library. The gene trap vector inactivated *Trib3* allele, thereby preventing the expression of the Trib3 protein. Salazar *et al.* confirmed Trib3 deletion by immunoblotting (Salazar, Lorente et al. 2015). Table 7 shows the list of mice used in this thesis.

No.	Line	Strain	Sectioning no.	MausDB no.	Genotype	Age	Weight (gm)
1	Trib3 KO	129S5_BL/6J	18/187	80013007	Mut/mut	11 weeks	24.75
2	Trib3 KO	129S5_BL/6J	18/188	80013008	Mut/mut	11 weeks	26.48
3	Trib3 KO	129S5_BL/6J	18/248	80015309	Mut/mut	11 weeks	25.78
4	Trib3 KO	129S5_BL/6J	18/249	80015314	Mut/mut	11 weeks	25.35
5	Trib3 KO	129S5_BL/6J	19/5	80015901	Mut/mut	11 weeks	30.75
6	Trib3 KO	129S5_BL/6J	19/6	80012995	Mut/mut	11 weeks	23.3
7	Trib3 KO	129S5_BL/6J	18/91	80011044	Wt/wt	11 weeks	25.2
8	Trib3 KO	129S5_BL/6J	18/92	80011045	Wt/wt	11 weeks	24.28
9	Trib3 KO	129S5_BL/6J	18/189	80012981	Wt/wt	11 weeks	27.3

10	Trib3 KO	129S5_BL/6J	18/190	80012987	Wt/wt	11 weeks	24.97
11	Trib3 KO	129S5_BL/6J	18/191	80012988	Wt/wt	11 weeks	22.21
12	Trib3 KO	129S5_BL/6J	18/192	80013022	Wt/wt	11 weeks	24.26

Table 7: List of Trib3 KO mice used in this study

Genotyping of *Trib3* KO mice

Genomic DNA isolated from mouse ear clips and was amplified by end-point PCR by using the following mTrib3 WT and KO primers:

Genotype	Primer	Sequence	Band size (bp)
WT	Forward	CCGCGACGAATGAAAGGTTTA	483 bp
	Reverse	AGACTCCGAGAGCTGCTCAGTTAGG	
KO	Forward	CCGCGACGAATGAAAGGTTTA	381 bp
	Reverse	AAATGGCGTTACTTAAGCTAGCTTGC	

Table 8: Mouse Trib3 primer sequences used for genotyping

GoTAq Colourless Master Mix (Promega) was used, with a final concentration of 25µl for each reaction. 12 µl of Master Mix, 0.1µM of forward and reverse primers (Sigma-Aldrich; Table 9), and 2 µl of DNA template was used. The reaction mixture was placed into an Eppendorf® Mastercycler X50i (Eppendorf) with the following functions:

PCR step	Temperature	Time	Cycle number
Initial denaturation	95°C	5 minutes	1
Denaturation	95°C	30 seconds	40
Annealing	65°C	30 seconds	
Extension	72°C	30 seconds	
Final Extension	72°C	5 minutes	1
Hold	4°C	∞	

Table 9: Endpoint PCR settings for *Trib3* KO mice genotyping

Samples and Quick-Load® 100 bp DNA Ladder (New England Biolabs, Frankfurt, Germany) were run on a 2% agarose gel. The results were qualitatively analysed by visualisation under UV-light through a gel documentation system as shown in Figure 2.1.3.

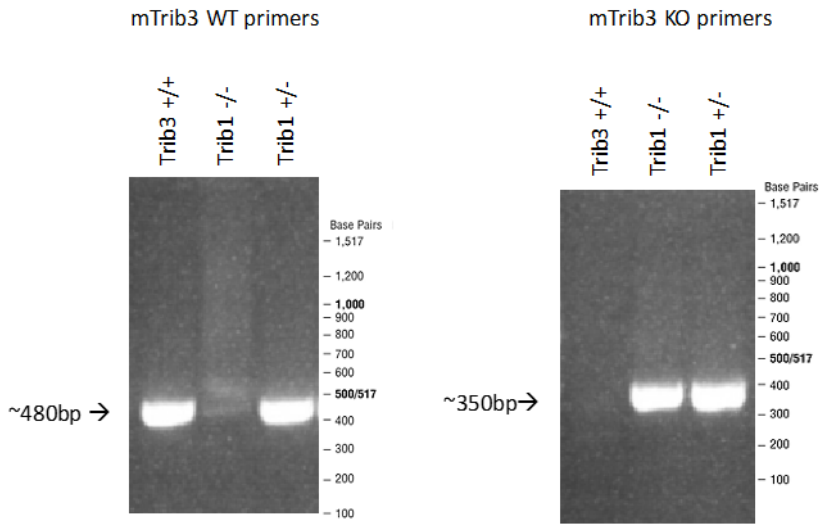

Figure 2.1.3: Genotyping results from *Trib3* KO mice
The band at 480 bp represents the WT allele and the band at 350 bp represents the mutant allele. Heterozygosity is indicated by the presence of both bands at 480 and 350bp.

2.1.5 Organ withdrawal

Mice were euthanized using CO_2 inhalation for 5 minutes according to animal welfare regulation. Death is confirmed by testing the reflexes. Mice were weighed immediately and blood for plasma was taken directly from the *vena cava*. Blood was centrifuged at 2000xg for 5 minutes at 4°C and resulting plasma was immediately stored at -20°C.

2.1.6 Tissue processing

The desired tissues were either collected in phosphate buffer saline (PBS) (Thermo Fisher Scientific, Wilmington, DE) with antibiotics, snap-frozen in liquid nitrogen and stored at -80°C. The remaining organs from the mice used for experiments were always collected in formalin for any future analysis.

2.1.7 Primary culture with adipose tissue from the mice

2.1.7.1 Mature adipocytes and SVF derived from adipose tissue of mice

scWAT and visWAT were used for primary culture in order to isolate mature adipocytes and SVF fraction. To mimic the conditions that appear in the natural tumour microenvironment, the mature adipocytes were taken directly from the adipose tissue and then cultured *in vitro*. Adipose tissues (scWAT and visWAT) were extracted from adult male 129S5_BL/6J mice (10-11 weeks old). The WAT was initially kept in PBS with antibiotics on ice and processed within 30 minutes after isolation. Initially, the fat piece was measured to get 500 mg of fat per collection (by pooling WAT from two mice). The adipose tissue was chopped in fine pieces using scalpels until a homogenous mixture was achieved. The mixture was transferred to a 50 ml falcon containing a collagenase solution (0.2% collagenase type I, Merck, Darmstadt, Germany) with 1% BSA and antibiotics. The solution was incubated at 37°C for 45 minutes and filtered using 50 µm filter. The remaining lysate was centrifuged at 1000 rpm at 5 minutes. Mature adipocytes were found in the upper floating layer and the SVF fraction was in the form of a pellet. The mature adipocytes were washed 3 times with culture media to eliminate collagenase and lastly transferred into a 75 cm^2 flask with 20 ml of culture media as shown in Figure 2.1.4. The SVF cells were plated in the 6-well plates.

2.1.7.2 Conditioned medium from mouse WAT

The conditioned media from both the mature adipocytes and SVF was harvested after 24 hours and filtered using 0.45 µM filters (Merk). The conditioned media was then distributed in 2 ml tubes, snap-frozen by liquid nitrogen and immediately stored at -80°C. The frozen aliquots were only used once.

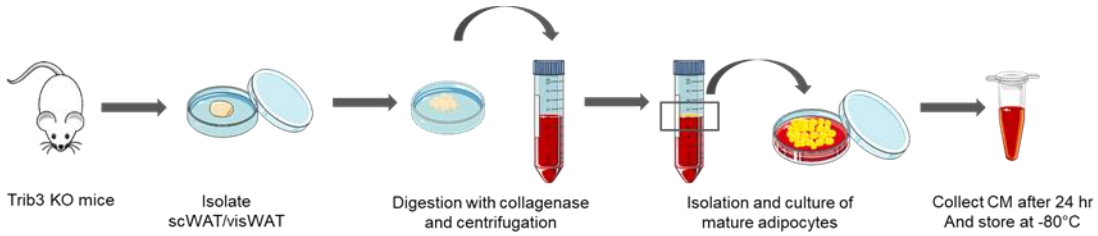

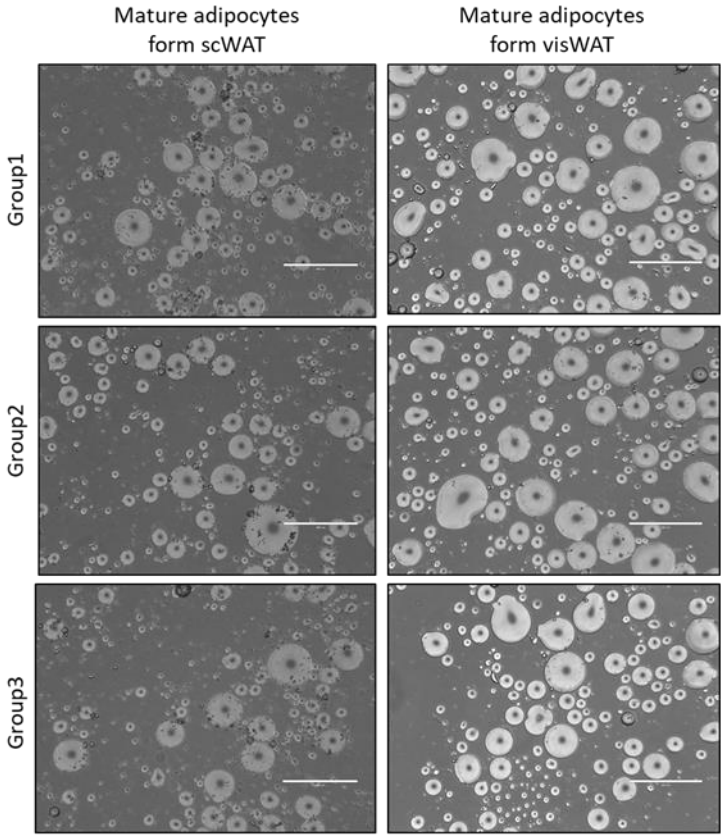

Figure 2.1.4: Isolation of CM from mature adipocytes from *Trib3* KO adipose tissue
(a) Schematic representation of mature adipocyte preparation from adipose tissue (mice). Isolated adipocytes were incubated for 24 hours in culture medium before transferring to 2ml tubes for storage in -80°C. (b) Mature adipocytes *in vitro* derived from scWAT and visWAT adipose tissue from *Trib3* KO mice.

2.2 Human samples

2.2.1 Human Ethics

Human PPAT was obtained from two patients that were undergoing radical prostatectomy as part of preliminary experiment (Therefore patient details are not mentioned). All the patients gave informed consent for this study and all the procedure is approved by ethics committee at the Technische Universität München (Ethics No. 70/19 S-SR).

2.2.2 Primary culture from human PPAT

2.2.2.1 Mature adipocytes and SVF derived from PPAT of human PCa patients

The tissue was transported from the hospital to the lab in PBS with antibiotics and was processed within 45 minutes after the surgery, to limit necrosis of the tissue. The adipose tissue was sliced into 1mm^2 pieces using scalpels; this homogenous mixture was then transferred to a collagenase solution with 1% BSA and antibiotics. This was incubated at 37°C for 45 minutes, and then filtered using a 50 µm filter (Merk) and centrifuged at 1000 rpm for 5 minutes. Mature adipocytes were found in the floating layer and the SVF fraction was in the form of a pellet. The mature adipocytes were washed 3 times with culture medium to eliminate collagenase and lastly transferred into a 75 cm^2 flask with 20 ml of the medium as shown in Figure 2.2.1. The SVF cells were plated in the 6-well plates.

2.2.2.2 Conditioned medium from mouse WAT

The conditioned media from both the mature adipocytes and SVF was harvested after 24 hours and filtered using 0.45 µM filters (Merk). The conditioned media was then distributed in 2 ml tubes, snap-frozen by liquid nitrogen and immediately stored at -80°C. The frozen aliquots were only used once.

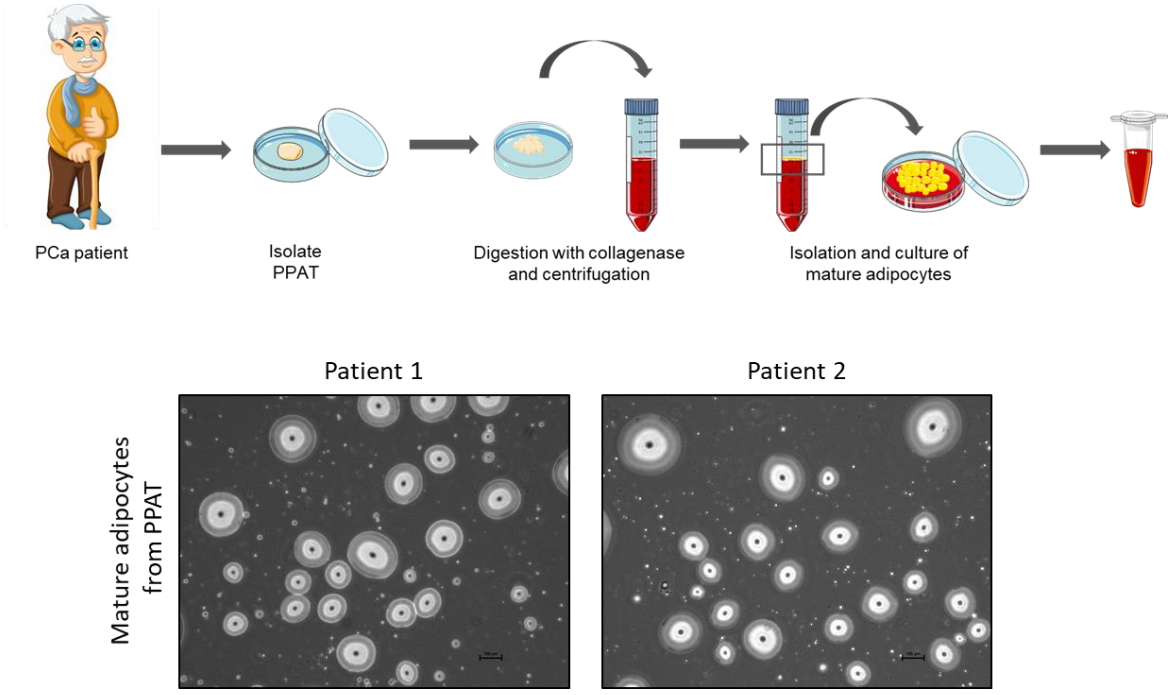

Figure 2.2.1: Schematic representation of mature adipocyte preparation from PPAT.
PPAT was minced into small pieces using a scalpel and transferred to a 50ml falcon with collagenase digestion solution. Mature adipocytes were found in the upper floating layer after the centrifugation step and they were culture for 24 hours. The resulting CM was transferred in 2ml tubes, snap-frozen and stored at -80°C. The lower panel shows mature adipocytes *in vitro* derived from PPAT tissue from locally advanced PCa patients.

2.3 Cell culture

2.3.1 Cell maintenance and passaging

Cell culture was performed using Class II laminar flow microbiological safety cabinet (Thermo Fisher Scientific) under aseptic conditions. Cell lines were routinely cultured in 75 cm^2 and 175 cm^2 tissue culture flasks (Greiner BioOne, Frickenhausen, Germany) and placed in the incubator (Thermo Fisher Scientific) at 37°C with 5% CO_2 supply. Cell lines were cultured with culture media described in Table 10 and 0.2% Amphotericin B was added to avoid any fungal contamination. All media was stored at 4°C and brought to room temperature before use. Cells were passaged every 2-4 days, once they reached 80% confluence. Cell passaging was performed by aspirating the culture medium and removing the dead cells by washing the cells with sterile PBS and then incubating with Trypsin (Thermo Fisher Scientific) for 5 minutes at 37°C. To neutralise the effect of Trypsin, the culture medium was added and centrifuged at 1000 rpm for 5 minutes at room temperature. The resulting supernatant was discarded, while the cell pellet was suspended in culture medium and used for passaging (1:3) and seeding cells. Cells were used for a maximum of 2 months after thawing. Following Table 10 shows the list of cell lines used in this thesis.

No	Cell line	Distributor/ Provider	Cat. No.	Culture media
1	PC3	ATCC and LGC Standards	ATCC® CRL-1435™	DMEM 10%FBS 1%Penicillin/Streptomycin (Life technologies)
2	Du145	ATCC and LGC Standards	ATCC® HTB-81™	DMEM 10%FBS 1%Penicillin/Streptomycin
3	TRAMP C2	ATCC and LGC Standards	ATCC® CRL-2731™	DMEM 0.005 mg/ml bovine insulin 10 nM dehydroisoandrosterone 5% FBS

				5% Nu-Serum IV 1%Penicillin/Streptomycin
5	HEK-293T	ATCC and LGC Standards	ATCC® CRL-11268™	DMEM 10%FBS 1%Penicillin/Streptomycin
6	3T3-L1	ATCC and LGC Standards	ATCC® CL-173™	DMEM media (1g/l Glucose) 10%FBS 1%Penicillin/Streptomycin
7	3T3-F44-2A	Gift from Dr Katrin Fischer (Helmholtz Centre Munich)	_	DMEM media (1g/l Glucose) 10%FBS 1%Penicillin/Streptomycin
9	MCF-7	ATCC and LGC Standards	ATCC® HTB-22™	RPMI 10%FBS 1%Penicillin/Streptomycin
10	MDA-MB-231	ATCC and LGC Standards	ATCC® CRM-HTB-26™	DMEM 10%FBS 1%Penicillin/Streptomycin
11	BT-474	ATCC and LGC Standards	ATCC® HTB-20™	DMEM 10%FBS 1%Penicillin/Streptomycin
13	TT	IRCCS Biobank	HTL98004	Hams F12K 15%FBS 1%Penicillin/Streptomycin
14	MZ-CRC-1	Gift from Dr. Mercedes Robledo (Centro Nacional de Investigaciones Oncológicas)	_	DMEM 15%FBS 1%Penicillin/Streptomycin

Table 10: List of cell lines used in this thesis

2.3.2 PCa cell lines

The initial study design was planned with PC3, Du145, LnCap and TRAMP-C2 cells. PC3 and Du145 cells are androgen unresponsive and are considered as highly aggressive PCa cell lines as they are derived from two different metastatic locations from PCa patients (Cunningham and You 2015). PC3 cells have high metastatic potential, while Du145 cells have moderate metastatic potential when injected *in vivo.* LnCap cells are androgen-responsive and were isolated from the lymph node of a prostate carcinoma patient and have low metastatic potential *in vivo* (Cunningham and You 2015). All three cells lines represent a diverse range of PCa conditions that cover hormone sensitivity and aggressiveness. TRAMP-C2 cells are PCa cells derived from mouse and can be used as controls in the study since the conditioned media used in this thesis is primarily derived from mice. To eliminate the cross-species effect, TRAMP-C2 cells were used as a control cell line. All the experiments in this thesis have been performed with PC3 and Du145 cells as a starting point, further experiments with LnCap and normal prostate epithelial cells are planned in section 3.7.

2.3.2.1 PC3

PC3 cells were obtained from 62-year old grade IV PCa patient with bone metastasis. They were obtained from the lumbar vertebral metastasized site, they are epithelial in nature and grow as androgen-independent cells and $PTEN^{-/-}$(Webber, Bello et al. 1997).

2.3.2.2 Du145

Du145 cell line is derived from a 69-year old PCa patient with brain metastasis. Du145 cells are generated from central nervous system lesion metastasized site, like PC3 cells these are also epithelial in nature and grow as androgen-independent cells however, they are $PTEN^{+/+}$(Webber, Bello et al. 1997).

2.3.2.3 TRAMP-C2

TRAMP-C2 is one of the three cell lines that were established from a 32-week tumour of the transgenic adenocarcinoma mouse prostate (TRAMP) model. TRAMP model is a transgenic mouse line, established to study PCa since the development and progression of cancer mimic human patients. TRAMP model develops PIN by 8-12 weeks of age that advances to

adenocarcinoma with distant metastases by 24-30 weeks of age. Out of the three cell lines, TRAMP-C1 and TRAMP-C2 form tumours when injected in CS7BL/6 hosts. TRAMP-C3 cells are used *in vitro* since they do not form tumours *in vivo* (Foster, Gingrich et al. 1997).

2.3.3 Adipose cell lines

2.3.3.1 3T3L1

The 3T3-L1 cell line is a well-established pre-adipose cell line that was generated from 17- to 19-day-old Swiss 3T3 mouse embryos. Their morphology appears like fibroblasts and they can be differentiated into mature adipocytes with the insulin, dexamethasone (DEX), and 3-isobutyl-1-methylxanthine (IBMX). 3T3-L1 cells are maintained in DMEM medium (1 g/l Glucose) (Thermo Fisher Scientific) before differentiation and to initiate differentiation, the cells are seeded on a 6-well plate (2 x 10^5cells/well) with DMEM media (4.5 g/l Glucose) (Thermo Fisher Scientific) and allowed to attain 80-90% confluence. After 2 days, the differentiation is initiated by adding 100 mM IBMAX (Sigma-Aldrich) and 1mM DEX (Sigma-Aldrich) and 10 mg/ml Insulin (Sigma-Aldrich). 4 days later the medium is supplemented with insulin (10 mg/ml) for 7-8 days. From day 9 onwards, large lipid droplets are visible under the microscope (Ruiz-Ojeda, Rupérez et al. 2016).

2.3.3.2 3T3-F442A

The 3T3-F442A cell line is also derived from Swiss 3T3 mouse embryos. Since it is isolated from the third selection of clones, 3T3-F442A cells show a higher frequency and more lipid droplets than the 3T3-L1 cells. They are maintained in DMEM medium (1 g/l Glucose) (Thermo Fisher Scientific) before differentiation. To initiate differentiation, the cells are seeded on a 6-well plate (2 x 10^5cells/well) with DMEM media (4.5 g/l Glucose) (Thermo Fisher Scientific) and allowed to reach 80-90% confluence. After 2 days, the differentiation is initiated by adding 0.005 mg/ml Insulin (Sigma-Aldrich) to the media. The culture media is changed every 3-4 days for up to 14 days when large lipid droplets can be visualised under the microscope (Ruiz-Ojeda, Rupérez et al. 2016). 3T3-L1 and 3T3-F442A cell lines are well established as good models for studying adipogenesis, as well as widely used for co-cultures and three-dimensional cell cultures

2.3.4 Breast cancer cell lines

2.3.4.1 BT-474

BT-474 cells were obtained from a 60-year-old Caucasian woman. The tumour, centrally located, was derived from a radical mastectomy. The cells are epithelial in nature and look like fibroblasts (Lasfargues, Coutinho et al. 1978).

2.3.4.2 MCF-7

MCF-7 cells were derived from a 69-year-old Caucasian female with metastatic breast cancer. The cells were isolated from the pleural effusion. MCF-7 cells are epithelial in nature and have polygonal morphology (Soule, Vazguez et al. 1973).

2.3.4.3 MDA-MB-231

MDA-MB-231 cells were obtained from a 51-year-old Caucasian female with metastatic breast cancer. The cells were isolated from the pleural effusion, and appear spindle-shaped (Cailleau, Olivé et al. 1978).

2.3.5 Thyroid cancer cell lines

2.3.5.1 TT

TT cells were derived by needle biopsy from a 77-year-old female with germline metastatic MTC. The cells express RET C634W mutation (Leong, Zeigel et al. 1981, Landa, Pozdeyev et al. 2019).

2.3.5.2 MZ-CRC-1

MZ-CRC-1 cell line was derived from a 43-year-old white female with sporadic metastatic MTC. The cells were obtained from pleural effusion and express RET M918T mutation (Knuth A., Gabbert H.E. et al. 1987, Landa, Pozdeyev et al. 2019).

2.3.6 Other cell lines

2.3.6.1 HEK-293T

293 cells were generated from human embryonic kidney cells in 1977. 293T cells are a subline containing simn virus 40 large tumour antigen, this increases the transfection efficiency of the cells. The HEK-293T cell line was used for the generation of Lenti-virus due to its high transfection efficiency. (Graham, Smiley et al. 1977, DuBridge, Tang et al. 1987)

2.3.7 Cryopreservation of cells

The cells were cryopreserved at early passages to generate large volumes of frozen stocks. Cryopreservation was performed using 10% dimethyl sulphoxide (DMSO) in FBS and aliquoted in 1.5 ml cryovials (BD Biosciences, Heidelberg, Germany). Cells were frozen by placing the cryovials in Mr frosty (Thermo Fisher Scientific) and stored at -80°C. For long-term storage, they were stored in liquid nitrogen. When needed, the frozen vials were thawed immediately by placing them in a water bath with 37°C. The cells were suspended in complete media and centrifuged at 1000x rpm for 5 minutes at room temperature. Cell pellet was suspended in complete media and placed in a 125 cm^2 tissue culture flask (Greiner BioOne) in the beginning and later transferred to bigger flasks for experiments.

2.3.8 Cell counting

The cells were counted using Countess II Automated Cell Counter (Thermo Fisher Scientific). The cell pellet was isolated, as mentioned in section 2.3.1. The cells were then re-suspended in 5ml of complete media and 10 µl of cells were mixed with 10 µl of Trypan Blue (0.4%) (Thermo Fisher Scientific). 10 µl of the Trypan blue mixture was directly loaded on the Countess™ Cell Counting Chamber Slides (Thermo Fisher Scientific) and placed in the Countess II. The Trypan Blue stains the dead cells and the viable cells are counted using an image analysis algorithm.

2.3.9 Mycoplasma testing

Presence of mycoplasma was tested in the cell culture supernatant using PCR Mycoplasma Test Kit I/C (PromoKine, Germany). The procedure was performed using the manufacture's protocol. Each cell line used in this study was tested for mycoplasma contamination at the end of each month. Figure 2.3.1 shows an example from Mycoplasma testing.

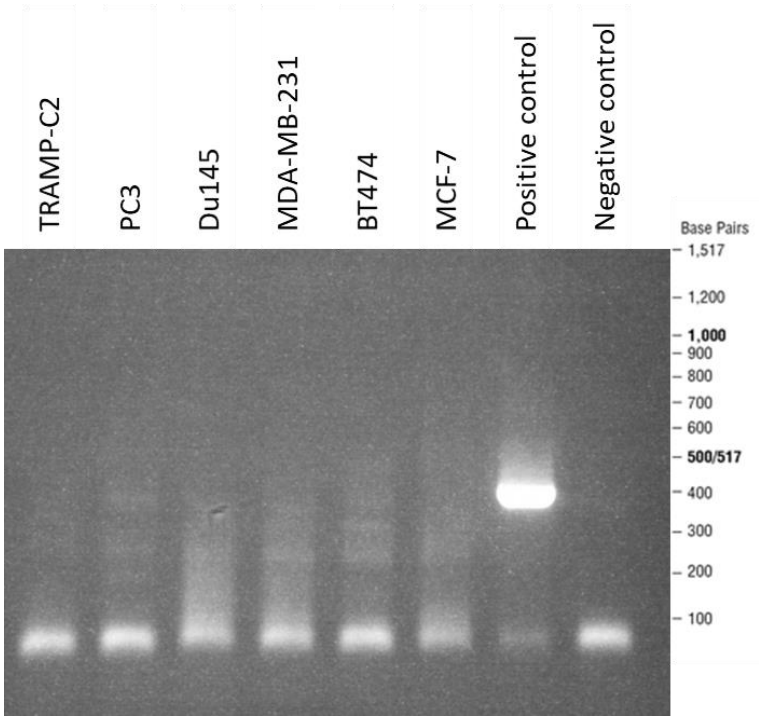

Figure 2.3.1: Endpoint PCR to test the presence of mycoplasma in cell lines.
PCR products from the cell lines were loaded on an agarose gel along with positive control and negative control DNA for mycoplasma.

2.4 Cell culture based assays

2.4.1 3D cell culture

For 3D cell culture, initially, the individual cell density for each cell line was determined by seeding different concentrations of cells. 100, 1000 and 5000 cells per cell line were seeded on an ultra-low attachment (ULA) plate (Corning) as shown in Figure 2.4.1 and incubated at 37°C for five days. The cell density should not exceed the magnification field of the microscope. Each cell line has variable cell densities, PC3 cells form 3D spheres with just 100 cells, while for Du145 and TRAMP-C2 cells need a seeding density of 1000 cells to obtain the same size. The size of the spheroids is especially important for consistent statistical analysis and should be consistent for each cell line once selected. After the preliminary testing of spheroid densities, we selected 100 cells for PC3 and HEK-293T cells and 1000 cells for all the other cell lines.

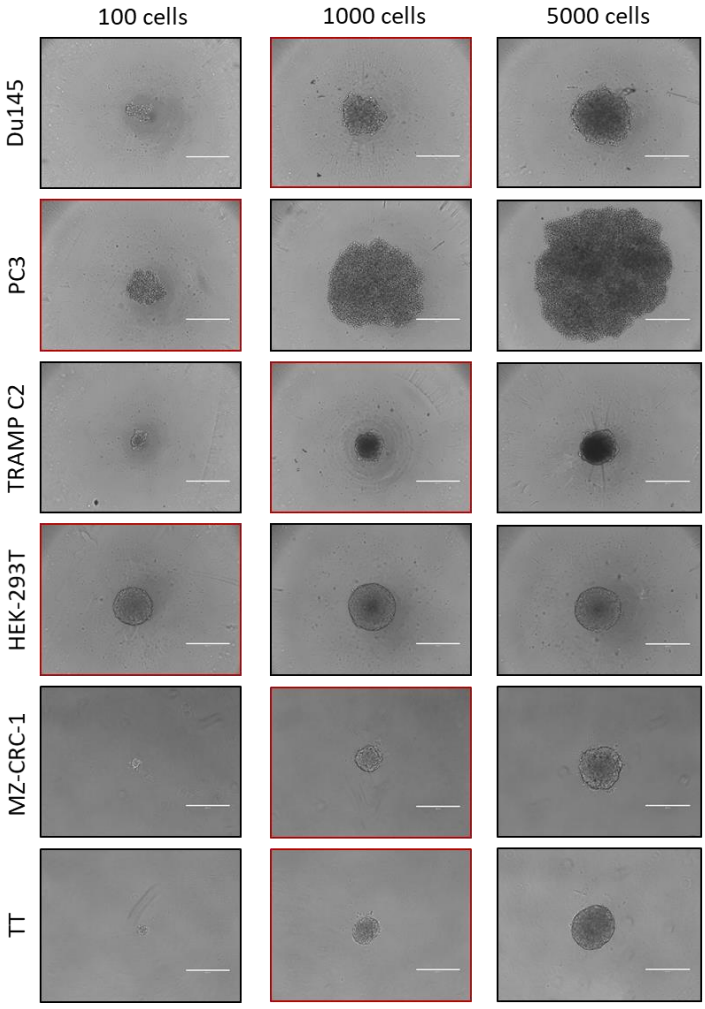

Figure 2.4.1: Optimisation of cell densities for 3D culture
Cell lines were seeded at 100, 1000 and 5000 cells per well in ULA plate. Images were taken on the fifth day after seeding. Higher seeding densities show a dark apoptotic core in the centre.

2.4.2 3D cell viability

Viability of 3D spheres was determined using RealTime-Glo™ MT Cell Viability Assay (Promega). The assay uses a substrate that is specifically taken up by viable cells and the viable cells can therefore reduce the substrate and produce luminescence. Dead cells are not able to reduce the substrate. Unlike other cell viability methods, this assay is ATP independent and an excellent method to estimate the viable cells. Once the reagents are added to the cells, the cell viability can be measured up to 72 hours without changing the media, thus without disturbing the 3D spheroids. Figure 2.4.2 shows a schematic representation of the assay. The reagents were added according to the manufacturer's protocol and luminesces was measured on a Varioskan Lux plate reader (Thermo Fisher Scientific) every day for 72 hours.

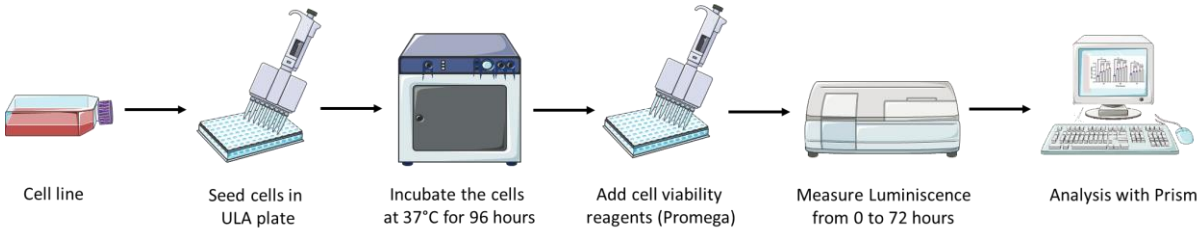

Figure 2.4.2: Cell viability assay for 3D cultures
Cells were seeded on an ULA plate and incubated at 37°C for four days to allow spheroid formation. Cell viability reagents were added, and measurements were taken every 24 hours for 3 days without changing the media.

2.4.3 3D invasion assay

The 3D invasion was performed using 96-well 3D Spheroid BME Cell Invasion Assay kit (Cultrex®) according to the manufacturer's instruction. Briefly, 3D spheroids were generated by seeding the appropriate number of cells (three technical replicates per sample) and adding spheroid formation ECM from the kit. After 96 hours, the spheres were centrifuged and invasion matrix was added to each well. Control wells with 3D spheroids did not have Matrigel. The ULA plate was placed back in the incubator for an hour and fresh medium/conditioned media was added on the solidified matrix. Pictures to measure the cell invasion were taken every 2-4 days, depending on the invasion potential of each cell lines. The pictures were saved as jpeg files and opened in ImageJ software. The invasion area or for control well the spheroid area was measured by drawing margin along the invaded spheroid. The pixel densities were then copied into Microsoft Excel and percentage of invasion was calculated by dividing the mean average of cells invading through the Matrigel divided by the

mean average of the corresponding 3D spheroid multiplied by 100. The values were copied to Graphpad Prism software and statistical analysis was carried out. Figure 2.4.3 shows a schematic representation of the assay.

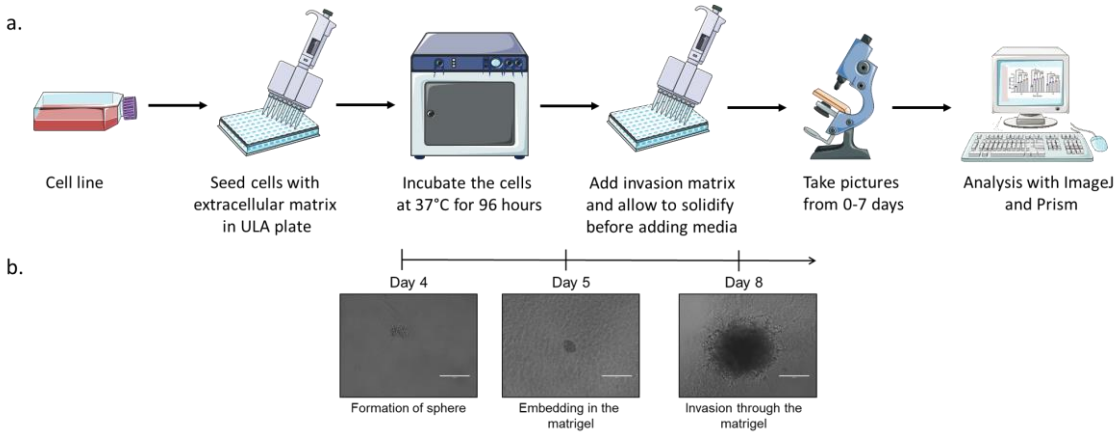

Figure 2.4.3: Cell invasion assay for 3D cultures
(a) Cells were seeded on a ULA plate and incubated at 37°C for four days to allow spheroid formation. Invasion matrix was added and allowed to solidify for an hour. Culture media was added after the matrix was solidified and pictures were taken every day for 3-7 days. The extent of invasion was measured with ImageJ software. (b) Example for 3D invasion for TRAMP-C2 cells on day 4, 5 and 8.

2.4.4 2D invasion assay

The 2D invasion assay was performed using Corning® BioCoat™ Matrigel® Invasion Chambers (Corning). The invasion inserts had 8-micron pore size PET membrane with a thin layer of Matrigel Basement Membrane Matrix. The assay was performed according to the suggested protocol. Briefly, the inserts with Matrigel were re-hydrated with culture media prior to use. Cells in the ratio 5 x 10^4 cells/ml were seeded on the insert and the ULA plate was incubated at 37°C overnight. The following day, conditioned media/culture media was added to the bottom 24-well plate and the cells were allowed to migrate for 24 hours. The non-invading cells were removed by scrubbing with a cotton swab and invading cells were fixed with 1% Toluidine blue (Sigma). Pictures were taken with the microscope and the percentage of invasion was calculated.

2.4.5 2D migration assay

Cell migration assay was performed using 4-well culture inserts in a 35 mm µ-Dish (IBIDI, Germany). The assay is based on the principle of the ability of the cells to migrate when an artificial gap is created, commonly known as gap closure assay. 1 x 10^5 cells were seeded per well and allowed to attain a confluent layer in the well. Once the confluent layer was achieved (usually 2-3 days' post-seeding), culture media was aspirated and the insert separating the wells was removed using forceps. Next, the desired media with chemoattractant or conditioned media was added to the µ-Dish. The appropriate duration for migration was determined for each cell line and pictures were taken immediately after addition of chemoattractant and after desired migration was obtained. The space between the cells was measure using ImageJ software. Figure 2.4.4 shows a schematic representation of the assay.

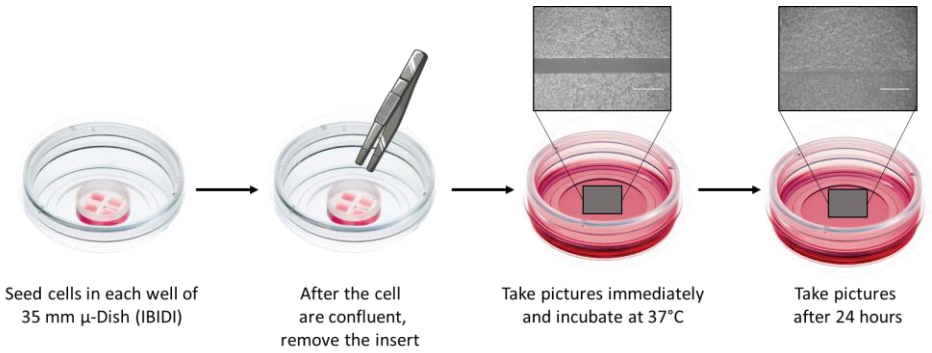

Figure 2.4.4: Gap closure assay for 2D cultures
Cell lines were seeded in each of the 4-wells of 35 mm µ-Dish (IBIDI). After the cells reached confluence, the insert separating the wells was removed using forceps and culture medium was added. Pictures were taken to visualise the gap closure every day for 2-7 days. The analysis was carried out in ImageJ software.

2.4.6 2D cell proliferation assay

Cell proliferation was measured using the CyQUANT® NF kit (Thermo Fisher Scientific). This kit measures cellular DNA content by quantifying the fluorescence signal. Cells are seeded on a black wall, clear-bottom 96-well plate at a concentration of 1 x 10^4 cells/well. Four to six hours after seeding, the culture medium is aspirated and reagents from the kit are added according to manufacturer's instructions. The plate is placed back in the incubator for 1 hour and the fluorescence is measured using an excitation wavelength of ~485 nm and an emission wavelength of ~530 nm.

2.5 Generation of stably transfected cell lines using Lenti-virus

Figure 2.5.1 shows a schematic representation of the overall process involved in the generation of stably transfected cells. Each step is described in detail ahead.

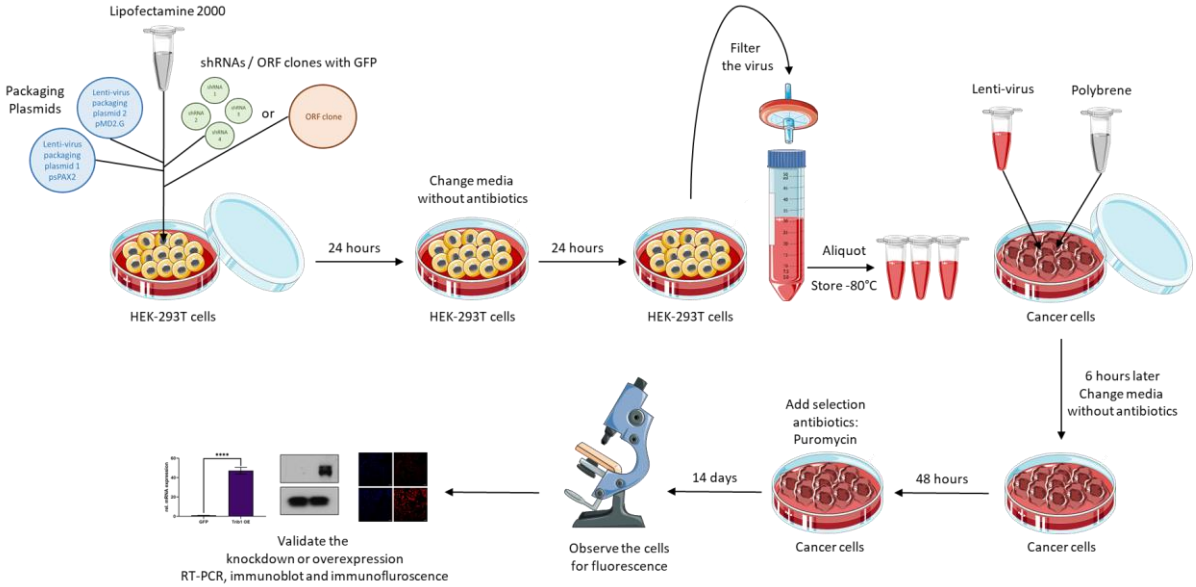

Figure 2.5.1: Generation of stably transfected cell lines using Lenti-virus
HEK-293T cells were used for Lenti-virus production due to their high transfection efficiency. HEK-293T cells were transfected with Lenti-viral packaging plasmids and knockdown or overexpression constructs for the desired gene. After 48 hours, the Lenti-virus was filtered, collected and snap-frozen with liquid nitrogen for storage at -80°C. Cancer cell lines were transduced with Lenti-virus with Polybrene transfection reagent and selection antibiotics were added after 48 hours. The cells were kept in culture for 14 days and validated using RT-PCR, immunoblot and immunofluorescence.

2.5.1 Transformation of plasmids

Lenti-virus plasmids were purchased from Origene (Table 11). Plasmids were transformation using NEB 5-alpha Competent E. coli (High Efficiency) (New England Biolabs) as per manufacturer's instructions. 10 µl of competent cells were used per reaction.

Company	Plasmid	Gene	Species	Catalogue no.
Origene	pGFP-C-shLenti (4 shRNAs)	TRIB1	Human	TL320635
Origene	pLenti-C-mGFP-P2A-Puro	TRIB1	Human	RC209219L4
Origene	pLenti-C-mGFP-P2A-Puro	TRIB2	Human	RC201210L4
Origene	pGFP-C-shLenti (4 shRNAs)	TRIB3	Human	TL300856
Origene	pGFP-C-shLenti	Scramble control for shRNAs		TR30021
Origene	pLenti-C-mGFP-P2A-Puro	GFP control for cDNA constructs		PS100093
-	psPAX2	2nd generation Lenti-viral packaging plasmid		Provided by IDC, Helmholtz Zentrum München
-	pMD2.G	2nd generation Lenti-viral packaging plasmid		Provided by IDC, Helmholtz Zentrum München

Table 11: List of Lentiviral vectors used in the study

2.5.2 Plasmid isolation

Plasmid isolation was performed using QIAGEN Plasmid Mega Kit (Qiagen) according to the manufacturer's protocol. The DNA concentration was measured using Nanodrop 2000 (Thermo Fisher Scientific).

2.5.3 Virus generation in HEK-293T cells

HEK-293T cells were plated in a 15 cm dish at a seeding density of 6 x 10^6 cells. The following day, once the cells reached 80% confluence, they were used for transfection. In 15 ml tube, 2 ml of Optimum media (Thermo Fisher Scientific) and 62.5 µl of Lipofectamine 2000 (Thermo Fisher Scientific) were added. In another 15 ml tube, 2 ml of Optimum media and 12.5 µg Lenti-vector were mixed with 12.5 µg of psPAX2 and 1.25 µg of pMD2G. Then, the contents of both the tubes were mixed together and incubated for 30 minutes at room temperature. Meanwhile, the fresh culture medium was added to the HEK-293T cells. After 30 minutes, the transfection mixture was added to the cells dropwise and incubated for 24 hours at 37°C. Cells were replenished with media without antibiotics the following day and again incubated for 24 hours. The virus was collected by first filtering the culture media with 0.22 µM filter system (Millipore-Stericup Quick Release-GP Sterile Vacuum Filtration System, Merk) in 1 ml aliquots and immediately snap-frozen with liquid nitrogen and stored at -80°C. Lenti-X GoStix Plus kit (Takara Bio, USA) was used to determine the viral concentration and the kit was used according to the manufacturer's protocol.

2.5.4 Dose response for antibiotic selection of mammalian cells

To eliminate the non-transfected cells after Lenti-viral transduction, the selection antibiotics were added. These antibiotics only allow transfected cells with the selection marker to survive and therefore desired cells can be maintained in culture. Kill curve analysis was performed by adding Puromycin (Sigma) to the cells at concentrations of 0.5 µg/ml, 1 µg/ml, 2 µg/ml, 3 µg/ml and 4 µg/ml for 48 to 72 hours. The lowest antibiotic concentration was selected at which all cells were dead. Figure 2.5.2 shows pictures taken on the seventh day after adding the antibiotics to the medium. At 1 µg/ml, all the Du145 and PC3 cells were dead and the concentration of 2 µg/ml was required for killing all MZ-CRC-1 and TT cells.

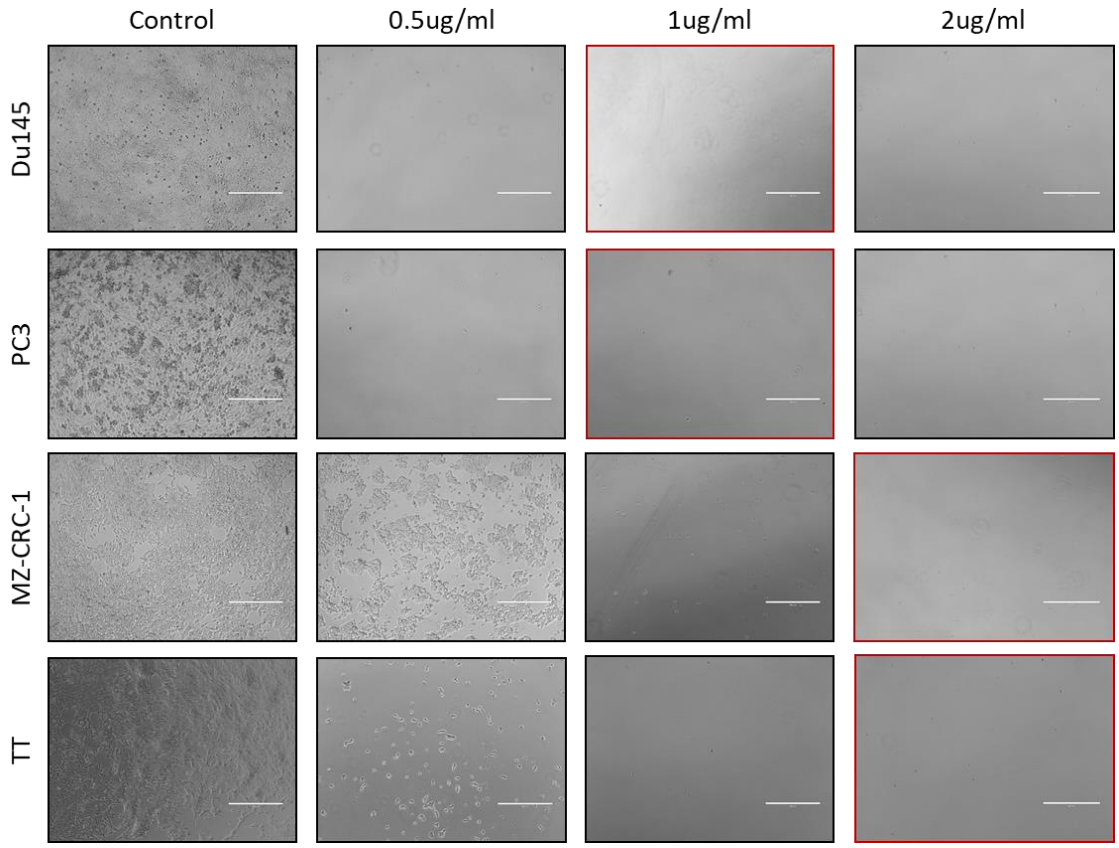

Figure 2.5.2: Picture with cell lines with different concentration of Puromycin
Pictures were taken on day 7, showing all the cell lines after treatment with different concentrations of Puromycin. The images from which the desired antibiotic concentration was selected are highlighted in red.

2.5.5 Viral transduction in desired cell lines

For viral transduction, the cancer cells were plated on a 6-well plated at a seeding density of 1 x 10^6 cells/well without antibiotics. The following day, cells attained approximately 90% confluence. The viral aliquots were thawed on ice, and appropriate amount of Lenti-virus was used for each transduction. The Lenti-virus was combined with 8 µg/ml Polybrene (Santa Cruz Biotechnology, Heidelberg, Germany) and added to each well. After 6 hours, the medium was replenished with culture medium without antibiotics and incubated for another 24 hours. The next day, the culture medium with antibiotics was added with appropriate concentrations of Puromycin. The culture media was changed 3 times a week and Puromycin was used for 2 weeks. 2 weeks post-transduction; the cells were expanded and stably transfected cells frozen down. The stable cell lines used in this thesis are polyclonal (the transgene is integrated into various locations in different cells) mainly due to time constraints for generating stable cell lines from single positively transduced cells and to avoid any clonal effect from cell lines generated from single clones. The efficiency of transfection was analysed every 2 weeks by western blotting while performing tumour cell behavioural assays. Since the overexpression constructs are GFP fusion proteins, the fluorescence was monitored under a fluorescent microscope during routine cell culture.

2.6 Co-culture and conditioned media culture

2.6.1 Co-culture

PCa cells and adipocytes were co-cultured using a 0.4 µM pore size Transwell system (Merk). 1.5 x 10^5 pre-adipocytes cells were seeded on a 6-well plate and differentiated to mature adipocytes as described in sections 2.3.3.1 and 2.3.3.2. Later, 1.5 x 10^5 tumour cells were seeded on the Transwell inserts. After 24 hours, the inserts were transferred on to the 6-well plate containing pre-adipocytes/mature adipocytes, as shown in Figure 2.6.1. Tumour cells were cultivated alone as negative control. After 48 hours, RNA and proteins were isolated for further analysis.

2.6.2 Conditioned media generation and culture

To investigate the secretory factors from adipocytes, conditioned media (CM) was generated from adipocytes. Fresh media was added on pre-/mature adipocytes and incubated overnight at 37°C. The following day the media was filtered using 0.45 µM filters (Merk), aliquoted in 2 ml tubes and snap-frozen immediately using liquid nitrogen. The aliquoted CM then store at -80°C until further use. For CM culture with tumour cells, the CM was thawed on ice and brought to room temperature before directly adding onto the tumour cells and incubated for 48 hours at 37°C.

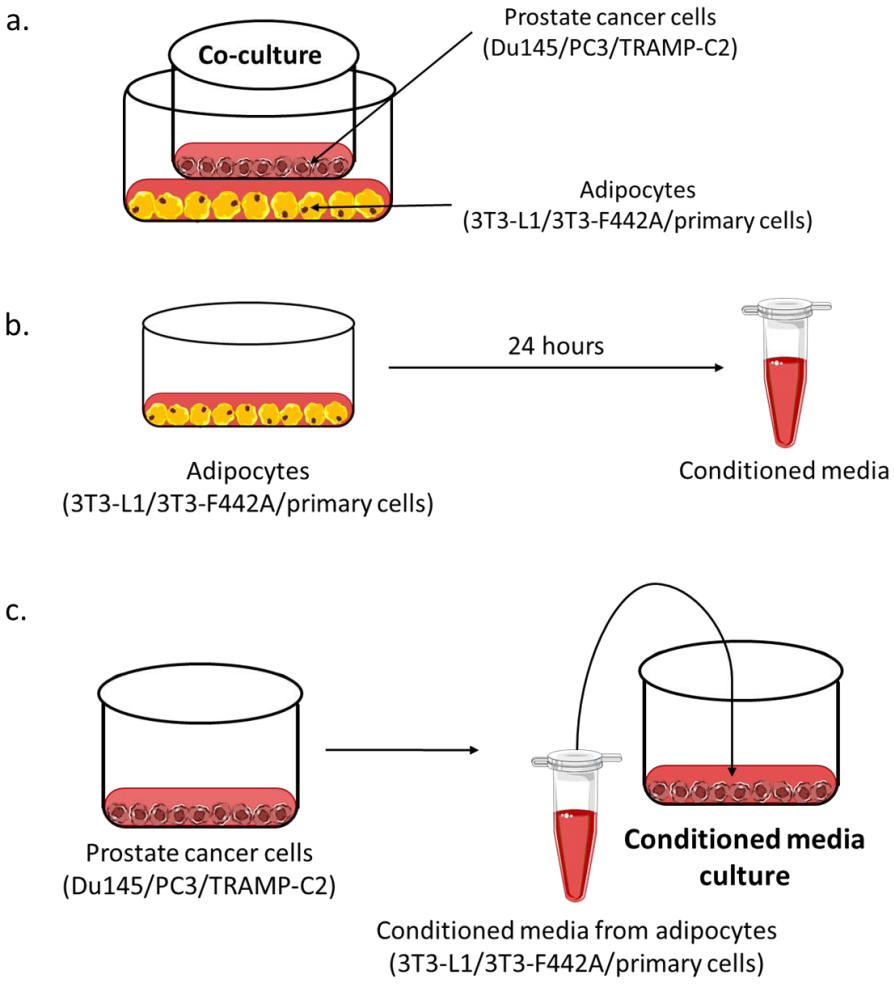

Figure 2.6.1: Co-culture and CM culture of cancer cells
(a) Pre-adipocytes were seeded on a 6-well plate and differentiated into mature adipocytes. Co-culture inserts were added on top of the wells with PCa cells. Thus, the two cell populations were in close contact with each other in the co-culture system. The co-culture membrane allowed the exchange of soluble nutrients but did not allow the exchange of cells. (b) CM from adipocytes was generated by isolating the media after 24 hours. The CM was snap-frozen immediately and stored at -80°C. (c) CM culture was carried out by adding the CM from the adipocytes on the cancer cells and incubating at 37 °C for 48 hours.

2.7 Expression Analysis

2.7.1 RNA extraction and quantification

2.7.1.1 RNA extraction from tissues

For isolating the RNA from adipose tissues, RNeasy Lipid Tissue Mini Kit (Qiagen) was used. 80 mg of frozen tissue were collected in a 1.5 ml tube with one 5 mm stainless steel bead (Qiagen). Tubes were placed on dry ice until 1 ml of QIAzol Lysis Reagent was added from the kit. The tubes were immediately transferred to Tissue Lyser Adapter Set and placed in Tissue Lyser MM 400 (Retsch, Haan, Germany) for 2 minutes at 20Hz. The tubes were rotated and again placed in the Tissue Lyser for 2 more minutes. The resulting protein lysates were transferred to a new 1.5ml tube and RNA isolation was performed according to the manufacturer's protocol. RNA quality was tested by measuring OD using Nanodrop 2000 (Thermo Fisher Scientific), an A260/280 ratio of 1.8-2.2 and an A260/230 of 2.0-2.2 was used in this study. RNA was stored at −80°C until further use.

2.7.1.2 RNA extraction from cells

RNA isolation from cells was performed using Maxwell® 16 LEV simply RNA Tissue Kit (Promega) and Maxwell® 16 Instrument (Promega) according to the manufacturer's protocol. RNA quality was tested by measuring OD using Nanodrop 2000 (Thermo Fisher Scientific), an A260/280 ratio of 1.8-2.2 and an A260/230 of 2.0-2.2 was used in this study. RNA was stored at −80°C until further use.

2.7.2 Reverse transcription (RT)

cDNA was generated using 2 µg of RNA using High-Capacity RNA-to-cDNA™ Kit (Thermo Fisher Scientific). The reaction mixture was prepared according to Table 12. For each sample, a Reverse transcription (Enzyme Mix) negative control was used. The reaction mixture was placed into Eppendorf® Mastercycler X50i (Eppendorf) at 37°C for 60min, 95°C for 5min and held at 4°C. The cDNA was diluted by adding 80 µl of nuclease-free water, for a final volume of 100 µl.

Reagents	Volume per reaction	
	RT reaction (+)	RT reaction (-)
2X RT Buffer Mix	10.0 µL	10.0 µL
20X RT Enzyme Mix	1.0 µL	-
RNA sample	up to 9 µL	up to 9 µL
Nuclease-free H_2O	up to 20 µL	up to 20 µL
Total per reaction	20.0 µL	20.0 µL

Table 12: Reagents used for cDNA synthesis

2.7.3 RT-PCR

RT-PCR was performed using QuantStudio™ 7 Flex (Thermo Fisher Scientific). Multiplex RT-PCR was used to amplify and relatively quantify *TRIBs* expression and endogenous control in a single tube. TaqMan® probes designed with FAM™ and VIC™ dyes allow the amplification of two genes in a single reaction. All experiments were performed in triplicate and were normalised to the housekeeping gene, either Beta-actin or GAPDH. Each reaction had a final volume of 10 µL, which include 5 µL of TaqMan® Multiplex Master Mix (Thermo Fisher Scientific), 1 µL of template cDNA, TaqMan® probes with FAM™ or VIC™ 0.5 µL each and up to 10 µL nuclease-free water. Table 13 shows the list of TaqMan assays used in this thesis. Data analysis was performed by exporting the raw data in Excel and fold changes were determined by using $2^{-\Delta Ct}$ method. Briefly, average Ct value was calculated for each sample and ΔCt was calculated taking the average Ct of the gene of interest subtracted by the average Ct of the housekeeping gene. Next, ΔΔCt was calculated by subtracting ΔCt (test sample) with ΔCt (control sample). Lastly, $2^{-\Delta Ct}$ for test sample and control sample was calculated using 2 to the power of negative ΔΔCt.

No.	Species	Name	Assay ID	Amplicon Length	Dye
1	Human	TRIB1	Hs00921832_m1	88	FAM-MGB
2	Human	TRIB2	Hs01120543_m1	93	FAM-MGB
3	Human	TRIB3	Hs00221754_m1	115	FAM-MGB
4	Human	Beta actin	Hs01060665_g1	63	VIC-PL
5	Mouse	Trib1	Mm00454875_m1	99	FAM-MGB
6	Mouse	Trib2	Mm00454876_m1	115	FAM-MGB
7	Mouse	Trib3	Mm00454879_m1	79	FAM-MGB
8	Mouse	GAPDH	Mm99999915_g1	107	VIC-PL

Table 13: List of TaqMan® Assays used for RT-PCR

2.7.4 Protein isolation and BCA assay

The cells were washed twice with ice-cold 1x PBS (Thermo Fisher Scientific). RIPA buffer (Sigma-Aldrich) containing Halt™ Protease and Phosphatase Inhibitor Cocktail (1x) added immediately before use. The cells were scrapped with ice-cold RIPA buffer and transferred into a 1.5 ml tube. To get rid of cell debris, the lysates were centrifuged at 14,000g at 4°C for 15 minutes and the supernatant was transferred to a fresh tube. Protein quantification was carried out using Pierce™ BCA Protein Assay Kit (Thermo Fisher Scientific) following the manufacture's protocol and the absorbance was measured at 560 nm.

2.7.5 Immunoblot

35ug of cell lysates from each sample were resolved on Novex™ 10% Tris-Glycine Mini Gels and transferred onto a nitrocellulose membrane (Bio-Rad Lab., Munich, Germany) using Trans-Blot® Turbo™ Transfer System (Bio-Rad Lab). After blocking the membrane with 5% BSA (Sigma-Aldrich) or 5% non-fat dry milk (Bio-Rad Lab) for 1 hour at room temperature, the membranes were incubated with primary antibodies (Table 14) at 4°C overnight. The following day the membrane was washed with TBST (Roth - Carl Roth) 3 times for 10 minutes and then incubated with secondary antibody for one hour at room temperature (Table 14). Finally, to remove the non-specific antibody binding, the membranes were washed with TBST

for 10 minutes (3 times). Proteins were detected using enhanced chemiluminescent reagents (Thermo Fisher Scientific) using hyperfilm ECL (GE healthcare, Buckinghamshire, UK). The intensity of protein bands were quantified by using ImageJ software. Briefly, the western blot films were scanned and saved as jpg files. In the ImageJ programme, the protein bands were marked by drawing a rectangular box around the band and the intensity of each band corresponded to the peak intensity in the software. The resulting values were copied in Microsoft Excel and further normalized to housekeeping protein (α-Tubulin). The values were copied to GraphPad Prism software and statistical analysis was carried out.

No.	Antigen	Clonality	Source	Catalogue no.	Lot. no.	Working dilution	
						Immuno-blot	IF
Primary antibodies							
1	TRIB1	Rabbit polyclonal	Millipore	09-126	2910011; 2990222	1:1500	1:100
2	TRIB2	Rabbit polyclonal	abcam	HPA001305	A114362	1:1500	1:100
3	TRIB3	Rabbit polyclonal	abcam	ab75846	GR83698-16;11;24	1:2000	1:150
4	α-Tubulin	Mouse monoclonal	Cell Signalling	12351S	1	1:5000	-
5	mGFP	Mouse monoclonal	Origene	TA180076	F004	1:500	-
6	Akt	Rabbit polyclonal	Cell Signalling	9272S	28	1:1000	-
7	P-Akt (Ser473)	Rabbit polyclonal	Cell Signalling	4060S	25	1:500	-
8	p44/42 MAPK (Erk1/2)	Rabbit polyclonal	Cell Signalling	4695S	28	1:500	-

9	P-p44/42 MAPK (Erk1/2) (Thr202/ Tyr204)	Rabbit polyclonal	Cell Signalling	4376S	18	1:1000	-
Secondary antibodies							
10	Mouse IGG HRP linked whole Ab		GE Healthcare	NA931V	17016967	1:2000	-
11	Rabbit IGG HRP linked whole Ab		GE Healthcare	NA934V	17041907	1:2000	-
12	Rabbit-IgG Alexa Fluor® 555		Cell Signalling	4413S	16	-	1:1000

Table 14: List of antibodies used for Immunoblotting

2.7.6 Immunofluorescence

Immunofluorescence was performed by using Thermo Scientific™ Nunc™ Lab-Tek™ II Chamber Slide™ System (Thermo Fisher Scientific). 1 x 10^5 cells were seeded in each well of the chamber slides and incubated overnight at 37°C. After 24 hours, cells were washed three times with PBS, and fixed with 4% paraformaldehyde at room temperature for 30 minutes. Next, the cells were washed with PBS and incubated with 0.1% TritonX for 3 minutes at room temperature. After permeabilization, primary antibody diluted in 5% normal goat serum was added and incubated overnight at 4°C. The next day, cells were washed with PBS to remove the non-specific binding and then incubated for one hour at room temperature with the secondary antibodies conjugated to Alexa Fluor® 555 channel. The non-specific antibody binding was removed by washing the cells with PBS. Finally, the cells were mounted with

ProLong Gold Antifade Mountant with DAPI (Thermo Fisher Scientific) and left overnight at 4°C for drying. Immunofluorescence images were taken using Confocal Olympus FV1200 microscope.

2.7.7 Immunohistochemistry

Immunohistochemistry was performed using the standard protocol suggested by abcam. The tissues were purchased from Biochain and Origene (Table 16). The slides were first deparaffinized by incubating them at 60°C for 10-30 minutes. Followed by a series of rehydration steps: xylene (30 minutes), 100% EtOH (10 minutes), 95% EtOH (1 minute), 85% EtOH (1 minute), 75% EtOH (1 minute) and distilled water (6 minutes). Antigen retrieval was performed by incubating the slides in a pressure cooker for 18 minutes in Citrate buffer pH 6.0 (abcam). The slides were rinsed again with distilled water (5 minutes). Endogenous peroxidase was inactivated by incubating the tissue sections with hydrogen peroxide (abcam) for 15 minutes. Multiple washing steps were performed using TBST solution (15 minutes). The non-specific antibody binding was blocked using protein block (abcam) for 15 minutes. Thereafter, primary antibodies shown in Table 15 were diluted with antibody diluent (abcam) and incubated overnight at 4°C in a humidified chamber. Subsequently, the slides were washed with TBST and pre-diluted secondary antibody was applied to the sections for 15 minutes at room temperature. Slides were washed with TBST in order to remove non-specific binding, and incubated with Streptavidin peroxide for 10 minutes at room temperature. Peroxidase activity was detected by freshly prepared DAB substrate (30 µl DAB chromogen + 1.5 ml DAB substrate) (abcam). After washing the slides with TBST, counterstaining was performed using Haematoxylin for 1 minute, followed by rinsing the slides with tap water. The slides were de-hydrated through series of de-hydration steps: 75% EtOH (1 minute), 85% EtOH (1 minute), 95% EtOH (1 minute), 100% EtOH (3 minutes) and xylene (3 minutes). The sections were mounted using Permanent Mounting media (abcam) and allowed to dry overnight at room temperature. The next day, pictures were taken using Nikon Eclipse Ci Upright microscope.

No.	Antigen	Clonality	Source	Catalogue no.	Lot. no.	Working dilution
Primary antibodies						
1	TRIB1	Rabbit polyclonal	Millipore	09-126	2990222	1:900
2	TRIB2	Mouse monoclonal	abcam	ab117981	GR3272671-3	1:400
3	TRIB3	Rabbit polyclonal	abcam	ab137526	GR107883-12	1:900
4	PSMA	Rabbit polyclonal	abcam	ab133579	GR3258749-1	1:500
5	Calcitonin	Rabbit polyclonal	abcam	ab75368	GR3333626-1	Pre-diluted
Secondary antibodies						
6	Mouse IgG H&L		abcam	ab214879	-	Pre-diluted
7	Rabbit specific HRP		abacm	ab64261	-	Pre-diluted

Table 15: List of antibodies used for Immunohistochemistry

Tissue	Catalogue no.	Lot no.	Source	Donor	Age
Normal prostate tissue	T2234201	C404083	Biochain	Male	38
Prostate tumour tissue	T2235201-D01	C102061	Biochain	Male	78
Normal thyroid tissue	CS703460	PA00005086	Origene	Female	42

Table 16 List of human tissues used for Immunohistochemistry

2.8 Statistical Analysis

All the experiments were performed at least three times unless otherwise stated and statistical analysis was performed with three or more biological replicates by using Graph Pad Prism software (GraphPad Software Inc., San Diego, USA). Student's t-test or analysis of variance (ANOVA) was performed to determine statistically significant differences between groups. Appropriate statistical test for each experiment is mentioned in the figure legends. All data presented in the thesis are shown as mean ± SD. Statistical significance is shown as follows *=$p<0.05$, **=$p<0.01$, ***=$p<0.001$. All graphs and analysis were performed using GraphPad Prism 8.0 unless otherwise stated.

Chapter 3 : Adipocyte microenvironment contributes to increase in TRIB1 and TRIB3 expression and TRIB3 promotes PCa progression *in vitro*

3.1 Declaration

The results reported in this chapter are intended to be published along with some additionally planned experiments (manuscript in preparation). All the experiments described in this chapter were performed by myself, with some technical support for immunohistochemistry from an Erasmus Master's student Amy Rose Fumo in our group.

3.2 Abstract

Prostate cancer (PCa) is the most common cancer in ageing men and it is associated with high mortality rates due to distant metastasis. Adipose tissue forms a major part of the tumour microenvironment in PCa. Adipocytes secrete adipokines that are involved in promoting PCa aggressiveness. Therefore, obese PCa patients generally tend to have poor prognosis upon detection. Tribbles proteins (TRIBs1/2/3) belong to a family of pseudokinases which are involved in the development of various cancers including leukaemia, colorectal, breast and prostate. *TRIB1* contributes to PCa tumorigenesis by regulating the ER chaperone expression, which is necessary for cell survival. However, the influence of adipose tissue microenvironment on *TRIBs* expression in cancer cells has not been studied. By co-culturing, we found that adipocytes increase TRIB1 and TRIB3 expression in Du145 and PC3 PCa cells. Furthermore, we also identified, CXCL13, IL6 and Leptin adipokines involved in upregulating TRIB1 and TRIB3 expression in PCa cells. Moreover, our *in vitro* assays indicate that *TRIB3* silencing in PCa cells inhibits cell survival, migration and invasion and this effect is even more prominent under the influence of conditioned media from adipocytes. In summary, we describe the impact of adipokines in regulating TRIB1 and TRIB3 expression in PCa cells and also show the novel role of *TRIB3* as an oncogene in PCa. Taken together, the findings of this thesis have provided deeper insights into the effect of adipose tissue microenvironment on PCa progression.

3.3 Introduction

PCa is the most commonly detected cancer in ageing men and responsible for a high number of cancer-associated mortalities (Kypta, Unda et al. 2012). The cancer cells are surrounded by the stroma that consists of diverse cell types including, immune cell, epithelial cells and fibroblasts, which display altered biological properties in the presence of cancer cells. Cells in the tumour microenvironment can primarily affect tumour growth and progression (Hoy, Balaban et al. 2017). The prostate gland is surrounded by periprostatic adipose tissue (PPAT) and it has been previously reported that the adipose tissue microenvironment promotes PCa aggressiveness (Laurent, Guerard et al. 2016).

In recent years, there has been increasing interest to understand the function of the adipose tissue microenvironment in PCa. Recent evidence suggests that obesity directly co-relates to aggressive PCa and recurrence (Wolin, Carson et al. 2010, Langlais, Cowan et al. 2019). Comba *et al.* described how fatty acids and their derivatives could control and modulate gene expression during tumorigenesis (Comba, Lin et al. 2011). Further studies have reported an altered gene expression profile in breast cancer cells after co-culturing with adipocytes (Strong, Strong et al. 2013, Lee Isla Crake, Phillips et al. 2019). In a recent study on breast cancer, the cancer-associated adipocytes influenced protein expression in breast cancer cells and after performing pathway analysis, the proteins that were upregulated in tumour cells were mainly involved in metabolism, purine synthesis and ubiquitination (Lee Isla Crake, Phillips et al. 2019). Overall, these studies suggest that adipocytes can modulate gene expression in cancer cells that might lead to poor prognosis. Therefore, further studies are needed to understand the cross-talk between adipocytes and cancer cells in various tumour types for developing better treatment options.

Tribbles pseudokinases (TRIB1, TRIB2 and TRIB3) are associated with the development of various cancers and can also contribute to drug resistance (O'Connor, Yalla et al. 2018, Richmond and Keeshan 2019). Depending on the cellular context, TRIBs can function as a tumour suppressor or oncogene (Richmond and Keeshan 2019). *TRIB1* is upregulated in breast and ovarian cancer and associated with poor prognosis (Puiffe, Le Page et al. 2007, Gendelman, Xing et al. 2017). As for PCa, several studies have shown *TRIB1* acts as an

oncogene by promoting cell growth and survival (Lin, Huang et al. 2014, Mashima, Soma-Nagae et al. 2014, Shahrouzi, Astobiza et al. 2020). The role of *TRIB2* in AML tumorigenesis is well established and it involves the regulation of cell cycle signalling and apoptosis (Rishi, Hannon et al. 2014). Furthermore, *TRIB2* has also been reported to confer drug resistance to standard therapies and PI3K inhibitors via AKT activation (Hill, Madureira et al. 2017). In endometrial cancer, *TRIB3* promoted apoptosis and reduced proliferation and migration in endometrial cancer cells (Qu, Liu et al. 2019), while in gastric cancer, *TRIB3* correlates to increased angiogenesis and aggressiveness (Dong, Xia et al. 2016). Very little is currently known about the role of *TRIB2* and *TRIB3* on PCa tumorigenesis. This thesis would investigate the impact of adipose tissue microenvironment on TRIBs expression in PCa cells and further determine the biological role of TRIBs in PCa tumorigenesis.

3.4 Hypothesis

Based on the available literature and the gaps in the field, we hypothesise that adipocytes modulate *TRIBs* expression in PCa cells and that increased *TRIBs* levels can influence PCa aggressiveness.

To test this hypothesis, we used the following objectives:

1. Co-culture adipocytes with PCa cells and analyse TRIBs expression
2. Identify the secretory factors that modulate the expression of TRIBs
3. Determine the biological role of *TRIBs* in PCa under the influence of adipocyte conditioned media

3.5 Materials and Methods

3.5.1 Mouse cytokine array analysis

To detect differentially secreted cytokines, Mouse Cytokine Array Panel A was performed (R&D systems, ARY006). Nitrocellulose membranes from the kit were blocked with Array Buffer 6 for an hour at room temperature. Meanwhile, samples from CM of adipocytes are diluted with Array Buffer 4 and antibody cocktail was added. The membranes were incubated overnight with constant agitation at 4°C. Washing steps were performed using TBST. Streptavidin-HRP secondary antibody was added to the membrane after the washing steps and chemiluminescent reagents were applied. The protein spots were detected using hyper film ECL (GE healthcare) and quantification of spot densities was carried out using ImageJ software.

3.5.2 Recombinant chemokine treatment

Human recombinant proteins for CCL7, IL6, Leptin and CXCL13 were purchased from Peprotech. These recombinant proteins were used at a concentration from 10 ng/ml to 500 ng/ml per well in a 6-wells plate. For treatment, 1.5 x 10^5 cells were seeded in a 6-well plate and treated with the recombinant proteins for 48 hours. After 2 days, RNA and proteins were collected and stored at -20°C.

3.5.3 Validation of TRIB1 and TRIB3 constructs using HEK-293T cells

Lentiviral vectors were used to overexpress or knockdown *TRIB1* and *TRIB3* in PCa cells. These vectors were first tested in HEK-293T cells and transfection efficiency was confirmed by observing GFP positive cells under a fluorescent microscope. Around 90% of the cells showed fluorescence and 48 hours after transfection and cells were collected for protein isolation. TRIB1 knockdown and overexpression and TRIB3 knockdown were confirmed by performing immunoblot, as shown in Figure 3.5.3. After the validation, HEK-293T cells were used further to generate lentivirus for transducing PCa cell lines (Du145 and PC3). TRIB1 shRNAs did not show any knockdown in HEK-293T cells; therefore, we decided to overexpress TRIB1 in both the cell lines.

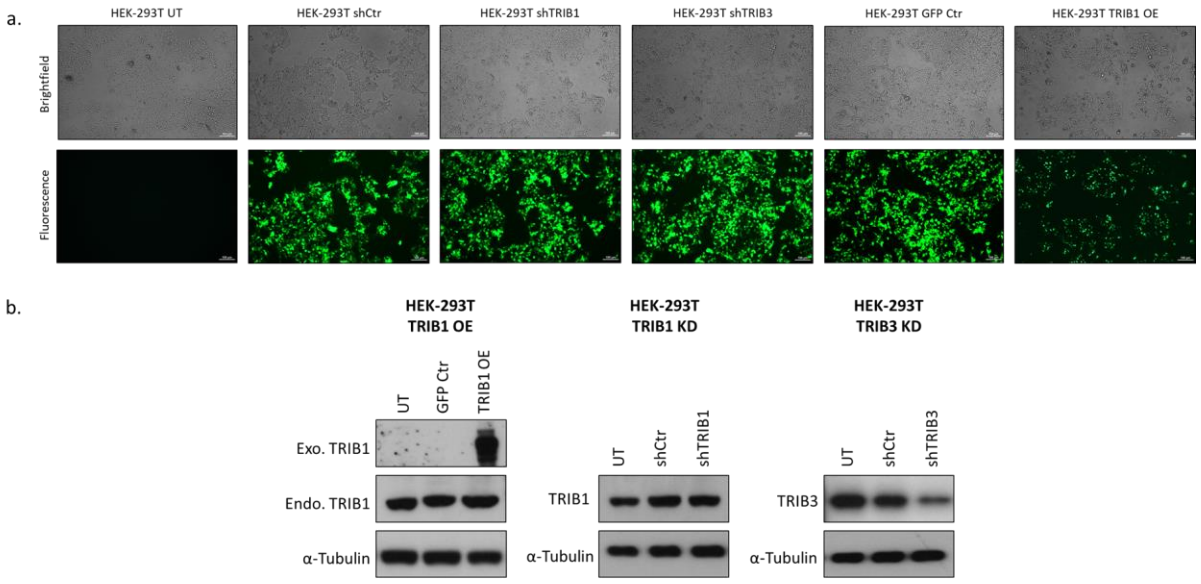

Figure 3.5.3: TRIBs modulation in HEK-293T cells.
(a) HEK-293T cells were transduced with lentivirus containing shRNAs for TRIB1 or TRIB3 and cDNA constructs for TRIBs. No virus control is shown by untreated cells (UT). shRNA Ctr was used as a control for cells transduced with shRNA and GFP Ctr was used as a control for TRIB1 OE. GFP positive cells were observed by fluorescence microscope. (b) TRIB1 overexpression (TRIB1 OE), TRIB1 knockdown (TRIB1 KD) and TRIB3 knockdown (TRIB3 KD) was confirmed by performing immunoblot.

3.6 Results

3.6.1 Effect of co-culturing between adipocyte cells and PCa cells on TRIBs levels

To investigate whether adipocytes influence TRIBs expression in PCa cells, a co-culture system was applied. Pre- and mature adipocytes from 3T3-L1 and 3T3-F442A cells were seeded on a 6-well plate and the PCa cell lines Du145, PC3 and TRAMP-C2 were placed above in the Transwell inserts. After co-culturing with adipocytes for 48 hours, we saw a significant increase in TRIB1 and TRIB3 mRNA and protein expression in Du145 and PC3 cells (Figure 3.6.1). This increase in TRIBs expression was cell type specific: PC3 cells showed increased TRIB1 and TRIB3 expression when co-cultured with 3T3-L1 adipocytes, while Du145 cells showed higher TRIB1 and TRIB3 levels when cultured with 3T3-F442A adipocytes. Furthermore, we only saw the increase in TRIBs expression with differentiated adipocytes from both the cell lines, thereby suggesting that only differentiated adipocytes could modulate the TRIBs expression. For TRAMP-C2 cells, we did not observe any differences in TRIBs expression. The TRIB2 levels remain unaffected in all three PCa cell lines. Since the mRNA levels and protein levels correlate in this experiment, we decided to perform only immunoblotting in future experiments.

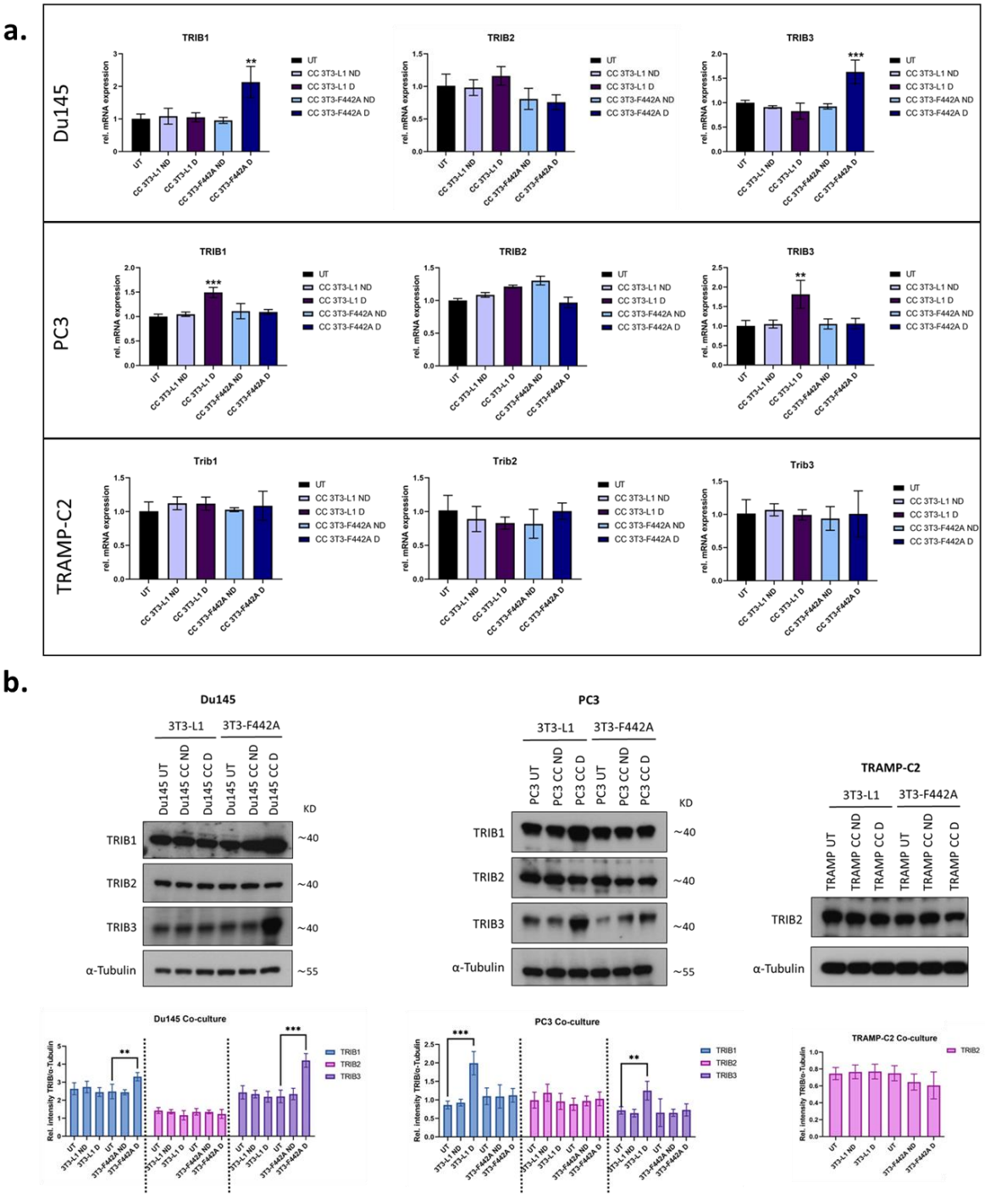

Figure 3.6.1: Increase in TRIB1 and TRIB3 at mRNA and protein levels in Du145 and PC3 cells after co-culture with adipocytes.

(a.) *TRIB1*, *TRIB2* and *TRIB3* mRNA levels in Du145 and PC3 cells after co-culture with non-differentiated (ND) and differentiated (D) adipocytes from 3T3-L1 and 3T3-F442A. The last panel shows *Trib1*, *Trib2* and *Trib3* mRNA levels from TRAMP-C2 cells showing no significant differences. Data represent the mean ±SD from three independent biological replicates. Ordinary One Way ANOVA, ** P ≤ 0.01, ***P ≤ 0.001 compared to the UT group. (b.) PCa cells were co-cultured with both non-differentiated (ND) and differentiated (D) adipocytes. For the untreated (UT) control, tumour cells were cultured alone in the Transwell inserts. Immunoblots were performed to detect changes in TRIBs expression in the tumour cells. The bar charts below represent relative quantification of immunoblot band intensities normalised to α-Tubulin. Data represent the mean ±SD from three independent biological replicates. Ordinary One Way ANOVA, ** P ≤ 0.01, ***P ≤ 0.001 compared to the UT group.

3.6.2 Factors secreted factors by 3T3-L1 and 3T3-F442A cells increase TRIB1 and TRIB3 expression in PCa cells

Next, we determined whether the increase in the TRIBs expression is due to secretory factors from adipocytes. We used only conditioned media (CM) derived from adipocytes to perform CM culture. As we did not observe any differences in TRIBs expression when co-culturing with non-differentiated adipocytes, here we only used the CM from differentiated adipocytes. Additionally, we performed these experiments with Du145 and PC3 cells since these cells showed differences with TRIBs expression. Interestingly, we observed similar results as our initial co-culture experiment and found an increase in TRIBs expression, which was cell type specific, as shown in Figure 3.6.2. Du145 and PC3 cells showed increased TRIB1 and TRIB3 expression as compared to untreated controls upon incubation with CM, thus confirming that adipocyte secretory factors mediate the increase in TRIBs levels.

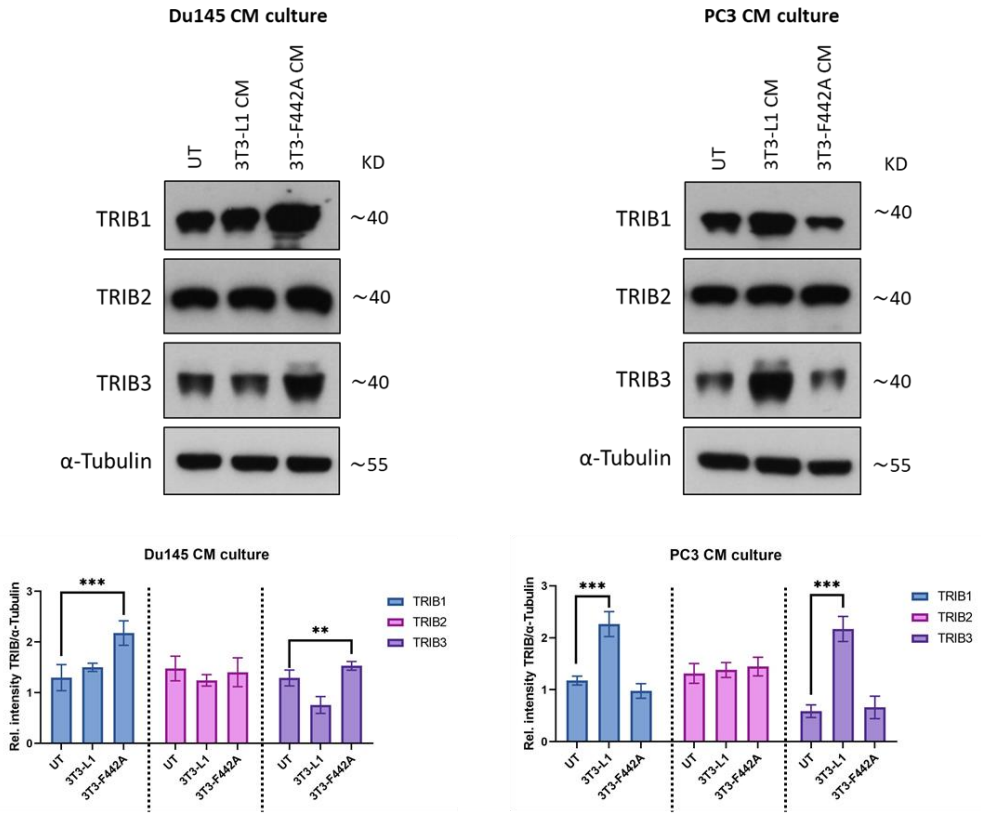

Figure 3.6.2: CM from 3T3-L1 and 3T3-F442A contribute to the increase in TRIB1 and TRIB3 expression in Du145 and PC3 cells.

PCa cells were cultured with conditioned media (CM) from 3T3-L1 and 3T3-F442A cells. For UT control, tumour cells were cultured with culture media alone. Immunoblots were performed to detect changes in TRIBs expression in the tumour cells. The bar charts below represent the relative quantification of immunoblot band intensities normalised to α-Tubulin. Data represent the mean ±SD from three independent biological replicates. Ordinary One Way ANOVA, ** P ≤ 0.01, ***P ≤ 0.001 compared to the UT.

3.6.3 CM derived from visWAT of mice shows an increase in TRIB1 and TRIB3 expression

Given the effect of CM from adipose cell lines on TRIBs expression in PCa cells, we evaluated the effect of CM from primary adipocytes from adipose tissue of mice on PCa cells. Since mice do not have an adipose capsule surrounding the prostate gland, we isolated the visceral adipose tissue (visWAT), which is the closest fat deposit to the prostate. We used the CM from the visWAT of Trib3 WT mice that were generated in Chapter 4 for this experiment. We also included the non-differentiated adipocyte CM that was obtained from the SVF cells as an additional control. Du145 and PC3 cells were incubated with CM of mouse visWAT for 48 hours. After the CM culturing, we saw a significant increase in TRIB1 protein levels in Du145 cells and an increase in TRIB3 protein levels in PC3 cells, as observed in Figure 3.6.3. These results complemented our *in vitro* data from 3T3-L1 and 3T3-F442A adipose cell lines and also showed a cell type specific increase in the TRIB1 and TRIB3 expression.

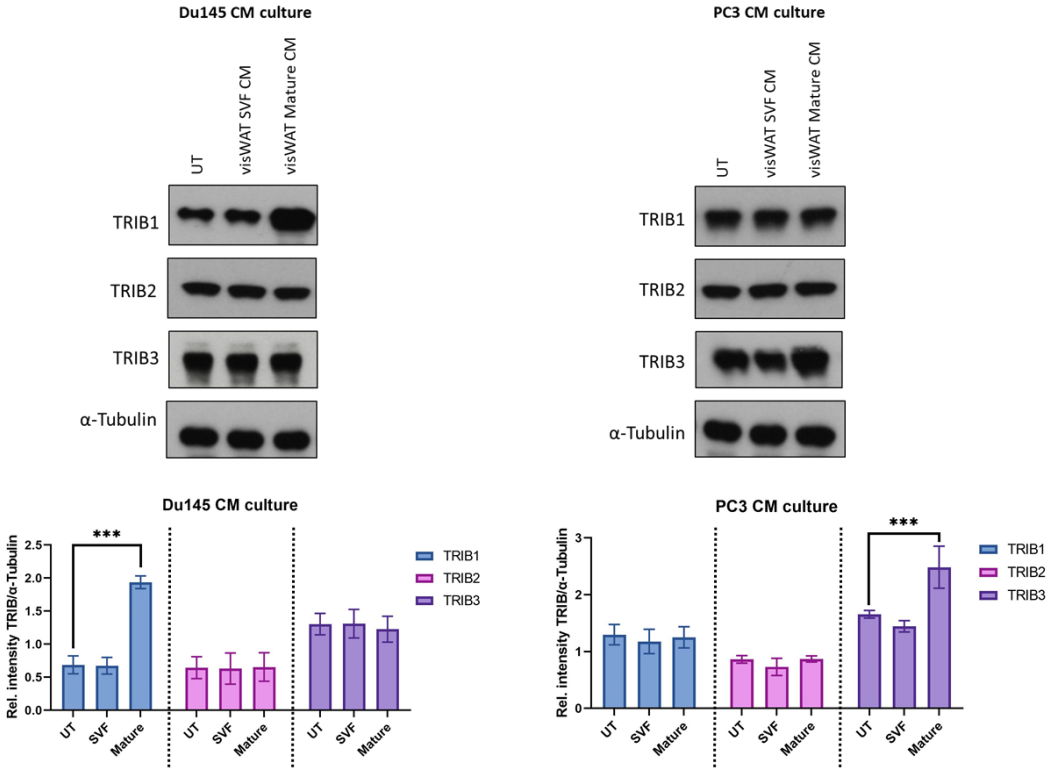

Figure 3.6.3: CM from visWAT increases TRIB1 levels in Du145 cells and TRIB3 levels in PC3 cells.
PCa cells were cultured with CM of mature adipocytes from mouse visWAT. As a control, tumour cells were cultured with culture media alone and CM from SVF cells. Immunoblots were performed to detect changes in TRIBs expression in the tumour cells. The bar charts below represent the relative quantification of immunoblot band intensities normalised to α-Tubulin. Data represent the mean ±SD of the CM from 6 mice. Ordinary One Way ANOVA, ***P ≤ 0.001 compared to the UT.

3.6.4 CM derived from PPAT of PCa patients increases in TRIB3 levels in Du145 and PC3 cells

Following the increase of TRIB1 and TRIB3 expression in PCa upon incubation with CM of adipocytes from both cell lines and primary adipocytes from mice. It was interesting to determine whether we would see a similar effect with the CM from PCa patients. We obtained PPAT from PCa patients undergoing radical prostatectomy and isolated mature adipocytes, as described in section 2.2.2. CM from mature adipocytes and SVF cells was cultured with Du145 and PC3 cells for 48 hours. As observed in Figure 3.6.4, there was an increase in TRIB3 expression in both the PCa cell lines. This time we did not detect any modulation of TRIB1 expression. The data represents CM from two PCa patients as part of preliminary experiment and additional experiments should be performed to confirm our observation by increasing the number of patient samples.

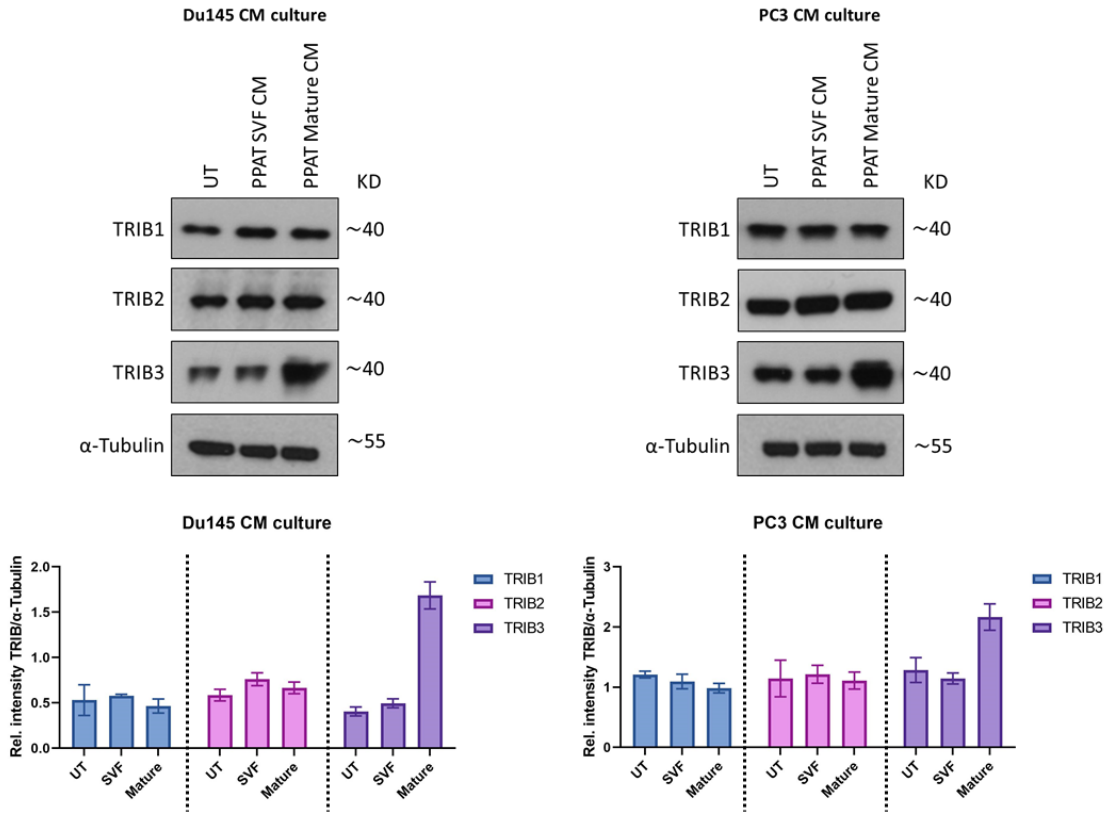

Figure 3.6.4: CM from PPAT increase TRIB3 protein levels in Du145 and PC3 cells.
PCa cells were cultured with CM from PPAT of two PCa patients. For control, tumour cells were cultured with culture media alone and CM from SVF cells. Immunoblots were performed to detect changes in TRIBs expression in the tumour cells. The bar charts represent relative quantification of immunoblot band intensities normalised to α-Tubulin.

3.6.5 Effect of adipose tissue microenvironment on TRIBs expression in Breast cancer cells

To verify whether the increase of TRIB1 and TRIB3 expression was specific to PCa, we used another type of cancer with a similar adipose tissue microenvironment, i.e. breast cancer. Several studies have shown that adipocytes surrounding the breast contribute to breast cancer tumorigenesis (Bertolini 2013, Wu, Li et al. 2019). We used cell lines that represent the three major types of breast cancer: HER2 positive (BT-474), triple-negative (MDA-MB-231) and estrogen-receptor-positive (MCF-7). Breast cancer cells were co-cultured with non-differentiated and differentiated adipocytes from 3T3-L1 and 3T3-F442A cells. After the co-culture, the TRIBs protein expression was analysed by immunoblotting. Interestingly, we did not detect any significant differences in TRIB1, TRIB2 and TRIB3 expression upon co-culturing. Therefore, showed that the increase in TRIB1 and TRIB3 expression was specific to the adipose tissue microenvironment surrounding the PCa cells.

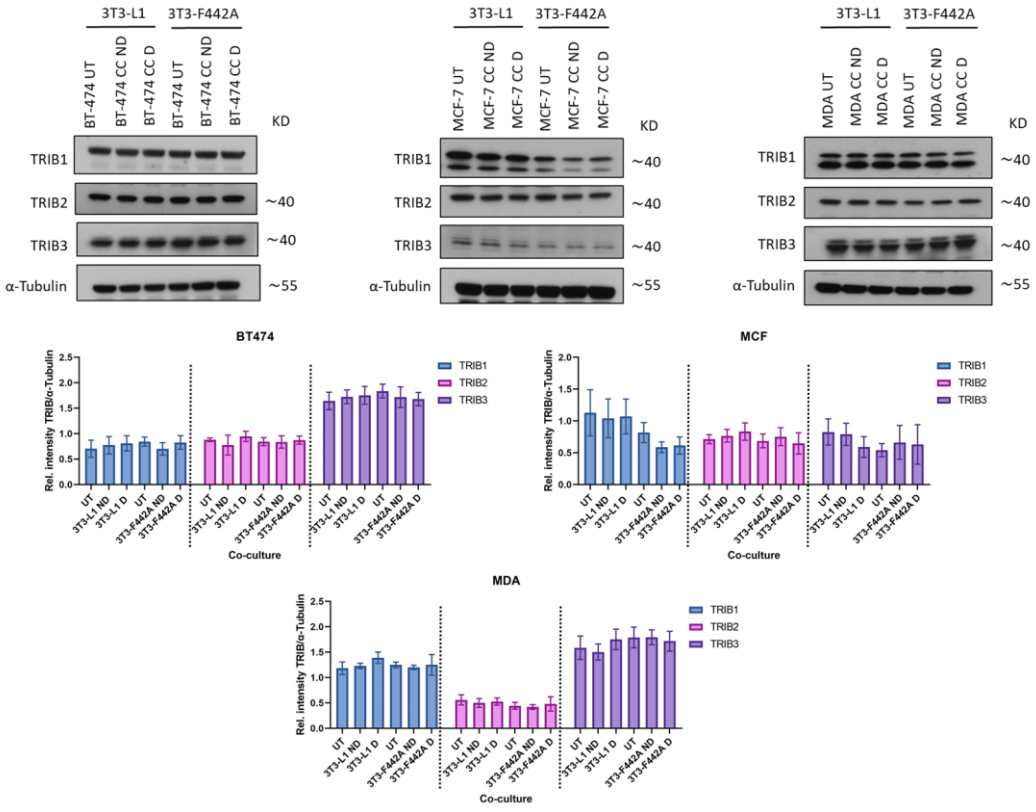

Figure 3.6.5: Breast cancer cells showing no differences in TRIBs expression after co-culturing with adipose cell lines.

Breast cancer cells were co-cultured with both non-differentiated (ND) and differentiated (D) adipocyte cell lines. For control, tumour cells were cultured alone in the co-culture inserts. Immunoblots were performed to detect changes in TRIBs expression in the tumour cells. The bar charts represent relative quantification of immunoblot band intensities normalised to α-Tubulin. Data represent the mean ±SD from three independent biological replicates. Ordinary One Way ANOVA, p>0.05.

3.6.6 Cytokine expression levels in CM from 3T3-L1 and 3T3-F442A cells

Next, to identify chemokines responsible for the increase in TRIB1 and TRIB3 expression in PCa cells, we performed Mouse Cytokine Array on the CM from 3T3-L1 and 3T3-F442A cells. Out of the 40 different cytokines present on the membrane, CXCL13, CXCL10, TIMP-1, CXCL1, M-CSF, CCL2, IL-1F3, CXCL12, CCL5 and TNF-α were detected from the CM of 3T3-L1 and 3T3-F442A cells. Since our previous results showed a cell type specific increase in TRIB1 and TRIB3 levels upon co-culture and CM culture, we only selected the chemokines that were differentially expressed by either 3T3-L1 or 3T3-F442A. Since TNF-α was detected in small amounts and present in only one of the samples, we selected CXCL13 as a candidate chemokine for future analysis, which was secreted explicitly by 3T3-L1 CM.

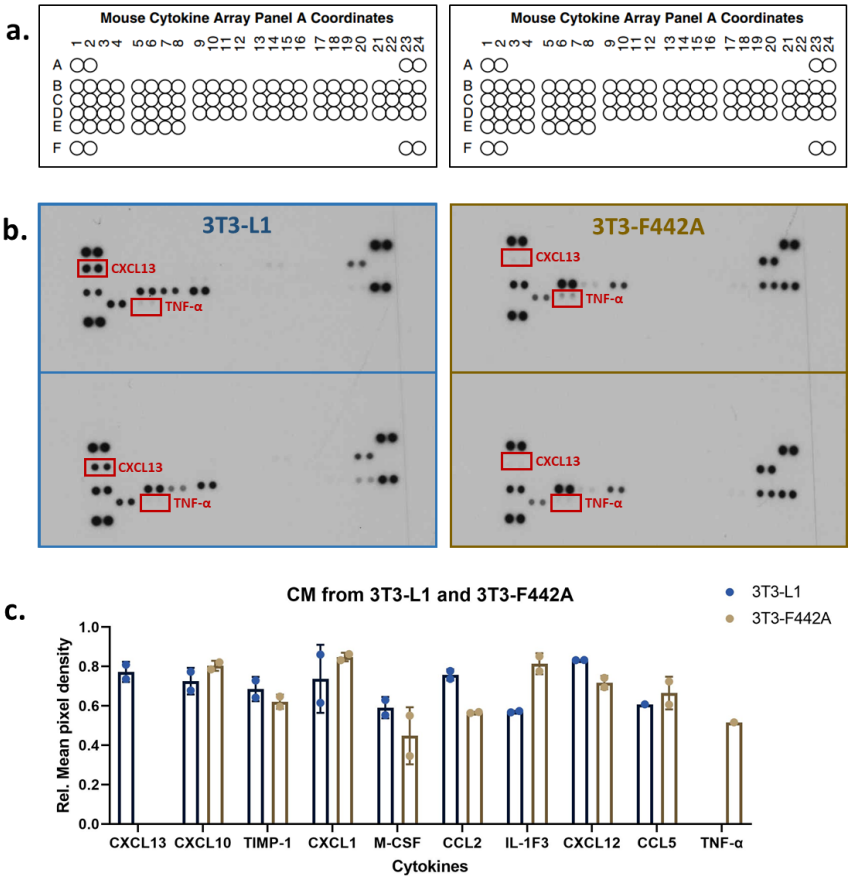

Figure 3.6.6: Cytokine expression levels in the CM from 3T3-L1 and 3T3-F442A cells
(a) Mouse Cytokine Array Panel A contains 40 different cytokines spotted in duplicates (b) Nitrocellulose blot representing two independent experiments using CM from 3T3-L1 and 3T3-F442A differentiated cells. (c) Relative expression levels of cytokines were normalised to the manufacturer's positive control samples. In particular, the expression of CXCL13 and TNF-α was specific to each cell line. Data represent the mean ±SD from two independent biological replicates.

3.6.7 IL6, Leptin and CXCL13 contribute to changes in TRIBs expression in Du145 and PC3 cells

Following the detection of CXCL13, which was solely secreted by 3T3L-1 cells, we planned to investigate whether this chemokine was involved in modulating TRIBs expression in PCa cells. In addition to CXCL13, we selected three other adipokines, i.e. CCL7, IL6 and Leptin based on the available literature described in section 1.4.3 (Rojas, Liu et al. 2011, Alshaker, Sacco et al. 2015, Laurent, Guerard et al. 2016). To determine the effect of these chemokines on Du145 and PC3 cells, we used recombinant proteins at concentrations ranging from 10-500ng/ml. Furthermore, after the addition of the recombinant proteins on PCa cells, we incubated the plates at 37°C for 48 hours, the same duration as the CM culture experiments. Figure 3.6.7 illustrates the increase in TRIB1 and TRIB3 expression in Du145 cells by Leptin treatment over 250 ng/ml. Recombinant IL6 protein promoted an increase in TRIB3 expression in Du145 cells. As for PC3 cells, the immunoblots (Figure 3.6.7b) show increase of TRIB3 expression with CXCL13 from the doses above 50ng/ml. Overall, we observe cell type specific increase of TRIBs levels following the recombinant chemokine treatment as seen with CM culture experiment.

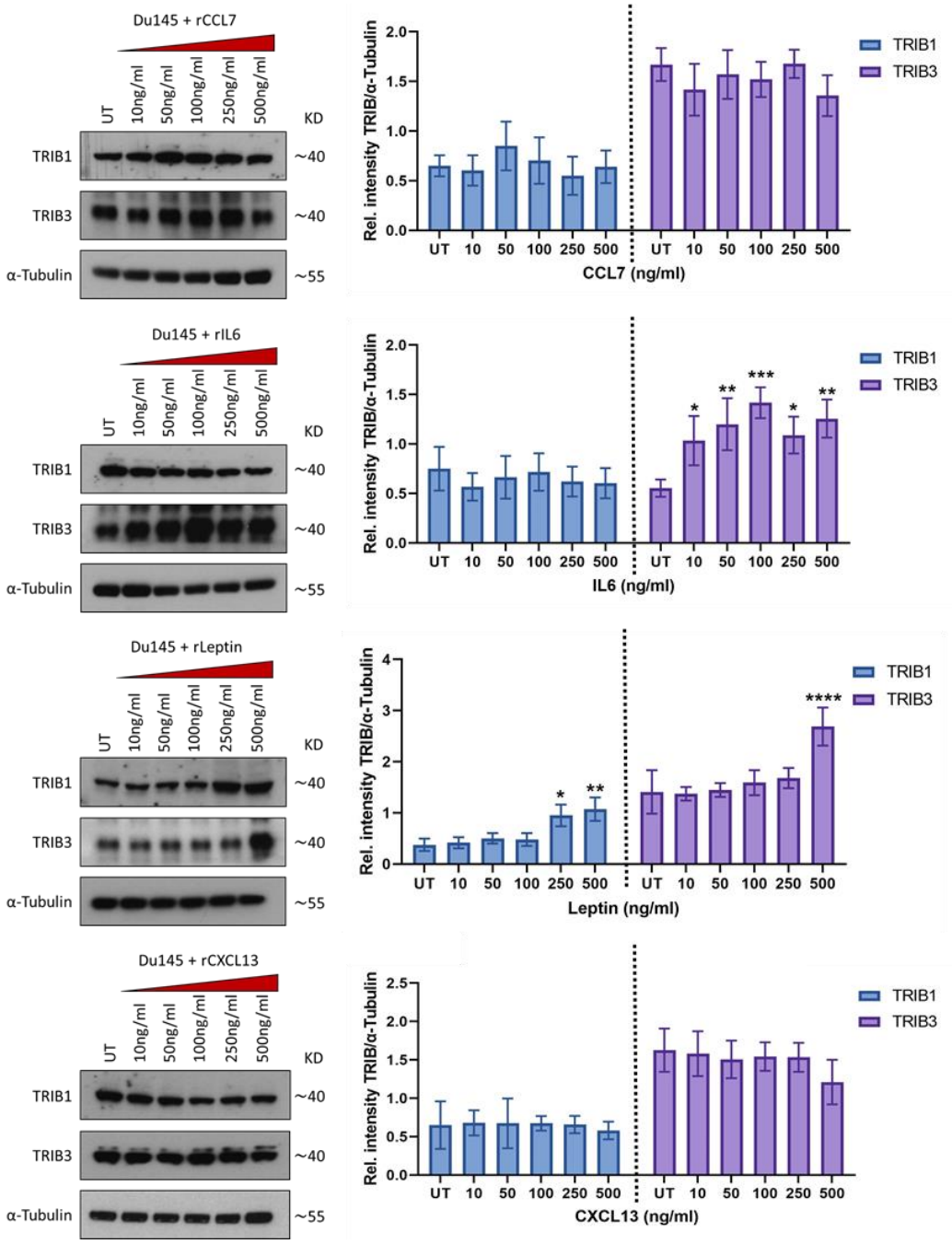

Figure 3.6.7: PCa cells treated with human recombinant chemokines (rCCL7, rIL6, rLeptin, rCXCL13)
Du145 cells treated with human recombinant chemokines (rCCL7, rIL6, rLeptin, rCXCL13) from 10-500ng/ml. After 48 hours, immunoblots were performed to identify any differences in TRIB1 and TRIB3 protein expression. The bar charts represent relative quantification of immunoblot band intensities normalised to α-Tubulin. Data represent the mean ±SD from three independent biological replicates. Ordinary One Way ANOVA,* P ≤ 0.05, ** P ≤ 0.01, ***P ≤ 0.001, **** P ≤ 0.0001 compared to the UT.

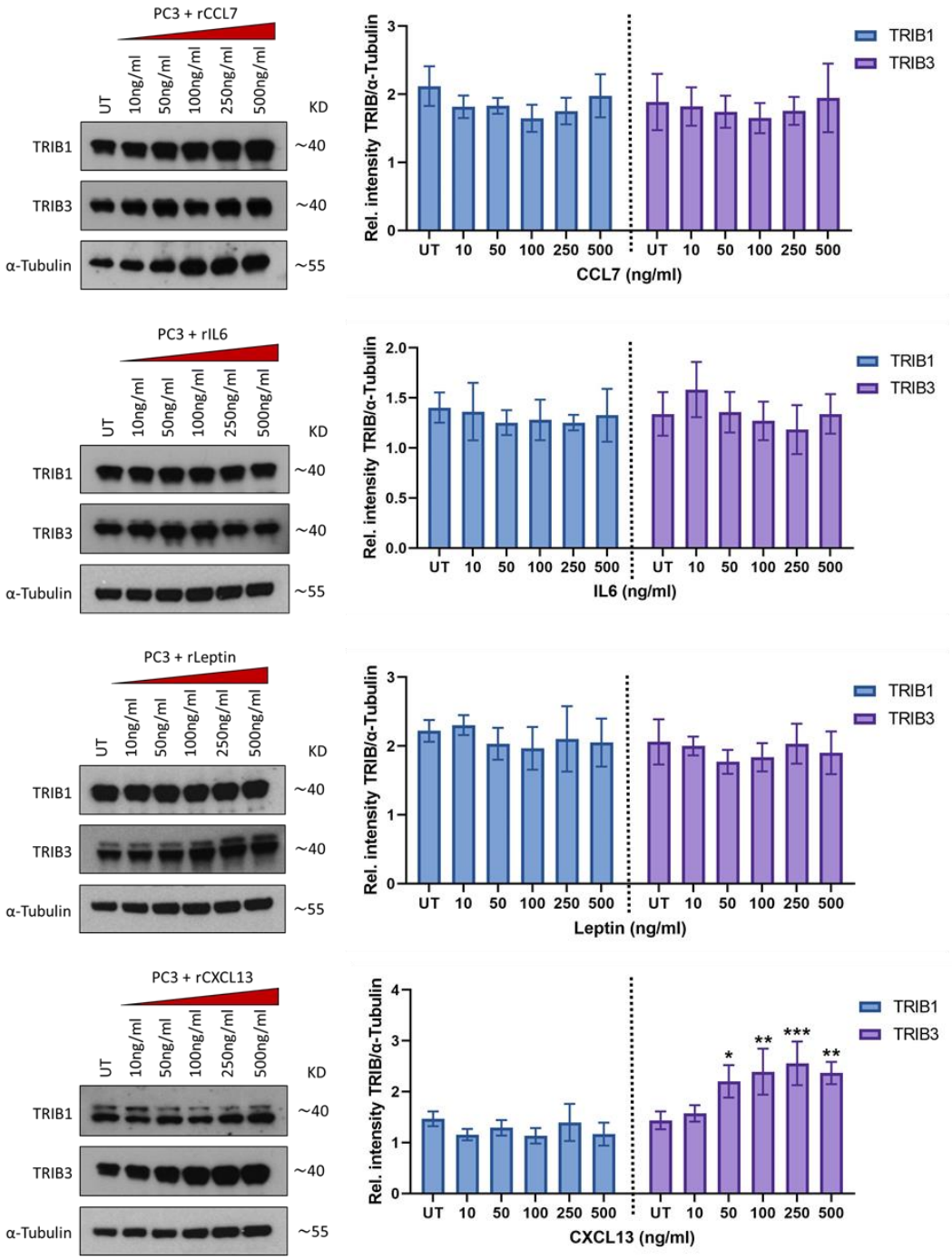

Figure 3.6.7b: PCa cells treated with human recombinant chemokines (rCCL7, rIL6, rLeptin, rCXCL13)
Recombinant chemokine proteins (10-500ng/ml) were incubated with PC3 cells for 48 hours. Thereafter, immunoblots were performed to identify any differences in TRIB1 and TRIB3 protein expression. The bar charts represent relative quantification of immunoblot band intensities normalised to α-Tubulin. Data represent the mean ±SD from three independent biological replicates. Ordinary One Way Anova, * P ≤ 0.05, ** P ≤ 0.01, ***P ≤ 0.001 compared to the UT.

3.6.8 Generation of stable PCa cells with *TRIB1* and *TRIB3* modulation

After our initial findings of *TRIB1* and *TRIB3* modulation in PCa cells upon incubation with adipocyte CM culture, we continued with our next objective to investigate the role of *TRIB1* and *TRIB3* in PCa progression. Generation of stable cell lines by knockdown or overexpression of the genes of interest is used to characterize their functional role *in vitro*. Lenti-virus transfection is a gene delivery method to generate stable cell lines (Scherr, Venturini et al. 2010). Based on the basal levels of TRIBs expression in PCa cells (Data not shown), we generated stable TRIB3 knockdown (KD) and TRIB1 overexpressing (OE) cells using Lentiviral vectors. The efficiency of knockdown and overexpression mediated by the shRNAs and cDNA constructs was first validated in HEK-293T cells (Figure 3.5.3). Thereafter, HEK-293T cells were used for Lentivirus production, as described in section 2.5. In PCa cells, TRIBs modulation was confirmed using RT- PCR, immunoblot and immunofluorescence, as shown in Figure 3.6.8 and Figure 3.6.8b. Furthermore, TRIBs modulated Du145 and PC3 cells were used for tumour behavioural studies such as cell viability, proliferation, migration and invasion in the presence or absence of the CM of adipocytes.

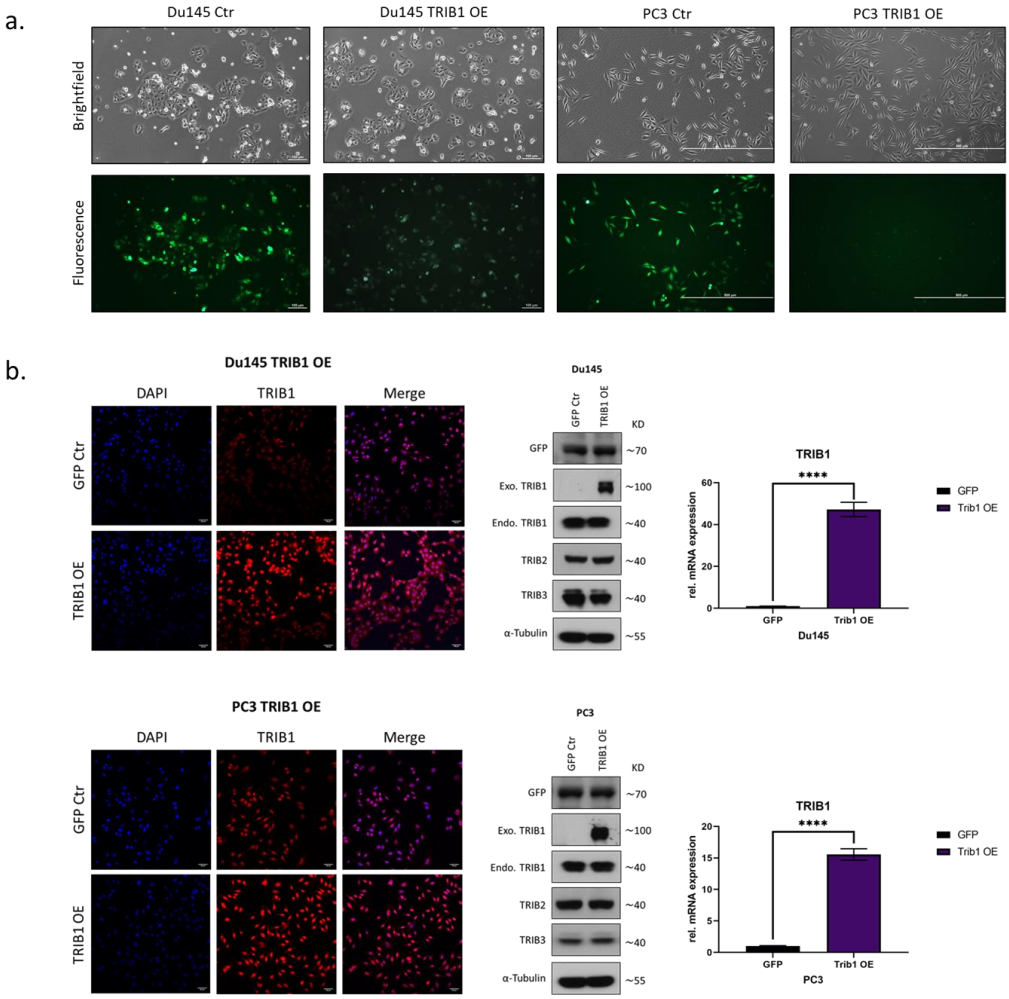

Figure 3.6.8: TRIBs modulation in Du145 and PC3 cells.
(a) Du145 and PC3 cells with TRIB1 overexpression. GFP positive cells were observed by fluorescence microscope. (b) TRIB1 overexpression was confirmed by performing immunofluorescence, immunoblot and RT-PCR. Data represent the mean ±SD from three independent biological replicates. Unpaired t-test, **** P ≤ 0.0001 compared to the GFP control.

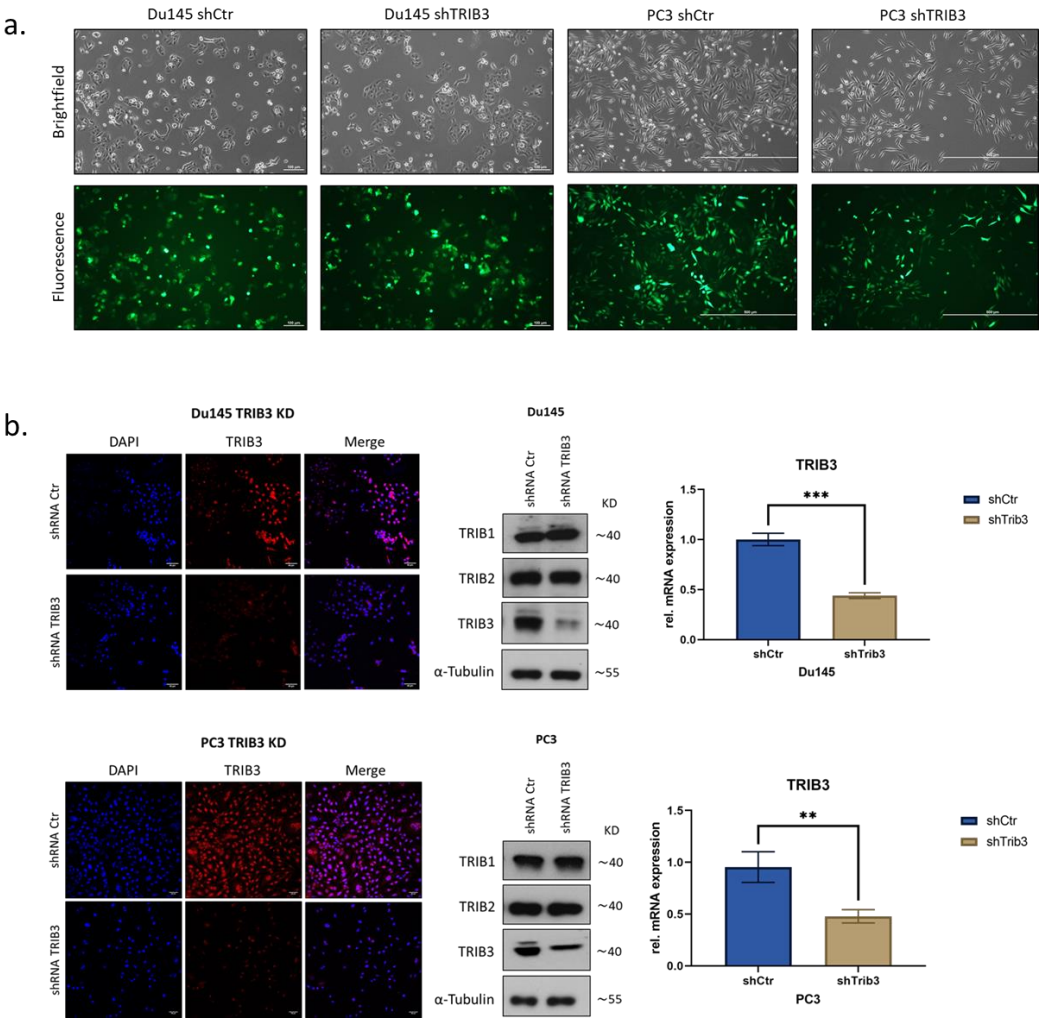

Figure 3.6.8b: TRIBs modulation in Du145 and PC3 cells.
(a) Du145 and PC3 cells with TRIB3 knockdown. GFP cells were observed by fluorescence microscope. (b) TRIB1 knockdown was confirmed by performing immunofluorescence, immunoblot and RT-PCR. Data represent the mean ±SD from three independent biological replicates. Unpaired t-test ** P ≤ 0.01, ***P ≤ 0.001 compared to the GFP control.

3.6.9 *TRIB3* knockdown inhibits cell viability in Du145 cells upon CM culture

First, we started with Du145 and PC3 cells with *TRIB3* KD and tested their cell viability compared to the control cells. Du145 and PC3 cells were seeded in 96-well ULA plate and 3D spheroids were generated. 4 days after the spheroid formation, CM of 3T3-L1 and 3T3-F442A cells and cell viability reagents were added and the measurements were taken every 24 hours for 3 days. For Du145 cells, the culture media did not show any differences in viability at 48 and 72 hours, as shown in Figure 3.6.9. However, after CM was added, Du145 cells with *TRIB3* KD showed a significant decrease in viability when compared to shCtr cells at 48 and 72 hours. The PC3 cells with *TRIB3* KD showed reduced viability with the culture media at 48 hours and no effect was observed with the CM. We also compared the group shCtr cells UT with shCtr cells CM to confirm our experimental system since it has been previously reported that PCa cells should have increased growth and migration when in cultured with CM (Laurent, Guerard et al. 2016).

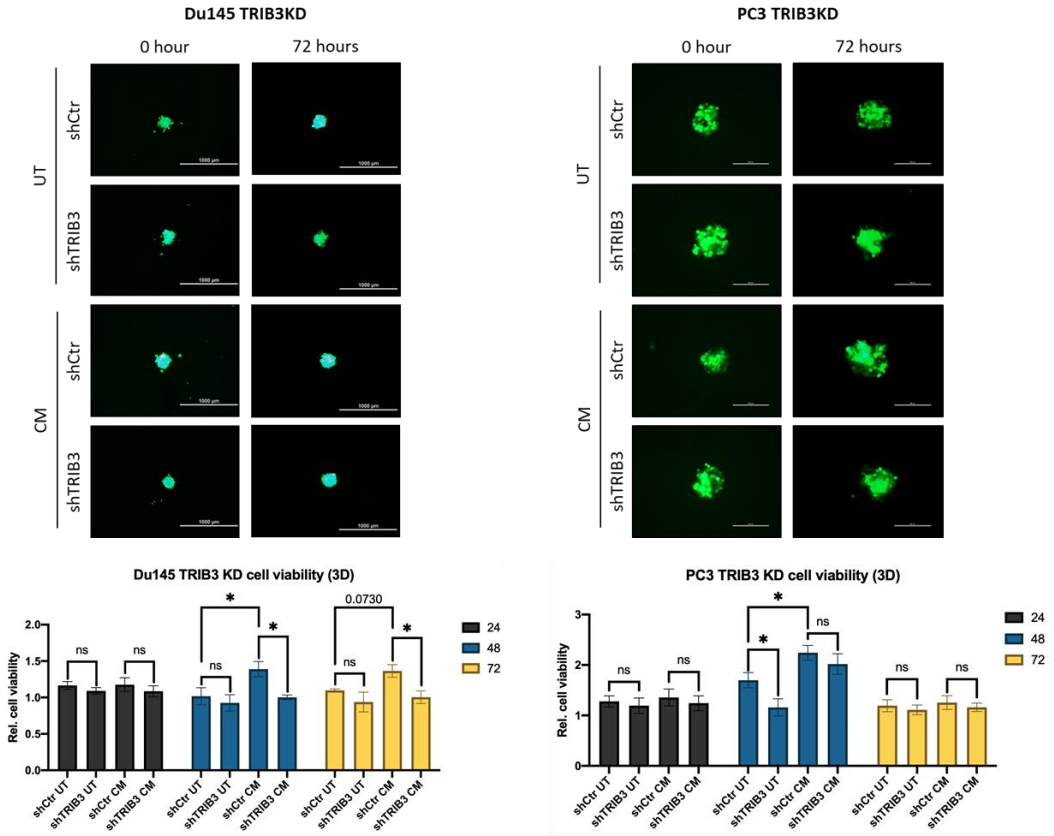

Figure 3.6.9: 3D cell viability of PCa cells having *TRIB3* KD upon CM from adipocytes
The Du145 and PC3 cells were seeded as 3D spheroids and pictures were taken after the addition of CM at 0 hour and 72 hours. The bar charts represent cell viability over 72 hours compared to shCtr (UT/CM). Data show the mean ±SD from three independent experiments. 2way ANOVA, * P ≤ 0.05, ns p>0.05 compared to shCtr UT/CM.

3.6.10 *TRIB3* knockdown inhibits cell proliferation in PC3 cells upon CM culture

Next, we assessed cell proliferation by measuring the dividing cells using CyQUANT® Cell Proliferation Assay. Du145 and PC3 cells were seeded in a black-wall 96-well plate, the following day cell proliferation reagents were added and measurements were taken every 24 hours for 3 days. Figure 3.6.10 showed a significant reduction in proliferation with culture media alone for Du145 *TRIB3* KD cells at 48 and 72 hours. However, for PC3 cells we observed a significant decrease in proliferation with both culture and CM. The data suggested that *TRIB3* KD lowered cell proliferation for both the cell lines at 48 hours. We also saw a significant increase in proliferation when we compared PC3 UT cells with PC3 cells incubated with CM at 48 hours.

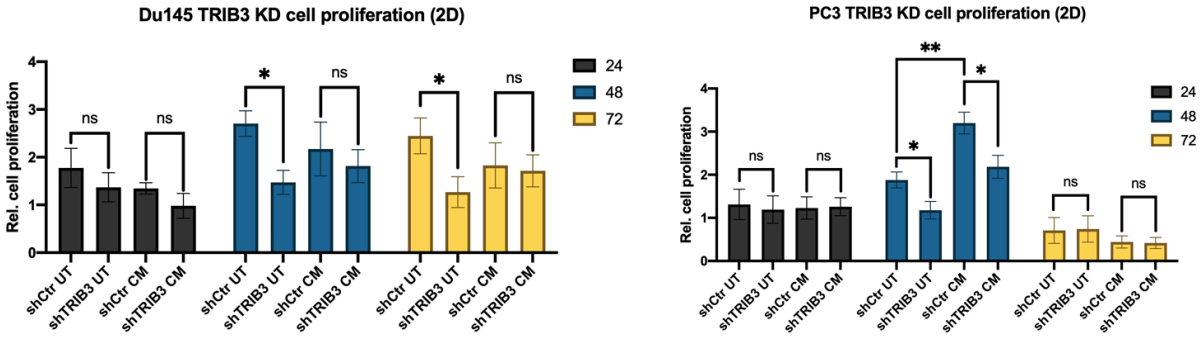

Figure 3.6.10: 2D cell proliferation with PCa having *TRIB3* KD upon CM culture
Du145 and PC3 cells were seeded as 2D culture in 96-well plate and cell proliferation reagents were added every day over 3 days. The graphs represent cell proliferation measurements over 72 hours compared to shCtr (UT/CM). Data show the mean ±SD from three independent experiments. 2way ANOVA, * P ≤ 0.05, ** P ≤ 0.01, ns p>0.05 compared to the shCtr UT/CM.

3.6.11 *TRIB3* knockdown significantly reduces cell migration in Du145 and PC3 cells upon CM culture

To gain insight into *TRIB3* KD on cell motility, the 2D scratch assay was performed. Du145 and PC3 cells were seeded onto four wells of IBIDI chambers. After the desired cell confluence was achieved, the insert between the wells was removed and 0% or 10% serum culture medium and CM was added. Pictures were taken immediately and after 24 hours. All the images were quantified using ImageJ software and the percentage of cell migration was calculated. Figure 3.6.11, as expected shows an increase in migration of Du145 and PC3 Ctr cells, after the addition of CM. However, this effect was abolished when *TRIB3* KD cells were treated with CM in both the cell lines. Thus suggesting the oncogenic role of TRIB3 in promoting cell migration upon incubation with CM.

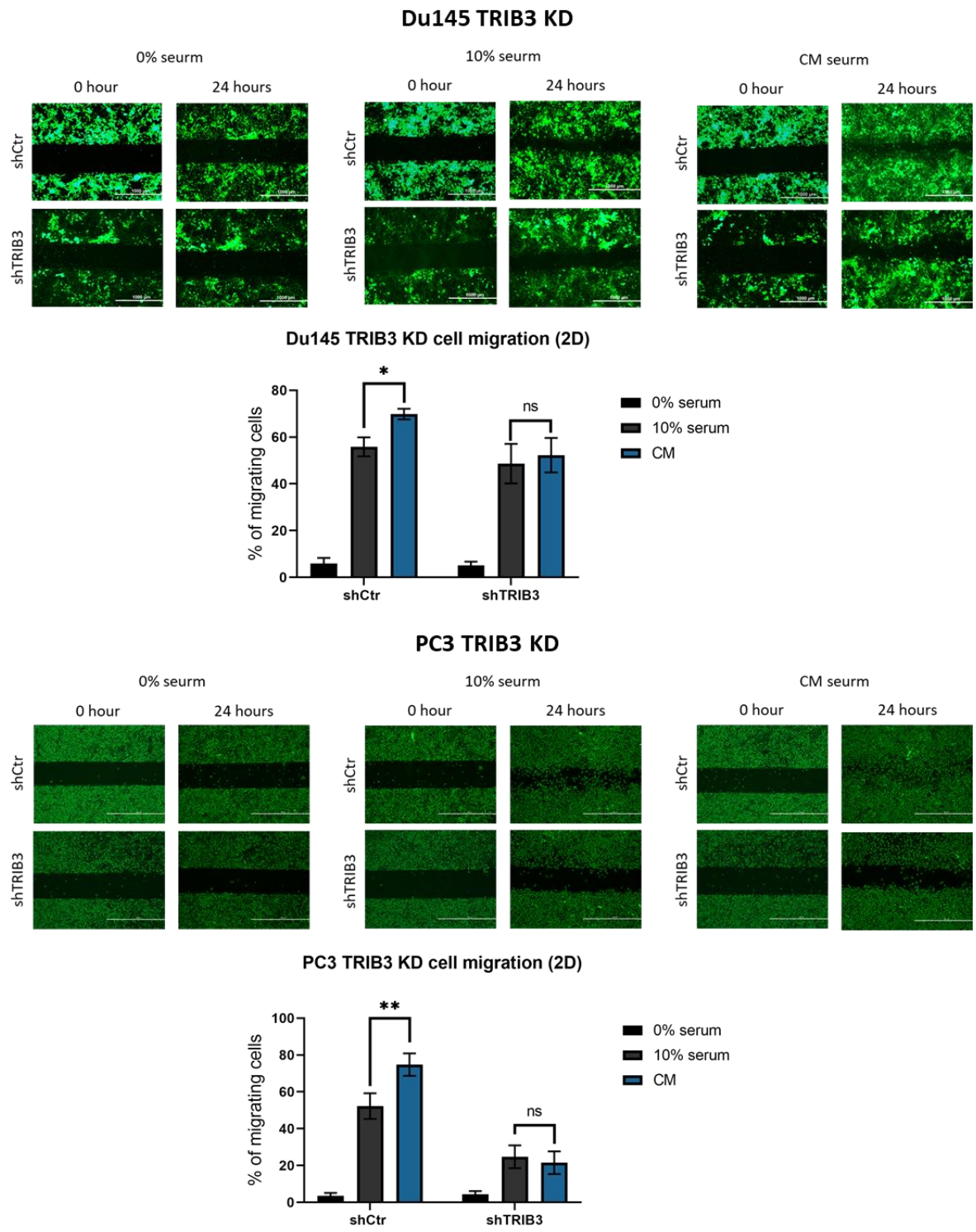

Figure 3.6.11: 2D cell migration with PCa having *TRIB3* KD upon CM culture
PCa cells were seeded in four wells of an IBIDI chamber, culture media or CM was added and pictures were taken at 0 hours and 24 hours. Du145 and PC3 shCtr cells show a significant increase in cell migration upon addition of CM. Du145 and PC3 TRIB3 KD cells has lowered migration as compared to the control cells and the tumorigenic effect of CM was suppressed. Data show the mean ±SD from three independent experiments. 2way ANOVA, * P ≤ 0.05, ** P ≤ 0.01, ns p>0.05 compared to the 10% serum group.

3.6.12 *TRIB3* knockdown significantly reduces cell invasion in PC3 cells upon CM culture

Lastly, to investigate the invasion potential of the cells through the Matrigel, we performed invasion assays. We used the 2D system to measure the cell invasion for Du145 cells since we observed that these cells do not invade in the 3D systems (Figure 4.5.5). 2D invasion assays were performed using Transwell inserts coated with Matrigel. Du145 cells were seeded on Transwell inserts and control inserts. After 24 hours, the culture medium or CM was added to the bottom well. Control inserts represent the migrating cells; these were used to calculate the percentage of invading cells in the end. As seen in Figure 3.6.12, Du145 TRIB3 KD and Ctr cells do not affect cell invasion after adding CM. While PC3 Ctr cells show a significant increase in the invasion upon CM addition, similar to the results from cell migration, the invasion was abolished when cells with TRIB3 KD were used.

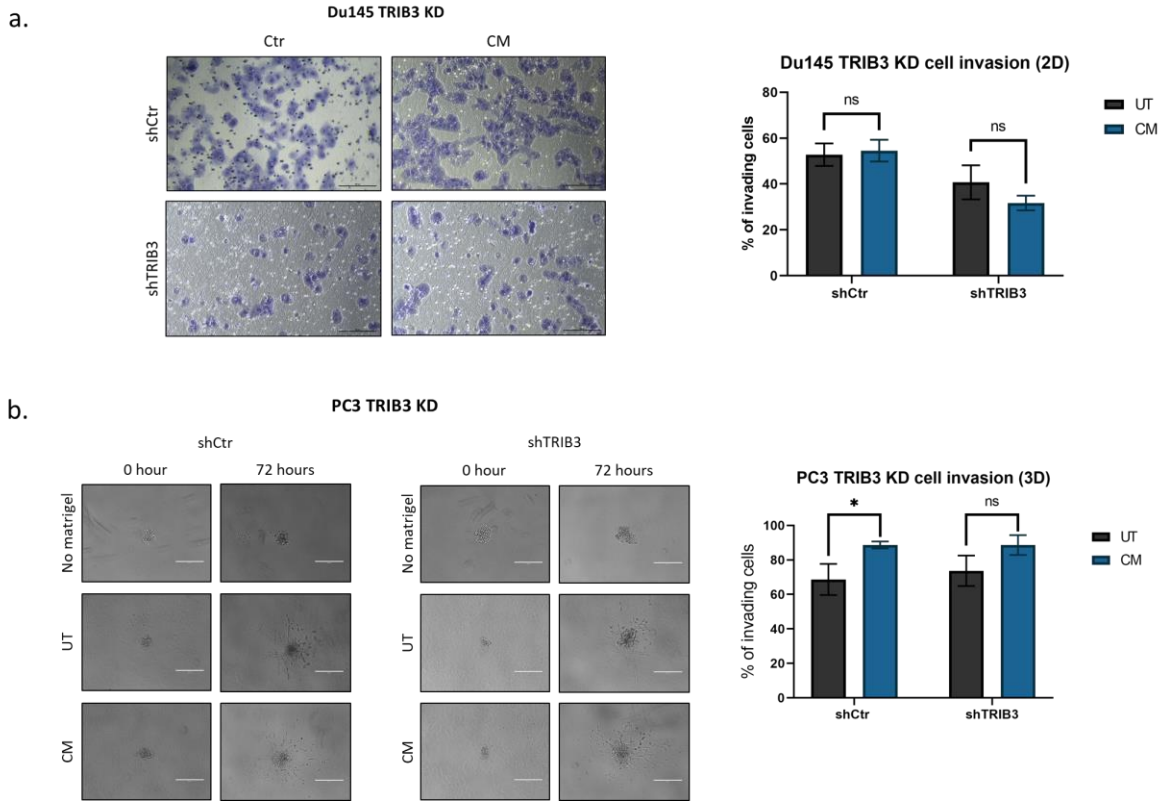

Figure 3.6.12: 2D and 3D cell invasion with PCa having *TRIB3* KD upon CM culture
(a) Du145 cells invading through the 2D Matrigel were photographed (3 technical replicates for each cell line) and pictures were taken for 3 representative fields per sample for calculating the average. Quantification was carried out in Excel by calculating the percentage of invading cells. (b) For PC3 Ctr cells, the graph shows a significant increase in the cell migration upon addition of CM. PC3 cells with TRIB3 KD do not show any differences with CM. All the data represent the mean ±SD from three independent experiments. 2way ANOVA, * $P \leq 0.05$, ns $p>0.05$ compared to the UT group.

3.6.13 *TRIB1* overexpression has no effect on cell viability of Du145 and PC3 cells upon CM culture

After performing tumour cell behavioural assays for PCa cells with *TRIB3* KD, we repeated all the experiments using Du145 and PC3 cells with *TRIB1* overexpression (OE). To determine the differences in cell viability, PCa cells were seeded in the ULA plate. 5 days after the spheroid formation, CM and cell viability reagents were added and the measurements were taken every 24 hours for 3 days. Since faint fluorescent signal was observed with *TRIB1* OE cells (Figure 3.6.8a), we took pictures of the spheroids with the light microscope for clearer images. PC3 and Du145 cells with *TRIB1* OE showed no difference in cell viability, both with culture medium and CM. However, as reported in the literature, the control cells had higher viability with CM as compared to the culture media.

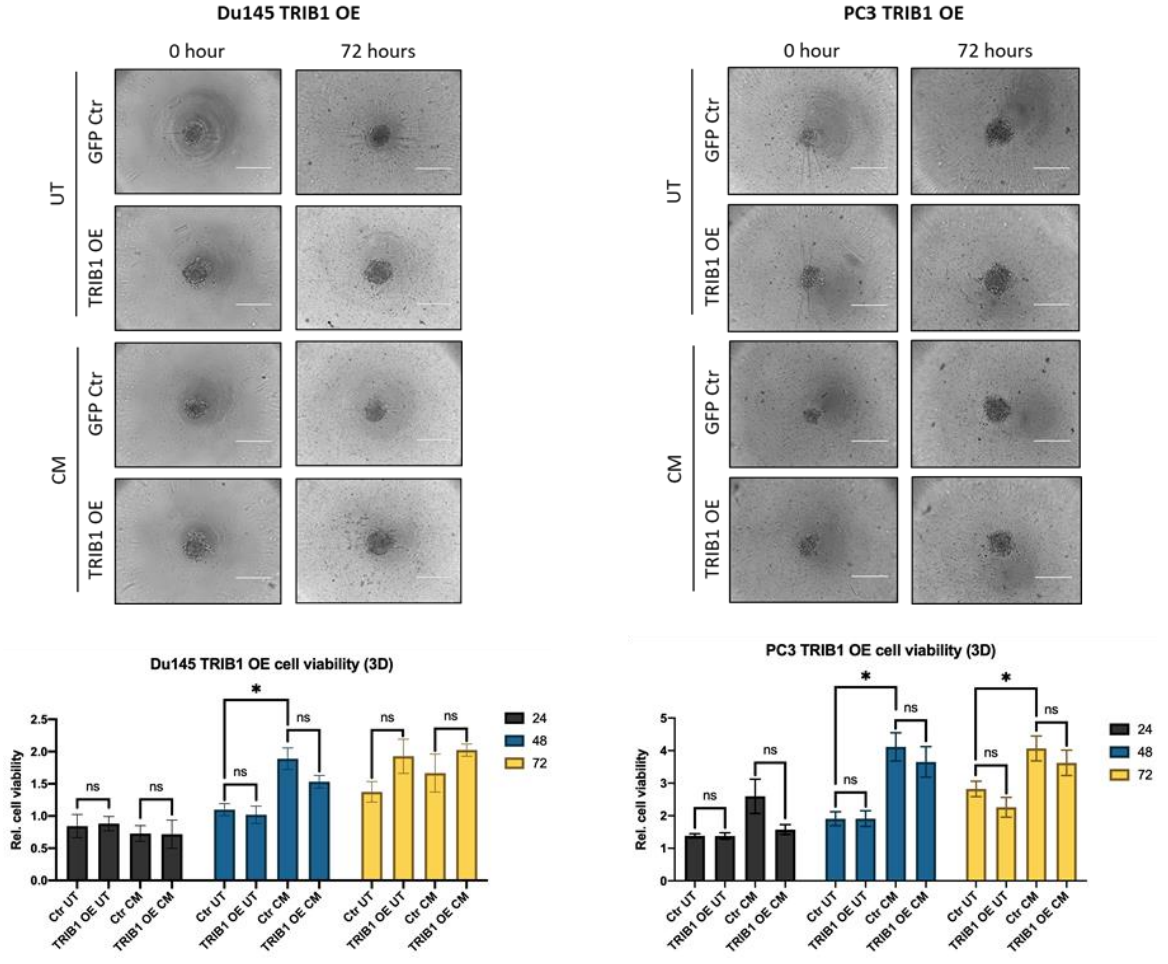

Figure 3.6.13: 3D cell viability with PCa having *TRIB1* OE upon CM culture
The Du145 and PC3 cells were seeded as 3D spheroids and pictures were taken 0 and 72 hours after spheroid formation. The bar charts represent cell viability over 72 hours compared to shCtr (UT/CM). Data show the mean ±SD from three independent experiments. 2way ANOVA, * P ≤ 0.05, ns p>0.05 compared to shCtr UT/CM.

3.6.14 *TRIB1* overexpression has no effect on cell proliferation of Du145 and PC3 cells upon CM culture

Next, we assessed cell proliferation by measuring the dividing cells using CyQUANT® Cell Proliferation Assay. Du145 and PC3 cells were seeded in a black-wall 96-well plate and the following day cell proliferation reagents were added and measurements were taken every 24 hours for 3 days. Similar to the cell viability results, PC3 and Du145 cells with *TRIB1* OE showed no differences in cell proliferation with and without CM.

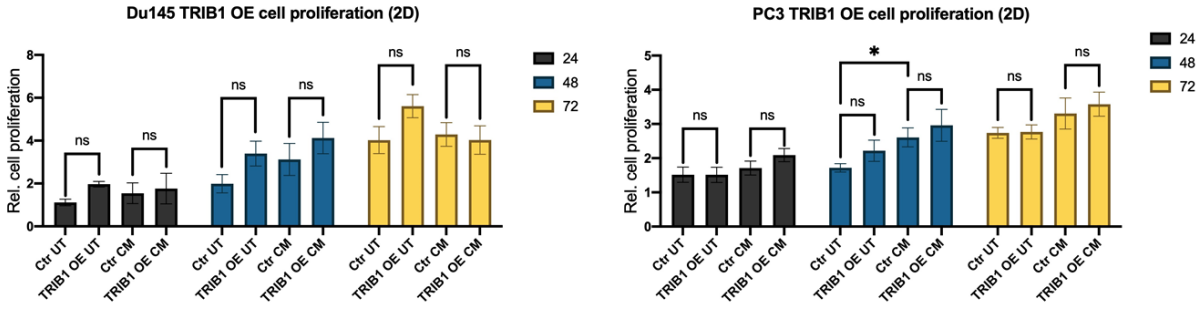

Figure 3.6.14: 2D cell proliferation with PCa having *TRIB1* OE upon CM culture
The Du145 and PC3 cells were seeded in 2D culture and cell proliferation reagents were added every day over 3 days. The graphs represent cell proliferation over 72 hours compared to shCtr (UT/CM). Data show the mean ±SD from three independent experiments. 2way ANOVA, * P ≤ 0.05, ns p>0.05 compared to the shCtr UT/CM.

3.6.15 *TRIB1* overexpression has no effect on cell migration Du145 and PC3 cells upon CM culture

To observe the effect of *TRIB1* OE on cell motility, the 2D scratch assay was performed. Du145 and PC3 cells were seeded onto four wells of IBIDI chamber. After desired cell confluence was achieved, the insert between the wells was removed and 0% or 10% serum culture medium and CM was added. Pictures were taken immediately and after 24 hours. All the images were quantified using ImageJ software and the percentage of cell migration was calculated by measuring the empty spaces between the cells. Both Du145 and PC3 *TRIB1* OE cells show a similar increase in the cell migration compared to Ctr cells upon addition of CM, thus suggesting the effect observed with CM did not depend on *TRIB1* expression.

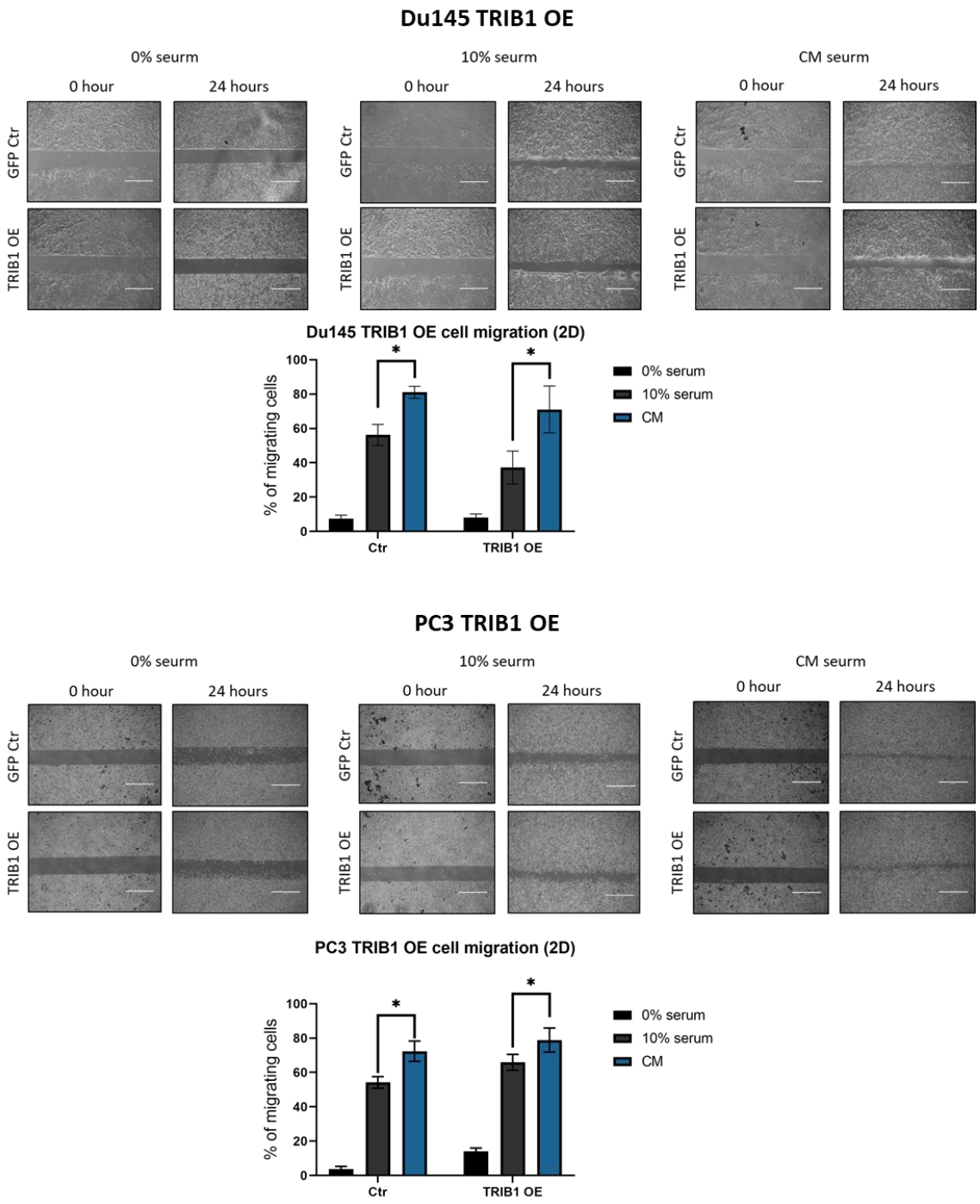

Figure 3.6.15: 2D cell migration with PCa having *TRIB1* OE upon CM culture
The PCa cells were seeded in four wells of an IBIDI chamber, once the cells were confluent, the inserts were removed and culture media or CM was added and pictures were taken at 0 hours and after 24 hours. Du145 and PC3 cells with *TRIB1* OE and Ctr cells showed increase in migration with CM. Data show the mean ±SD from three independent experiments. 2way ANOVA, * P ≤ 0.05 compared to the 10% serum group.

3.6.16 *TRIB1* OE significantly reduces cell invasion in PC3 cells upon CM culture

Lastly, to investigate the invasion potential of the cells through Matrigel, we performed invasion assays. We used the 2D system to measure the invasion of Du145 cells by seeding the cells on Transwell inserts and control inserts. After 24 hours, the culture medium or CM was added to the bottom well. Control inserts represent the migrating cells; these were used to calculate the percentage of invading cells in the end. Du145 *TRIB1* OE and Ctr cells had no effect on invasion when CM was added. PC3 cells were grown in ULA plate and 5 days after spheroid formation, Matrigel was added. Pictures of the invading cells were taken 0 and 72 hours later. PC3 cells show an increase in cell invasion upon addition of CM and this effect was abolished in *TRIB1* OE cells. Therefore suggesting the tumour suppressive role of TRIB1 for PC3 cell invasion.

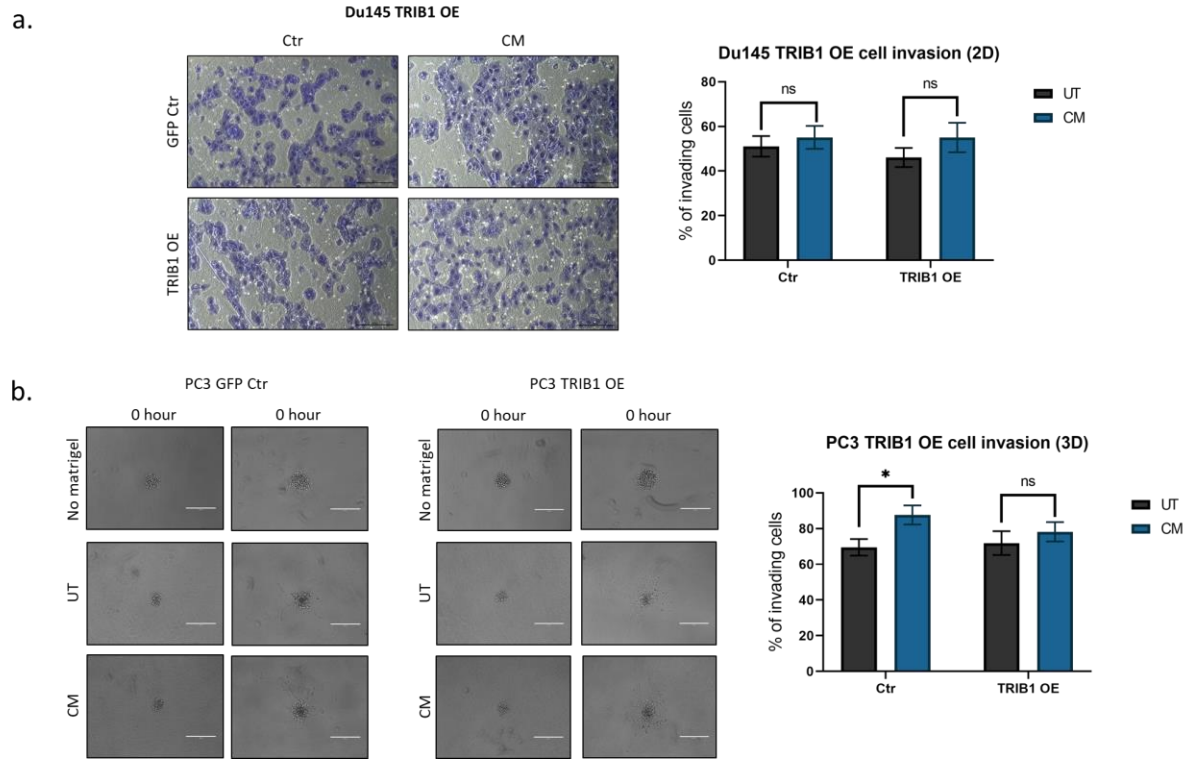

Figure 3.6.16: 2D and 3D cell invasion with PCa having *TRIB1* OE upon CM culture
(a) Du145 cells invading through the 2D Matrigel were photographed (3 technical replicates for each cell line) and pictures were taken for 3 representative fields per sample for calculating the average. Quantification was carried out in Excel by calculating the percentage of invading cells. (b) In PC3 Ctr cells, graph showed increase in cell invasion upon addition of CM while for Du145 cells with *TRIB1* OE showed no differences in invasion between culture media and CM. All the data represent the mean ±SD from three independent experiments. 2way ANOVA, * P ≤ 0.05, ns p>0.05 compared to the UT group.

3.6.17 TRIB1 and TRIB3 expression in normal and PCa tissue

Finally, we wanted to determine the basal TRIBs expression in prostate normal and tumour tissue sections. As part of a preliminary experiment, PCa serial sections were used to optimise IHC staining with the TRIBs antibodies. The tissue itself did now show any background when the primary or the secondary antibodies were added (Data not shown). Additionally, only primary and secondary antibody controls were used to detect any unspecific binding. As seen in Figure 3.6.17, the TRIB1 antibody alone gave high non-specific positivity on the tissue suggesting unspecific staining. The other primary antibodies and secondary antibodies did not show any background staining (Figure 3.6.17). Next, we tested the antibody concentrations on normal and tumour prostate tissue and we observed higher TRIB3 staining in tumour tissue compared to the normal tissue (Figure 3.6.17b). This was a preliminary experiment. To confirm the specificity of the staining, we will show the slides to a pathologist for further feedback.

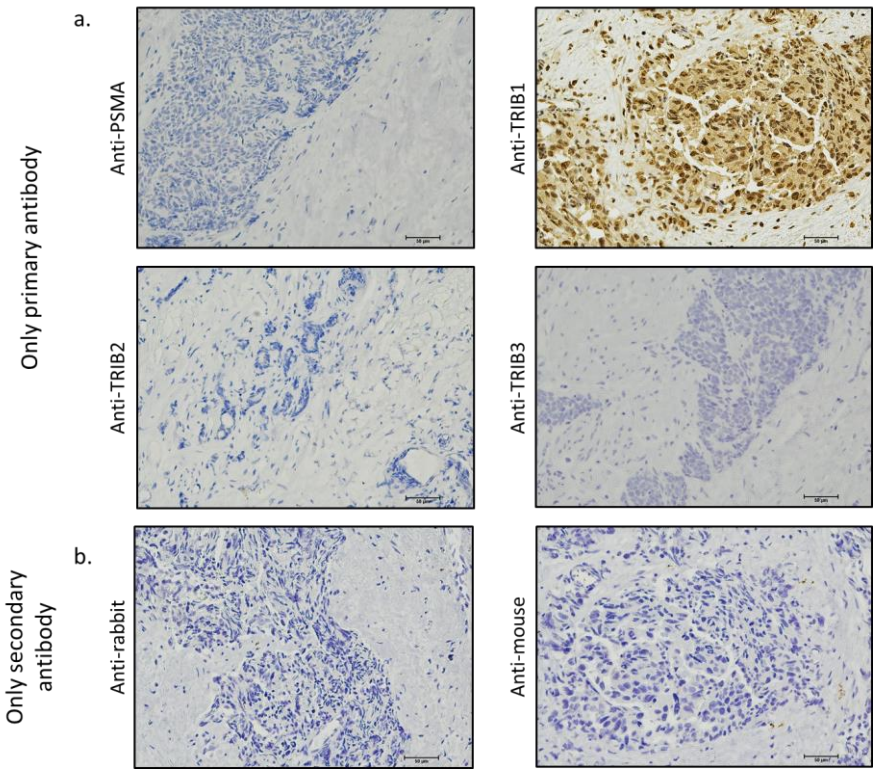

Figure 3.6.17: Optimisation of IHC controls for TRIBs antibodies
IHC staining was performed on serial sections (one sample) of PCa tissue using TRIBs antibodies. (a) Only primary antibody control was added to the tissues to identify any unspecific staining. (b) No primary control, only secondary antibody was added to the tissue and did not show any unspecific background staining.

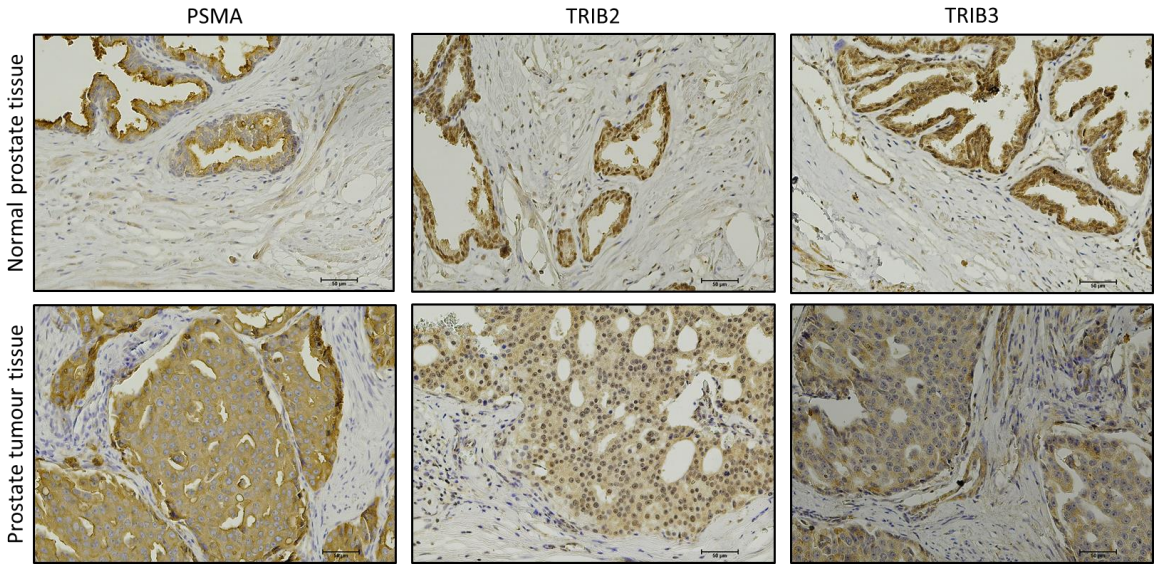

Figure 3.6.17b: Expression of TRIB2 and TRIB3 in normal and prostate tumour tissue

PSMA protein expression (positive marker) showed a week cytoplasmic staining in normal prostate tissue (one sample) as compared to the prostate tumour tissue that showed a strong cytoplasmic and membranous staining. TRIB2 and TRIB3 expression in the normal tissue (one sample), there was a weak nuclear and cytoplasmic staining. In tumour tissue, the TRIB2 and TRIB3 staining were higher and it was mainly localised in the cytoplasm.

3.7 Discussion

Previous studies have reported that the tumour microenvironment is an essential factor in cancer initiation and progression. The interaction between cancer cells and adipocytes results in the development of cancer-associated adipocytes. These cancer-associated adipocytes change the phenotypic characteristics of the cancer cells by promoting cell proliferation and migration through the secretion of adipokines (Laurent, Guerard et al. 2016).

The first question in this study was to determine whether the crosstalk between adipocytes and PCa cells could influence *TRIBs* expression in the latter. We used PCa cell lines, i.e. Du145 and PC3 cells for this study as both are highly invasive cell lines that represent aggressive type of PCa. Co-culture is a conventional technique to mimic interactions between two different cell populations *in vitro*. Firstly, we co-cultured non-differentiated and differentiated adipocytes from the mouse adipose cell lines 3T3-L1 and 3T3-F442A with Du145, PC3 and TRAMP-C2 cells. After co-culturing, we saw an increase of TRIB1 and TRIB3 expression at both mRNA and protein levels in Du145 and PC3 cells. This increase was cell type-specific since PC3 cells showed an increase in TRIB1 and TRIB3 levels only when co-cultured with 3T3-L1 cells and not with the 3T3-F442A cells and vice versa for Du145 cells. A possible explanation for this might be because both PCa cell lines are derived from two different metastatic locations: Du145 from a brain metastasis and PC3 cells were isolated from a bone metastasis and have different characteristics. Another possible explanation for this cell-type specificity might be the different *PTEN* status in these cell lines Du145 and PC3. Finally, we cannot exclude the possibility that the two adipose cell lines have various secretory factors and Du145 and PC3 cells may lack the receptor for that specific ligand.

Next, to confirm our second objective that the secretory factors from adipocytes mediate the TRIBs upregulation in cancer cells, we added the conditioned media (CM) from the differentiated and non-differentiated 3T3-L1 and 3T3-F442A cells on PCa cells to see if we could replicate the results obtained with the co-culturing. Interestingly, we found a similar increase in TRIB1 and TRIB3 protein levels in PC3 and Du145 cells with the same cell type specificity that was detected with co-culture system. Furthermore, this effect was only observed with differentiated adipocytes in both co-culture and CM culture system, suggesting

that the secretory factors come from mature adipocytes. This suggests that mature adipocytes secrete adipokines that influence TRIB1 and TRIB3 expression in PCa cells. This effect was further validated by using CM of primary mouse adipocyte from visWAT; we observed an increase of TRIB1 expression in Du145 cells and of TRIB3 expression in PC3 cells. Lastly, in a pilot study, we used CM from PPAT of two PCa patients. Interestingly, here we saw an increase in only TRIB3 protein levels in both Du145 and PC3 cells. Overall, we found that the CM obtained from adipose cell lines and primary adipocytes from both mice and two PCa patients increased TRIB1 and TRIB3 protein levels in cancer cells. The changes in the TRIBs expression were cell type-specific, but this could be due to various reasons discussed above. Moreover, it would be clinically relevant to see if the increased TRIBs expression is restricted to cancer cells or if it also occurs in normal prostate epithelial cell or in the early stages of androgen sensitive PCa. RWRE1 and PWRE1 are non-tumorigenic human prostatic epithelium cell lines and LnCaP is androgen sensitive PCa cell line that can be used for CM culture experiments with adipocytes.

Further, to identify the chemokines that can regulate the increase of TRIB1 and TRIB3 expression in PCa cells, we selected adipokines based on secreted factors obtained from the cytokine array and available literature. We identified CXCL13 that was exclusively secreted by 3T3-L1 cells. We also investigated CCL7, IL6 and Leptin that were previously published in the literature to increase PCa aggressiveness (Rojas, Liu et al. 2011, Alshaker, Sacco et al. 2015, Laurent, Guerard et al. 2016). Interestingly, we found that in Du145 cells, TRIB3 expression was increased when cultured with recombinant IL6 and Leptin. In contrast, TRIB1 expression was only altered by Leptin. For PC3 cells, CXCL13 increased the TRIB3 expression. Similar to our previous results, we observed a cell type specific increase with recombinant chemokine proteins. Chemokines, especially CXC-chemokine ligand and their corresponding receptors contribute to cancer migration, invasion and metastasis (Keeley, Mehrad et al. 2010). It has been well established that CXCL13: CXCR5 axis contribute to PCa aggressiveness. PCa cells express high levels of CXCR5 compared to the adjacent normal tissue (Kazanietz, Durando et al. 2019). PCa cell lines LnCap and PC3 cells express CXCR5 receptor on its cell surface and contribute to cell proliferation via JNK signalling and invasion through ERK activation (El-Haibi, Singh et al. 2011). Very little is known about Du145 cells expressing CXCR5 receptor. Taken together, it is clear that 3T3-L1 cells secrete CXCL13, which probably binds to CXCR5 present

on PC3 cells and increases TRIB3 protein expression. This could be one of the explanation of why we observe cell type specific TRIBs modulation in PCa cells. These results suggest that these chemokines alone or in combination with others, elevate TRIB1 and TRIB3 proteins levels in PCa. To determine the concentration of these chemokines in the adipocyte CM, ELISA will be performed. Furthermore, specific antibodies can be used to inhibit these chemokines for confirming their effect on TRIBs expression.

To verify whether the effect of adipose tissue microenvironment on cancer-related TRIBs expression was specific to PCa, we used another type of cancer with a similar tumour microenvironment such as breast cancer. We examined cell lines representing the three major types of breast cancers: HER2 positive, ER-positive and triple-negative subtype for the co-culture experiment. Surprisingly, we observed that TRIBs levels were unaffected in breast cancer cells. Thus suggesting that the phenotype that we observe is specific to PCa. We need to compare other cancer types such as ovarian and colon cancer for making a general conclusion.

Lastly, we wanted to determine the role of TRIBs in prostate tumorigenesis. Since our previous results show an increase of TRIB1 and TRIB3 expression in PCa cells when exposed to adipocytes or adipose-derived CM. We selected TRIB1 and TRIB3 to characterise their role in PCa aggressiveness. Previous studies have described the oncogenic role of TRIB1; however, there have not been many studies describing the role of TRIB3 in PCa (Mashima, Soma-Nagae et al. 2014). The Du145 and PC3 cells were stably transfected with *TRIB1* overexpression and *TRIB3* knockdown using lentivirus. *TRIB1* overexpression in Du145 and PC3 cells showed no effect on viability, proliferation and migration with and without CM from adipose cell lines. These results confirm recently published finding from the TRAIN consortium (Shahrouzi, Astobiza et al. 2020). Shahrouzi *et al.* generated stable Du145 and PC3 with *TRIB1* modulation and analysed the effect on 2D and 3D growth and invasion; they saw no effect on tumour behaviour. However, we observed the tumour suppressive role of TRIB1 overexpressing PC3 cells upon addition of CM. To further confirm this result, it is necessary to conduct additional experiments with CM from primary adipocytes from mice and humans.

As for *TRIB3* modulation, PC3 cells with *TRIB3* knockdown showed a decrease in cell proliferation. Whereas, Du145 cells showed an overall reduction in cell viability. Both the cells with TRIB3 KD abolished the pro-migratory effect of CM. Overall, the results suggest that *TRIB3* acts as an oncogene *in vitro* by suppressing viability, proliferation, migration and invasion of PCa cells. Moreover, cell migration was considerably reduced with TRIB3 KD cells when CM was added for both the cell lines, suggesting that high levels of *TRIB3* and adipose tumour microenvironment promote PCa aggressiveness. Further work is required to validate our *in vitro* results by injecting the stably transfected PCa cells in mice and characterising the growth *in vivo*.

3.8 Limitation

The work presented in this chapter has some limitations. We used CM from differentiated adipose cell lines 3T3-L1 and 3T3-F442A cells for tumour behavioural assays. However, we also need to repeat these assays with CM from mice and human PCa patients to confirm our findings. Furthermore, we overexpressed *TRIB1* in both Du145 and PC3 PCa cell lines. PC3 cells have a high endogenous expression of *TRIB1* and since at the beginning of the study, the shRNA constructs did not show any knockdown of *TRIB1*. Due to time constraints, we decided to generate overexpression in PC3 cells. We need to confirm if we would obtain similar results with the knockdown of *TRIB1* on PC3 cells.

3.9 Conclusion

It has been well established that the tumour microenvironment plays a significant role in cancer progression, invasion and metastasis. PPAT forms the major part of the tumour microenvironment in PCa. The invasion of PPAT by PCa cells is considered as one of the factors that determine the prognosis of patients undergoing radical prostatectomy. So far, all the studies have focused on PPAT and its effect on PCa aggressiveness. However, the mechanism underlying this is still unknown. Limited studies have investigated the involvement of TRIBs in PCa. To our knowledge, this is the first study to investigate the role of TRIBs in PCa tumour microenvironment.

Based on our *in vitro* experiments, we found that mature adipocytes secrete cytokines that are responsible for the increase in TRIB1 and TRIB3 protein levels in PCa cell lines, Du145 and PC3. To further confirm this result, we also used CM from mouse primary adipocytes and PPAT of PCa patients. Adipokines such as Leptin and IL6 increase TRIB1/3 expression in Du145 cells, while well-characterised chemokine CXCL13 increases TRIB3 protein expression in PC3 cells. Concerning the effect of TRIBs in PCa, we found that KD of *TRIB3* reduces the migration of both Du145 and PC3 cells which was promoted by the CM of adipocytes. Thus, it is quite tempting to speculate that *TRIB3* might be involved in the migration of PCa cells upon contact with the secretory factors from adipocytes.

In conclusion, the findings of this study provide new insights into the crosstalk between the PCa and adipocytes present in the tumour microenvironment. The latter contributes to increased *TRIB3* expression in the PCa cells. This increased promoted by adipocyte-secreted adipokines further improves the migration capacity of cancer cells, thus contributing to an aggressive phenotype. The preliminary results in this study are promising, and further experiments will broaden our understanding of PCa progression and the role of the tumour microenvironment.

Chapter 4 : *Trib3* in the adipose tissue has no effect on tumour cell behaviour of PCa cells *in vitro*

4.1 Declaration

The data presented in this chapter reports one of the research objectives from TRAIN ITN Consortium (Work package 3). I have performed 95% of the experiments in this chapter with help for genotyping of mice from Elke Pultz. I want to thank Adam Lindford (ESR 5) for breeding the *Trib1* transgenic mice as part of his project and to provide us with the tissues of the testing cohorts and mice from high-fat diet for further analysis. I would also like to thank Laura Martinez Campesino (ESR 3) for allowing me to use her unpublished data for RT-PCR on *Trib3* expression in mature adipocytes from scWAT and visWAT of Trib3 KO mice and data on differentiated adipocyte gene expression and adipocyte size between Trib3 KO and WT mice (section 4.5.2).

4.2 Abstract

Tribbles proteins (Trib1/2/3) are a family of pseudo-kinases involved in multiple cellular processes, including glucose and lipid metabolism. Specifically, *Trib3* regulates lipid metabolism and insulin sensitivity, whereas *Trib1* affects inflammatory responses in adipose tissue by regulating cytokine gene expression. The interaction between cancer cells and cells of the tumour microenvironment, including mesenchymal stem cells, endothelial cells, immune cells, fibroblasts and adipocytes promotes cancer progression and metastasis. In prostate cancer (PCa), the interaction between periprostatic adipose tissue and cancer cells enhances tumour invasion and aggressiveness. Our project focuses on the role of *Trib1* and *Trib3* in the cross-talk between the adipocytes and tumour cells in the tumour microenvironment. We hypothesize that abnormal *Trib1* and *Trib3* function in adipose cells influences PCa progression. To address this issue, we used mice with Tamoxifen-inducible *Trib1* overexpression in the adipose tissue and *Trib3* whole-body KO mice. We encountered several problems with the breeding of mice with Tamoxifen-inducible overexpression of *Trib1* in the adipose tissue and in the three cohorts tested. We could not observe any *Trib1* overexpression in adipose tissue. Therefore, we did not continue further with these mice. The CM from primary adipocytes isolated from *Trib3* whole-body KO mice were cultured with PCa cell lines and their effect on tumour cell viability, invasion and migration were assessed. Our results suggest that *Trib3* deletion in the adipose tissue does not affect the viability, invasion and migration of PCa cells, Du145, PC3 and TRAMP-C2. Overall, this study suggests that *Trib3* in the adipose tissue does not contribute to PCa aggressiveness.

4.3 Introduction

Adipose tissue plays a critical role in metabolism. It acts as an endocrine organ by secreting adipokines that regulate lipid and glucose metabolism, insulin sensitivity, control appetite and blood pressure and regulates angiogenesis and inflammatory processes in the body (Sethi and Vidal-Puig 2007). Ostertag *et al.* reported that *Trib1* is upregulated during acute and chronic inflammation in WAT of mice. *Trib1* heterozygous KO mice protected them against high-fat diet-induced obesity and showed a significant reduction of cytokine expression in adipocytes (Ostertag, Jones et al. 2010). While, *Trib3* controls adipocyte differentiation by blocking the activity of C/EBPβ dependent induction of PPARγ2 (Bezy, Vernochet et al. 2007). Several studies have described the role of adipose tissue in contributing to PCa aggressiveness by modulating tumour growth, invasion and metastasis (Uehara, Kobayashi et al. 2018). Thus, adipose tissue dysfunction can affect PCa progression and could lead to a more aggressive phenotype.

To investigate the function of a specific gene in adipose tissue, the Cre-loxP system is widely used to generate transgenic mice with adipose-specific modulation of the desired gene (Sassmann, Offermanns et al. 2010). Wang *et al.* generated adipose-specific transgenic mice using the promoter of *adiponectin (Adipoq)* (Wang, Deng et al. 2010). Adiponectin is a well-studied adipokine found abundantly in differentiated white and brown adipocytes (Das, Lin et al. 2001). Further characterisation of this transgenic line showed that Tamoxifen induction showed complete recombination in WAT in AdipoqCreER^{T2} line (96%-99%). This was specific to adipose tissue and was not seen in other orangs. Moreover, metabolic functions such as glucose tolerance, lipolysis, or energy expenditure were not altered (Sassmann, Offermanns et al. 2010). Henceforth several studies have used AdipoqCreER^{T2} to determine the biological function of various genes (Sassmann, Offermanns et al. 2010). Our study aims to investigate the gap in the literature by modulating *Trib1* and *Trib3* expression in mice adipose tissue and determine their role in PCa. To generate *Trib1* modulation in adipocytes, *Trib1* adipose-specific knockout (KO) and overexpression (OE) mice were generated by crossing them with tamoxifen inducible Adipoq CreER^{T2} line (Figure 2.1.1). Using this approach, it was possible to delete or overexpress *Trib1* in mouse adipose tissue. For *Trib3* modulation in adipocytes, due to lack of time and breeding capacities in the facility, we used *Trib3* whole-body KO mice that

were previously published and well characterised (Salazar, Lorente et al. 2015). We were aware of the limitations due to whole-body KO mechanism and any results would be interpreted accordingly.

4.4 Hypothesis

Previous studies report the important functions of *Trib1* and *Trib3* in adipose tissue and the influence of adipose tissue microenvironment on PCa aggressiveness is also well described. Therefore, we hypothesise that *Trib1* or *Trib3* modulation in adipose tissue affects PCa progression by affecting tumour cell behaviour.

To test this hypothesis, we used the following objectives:

1. To isolate mature adipocytes and SVF from adipose tissue of *Trib1* overexpression tamoxifen-inducible Adipoq CreER^{T2} line and *Trib3* whole-body KO mice and generate CM
2. Perform *in vitro* tumour behavioural assays such as cell viability, migration and invasion on PCa cell lines using the above mentioned CM
3. Identify secretory factors that promote aggressive tumour behaviour.
4. Characterise the mechanism underlying the crosstalk between *Trib1* and *Trib3* modulated adipocytes and their involvement in PCa progression.

4.5 Results

4.5.1 *Trib3* expression levels in BAT, liver and mature adipocytes of *Trib3* KO mice

To confirm the *Trib3* deficiency in the mice used for this study in addition to the genotyping results, we isolated the BAT and Liver from the animals and assessed *Trib3* expression by RT-PCR. As expected, *Trib3* levels are significantly lower as compared to the WT mice (Figure 4.5.1a). Data in Figure 4.5.1b is from Laura Martínez Campesino, who further confirmed the reduced *Trib3* expression in mature adipocytes from scWAT and visWAT from *Trib3* KO mice as part of her project (unpublished data). After the validation of *Trib3* expression in the tissues, we bred cohorts from *Trib3* KO and WT mice (section 2.1.4) and isolated both, scWAT and visWAT fat deposits and collected CM for our next experiment as described in section 2.1.7.

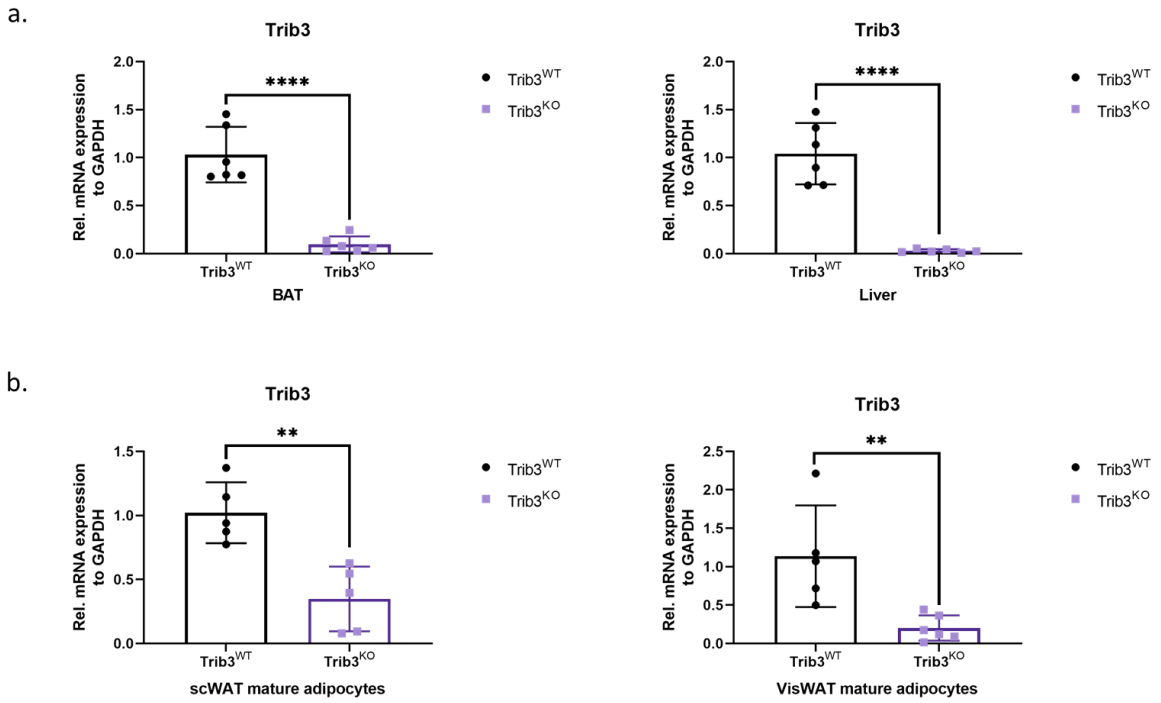

Figure 4.5.1: Trib3 mRNA expression of BAT, liver and mature adipocytes from *Trib3* KO mice
(a) The BAT and liver tissues were isolated while taking scWAT and visWAT for primary culture from $Trib3^{KO}$ mice. Trib3 mRNA expression in BAT and Liver. Data show the mean ±SD from a cohort of six mice per group. **** P ≤ 0.0001 compared to $Trib3^{WT}$ group. (b) Trib3 mRNA expression in mature adipocytes from scWAT and visWAT of $Trib3^{KO}$ mice. Data show the mean ±SD from a group of 5 mice per group. Unpaired t-test, ** P ≤ 0.01 compared to $Trib3^{WT}$ group.

4.5.2 Differences in adipocyte tissues between *Trib3* KO and WT mice

During the isolation of adipose tissue from *Trib3* KO and WT mice, we observed a difference in the size of the depots. The KO mice had increased adiposity compared to the WT mice. One of the projects from TRAIN was to investigate the impact of *Trib3* deficiency in adipose tissue on macrophage and adipocyte function. The project was carried out by ESR3 Laura Martínez Campesino, who characterised the differences in adipose tissue depots in *Trib3* KO and WT mice. She observed that Trib3 KO mice have significantly higher body weights when compared to WT mice after 10 weeks (Unpublished data). Furthermore, Figure 4.5.2a shows PPAR-γ expression in *ex vivo* differentiated adipocytes scWAT and visWAT. *Trib3* deficiency in the subcutaneous depot significantly increases the expression of PPAR-γ, a critical regulator of adipose tissue function. This data supports previous research that shows *Trib3* regulates adipocyte differentiation by binding to PPAR-γ in 3T3-L1 pre-adipocytes and inhibiting PPAR-γ and CEBPA production (Takahashi, Ohoka et al. 2008). Figure 4.5.2b shows differences in H&E staining of mature adipocytes from scWAT and visWAT depots from *Trib3* KO and WT mice. Subcutaneous adipose tissue from *Trib3* KO mice have a reduction in adipocyte size, therefore the expansion of this adipose depot is not due to adipocyte enlargement, but to an increased adipocyte proliferation. These data suggest that *Trib3* is an important modulator of adipose tissue expansion and function, highly affecting the subcutaneous adipose depot.

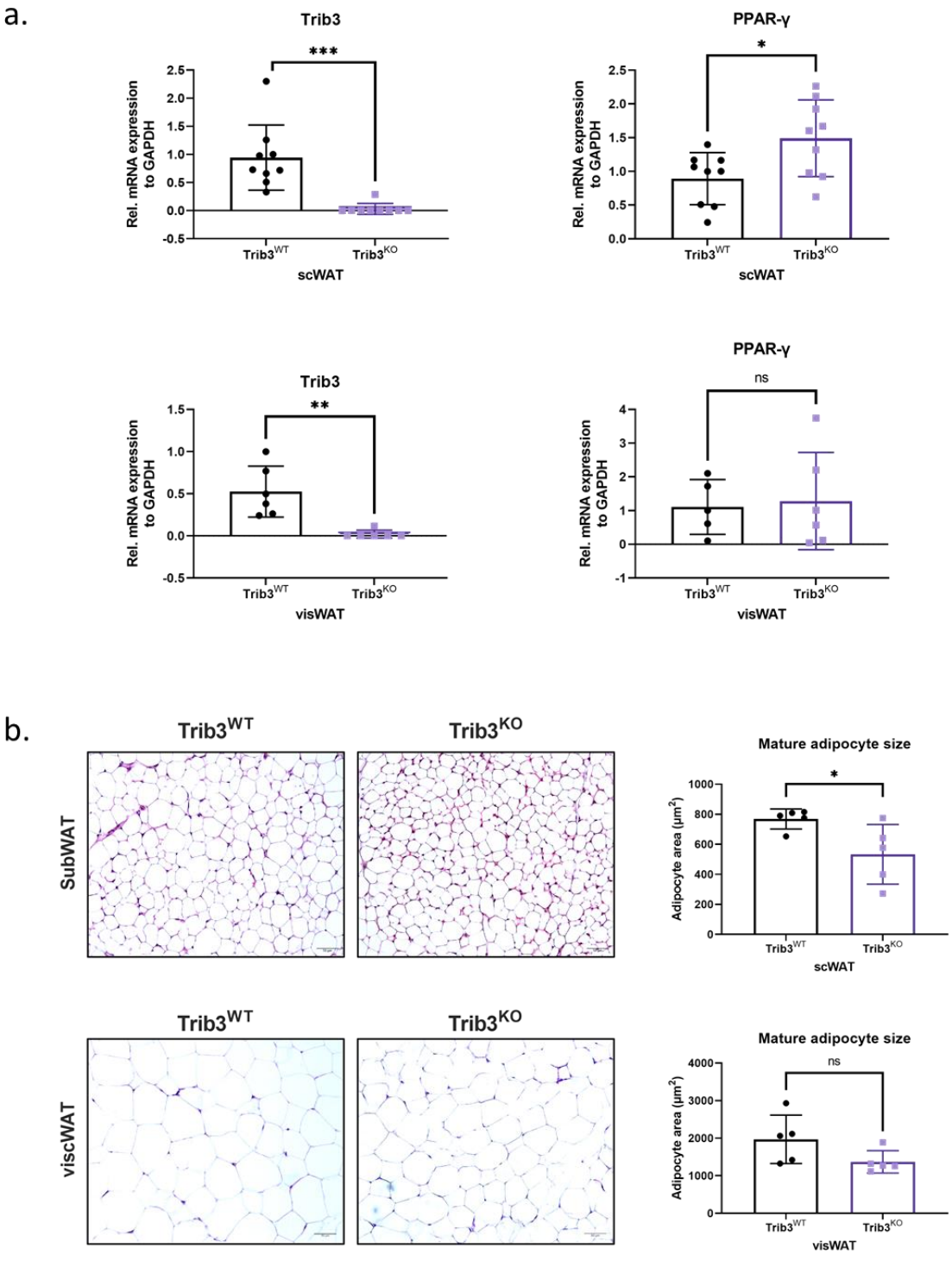

Figure 4.5.2: PPAR-γ expression and adipocyte size comparison in scWAT and visWAT of Trib3 KO and WT mice.

(a) *Trib3* and *PPAR-γ* mRNA expression in scWAT and visWAT of Trib3^{KO} and Trib3^{WT} mice. Data show the mean ±SD from a cohort from 6-9 mice per group. Unpaired t-test, * P ≤ 0.05, ** P ≤ 0.01, *** P ≤ 0.001 compared to Trib3^{WT} group. (b) H&E sections from Trib3^{KO} and Trib3^{WT} mice and corresponding measurements for adipocyte area. Data show the mean ±SD from a group of 5 mice per group. Unpaired t-test, * P ≤ 0.05 compared to Trib3^{WT} group.

4.5.3 The CM from adipose cells of *Trib3* KO mice does not affect the viability of PCa cells

Firstly, to identify the effect of CM from mature adipocytes isolated from *Trib3* KO mice on cell viability of PCa cells, we used 3D cell viability assay. Du145, PC3 and TRAMP-C2 cells were seeded on the ULA plates for 3D spheroids formation. Five days later, CM from mouse adipose tissue (scWAT and VisWAT) and cell viability reagents were added and the measurements were taken every 24 hours for 3 days. For untreated control (UT), PCa cells were cultured with culture media alone. At 24 hours, all the PCa cell lines showed a significant increase in viability when the UT controls were compared with the CM samples, as shown in Figure 4.5.3. This is in line with previously reported studies (Laurent, Guerard et al. 2016). However, there were no differences observed between the viability of cells incubated with the CM from scWAT and visWAT, of both *Trib3* KO and *Trib3* WT mice. Thus, suggesting that even if possible changes in the secretome of adipose cells occurred after *Trib3* deletion, they did not affect the cell viability.

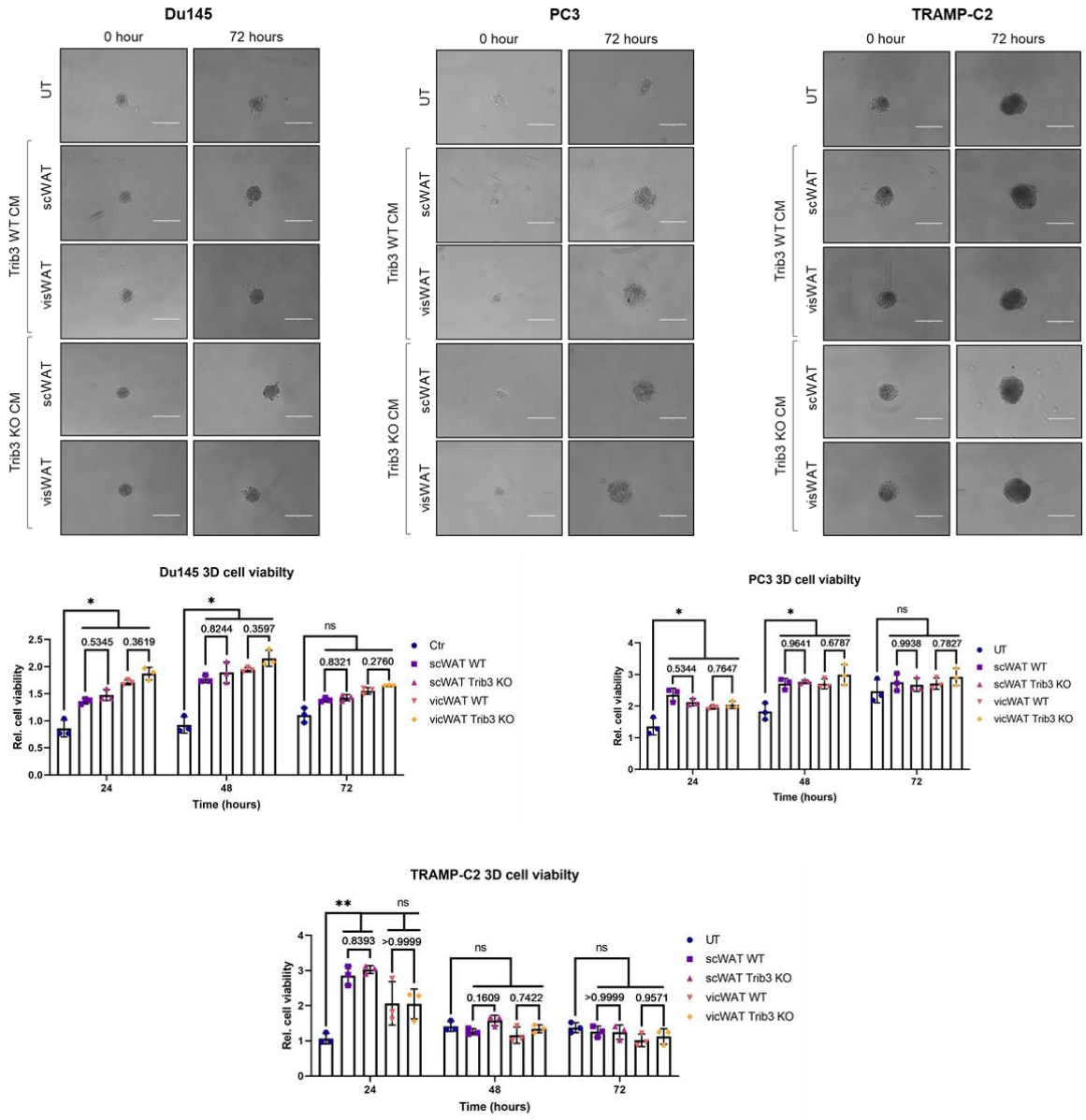

Figure 4.5.3: CM from *Trib3* KO adipose tissue does not affect cell viability of PCa cells.
PCa cell lines were seeded as 3D spheroids and pictures were taken on Day 5 and Day 8 post spheroid formation. Graphs represent cell viability of PCa cell lines over 3 days compared with the UT control. Data show the mean ±SD from a cohort of six mice per group. 2way ANOVA, * P ≤ 0.05, ** P ≤ 0.01, ns p>0.05 compared to UT.

4.5.4 PCa cells do not differentially migrate when cultured with the CM from adipocytes of *Trib3* KO mice

Next, we analysed the effect of CM from adipocytes of *Trib3* KO mice on the migration of PCa cells using the gap closure assay. Cells were seeded on four wells of an IBIDI chamber. Once the confluence was achieved, the insert between the wells was removed and 0% or 10% serum culture medium or CM was added. Pictures were taken from 0 up to 15 hours after adding the CM. All the pictures were quantified in ImageJ software and the percentage of migration was calculated by measuring the space between the cells. As seen previously with the cell viability results, we saw a significant increase in the migration of PCa when cultured with CM from either the *Trib3* KO or *Trib3* WT mice when compared to culture media. However, we did not observe any CM-dependent differences between *Trib3 KO* and *Trib3 WT* mice in the migration of cells, as shown in Figure 4.5.4.

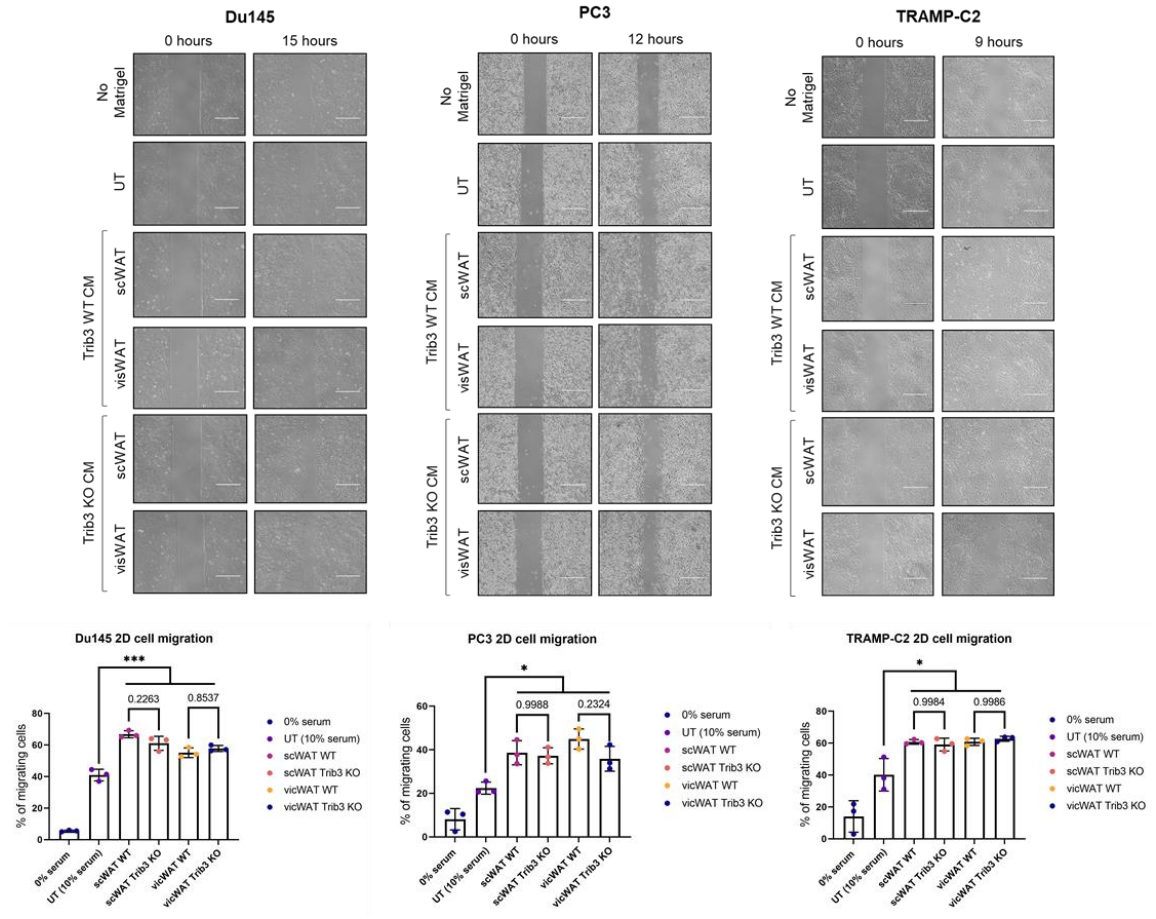

Figure 4.5.4: CM from *Trib3* KO adipose tissue has no effect on cell migration of PCa cells.
(a) The PCa cells were seeded in four wells of an IBIDI chamber and allowed to attach for at least 24 hours. Immediately after the insert was removed, CM or culture media was added and pictures were taken. (b) Graphs represent cell migration of PCa cell lines with culture media and the CM from mice. Data show the mean ±SD from a cohort of six mice. 2way ANOVA, * P ≤ 0.05, ***P ≤ 0.001, ns p>0.05 compared to UT.

4.5.5 PCa cell invasion is not affected by the addition of CM from adipocytes of *Trib3* KO mice

Lastly, the invasion potential of PCa cells upon incubation with CM of mouse adipocytes was measured using a 3D invasion assay. PCa cells were seeded on the ULA plates to form spheroids and Matrigel was added to the wells. Cells were cultured with CM and culture media alone as UT control. Pictures of the invading cells were taken from 0 hours and up to twelve days after adding the CM. For PC3 and TRAMP-C2 cells, we did not observe any difference in cell invasion with the CM from *Trib3* KO or *Trib3* WT mice. However, as expected, we did see a significant increase in invasion potential when compared with the UT control. As for Du145 cells, the 3D spheroids grew in Matrigel without invading through them even after 12 days. Therefore, for Du145 cells, we opted for a 2D invasion method. Du145 cells were seeded on culture inserts coated with Matrigel and control inserts. These cells showed invasion in the 2D system, as shown in Figure 4.5.5. However, Du145 cells also did not show any significant differences between the CM from *Trib3* KO and *Trib3* WT mice. Overall, the CM from *Trib3 KO* mice showed no difference in cell viability, migration and invasion of PCa cells.

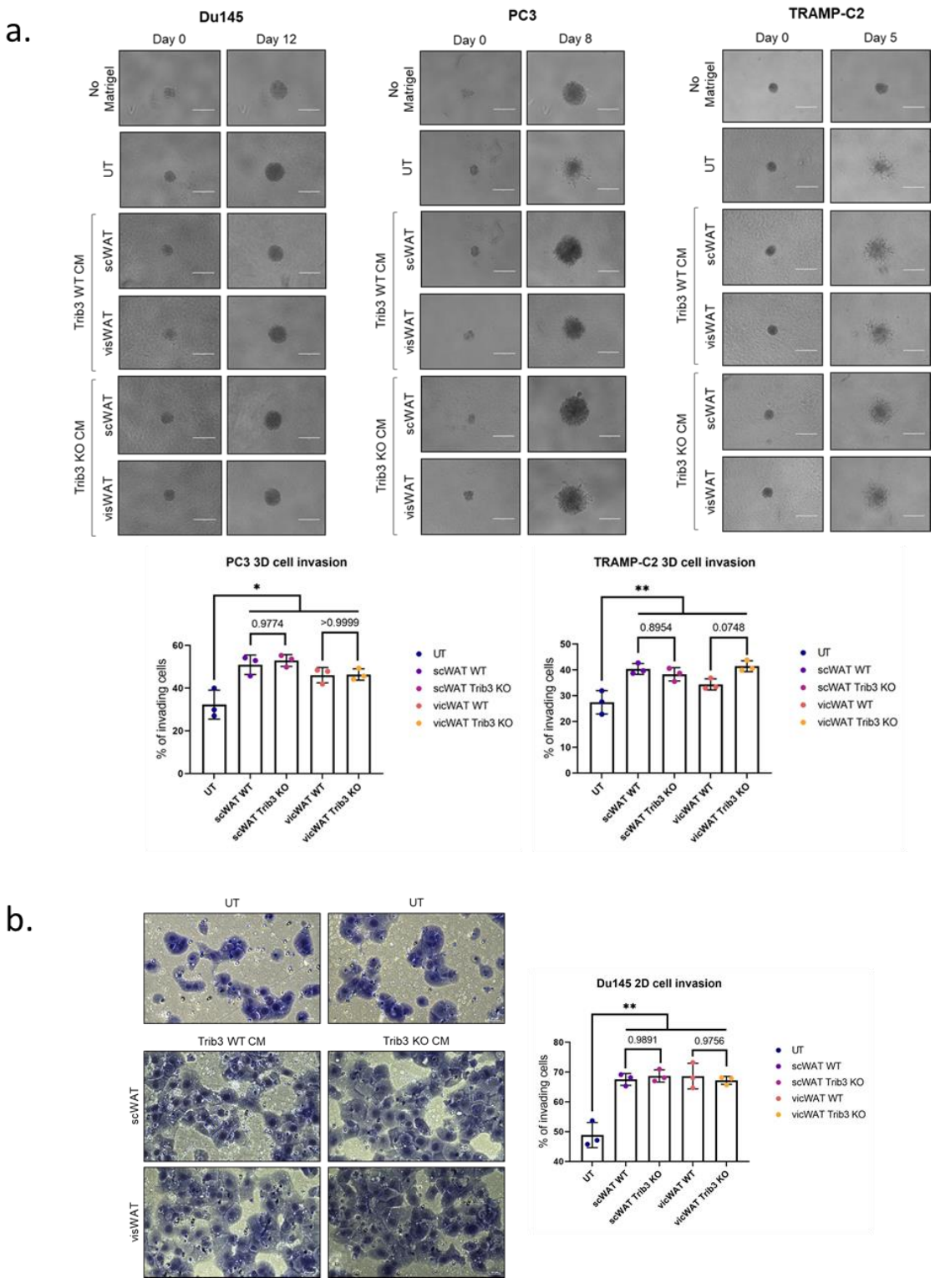

Figure 4.5.5: CM from *Trib3* KO adipose tissue has no effect on cell invasion of PCa cells.
(a) The PCa cells, Du145, PC3 and TRAMP-C2, invading into the Matrigel in a 3D system. Images taken on the first and final day of the quantification using ImageJ software. Quantification of the percentage of invading cells for PC3 and TRAMP-C2 are shown in the bar graph below. (c) Du145 cells invading through the 2D Matrigel were photographed (3 technical replicates for each cell line) and pictures were taken for three representative fields per sample for calculating the average. Quantification was carried out in Excel by calculating the percentage of invading cells. All the data represent the mean ±SD from a cohort of six mice. 2way ANOVA, * $P \leq 0.05$, ** $P \leq 0.01$, ns $p>0.05$ compared to UT.

4.5.6 *Trib1* expression in the first cohorts of *Trib1* adipose-specific OE mice

Generation of *Trib1* adipose-specific KO and OE mice was part of Adam Linford's (ESR 5) PhD project entitled: *Tribs*-dependent reprogramming of adipocytes and its implications for immuno-metabolic conditions. At the beginning of his PhD, he started crossing the *Trib1*$^{fl/fl}$ mice with tamoxifen-inducible Adipoq CreER^{T2} line. The resulting mice would have either the *Trib1* knockdown or overexpression specifically in the adipose tissue upon tamoxifen induction. However, a number of problems were encountered during the breeding of these mice. The KO line did not breed normally, and from July 2017 until July 2019 there were only six generations of the transgenic line. These were never used for validation and only used to continue the breeding. On the other hand, the overexpression line had better results in terms of breeding. From December 2017 until July 2019, Adam generated three cohorts of mice. In July 2019, he resigned from the PhD and after that, I temporality took over the project. The first two groups, consisting of four Cre+ and two Cre- mice, were subjected to Tamoxifen treatment and the tissues were collected 2 and 4 weeks after the Tamoxifen induction. I isolated the RNA from scWAT, visWAT and BAT samples and performed RT-PCR to analyse the *Trib1* levels in Cre+ and Cre- mice, as shown in Figure 4.5.6. Unfortunately, due to the low number, we could not perform a statistical test. Adam used the final cohort for an experiment by placing the mice on a high-fat diet as described ahead.

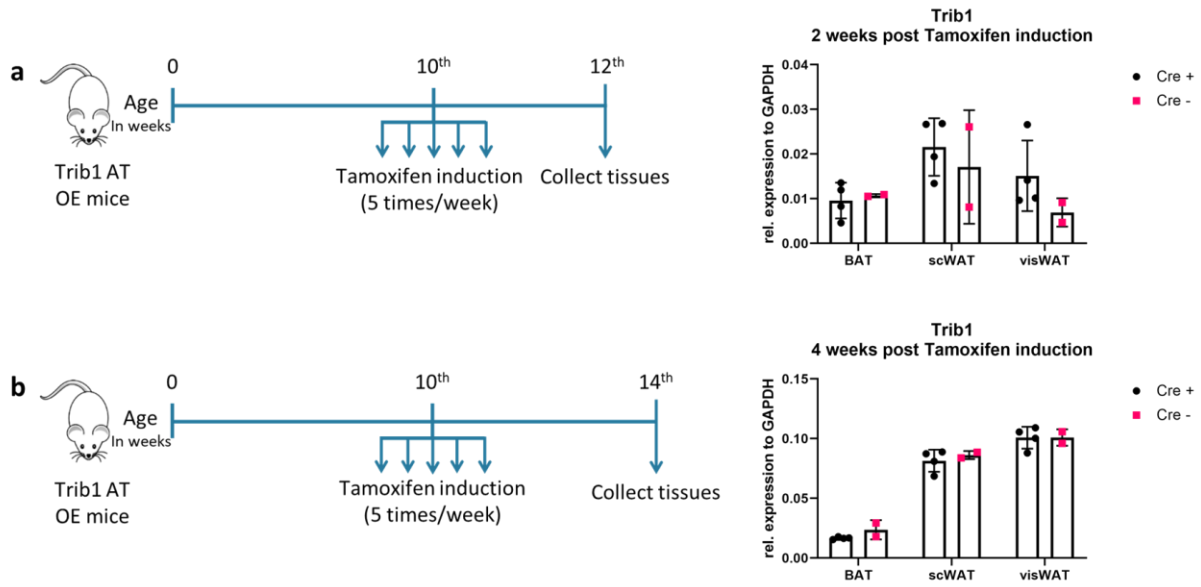

Figure 4.5.6: *Trib1* expression in the first cohorts of *Trib1* adipose-specific OE mice
(a) The first cohort consisted of 6 male mice (4 Cre+ and 2 Cre-). They were subjected to tamoxifen induction 5 times per week when they were 10 weeks old. 2 weeks later, these mice were euthanized and BAT, scWAT and visWAT was collected. The differences in mRNA levels for Trib1 expression was analysed. (b) The second cohort was similar to the first one, but the mice were euthanized after 4 weeks' post tamoxifen induction.

4.5.7 *Trib1* expression in *Trib1* adipose-specific OE mice kept on a high-fat diet for 14 weeks

The last cohort of mice consisted of nine cre+ and eight cre- male mice (Table 17), which were kept on a high-fat diet (HFD) for 14 weeks and Tamoxifen injections were given 5 times per week for 3 weeks. At the end of the study after taking over the project, I euthanized the mice and collected the adipose tissue to determine the levels of *Trib1* at mRNA level. Four mice were used for RNA extraction of scWAT, visWAT and BAT and the remaining four mice were fixed with formalin. RT-PCR was performed to analyse *Trib1* expression and body weight was evaluated as seen in Figure 4.5.7. We did not see any difference both in *Trib1* mRNA expression and in body weight between the Cre+ and Cre- groups.

No	Line	Strain	Sectioning no.	MausDB no.	Genotype	Age	Wt (gm)
1	Adipoq CreERT2:Cre+; Trib1 flox:f/f	C57BL/6N-BL/6J	19/77	80017286	Cre+ Trib1 f/f	6 months	28.95
2	Adipoq CreERT2:Cre+; Trib1 flox:f/f	C57BL/6N-BL/6J	19/78	80017297	Cre+ Trib1 f/f	6 months	34.6

3	Adipoq CreERT2:Cre+; Trib1 flox:f/f	C57BL/6N-BL/6J	19/79	80017299	Cre+ Trib1 f/f	6 months	39.8
4	Adipoq CreERT2:Cre+; Trib1 flox:f/f	C57BL/6N-BL/6J	19/80	80017301	Cre+ Trib1 f/f	6 months	34.33
5	Adipoq CreERT2:Cre+; Trib1 flox:f/f	C57BL/6N-BL/6J	19/81	80017302	Cre+ Trib1 f/f	6 months	25.5
6	Adipoq CreERT2:Cre+; Trib1 flox:f/f	C57BL/6N-BL/6J	19/82	80017305	Cre+ Trib1 f/f	6 months	34.7
7	Adipoq CreERT2:Cre+; Trib1 flox:f/f	C57BL/6N-BL/6J	19/83	80017306	Cre+ Trib1 f/f	6 months	38.11
8	Adipoq CreERT2:Cre+; Trib1 flox:f/f	C57BL/6N-BL/6J	19/84	80017318	Cre+ Trib1 f/f	6 months	33.52
9	Adipoq CreERT2:Cre+; Trib1 flox:f/f	C57BL/6N-BL/6J	19/85	80017319	Cre+ Trib1 f/f	6 months	36.3
10	Adipoq CreERT2:Cre-; Trib1 flox:f/f	C57BL/6N-BL/6J	19/86	80017287	Cre- Trib1 f/f	6 months	22.5
11	Adipoq CreERT2:Cre-; Trib1 flox:f/f	C57BL/6N-BL/6J	19/87	80017294	Cre- Trib1 f/f	6 months	28.34
12	Adipoq CreERT2:Cre-; Trib1 flox:f/f	C57BL/6N-BL/6J	19/88	80017296	Cre- Trib1 f/f	6 months	36.35
13	Adipoq CreERT2:Cre-; Trib1 flox:f/f	C57BL/6N-BL/6J	19/89	80017303	Cre- Trib1 f/f	6 months	38.2
14	Adipoq CreERT2:Cre-; Trib1 flox:f/f	C57BL/6N-BL/6J	19/90	80017314	Cre- Trib1 f/f	6 months	36.6
15	Adipoq CreERT2:Cre-; Trib1 flox:f/f	C57BL/6N-BL/6J	19/91	80017315	Cre- Trib1 f/f	6 months	43.7
16	Adipoq CreERT2:Cre-; Trib1 flox:f/f	C57BL/6N-BL/6J	19/92	80017316	Cre- Trib1 f/f	6 months	48.9
17	Adipoq CreERT2:Cre-; Trib1 flox:f/f	C57BL/6N-BL/6J	19/93	80017317	Cre- Trib1 f/f	6 months	31.56

Table 17: Cohort of *Trib1* adipose-specific OE mice on HDF

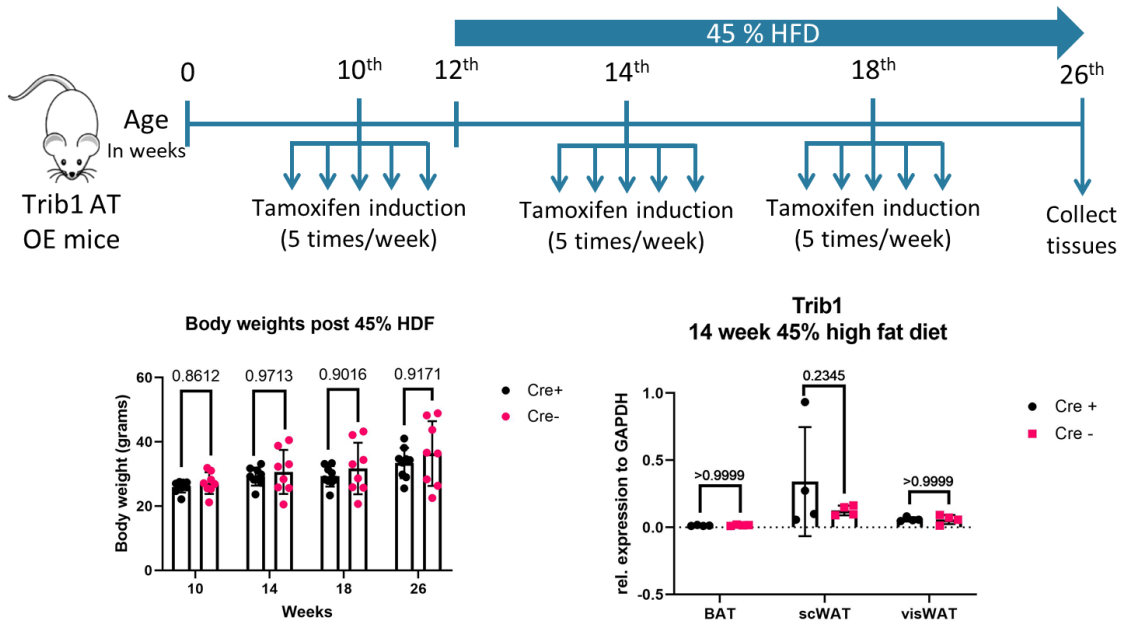

Figure 4.5.7: *Trib1* expression in *Trib1* adipose-specific OE mice on 14 weeks HFD
The final cohort was subjected to 14 weeks HFD (45%) and the mice were given tamoxifen injections 5 times per week for 3 weeks. Bodyweights are represented with the mean ±SD from a cohort of nine cre+ and eight cre-, 2way ANOVA, p>0.05. *Trib1* mRNA levels are represented with the mean ±SD from a cohort of four cre+ and four cre-, 2way ANOVA, p>0.05.

4.6 Discussion and future work

Tribbles play a multifactorial role in regulating various metabolic processes (Richmond and Keeshan 2019). Qi *et al*. reported that *Trib3* regulates lipid synthesis in the adipose tissue by degrading acetyl coenzyme A, a rate-limiting enzyme for fatty acid synthesis (Qi, Heredia et al. 2006). In the liver, under fasting condition, *Trib3* is upregulated and it was shown to downregulate AKT activation, therefore contributing to insulin resistance (Du, Herzig et al. 2003), as well as potentially regulating other signalling pathways (Kiss-Toth, Bagstaff et al. 2004, Sung, Francis et al. 2006). A further study reported *Trib3* as an essential negative regulator of adipogenesis by inhibiting the activation of C/EBPβ, an important adipogenic transcription factor (Bezy, Vernochet et al. 2007). On the other hand, the biological role of *Trib1* in adipose tissue has not been well characterised. There is only one study that shows *Trib1* regulation in WAT in diabetes mouse models. *Trib1* enhanced the secretion of IL-6, IL-1β, tumour necrosis factor-α (TNF-α) and nuclear factor kappa B (NF-κB) in Trib1 heterozygous K mice (Ostertag, Jones et al. 2010). In the same study, they reported that homozygous *Trib1* knockout mice had high perinatal mortality and the underlying basis is still unknown (Ostertag, Jones et al. 2010). Clearly, more studies are needed to understand the biological role of *Trib1* in metabolism.

To understand the role of *Trib1* in adipose tissue metabolism (TRAIN project 5) and further characterise its role in PCa progression (TRAIN project 7), Adam Lindford (ESR 5) started breeding adipose-specific *Trib1* overexpression and knockout mice. Unfortunately, both lines had breeding problems since the beginning of the project. Due to insufficient breeding and consistently low number of pups, these mice were always used for further breeding. In March 2019, the breeding for Trib1 adipose-specific KO was stopped and three of the transgenic Trib1 adipose-specific KO Cre positive mice were used for sperm freezing. For the *Trib1* adipose-specific overexpressing line, there were two cohorts used for validation of *Trib1* expression. However, we did not observe any difference in the *Trib1* mRNA levels.

The final cohort from this line was used for high-fat diet experiment by placing them on 45% high-fat diet for 14 weeks. Even here in the last experimental group, we failed to see any differences in the *Trib1* levels. After validating the *Trib1* expression in these three cohorts, we

were confident the problem was not from the *Trib1*$^{fl/fl}$ mice, since they were used to generate other transgenic lines within the TRAIN consortium. We assumed that there might be an issue with the Tamoxifen inducible adiponectin CreER^{T2} line. Therefore, we looked through the literature to investigate. It has been previously reported that in some transgenic mouse lines, CreER^{T2} is active independent of Tamoxifen inductions (Kristianto, Johnson et al. 2017), and can regulate the expression of the target gene in an age-dependent manner (Fonseca, Chu et al. 2017). Furthermore, we cannot exclude the possibility that the Adipoq CreER^{T2} mice were leaky and during early weeks, there could be overexpression of *Trib1* without Tamoxifen injections that decreased over time as previously reported in the literature with Adipoq CreER^{T2} lines (Fonseca, Chu et al. 2017, Kristianto, Johnson et al. 2017). However, we do not have the tissue from young mice to confirm this assumption. Some studies have also reported that Tamoxifen inducible models are not reliable for functional studies with adipose tissue, since Tamoxifen injection reduces fat mass accumulation in the adipose tissue. However, the reduction in the body weight was temporary as the mice restored their body weight ten days after the last Tamoxifen injection (Ye, Wang et al. 2015). The *Trib1* adipose-specific OE mice that were subjected to 45% high fat-diet for 14 weeks, we observed a trend of lower body weights for Cre+ mice when compared to Cre- mice, although it was not significant. Overall, this study was unable to demonstrate the effect of *Trib1* modulation in adipose tissue on PCa cell behaviours. Further studies to generate a constitutive overexpressing *Trib1* adipose-specific model can help us understand its mechanistic role of *Trib1* on adipogenesis and obesity. Moreover, to further evaluate if *Trib1* dysfunction in adipose tissue has an influence on PCa aggressiveness.

Due to a delay in the generation of *Trib1* mice, we focused on *Trib3* KO mice for this study. We used CM from mature adipocytes of *Trib3* KO and WT mice to investigate tumour cell behaviour in PCa cell lines Du145, PC3 and TRAMP-C2. Surprisingly, we did not observe any difference in the cell viability, migration and invasion of PCa cells when compared to CM of adipocytes between *Trib3* KO and *Trib3* WT mice. However, care should be taken in the interpretation of data derived from whole-body *Trib3* KO mice. It has been reported that whole-body KO mice can have some secondary effect due to interactions in other organs and can be challenging to identify or distinguish these effects (Davey and MacLean 2006).

Therefore, it is plausible that since we do not have a clean knockdown in the adipose tissue, it can alter the results obtained.

4.7 Limitations

One of the major limitations of this study were the breeding problems that were encountered during the generation of *Trib1* transgenic mice. By the time we could validate the *Trib1* expression in these mice, it was too late to realise the problems we encountered were due to Tamoxifen inducible Adipoq CreER^{T2} line. Moreover, we also did not have *Trib3* adipose-specific KO mice for functional experiments with PCa cells. Overall, due to major issues encountered with the animals, we could not address the particular hypothesis that was initially proposed.

4.8 Conclusion

In conclusion, in our experimental model, we observed that *Trib3*, an important regulator of adipogenesis, did not contribute to any notable differences in PCa cell behaviour *in vitro*. We performed cell behavioural assays such as cell viability, migration and invasion using the CM from adipocytes. We observed an increase in cell viability, migration and invasion upon incubation with CM, thereby confirming our experimental system to what was previously shown in the literature (Laurent, Guerard et al. 2016). However, these effects were independent of the presence of *Trib3* in adipocytes.

Chapter 5 : *TRIB2* functions as a tumour suppressor in MTC by inhibiting tumour cell behaviour *in vitro*

5.1 Declaration

The results reported in this chapter are intended to be published along with some additionally planned experiments (manuscript in preparation). All the experiments described in this chapter are performed by myself, with some technical support for immunohistochemistry from an Erasmus Master's student Amy Rose Fumo in our group.

5.2 Abstract

Medullary thyroid cancer (MTC) accounts for 5-10% of all thyroid cancers and arises from para-follicular C cells that produce calcitonin. *RET* proto-oncogene alterations result in the development of both hereditary and somatic MTCs. Clinical management of MTC patients is challenging due to lymph node metastasis at an early stage, thus resulting in poor prognosis. Receptor tyrosine kinases inhibitors, e.g. Cabozantinib and Vandetanib, are prescribed for the treatment of MTCs; however, most of the patients develop drug resistance over time. Therefore, currently, there are no effective treatments options available for advanced MTC patients, and new biomarkers and therapies are urgently needed. In the present study, we show that *TRIB2* acts as a tumour suppressor in human MTC cell lines MZ-CRC-1 and TT *in vitro*, and it promotes drug sensitivity to Cabozantinib treatment. Here we used MZ-CRC-1 and TT cells stably transfected with *TRIB2* overexpression to analyse tumour cell behaviour. Our results indicate that *TRIB2* inhibits the viability, proliferation, migration and invasion of MTC cells *in vitro*. Next, we analysed the effect of Cabozantinib and Vandetanib treatment on MTC stably overexpressing *TRIB2*. Interestingly, we observed that *TRIB2* increases drug sensitivity in MZ-CRC-1 cells, carrying an aggressive RET M198T mutation. In summary, our research suggests that overexpression of *TRIB2* inhibits tumour growth properties *in vitro* and also affects drug sensitivity with Cabozantinib. Further studies are needed to confirm the role of *TRIB2 in vivo* and to determine whether it can be used as a potential therapy target for resistant MTC.

5.3 Introduction

p27 is a member of CDK inhibitors that negatively regulates cell cycle progression. p27 is downregulated in several cancers such as colon, breast, prostate, lung, stomach amongst others which ultimately lead to poor prognosis (Blain, Scher et al. 2003). Mice with functional loss of p27 develop multiple hyperplasias in several organs suggesting its tumour suppressive role in cancer (Fero, Rivkin et al. 1996, Kiyokawa, Kineman et al. 1996, Nakayama, Ishida et al. 1996). Our group has a rat model that develops a spontaneous germline mutation in *Cdkn1b* that promotes the production of unstable p27 protein, therefore developing multiple endocrine neoplasia (MEN) syndrome called MENX (Pellegata, Quintanilla-Martinez et al. 2006). MENX rats are excellent models for studying multiple neuroendocrine tumours as they develop pituitary adenomas, pheochromocytoma, parathyroid hyperplasia, and thyroid C-cell hyperplasia (Fritz, Walch et al. 2002). As previously described in Chapter 1 (section 1.5), medullary thyroid cancer (MTC) accounts for 5-10% of thyroid cancer cases (Pacini, Castagna et al. 2010). MTC is an aggressive type of thyroid cancer due to its late-stage diagnosis and presence of lymph node metastasis. MENX heterozygous rats develops C-cell hyperplasia that later develop into metastatic MTC by 16-18 months. While, MENX homozygous mutant rats have a shorter life span of 7-8 months and develop the MEN syndrome (Molatore, Kügler et al. 2018). The morphology of the tumours in MENX rats are comparable to that in human patients and in rats there is an increase in serum calcitonin levels with an increase in tumour size as in their human counterpart (Molatore, Kügler et al. 2018).

A recent study published by our group shows a transcriptome profiling of MTC in MENX rats. The gene expression profile of MENX heterozygous rats with advanced MTC was compared with previously published data on human MTCs carrying the RET-M918T mutation (Maliszewska, Leandro-Garcia et al. 2013). There were 26 genes dysregulated in both groups (Molatore, Kügler et al. 2018). One of the genes that were significantly upregulated in MTCs, bearing the aggressive M918T mutation was *TRIB2* (Molatore, Kügler et al. 2018). Interestingly, *Trib2* was first identified in dog thyroid by Wilkin *et al.* and was expressed predominantly in the dog thyroid (Wilkin, Suarez-Huerta et al. 1997). Since then, there have not been any studies focusing on *TRIB1* or *TRIB2* in the thyroid gland. The role of *TRIB3* in thyroid cancer is still unclear; there was one study that reported hyperthyroidism and thyroid

carcinoma in *Trib3* whole body heterozygous mice crossed with *Pten* whole body heterozygous mice (Salazar, Lorente et al. 2015).

Several studies have shown the role of TRIB2 in cancer malignancies that include acute leukaemia, melanoma, lung, liver and ovarian cancer. Depending on the tissue type, *TRIB2* can act as a tumour suppressor or as an oncogene (O'Connor, Yalla et al. 2018). A recent study by Salomé *et al*. show the tumour suppressive function of TRIB2 in AML, where TRIB2 was initially identified as an oncogene (Salomé, Magee et al. 2018). Thus suggesting that TRIB2 might play a dual role by regulating various signalling. Therefore, further studies are needed for understanding the underlying role of *TRIB2* in various cancers. Based on the genes dysregulated in the transcriptomic comparison between MENX rat model and human MTC tumours, we decided to investigate *TRIB2* in MTC.

5.4 Hypothesis

Based on the previous work performed in our group, we hypothesize that *TRIB2* might be involved in MTC tumorigenesis.

To test this hypothesis, we used the following objectives:

1. To generate stable MTC cell lines (MZ-CRC-1 and TT) with *TRIB2* modulation and to validate this using RT-PCR, immunoblot and immunofluorescence.
2. To investigate the *TRIB2* modulation in MTC cell lines *in vitro* by measuring cell viability, proliferation, migration and invasion and to identify potential signalling pathways regulating the above shown effect.
3. To verify whether *TRIB2* modulation in MTC cell lines has an effect on drug treatment *in vitro*.

5.5 Methods

5.5.1 Validation of TRIB2 overexpression in HEK-293T cells

Lentiviral vector was used to overexpress TRIB2 in MTC cells. This vector was first tested in HEK-293T cells and the transfection efficiency was confirmed by observing GFP positive cells under a fluorescent microscope. Around 90% of the cells showed fluorescence and 48 hours after transfection and cells were collected for protein isolation. TRIB2 overexpression was confirmed by performing immunoblot, as shown in Figure 5.5.1. After the validation, HEK-293T cells were further used to generate lentivirus to transduce MTC cell lines (MZ-CRC-1 and TT).

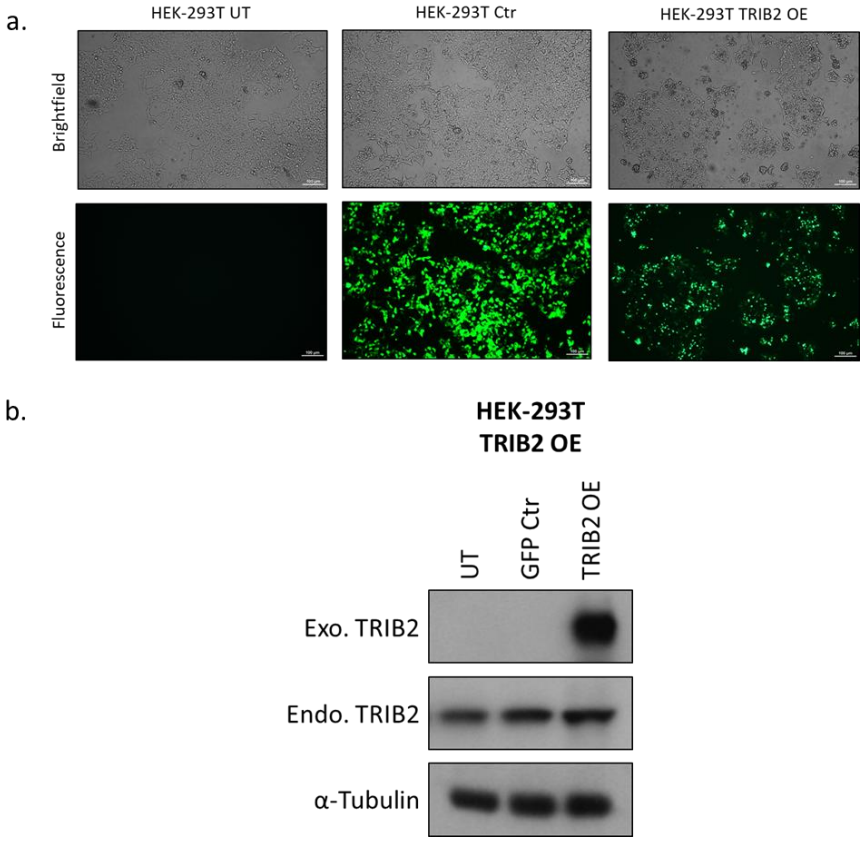

Figure 5.5.1: TRIB2 overexpression in HEK-293T cells.
(a) HEK-293T cells were transfected with TRIB2 cDNA lentiviral construct. No transfection control is shown by untreated cells (UT). GFP Ctr was used as a control for TRIB2 OE. GFP positive cells were observed by fluorescence microscope. (b) TRIB2 overexpression (TRIB2 OE) was confirmed by immunoblot.

5.5.2 Human phosphor-antibody array analysis

The phosphor-array analysis was performed using the Proteome profiler antibody array kit (R&D systems™, ARY003B) to detect the differences in phosphor-proteins. MZ-CRC-1 and TT cells were seeded at a concentration of 1 x 10^7 cells and incubated for 48 hours. Afterwards, 1 ml of Lysis Buffer 6 was added to lyse the cells. The homogenate mixture was kept with constant agitation at 4°C. Protein concentration was determined using BCA assay described in section 2.7.4. The samples were added on the nitrocellulose membrane blocked with 5% BSA in TBST. The membranes were incubated overnight with constant agitation at 4°C. Unbound proteins were removed by washing several times with TBST and primary detection antibody Cocktail A and B were added to the membranes for 2 hours at room temperature. Streptavidin-HRP secondary antibody was added to the membrane after the washing steps and chemiluminescent reagents were applied. The protein spots were detected using hyperfilm ECL (GE healthcare) and quantification of spot densities was carried out using ImageJ software.

5.6 Results:

5.6.1 Establishing *TRIB2* overexpression (OE) in MTC cell lines MZ-CRC-1 and TT

Generation of stable cell lines by knockdown or overexpression of the genes of interest is used to characterize their functional role *in vitro*. Lenti-virus transfection is a stable gene delivery method shown to generate stable cell lines (Scherr, Venturini et al. 2010). Human MTC cell lines MZ-CRC-1 and TT carrying different RET mutations were used in the study. To investigate the role of *TRIB2* in thyroid cancer, we decided to modulate *TRIB2* expression in MTC cells. We first started with the generation of stable *TRIB2* OE cells using Lentivirus. The detailed protocol is explained in section 2.5. The efficiency of the cDNA construct was validated as shown in Figure 5.5.1 in HEK-293T cells. Figure 5.6.1a shows the GFP-TRIB2 fusion protein showed a faint fluorescence signal in the *TRIB2* OE cells when compared to cells infected with GFP alone. TRIB2 OE in MZ-CRC-1 and TT cells was confirmed using immunofluorescence, immunoblotting and RT-PCR (Figure 5.6.1b).

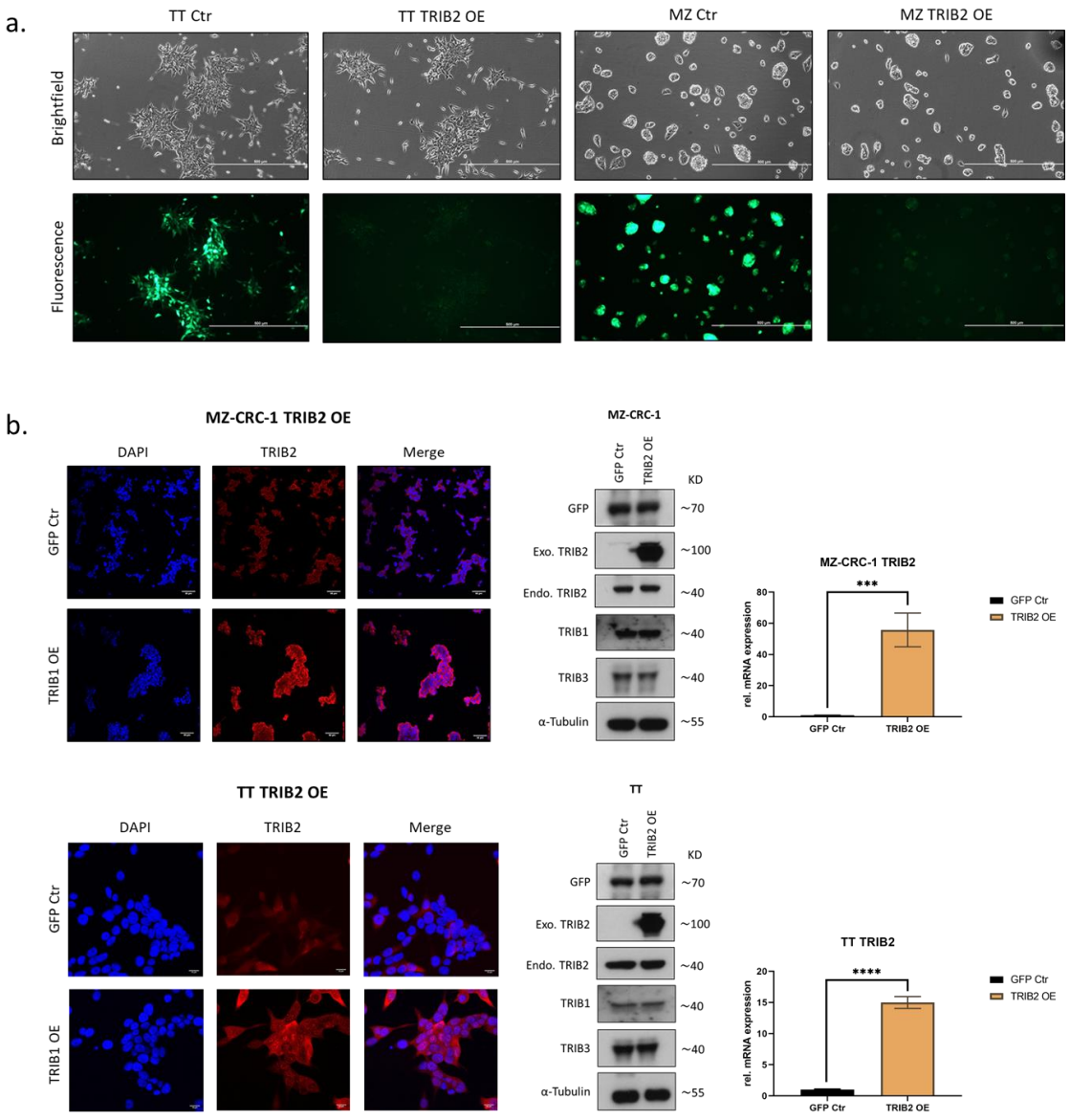

Figure 5.6.1: TRIB2 overexpression in MZ-CRC-1 and TT cells
(a) GFP expression in the MTC cell line following *TRIB2* lentivirus infection for 72 hours. (b) TRIB2 overexpression in MZ-CRC-1 and TT cells was assessed by immunofluorescence, immunoblotting and RT-qPCR. Data show the mean ±SD from three independent experiments. Unpaired t-test, ***P ≤ 0.001, **** P ≤ 0.0001 compared to the GFP Ctr group.

5.6.2 *TRIB2* overexpression inhibits cell viability of MZ-CRC-1 and TT cells

Next, we determined whether *TRIB2* OE could affect MTC cell viability. Therefore, we performed 3D cell viability assay by seeding MZ-CRC-1 and TT TRIB2 OE cells on the ULA plates. 5 days after the formation of spheroids, cell viability reagents were added and the measurements were taken every 24 hours for 3 days. Both the stable cell lines were validated for *TRIB2* OE before performing the experiments. As observed from the graph in Figure 5.6.2, at 72 hours, we observed a drastic decrease up to 50% in the viability of both MZ-CRC-1 and TT cells having TRIB2 overexpression. On the contrary, to our expectations we saw that *TRIB2* OE cells suppressed cell viability in 3D spheroids.

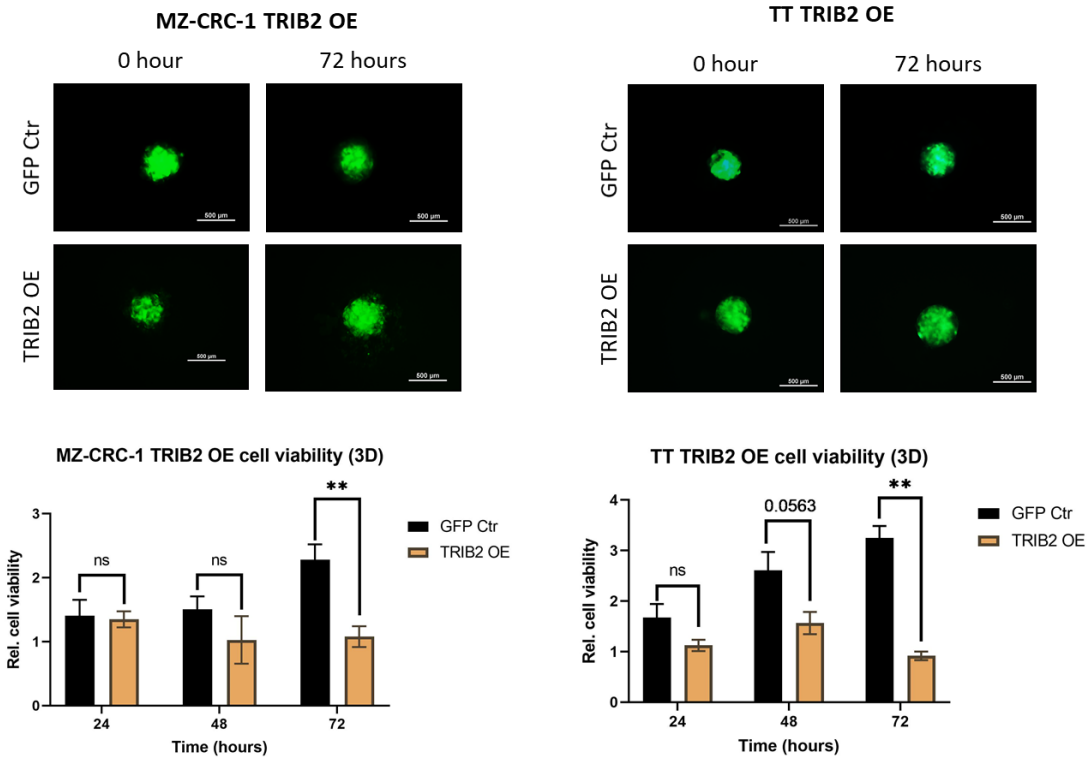

Figure 5.6.2: 3D Cell viability of MTC cell lines with *TRIB2* overexpression
The MTC cell lines as 3D spheroids were measured for their cell viability over 72 hours. Pictures were taken right after the addition of the cell viability reagents and at 72 hours. Graphs represent cell viability measurements taken every 24 hours for 3 days normalised to Day 0 measurements. Data show the mean ±SD from three independent experiments. 2way ANOVA, ** P ≤ 0.01, ns p>0.05 compared to the GFP Ctr group.

5.6.3 *TRIB2* overexpression inhibits cell proliferation in MZ-CRC-1 and TT cells

Based on our cell viability results, we further examined the effect of *TRIB2* OE on dividing cells by performing cell proliferation assays. MZ-CRC-1 and TT cells were seeded on black-wall 96-well plates and the following day, cell proliferation reagents were added to each well and measurements were taken every 24 hours for 3 days. Figure 5.6.3 shows a significant decrease in cell proliferation from 48 hours in both the cell lines over-expressing *TRIB2*. These results complement our previous data with cell viability. Therefore suggesting that high levels of *TRIB2* can reduce growth and proliferation of MTC cells.

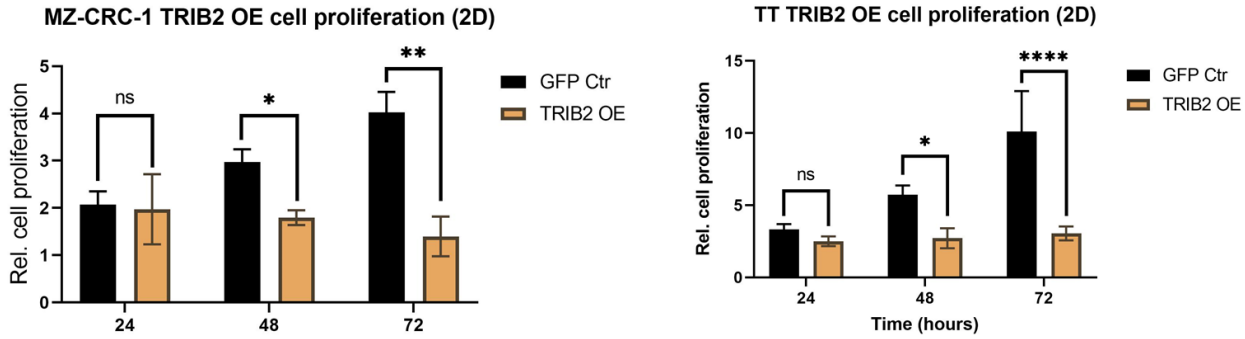

Figure 5.6.3: 2D Cell proliferation of MTC cell lines with TRIB2 overexpression
Cell proliferation in MTC cell lines was measured by taking fluorescence measurements every day over a 72 hours period. Bar graphs represent cell proliferation measurements normalised to Day 0 measurements. Data show the mean ±SD from three independent experiments. 2way ANOVA, * P ≤ 0.05, ** P ≤ 0.01, **** P ≤ 0.0001, ns p>0.05 compared to the GFP Ctr group.

5.6.4 *TRIB2* overexpression inhibits cell migration of MZ-CRC-1 and TT cells

To investigate the effect of *TRIB2* OE on MTC cell migration, the gap closure assay was performed. MZ-CRC-1 and TT cells were seeded on four wells of an IBIDI chamber. Once the desired confluence was achieved, the insert between the wells was removed and 0% or 10% serum culture medium was added. Pictures were taken at day 0 and day 7 and all the pictures were quantified using ImageJ software and the percentage of migrated cells was calculated. In both MZ-CRC-1 and TT cells, TRIB2 OE significantly inhibited cell migration (Figure 5.6.4).

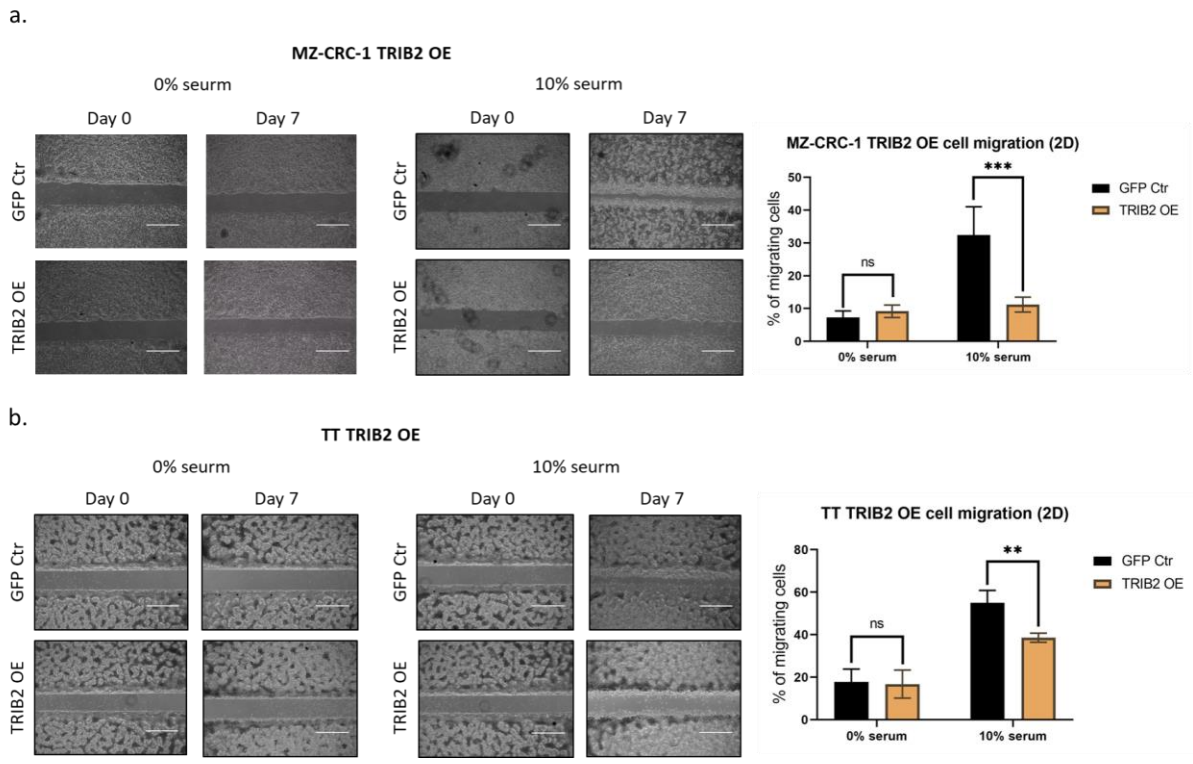

Figure 5.6.4: 2D Cell migration of MTC cell lines with *TRIB2* overexpression
Images were taken immediately after removing the inserts and 7 days later. MZ-CRC-1 cells with *TRIB2* overexpression show a significant reduction in cell migration as compared to control cells. (b) TT cells also show reduced cell migration when overexpressed with *TRIB2*. Bar graphs represent cell migration normalised to Day 0 measurements. Data show the mean ±SD from three independent experiments. 2way ANOVA, ** P ≤ 0.01, **** P ≤ 0.0001, ns p>0.05 compared to the GFP Ctr group.

5.6.5 *TRIB2* overexpression inhibits cell invasion of MZ-CRC-1 and TT cells

We further examined the function of *TRIB2* OE on the invasive capability of MTC cells. We performed 3D invasion assays where we seeded MZ-CRC-1 and TT cells in the ULA plates and 5 days after spheroid formation, Matrigel was added. Pictures of the invading cells were taken on day 0 and day 14. We switched to a 2D system to measure the invasion of TT cells since we saw that these cells do not invade in a 3D system (Data not shown). TT cells were seeded on Transwell inserts coated with/without Matrigel. After 24 hours, culture medium was added, the migrating cells were stained with Toluidine blue and photos were taken. *TRIB2* overexpression significantly reduced MZ-CRC-1 and TT cell invasion as compared to the control cells. Therefore, taking into account also the results from the migration assays, *TRIB2* inhibits both migration and invasion of MTC cell lines.

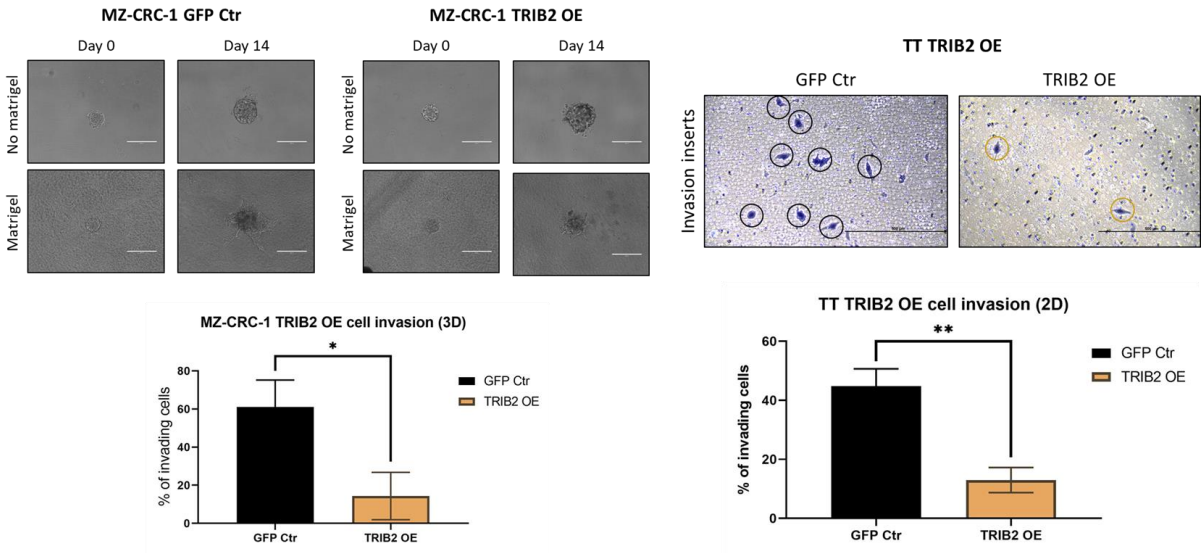

Figure 5.6.5: Cell invasion of MTC cell lines with *TRIB2* overexpression
Cell invasion was performed with 3D culture for MZ-CRC-1 cells and for TT cells, it was performed in 2D Transwell inserts with non-Matrigel or Matrigel-coated membranes. For MZ-CRC-1 cells, the pictures were taken immediately after adding the Matrigel and after 14 days once invasion through the Matrigel was visible. TT cells were stained with Toluidine blue and the cells invading through the 2D Matrigel were photographed (3 technical replicates for each cell line) and pictures were taken for 3 representative fields per sample for calculating the average. Quantification was carried out in Excel by calculating the percentage of invading cells. Data show the mean ±SD from three independent experiments. Unpaired t-test, * $P \leq 0.05$, ** $P \leq 0.01$, compared to the GFP Ctr group.

5.6.6 *TRIB2* overexpression inhibits cell migration in MZ-CRC-1 and TT cells

To investigate the underlying mechanisms by which *TRIB2* inhibits MTC cell growth and progression, we examined the effect of *TRIB2* OE on signalling pathways. Since *TRIB2* has been previously reported to affect AKT and MAPK signalling (Richmond and Keeshan 2019), we tested whether the MZ-CRC-1 and TT cells with TRIB2 overexpression show changes in the activation of AKT and MAPK pathways. As shown in Figure 5.6.6, surprisingly, *TRIB2* OE had no effect on AKT and ERK phosphorylation as compared to the control cell line. Therefore, to identify the specific effector signalling proteins affected by *TRIB2* overexpression, we examined 43 individual phosphor-proteins using a protein array kit.

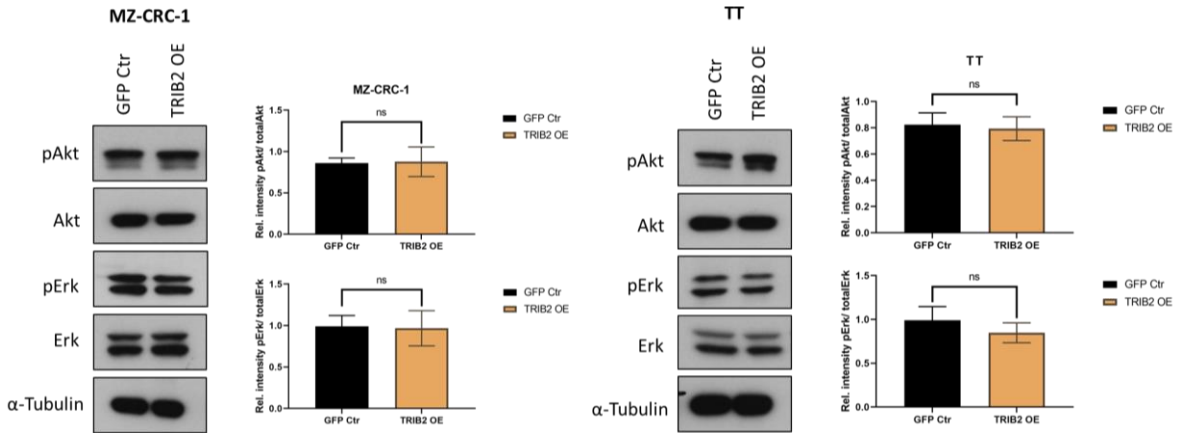

Figure 5.6.6: Effect of *TRIB2* overexpression in MTC cell lines on AKT and ERK signalling.
Immunoblots representing phosphor-Akt (pAKt), total Akt, phosphor- Erk (p-Erk) and total Erk. Graphs represent the ratio of pAkt over total Akt. Data show the mean ±SD from three independent experiments. Unpaired t-test, ns p>0.05 compared to the GFP Ctr group.

5.6.7 Human Phosphor-Kinase Array on MTC cells with *TRIB2* overexpression

To assess the effect of *TRIB2* OE on different phosphor-proteins, a commercially available protein array was probed with cell lysates. Relative expression levels of the phosphor-proteins were normalised to manufacturer's positive control samples. As shown in Figure 5.6.7, we did not detect any major changes in the levels of phosphor-proteins. However, TT *TRIB2* overexpressing cells showed an elevation in STAT6, JNK, AKT T308 and MSK levels compared to control cells. Because the experiment was only performed once, more replicates are needed to confirm if these changes are indeed reproducible. Furthermore, elevated phosphor-proteins should be confirmed by immunoblotting.

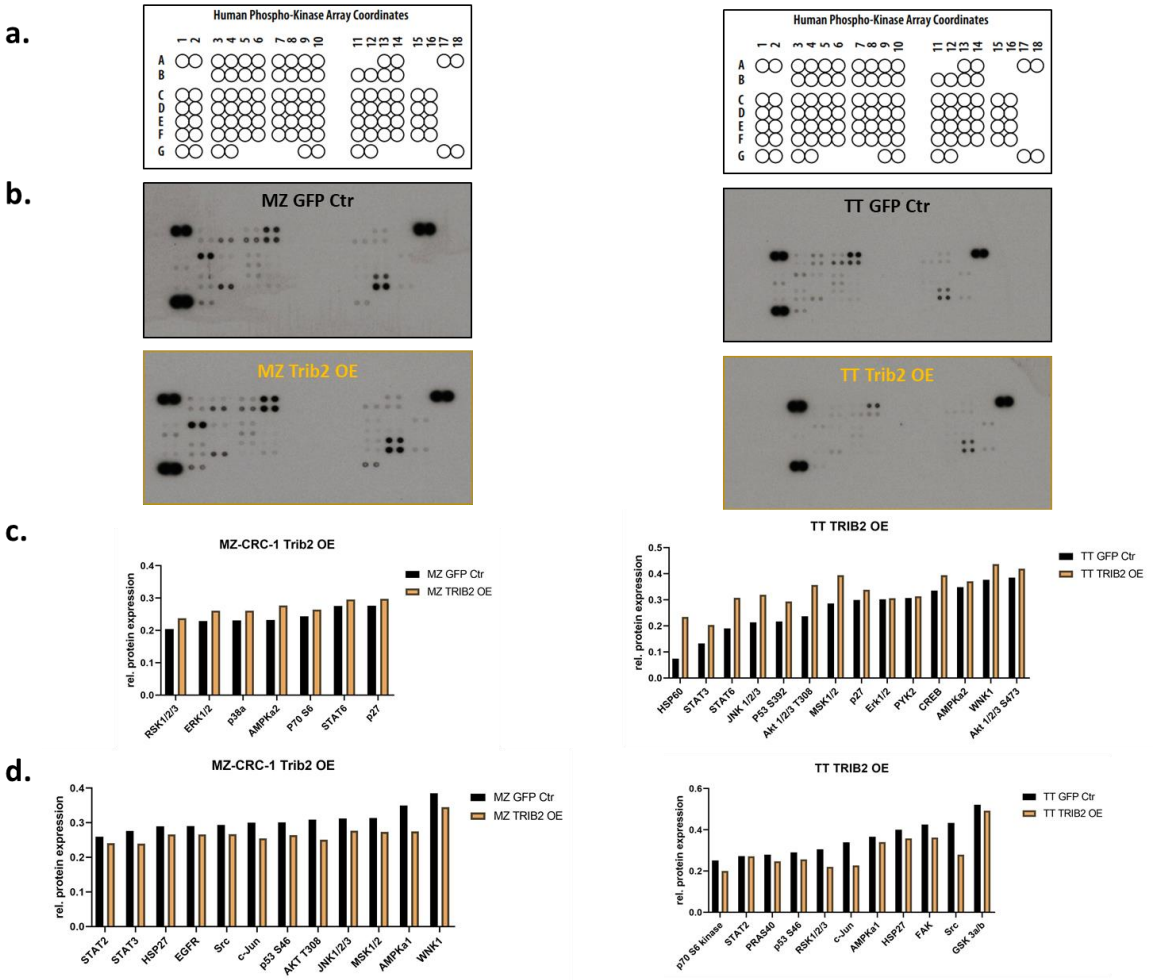

Figure 5.6.7: Proteome profiler analysis of MTC cells with *TRIB2* overexpression
(a) Human Phosphor-Kinase Array co-ordinates that detects relative levels of phosphorylation of 43 kinase phosphorylation sites in duplicates. (b) Nitrocellulose blot with total protein lysates from *TRIB2* OE and control cells. The quantification of the blots as two set of graphs with proteins that were up-regulated and proteins that were down-regulated (c) MZ-CRC-1 and TT *TRIB2* OE cells with phosphor-proteins upregulated. (c) MZ-CRC-1 and TT TRIB2 overexpression cells with phosphor-proteins downregulated. This experiment was performed once.

5.6.8 *TRIB2* overexpression in MZ-CRC-1 cells has decreased cell viability to Cabozantinib treatment

To further detect the effect of *TRIB2* OE on drug response, MTC cells were incubated with different concentrations of receptor tyrosine kinases inhibitors, Cabozantinib and Vandetanib. These drugs are FDA-approved for the treatment of advanced MTC. Cells were seeded in 96 well- plates and treated for 72 hours. We used a range of drug concentrations previously published for these cell lines (Starenki, Hong et al. 2017). Control wells were treated with 0.5% DMSO. As expected, we saw reduced cell viability at 0.25µM for Cabozantinib and 0.5µM for Vandetanib (Starenki, Hong et al. 2017). Overall, cells with *TRIB2* OE responded similarly to the Ctr cells. Interestingly, measurements taken at 72 hours showed 70% reduced viability for MZ-CRC-1 *TRIB2* overexpressing cells upon treatment with Cabozantinib, whereas Ctr cells had a 45% reduced viability. This suggests that *TRIB2* might be involved in the sensitivity of MZ-CRC-1 cells to Cabozantinib, however further studies are required to confirm this assumption. In contrast, amongst the other GFP control cells and *TRIB2* overexpression cells, we did not see a significant difference in drug response.

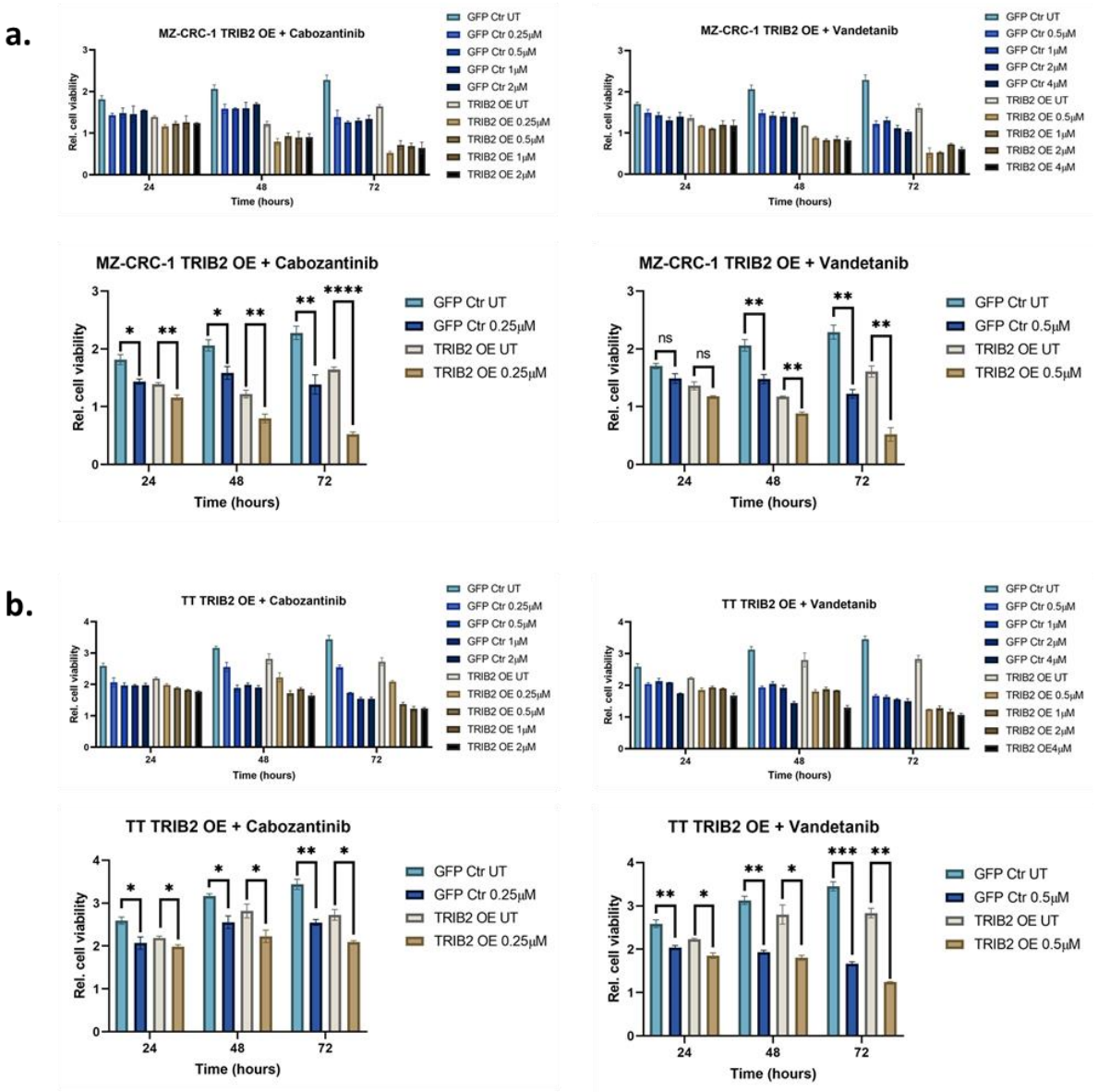

Figure 5.6.8: *TRIB2* overexpression decreases cell vaibilty for Cabozantinib treatment in MZ-CRC-1 cells
(a) Cell viability of MZ-CRC-1 cells treated with different concentrations of Cabozantinib and Vandetanib. The lower panels show graphs with 0.25µM for Cabozantinib and 0.5µM for Vandetanib treatment and statistical test performed (b) Effect on cell viability of TT cells treated with different concentrations of Cabozantinib and Vandetanib. The lower panels show graphs with 0.25µM for Cabozantinib and 0.5µM for Vandetanib treatment and statistical test performed Data shows the mean ±SD from three independent experiments. 2way ANOVA, * P ≤ 0.05, ** P ≤ 0.01, ***P ≤ 0.001, **** P ≤ 0.0001, ns p>0.05 compared to the GFP Ctr group.

5.6.9 TRIB2 expression in thyroid normal and tumour tissue

Lastly, we wanted to determine the expression of TRIB2 in normal thyroid and tumour tissues. Normal thyroid serial sections form one patient sample was used to optimise IHC staining for TRIB2 and calcitonin antibodies. The tissue itself did now show any background when none of the antibodies was added (Data not shown). Additionally, only primary and secondary antibody controls were used to detect any unspecific binding. The antibody controls did not show background staining, as shown in Figure 5.6.9. The preliminary staining illustrated in Figure 5.6.9c show that TRIB2 staining is comparable to calcitonin staining in the C-cells. For confirming the specificity of the staining, we plan to show the slides to a pathologist for further feedback.

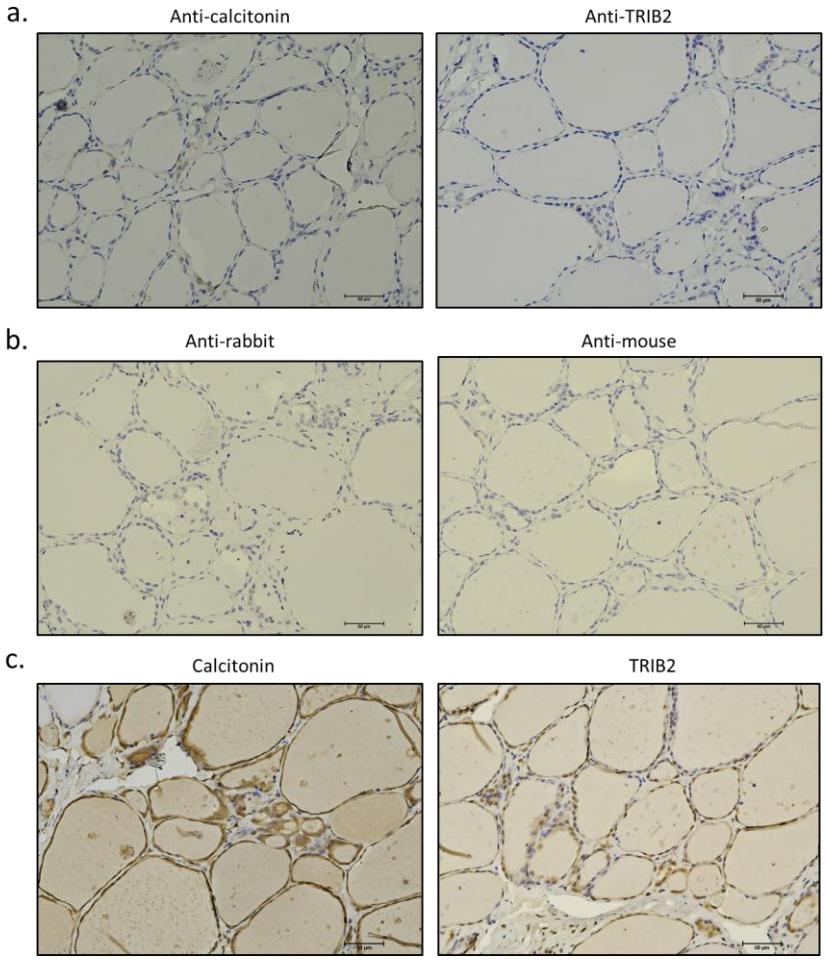

Figure 5.6.9: Optimisation of IHC controls for Calcitonin and TRIB2 antibodies
IHC staining was performed on serial sections of normal thyroid tissue with Calcitonin and TRIB2 antibodies. (a) Only primary antibody control was added to the tissues to identify any unspecific staining. (b) No primary control with only secondary antibody was added to the tissue and did not show any unspecific background staining. (c) Calcitonin protein expression (positive marker) and TRIB2 showed cytoplasmic staining in a few C cells in the normal thyroid tissue

5.7 Discussion and Future work

Medullary thyroid carcinoma (MTC) is a malignant neuroendocrine tumour developing from para-follicular C-cells of the thyroid gland. 75% of MTCs are sporadic and the remaining 25% arise due to hereditary mutations. Point mutations in *RET* proto-oncogene contribute to the majority of MTC cases (Castellone and Melillo 2018). RET-M918T mutation in exon 16 occurs in 94% of hereditary cases and up to 50% of somatic cases. RET-M918T mutation is associated with poor prognosis as it activates pathways involved in invasion and metastasis (Maliszewska, Leandro-Garcia et al. 2013). Gene expression profiles of human MTCs cases are guided by presence and type of RET mutations (Jain, Watson et al. 2004, Maliszewska, Leandro-Garcia et al. 2013, Oczko-Wojciechowska, Swierniak et al. 2017).

The MENX rat model develops multiple neuroendocrine tumours, including MTC. A previous study from our group performed transcriptome profiling on MTCs from MENX p27 heterozygous and homozygous mutant rats at 9 and 18 months of age (Molatore, Kügler et al. 2018). Heterozygous MENX rats survive for approximately 18 months whereas homozygous mutant rats develop C-cell thyroid hyperplasia already at 2 months of age. Homozygous mutant MENX rats do not survive beyond 8 months due to the development of other neuroendocrine tumours. When transcriptome profiling was carried out, referencing to the normal C-cells was challenging due to its low number in thyroid tissue under non-disease condition. Therefore, Molatore *et al.* compared tumours from MENX heterozygous 18-month rat, showing pre-malignant condition with MENX mutant 9-month rat representing advanced MTC (Molatore, Kügler et al. 2018). Furthermore, they identified genes differentially expressed between rat MENX MTCs and human MTCs. There were 26 genes that were differentially expressed in both the subsets. *In silico* analysis showed upregulation of *TRIB2, TUBB2B, GREM2, NREP, TUBB6, CA10* and *GRHL3.* While *PLA2G16, SMAD9, HSPB1* and *CLDN3* were found to be downregulated amongst others, between RET-M918T and RET-WT human MTCs versus early and advanced rat MTCs (Molatore, Kügler et al. 2018).

Previous studies have reported that Tribbles family members exhibit both tumour suppressor and oncogenic properties depending on the cellular type (Richmond and Keeshan 2019). Recent studies showed the involvement of *TRIB2* in regulating proliferation, apoptosis and

drug resistance in various cancers (Kritsch, Hoffmann et al. 2017, O'Connor, Yalla et al. 2018, Salomé, Magee et al. 2018). In AML and liver cancer, *TRIB2* overexpression promotes aggressiveness by downregulation of C/EBPα pathway (Keeshan, He et al. 2006, Grandinetti, Stevens et al. 2011). *TRIB2* promotes cell survival and transformation in liver cancer cells and protein stabilization through βTrCP ubiquitin ligase (Wang, Park et al. 2013). Kritsch *et al.* showed that *TRIB2* promotes drug sensitivity in ovarian cancer cells (Kritsch, Hoffmann et al. 2017). However, there are no available studies regarding the role of *TRIB2* in thyroid cancer. Based on the available literature, we selected *TRIB2* as a candidate gene for further analysis.

To study the functional role of *TRIB2* in MTC, we used two different MTC cell lines: MZ-CRC-1 (RET M918T) and TT (RET C634W mutation) as model systems. We first did overexpression of *TRIB2* using TRIB2 overexpressing Lentiviral vector in the MZ-CRC-1 and TT cells. The *in vitro* experiments demonstrated inhibition of cell viability and proliferation in cells with *TRIB2* overexpression. Furthermore, migration and invasion were also significantly reduced. These data suggest that *TRIB2* may play a tumour suppressive role by inhibiting the survival, migration and invasion of MTC cells. We want to confirm these results by downregulating *TRIB2* in the MTC cells where we expect to see the opposite effects. Initial work to generate Lentiviral vectors with TRIB2 knockdown has already started in our lab. In addition to the cellular phenotype, we tried to determine the molecular mechanisms underlying the tumour suppressive role of *TRIB2*. Several studies have reported the role of AKT and MAPK pathway for cell growth and metastasis (Johnson and Lapadat 2002, Manning and Cantley 2007). Furthermore, *TRIB2* has been shown to regulate AKT and MAPK signalling (Richmond and Keeshan 2019). Therefore, we investigated the effect of *TRIB2* overexpression on the activation of downstream signalling pathways in MTC cells. Surprising we found no difference in AKT and ERK1/2 phosphorylation between *TRIB2* OE and Ctr cells. To identify which kinases are phosphorylated due to *TRIB2* overexpression, we used human phosphor array kit. We identified upregulation of the following phosphor proteins: STAT6, JNK, AKT T308 and MSK in TT cells. However, we would like to repeat the experiment one more time and perform immunoblots with specific antibodies for validation. This would be beneficial to explore the exact mechanism of how *TRIB2* influences the downstream signalling pathways in MTC.

Next, we investigated the effect of TRIB2 on drug treatment. In MZ-CRC-1 cells bearing RET-M918T mutation upon treatment with Cabozantinib, we observed reduced cell viability. Interestingly, in TRIB2 overexpressing cells, there was a 70% decrease in cell viability as compared to the control GFP cells showing a decrease of 45%. It would be interesting to perform apoptosis assay after drug treatment and to determine whether this effect will be reversed when TRIB2 is knocked downed in the cells

We plan to further validate these results by performing *in vivo* study. MTC xenograft mouse models using MZ-CRC-1 and TT cells are widely used to monitor tumour growth *in vivo* and test the safety of multiple kinase inhibitors (Lopergolo, Nicolini et al. 2014). We have planned to inject *TRIB2* modulated MZ-CRC-1 and TT cells subcutaneously on the back of athymic nude mice. When tumours develop, mice will be randomly distributed into control and treatment groups. Mice will be treated with Cabozantinib and Vandetanib for 3 weeks and at the end of the study, the tumour will be collected for immunohistochemistry and molecular analysis. Moreover, we started optimising the TRIB2 antibody for immunohistochemistry on normal thyroid tissue. In the staining's we saw no background when using the TRIB2 or the calcitonin antibodies, suggesting that the staining are specific. In the normal tissue, we observe TRIB2 expression comparable to the calcitonin staining however; we need to further confirm the staining's by a pathologist. We intend to stain a tissue microarray of normal and tumour thyroid tissues for TRIB2 expression.

In conclusion, our results suggest that *TRIB2* functions as a tumour suppressor *in vitro* by inhibiting cell survival, migration and invasion. Further *in vivo* studies would be useful to investigate the biological role of *TRIB2* in MTC and its effect on drug treatment.

5.8 Limitations

The results presented in this chapter have some limitations. First, due to the low amount of C cells in the normal thyroid tissue, it was a challenge to normalise to the normal control while performing *in silico* analysis. Therefore, all the *in silico* analysis performed previously compared tumours with wild type RET and RET mutations. This might have an impact on the results concerning the differentially expressed genes. Additionally, for *in vitro* experiments, due to the unavailability of normal C-cells, we could only use tumour cell lines (MZ-CRC-1 and TT) and compare them with each other.

5.9 Conclusion

The main goal of the current study was to determine the biological role of *TRIB2* in MTC. Based on previous findings from our group, we hypothesised that *TRIB2* is an oncogene in MTC. However, based on our *in vitro* experiments, we report *TRIB2* as a tumour suppressor in MTC. We observed that stable *TRIB2* overexpression in MTC cells inhibits their viability, proliferation, migration and invasion *in vitro*. Due to time constraints, we could not identify the signalling pathways that mediate the *TRIB2*-dependent inhibition of cell growth and migration. However, based on our preliminary experiments of phosphor-proteins arrays, this approach might identify downstream pathways. Drug resistance is one of the major problems for the treatment of advanced MTC. Here we report that *TRIB2* has lowered cell viability in MZ-CRC-1 cells to Cabozantinib, a multiple tyrosine kinase inhibitors. Future work would be beneficial to determine the role of *TRIB2* drug response in MTC.

Chapter 6 : General discussion and conclusion

Cancer is the second leading cause of deaths globally behind cardiovascular diseases (The Lancet Diabetes 2020). International Agency for Research in Cancer, France conducted more than 1000 epidemiologic studies and concluded that higher BMI leads to increased risk of 13 types of cancers (Lauby-Secretan, Scoccianti et al. 2016). Despite the growing evidence about the association between obesity and cancer, the molecular mechanism underlying this still remains unclear. This thesis aims to identify and evaluate the role of target genes that might be involved in the cross-talk between obesity, with an increase in adiposity and cancer. Based on the previous studies, TRAIN consortium focuses on characterising the role of TRIBs in the context of immunity, metabolism, system biology and PCa. Therefore, my project focuses on determining the role of *TRIB1* and *TRIB3* in PCa progression under the influence of adipose tissue microenvironment. The results summarised below for the first time show the oncogenic role of *TRIB3* in PCa both cell-autonomously and under the influence of adipose tissue microenvironment. We observed that adipocytes contribute to an increase in the TRIB1 and TRIB3 expression in PCa cells. Next, by using 2D and 3D *in vitro* assays with PCa cells, we showed *TRIB3* expression promotes the viability, proliferation, migration and invasion. The second major finding of this study was to report the novel tumour suppressive role of *TRIB2* in MTC. In the following paragraphs, we would summarise the major findings of this study.

In recent years, there has been an increasing interest in studying the tumour microenvironment surrounding cancer. Adipose tissue primarily acts as a lipid-storing organ, which is located throughout the body and therefore found adjacent to various invasive cancers including colon, breast, melanoma and prostate (Park, Morley et al. 2014, Clement, Lazar et al. 2017, Lengyel, Makowski et al. 2018). The prostate gland is surrounded by a capsular structure called periprostatic adipose tissue (PPAT), which is directly in contact with the anterior surface of the prostate gland (Balaban, Nassar et al. 2019). Adipose tissue secretes cytokines, chemokines, growth factors and hormones collectively known as adipokines (Funcke and Scherer 2019). These adipokines mediate the cross-talk between cancer and surrounding adipose tissue and contribute to cancer progression (Attané and Muller 2020). In obese condition, PPAT show altered adipose tissue homeostasis by increased production and secretion of chemokines and proinflammatory cytokines (Attané and Muller 2020). Ribeiro *et al.* compared gene expression profiles of PPAT from obese men and saw overexpression of adipogenic, proliferative and mild immunoinflammatory genes compared

to lean men (Ribeiro, Monteiro et al. 2012). Therefore showing a prominent association between adipose tissue microenvironment and PCa. At this point, there is a clear need for identifying the factors that are involved between the cross-talk between adipocytes and cancer cells. There are very few studies focusing on the molecular pathways defining the role of PPAT in PCa progression.

Tribbles family of pseudokinases play an important role in cellular processes by regulating several key signalling pathways. Recent evidence has reported the multifunctional role of TRIBs in various cancer and drug resistance (Hill, Madureira et al. 2017, O'Connor, Yalla et al. 2018, Richmond and Keeshan 2019). However, their role in PCa is not well characterised. There are few studies showing the oncogenic role of TRIB1 in PCa (Lin, Huang et al. 2014, Mashima, Soma-Nagae et al. 2014, Shahrouzi, Astobiza et al. 2020), while there is insufficient data on the role of TRIB2 and TRIB3 in PCa.

In this thesis, we have described the effect of adipose tissue microenvironment on PCa in the context of TRIBs. We demonstrated that adipocytes secrete factors that regulate TRIB1 and TRIB3 expression in the PCa cell lines, Du145 and PC3. This effect was observed with differentiated adipocyte cell lines 3T3-L1 and 3T3-F442A, primary mature adipocytes from mice and primary mature adipocytes from PPAT of two PCa patients, as part of a preliminary experiment. We consistently observed that the conditioned media (CM) from mature adipocytes resulted in increased TRIB1 and TRIB3 expression in Du145 and PC3 cells. Both PCa cell lines represent aggressive tumours since both of them are isolated from different metastatic locations in PCa patients. As mature adipocytes are the major component of adipose tissue, and therefore we speculate, the mature adipocytes present in PPAT could upregulate the TRIB1 and TRIB3 levels in PCa cells *in vivo*. TRIBs immunohistochemistry staining on PCa tissue sections adjacent to adipose tissue could help us characterise the role of mature adipocyte secretory factors on TRIBs levels in PCa. We also reported the increase in the TRIB1 and TRIB3 expression due to adipose tissue microenvironment was specific to PCa, as we did not observe this effect when we used breast cancer cells. This suggests that the mechanisms underlying the regulation of TRIBs in cancer cells are somehow cell type specific. Further experiments using other types of cancer cells having adipose tissue in the

vicinity, such as ovarian cancer or colon cancer, can be useful further to understand the regulation of TRIBs in the tumour microenvironment.

We discovered that the results obtained from CM culture were cell type specific, meaning depending on the CM used we saw differences in TRIBs expression. For instance, when we cultured Du145 cells with the CM from 3T3-F442A adipocytes, there was an increase in TRIB1 and TRIB3 protein expression. In comparison, PC3 cells did not show any changes in TRIBs levels with CM from 3T3-F442A adipocytes. In PC3 cells, we detected an increase in TRIB1 and TRIB3 expression with CM from 3T3-L1 adipocytes. Additionally, CM from primary mouse adipocytes also showed these differences. In a pilot study with the CM culture from primary PPAT adipocytes, we saw both the cell lines showed TRIB3 upregulation. Therefore taken together these findings suggests that there might be different secretory factors from adipocytes that act alone or in combination to modulate the TRIBs levels in PCa cells. Therefore, in an exploratory experiment to determine which are the secretory factors modulating TRIBs expression in PCa cells, we identified CXCL13, IL6 and Leptin. Here we saw the TRIB1 and TRIB3 levels in PCa cells were increased upon adding the increasing concentration of recombinant adipokines. Previously it has been reported that adipokines regulate the expression of miRNAs; therefore, exerting oncogenic or tumour suppressive role depending on the cancer type (Jasinski-Bergner and Kielstein 2019). The current results highlight the role of adipokines secreted by adipocytes in modulating gene expression in cancer cells. To confirm that these adipokines indeed mediate TRIB1 and TRIB3 upregulation, we need to block these adipokines by using antibodies in the CM. Additionally, ELISA can be performed on the CM to determine each chemokine's concentration and correlate with their induction of TRIBs expression.

A follow-up study was conducted to understand the increase in *TRIB1* and *TRIB3* levels in PCa and how this can contribute to cancer progression. We used PCa cells with stable modulation of *TRIB1* and *TRIB3* and assessed the effect of adipocyte CM on them. On contrarily to our expectations, we did not observe any effect of *TRIB1* overexpressing Du145 and PC3 cells on tumour cell behaviour with or without CM. This was surprising since *TRIB1* was previously shown to behave as an oncogene in PCa (Lin, Huang et al. 2014, Mashima, Soma-Nagae et al. 2014). However, our results were in line with a recent study from Parastoo Shahrouzi from

the TRAIN consortium, who analysed the effect of *TRIB1* in PCa cells using normal culture media without looking at the effect of adipocytes. Shahrouzi *et al.* reported the transgenic *TRIB1* overexpression in the prostate epithelium of mice promoted cell proliferation in contrast to their *in vitro* data. At the same time, *TRIB3* knockdown in PCa cells caused a significant reduction in growth and migration. Additionally, when CM was added, the pro-migratory effect of the CM was abolished in Du145 and PC3 cells with *TRIB3* KD. Therefore suggesting that the presence of *TRIB3* in PCa cells supports the oncogenic behaviour of secretory factors from the CM of adipocytes. Overall, this study for the first time documents the role of *TRIB3* in PCa cell lines, Du145 and PC3. Our *in vitro* results support the oncogenic role of *TRIB3* in PCa and highlights the importance of adipose cells in the microenvironment that can further result in higher aggressiveness by *TRIB3* upregulation. Further research using the *in vivo* model is required to confirm our *in vitro* findings and identify the underlying molecular mechanisms mediating TRIB3 upregulation in PCa cells. These results can be clinically relevant as adipokines have been shown to promote PCa aggressiveness and identify TRIB3 as a target gene involved in this cross-talk to design specific therapeutic strategies, especially in obese patients.

As part of adipose tissue microenvironment, we also tried to understand the role of TRIBs in adipose tissue and their influence on PCa progression. It has been previously reported that *Trib1* heterozygous knockout mice show altered cytokine expression in adipocytes and protect the mice from high-fat diet-induced obesity (Ostertag, Jones et al. 2010). In adipose tissue, *Trib3* has been shown to regulate adipogenesis by suppressing the activity of C/EBPβ. In summary, *Trib1* and *Trib3* play a role in adipose tissue homeostasis. As previously discussed, adipose tissue microenvironment plays a critical role in PCa progression. We aimed to determine the *Trib1* and *Trib3* modulation in adipose tissue on PCa cell behaviour. Due to numerous problems encountered with the generation and breeding of Tamoxifen inducible adipocyte-specific *Trib1* overexpressing mice discussed in section 4.6, we focused on whole-body knockout *Trib3* mice in this thesis.

We bred experimental cohorts of *Trib3* knockout and wild type mice and isolated mature adipocytes from scWAT and visWAT deposits. Our tumour behavioural results with the CM from mature adipocytes of *Trib3* knockout and wild type mice showed no differences in PCa

cell viability, migration and invasion in Du145, PC3 and TRAMP-C2 cells. Thus suggesting that *Trib3* deletion in the adipose tissue does not secrete factors that can contribute to PCa aggressiveness. One of the limitations of the study was the use of whole-body knockout *Trib3* mice for experiments. Davey *et al.* previously reported that whole-body knockout mice could have secondary effects on other organs that might result in variability that are difficult to identify (Davey and MacLean 2006). Despite the limitation, in our experimental model, we saw that *Trib3* deletion in the adipose tissue does not affect tumour behaviour of Du145, PC3 and TRAMP-C2 cells.

The second aim of this thesis was to investigate the role of *TRIB2* in MTC. Previous experiments in our group showed that *TRIB2* was differentially regulated in human MTCs with RET-M198T and RET WT mutations as well as in MENX rat tumour model. And based on the mutational role of *TRIB2* in various cancers (Keeshan, He et al. 2006, Rishi, Hannon et al. 2014, Hou, Guo et al. 2018), we selected *TRIB2* for investigating its role in MTC. We generated MTC cell lines stably overexpression *TRIB2* and analysed the effect on tumour cell behaviour. Interestingly, we saw that *TRIB2* acts as a tumour suppressor by inhibiting viability, proliferation, migration and invasion of MTC cells *in vitro*. Furthermore, *TRIB2* decreased cell viability compared to control cells in MZ-CRC-1 cells towards Cabozantinib treatment; an FDA approved tyrosine kinase inhibitor used for the treatment of MTC. Taken together, these findings suggest that *TRIB2* acts as a tumour suppressor in MTC cells *in vitro*. Further research involving *in vivo* experiments are needed to confirm our findings and drug treatment studies can be carried out by injecting TRIB2 overexpressing cell in nude mice.

Currently, the treatment options for lean and obese PCa patient are the same. Our findings confirm the effect of normal culture media and adipose-derived CM on PCa progression as reported previously (Laurent, Guerard et al. 2016). Overall, this thesis tries to understand the mechanism behind the cross-talk between adipocytes and PCa cells. We identified chemokines that can contribute to an increase in *TRIB3* expression in PCa. Our finding supports the importance of adipose tissue microenvironment on PCa aggressiveness and we observed *TRIB3* as a novel oncogene that is involved in regulating this cross-talk. It has been well established that CM promotes PCa cell growth and migration. Therefore, in obese patients, specific therapies can be designed to inhibit the TRIB3 expression in PCa cells. Thus,

the effect of CM could be reversed. This would prolong the time of PCa cells to metastases out of the PPAT capsule and allowing better response to existing therapies. Further *in vivo* studies would give us insights into the mechanism underlying *TRIB3* contributing to PCa progression under the influence of adipose tissue microenvironments.

In MTC patients, the survival rates usually depend on the stage of diagnosis. Early detection can significantly improve the prognosis for MTC patients both for sporadic and hereditary cases. The response to drug treatment with multi-tyrosine kinase inhibitors Cabozantinib and Vandetanib is low and most of the patients develop drug resistance. Identifying factors that can improve drug treatment are crucial for patient response in MTC. The results obtained suggest the tumour suppressive role of TRIB2 in MTC *in vitro*. Further *in vivo* studies with drug treatment can help understand the role of TRIB2 during drug treatment. Therefore, TRIB2 expression in the tumour tissue could help determine disease progression and outcome.

References

Airaksinen, M. S. and M. Saarma (2002). "The GDNF family: signalling, biological functions and therapeutic value." Nature Reviews: Neuroscience 3(5): 383-394.

Alessi, D. R., S. R. James, C. P. Downes, A. B. Holmes, P. R. Gaffney, C. B. Reese and P. Cohen (1997). "Characterization of a 3-phosphoinositide-dependent protein kinase which phosphorylates and activates protein kinase Balpha." Current biology : CB 7(4): 261-269.

Alshaker, H., K. Sacco, A. Alfraidi, A. Muhammad, M. Winkler and D. Pchejetski (2015). "Leptin signalling, obesity and prostate cancer: molecular and clinical perspective on the old dilemma." Oncotarget 6(34): 35556-35563.

Amit, M., S. Na'ara, L. Leider-Trejo, Y. Binenbaum, N. Kulish, E. Fridman, A. Shabtai-Orbach, R. J. Wong and Z. Gil (2017). "Upregulation of RET induces perineurial invasion of pancreatic adenocarcinoma." Oncogene 36(23): 3232-3239.

Angyal, A. and E. Kiss-Toth (2012). "The tribbles gene family and lipoprotein metabolism." Current Opinion in Lipidology 23(2): 122-126.

Arai, Y., H. Akaza, T. Deguchi, M. Fujisawa, M. Hayashi, Y. Hirao, H. Kanetake, S. Naito, M. Namiki, M. Tachibana, M. Usami and Y. Ohashi (2008). "Evaluation of quality of life in patients with previously untreated advanced prostate cancer receiving maximum androgen blockade therapy or LHRHa monotherapy: a multicenter, randomized, double-blind, comparative study." Journal of Cancer Research and Clinical Oncology 134(12): 1385-1396.

Arighi, E., M. G. Borrello and H. Sariola (2005). "RET tyrosine kinase signaling in development and cancer." Cytokine and Growth Factor Reviews 16(4-5): 441-467.

Attané, C. and C. Muller (2020). "Drilling for Oil: Tumor-Surrounding Adipocytes Fueling Cancer." Trends Cancer 6(7): 593-604.

Attard, G., J. Richards and J. S. de Bono (2011). "New strategies in metastatic prostate cancer: targeting the androgen receptor signaling pathway." Clinical cancer research : an official journal of the American Association for Cancer Research 17(7): 1649-1657.

Audrito, V., V. G. Messana and S. Deaglio (2020). "NAMPT and NAPRT: Two Metabolic Enzymes With Key Roles in Inflammation." Frontiers in Oncology 10: 358.

Bailey, F. P., D. P. Byrne, K. Oruganty, C. E. Eyers, C. J. Novotny, K. M. Shokat, N. Kannan and P. A. Eyers (2015). "The Tribbles 2 (TRB2) pseudokinase binds to ATP and autophosphorylates in a metal-independent manner." Biochemical Journal 467(1): 47-62.

Balaban, S., Z. D. Nassar, A. Y. Zhang, E. Hosseini-Beheshti, M. M. Centenera, M. Schreuder, H. M. Lin, A. Aishah, B. Varney, F. Liu-Fu, L. S. Lee, S. R. Nagarajan, R. F. Shearer, R. A. Hardie, N. L. Raftopulos, M. S. Kakani, D. N. Saunders, J. Holst, L. G. Horvath, L. M. Butler and A. J. Hoy (2019). "Extracellular Fatty Acids Are the Major Contributor to Lipid Synthesis in Prostate Cancer." Molecular Cancer Research 17(4): 949-962.

Ballerini, P., S. Struski, C. Cresson, N. Prade, S. Toujani, C. Deswarte, S. Dobbelstein, A. Petit, H. Lapillonne, E. F. Gautier, C. Demur, E. Lippert, P. Pages, V. Mansat-De Mas, J. Donadieu, F. Huguet, N. Dastugue, C. Broccardo, C. Perot and E. Delabesse (2012). "RET fusion genes are associated with chronic myelomonocytic leukemia and enhance monocytic differentiation." Leukemia 26(11): 2384-2389.

Bapat, S. P., J. Myoung Suh, S. Fang, S. Liu, Y. Zhang, A. Cheng, C. Zhou, Y. Liang, M. LeBlanc, C. Liddle, A. R. Atkins, R. T. Yu, M. Downes, R. M. Evans and Y. Zheng (2015). "Depletion of fat-resident Treg cells prevents age-associated insulin resistance." Nature 528(7580): 137-141.

Bauer, R. C., M. Sasaki, D. M. Cohen, J. Cui, M. A. Smith, B. O. Yenilmez, D. J. Steger and D. J. Rader (2015). "Tribbles-1 regulates hepatic lipogenesis through posttranscriptional regulation of C/EBPalpha." Journal of Clinical Investigation 125(10): 3809-3818.

Bauer, R. C., B. O. Yenilmez and D. J. Rader (2015). "Tribbles-1: a novel regulator of hepatic lipid metabolism in humans." Biochemical Society Transactions 43(5): 1079-1084.

Becker, M., M. K. Levings and C. Daniel (2017). "Adipose-tissue regulatory T cells: Critical players in adipose-immune crosstalk." European Journal of Immunology 47(11): 1867-1874.

Bertolini, F. (2013). "Adipose tissue and breast cancer progression: a link between metabolism and cancer." Breast 22 Suppl 2: S48-49.

Bezy, O., C. Vernochet, S. Gesta, S. R. Farmer and C. R. Kahn (2007). "TRB3 blocks adipocyte differentiation through the inhibition of C/EBPbeta transcriptional activity." Molecular and Cellular Biology 27(19): 6818-6831.

Blain, S. W., H. I. Scher, C. Cordon-Cardo and A. Koff (2003). "p27 as a target for cancer therapeutics." Cancer Cell 3(2): 111-115.

Blüher, M. (2019). "Obesity: global epidemiology and pathogenesis." Nature Reviews: Endocrinology 15(5): 288-298.

Bostwick, D. G. and M. K. Brawer (1987). "Prostatic intra-epithelial neoplasia and early invasion in prostate cancer." Cancer 59(4): 788-794.

Bostwick, D. G., R. Montironi and I. A. Sesterhenn (2000). "Diagnosis of prostatic intraepithelial neoplasia: Prostate Working Group/consensus report." Scandinavian Journal of Urology and Nephrology Supplementum(205): 3-10.

Boutens, L., G. J. Hooiveld, S. Dhingra, R. A. Cramer, M. G. Netea and R. Stienstra (2018). "Unique metabolic activation of adipose tissue macrophages in obesity promotes inflammatory responses." Diabetologia 61(4): 942-953.

Brestoff, J. R. and D. Artis (2015). "Immune regulation of metabolic homeostasis in health and disease." Cell 161(1): 146-160.

Brinkmann, A. O. (2011). "Molecular mechanisms of androgen action--a historical perspective." Methods in Molecular Biology 776: 3-24.

Brisard, D., F. Chesnel, S. Elis, A. Desmarchais, L. Sánchez-Lazo, M. Chasles, V. Maillard and S. Uzbekova (2014). "Tribbles expression in cumulus cells is related to oocyte maturation and fatty acid metabolism." Journal of Ovarian Research 7: 44.

Cabanillas, M. E., M. I. Hu and C. Jimenez (2014). "Medullary thyroid cancer in the era of tyrosine kinase inhibitors: to treat or not to treat--and with which drug--those are the questions." Journal of Clinical Endocrinology and Metabolism 99(12): 4390-4396.

Cabanillas, M. E., D. G. McFadden and C. Durante (2016). "Thyroid cancer." Lancet 388(10061): 2783-2795.

Cailleau, R., M. Olivé and Q. V. Cruciger (1978). "Long-term human breast carcinoma cell lines of metastatic origin: preliminary characterization." In Vitro 14(11): 911-915.

Cancello, R. and K. Clément (2006). "Is obesity an inflammatory illness? Role of low-grade inflammation and macrophage infiltration in human white adipose tissue." BJOG: An International Journal of Obstetrics and Gynaecology 113(10): 1141-1147.

Cantley, L. C. (2002). "The phosphoinositide 3-kinase pathway." Science 296(5573): 1655-1657.

Carver, B. S., C. Chapinski, J. Wongvipat, H. Hieronymus, Y. Chen, S. Chandarlapaty, V. K. Arora, C. Le, J. Koutcher, H. Scher, P. T. Scardino, N. Rosen and C. L. Sawyers (2011). "Reciprocal feedback regulation of PI3K and androgen receptor signaling in PTEN-deficient prostate cancer." Cancer Cell 19(5): 575-586.

Castellone, M. D. and R. M. Melillo (2018). "RET-mediated modulation of tumor microenvironment and immune response in multiple endocrine neoplasia type 2 (MEN2)." Endocrine-Related Cancer 25(2): T105-t119.

Castinetti, F., J. Moley, L. Mulligan and S. G. Waguespack (2018). "A comprehensive review on MEN2B." Endocrine-Related Cancer 25(2): T29-t39.

Catrysse, L. and G. van Loo (2018). "Adipose tissue macrophages and their polarization in health and obesity." Cellular Immunology 330: 114-119.

Cawthorn, W. P. and J. K. Sethi (2008). "TNF-alpha and adipocyte biology." FEBS Letters 582(1): 117-131.

Ceolin, L., M. Duval, A. F. Benini, C. V. Ferreira and A. L. Maia (2019). "Medullary thyroid carcinoma beyond surgery: advances, challenges, and perspectives." Endocrine-Related Cancer 26(9): R499-r518.

Chavey, C., G. Lazennec, S. Lagarrigue, C. Clapé, I. Iankova, J. Teyssier, J. S. Annicotte, J. Schmidt, C. Mataki, H. Yamamoto, R. Sanches, A. Guma, V. Stich, M. Vitkova, B. Jardin-Watelet, E. Renard, R. Strieter, A. Tuthill, G. S. Hotamisligil, A. Vidal-Puig, A. Zorzano, D. Langin and L. Fajas (2009). "CXC ligand 5 is an adipose-tissue derived factor that links obesity to insulin resistance." Cell Metabolism 9(4): 339-349.

Chernock, R. D. and I. S. Hagemann (2015). "Molecular pathology of hereditary and sporadic medullary thyroid carcinomas." American Journal of Clinical Pathology 143(6): 768-777.

Chughtai, B., J. C. Forde, D. D. Thomas, L. Laor, T. Hossack, H. H. Woo, A. E. Te and S. A. Kaplan (2016). "Benign prostatic hyperplasia." Nature Reviews Disease Primers 2: 16031.

Cipolletta, D. (2014). "Adipose tissue-resident regulatory T cells: phenotypic specialization, functions and therapeutic potential." Immunology 142(4): 517-525.

Clement, E., I. Lazar, C. Muller and L. Nieto (2017). "Obesity and melanoma: could fat be fueling malignancy?" Pigment Cell & Melanoma Research 30(3): 294-306.

Comba, A., Y. H. Lin, A. R. Eynard, M. A. Valentich, M. E. Fernandez-Zapico and M. E. Pasqualini (2011). "Basic aspects of tumor cell fatty acid-regulated signaling and transcription factors." Cancer and Metastasis Reviews 30(3-4): 325-342.

Costa, E. C., A. F. Moreira, D. de Melo-Diogo, V. M. Gaspar, M. P. Carvalho and I. J. Correia (2016). "3D tumor spheroids: an overview on the tools and techniques used for their analysis." Biotechnology Advances 34(8): 1427-1441.

Cukierman, E., R. Pankov, D. R. Stevens and K. M. Yamada (2001). "Taking cell-matrix adhesions to the third dimension." Science 294(5547): 1708-1712.

Cunard, R. (2013). "Mammalian tribbles homologs at the crossroads of endoplasmic reticulum stress and Mammalian target of rapamycin pathways." Scientifica (Cairo) 2013: 750871.

Cunningham, D. and Z. You (2015). "In vitro and in vivo model systems used in prostate cancer research." Journal of Biological Methods 2(1).

Dam, V., T. Sikder and S. Santosa (2016). "From neutrophils to macrophages: differences in regional adipose tissue depots." Obesity Reviews 17(1): 1-17.

Das, K., Y. Lin, E. Widen, Y. Zhang and P. E. Scherer (2001). "Chromosomal localization, expression pattern, and promoter analysis of the mouse gene encoding adipocyte-specific secretory protein Acrp30." Biochemical and Biophysical Research Communications 280(4): 1120-1129.

Davey, R. A. and H. E. MacLean (2006). "Current and future approaches using genetically modified mice in endocrine research." American Journal of Physiology: Endocrinology and Metabolism 291(3): E429-438.

Davis, T. K., M. Hoshi and S. Jain (2014). "To bud or not to bud: the RET perspective in CAKUT." Pediatric Nephrology 29(4): 597-608.

De Marzo, A. M., M. C. Haffner, T. L. Lotan, S. Yegnasubramanian and W. G. Nelson (2016). "Premalignancy in Prostate Cancer: Rethinking What we Know." Cancer Prevention Research (Philadelphia, Pa) 9(8): 648-656.

Dehm, S. M. and D. J. Tindall (2011). "Alternatively spliced androgen receptor variants." Endocrine-Related Cancer 18(5): R183-196.

DePinho, R. A. (2000). "The age of cancer." Nature 408(6809): 248-254.

Desoize, B. and J. Jardillier (2000). "Multicellular resistance: a paradigm for clinical resistance?" Critical Reviews in Oncology/Hematology 36(2-3): 193-207.

Dirat, B. A., L. Bochet, G. Escourrou, P. Valet and C. Muller (2010). "Unraveling the obesity and breast cancer links: a role for cancer-associated adipocytes?" Endocrine Development 19: 45-52.

Do, E. K., J. K. Park, H. C. Cheon, Y. W. Kwon, S. C. Heo, E. J. Choi, J. K. Seo, I. H. Jang, S. C. Lee and J. H. Kim (2017). "Trib2 regulates the pluripotency of embryonic stem cells and enhances reprogramming efficiency." Experimental and Molecular Medicine 49(11): e401.

Dobens, L. L., Jr. and S. Bouyain (2012). "Developmental roles of tribbles protein family members." Developmental Dynamics 241(8): 1239-1248.

Dolznig, H., C. Rupp, C. Puri, C. Haslinger, N. Schweifer, E. Wieser, D. Kerjaschki and P. Garin-Chesa (2011). "Modeling colon adenocarcinomas in vitro a 3D co-culture system induces cancer-relevant pathways upon tumor cell and stromal fibroblast interaction." American Journal of Pathology 179(1): 487-501.

Dong, S., J. Xia, H. Wang, L. Sun, Z. Wu, J. Bin, Y. Liao, N. Li and W. Liao (2016). "Overexpression of TRIB3 promotes angiogenesis in human gastric cancer." Oncology Reports 36(4): 2339-2348.

Du, K., S. Herzig, R. N. Kulkarni and M. Montminy (2003). "TRB3: a tribbles homolog that inhibits Akt/PKB activation by insulin in liver." Science 300(5625): 1574-1577.

DuBridge, R. B., P. Tang, H. C. Hsia, P. M. Leong, J. H. Miller and M. P. Calos (1987). "Analysis of mutation in human cells by using an Epstein-Barr virus shuttle system." Molecular and Cellular Biology 7(1): 379-387.

Dugas, E., E. Kiss-Toth, J. P. Soulillou, S. Brouard and J. Ashton-Chess (2012). "The Tribbles-1 Protein in Humans Roles and Functions in Health and Disease." Current Molecular Medicine 13(1): 80-85.

Duong, M., A. Geneste, F. Fallone, X. Xia Li and C. Catherine Muller (2017). "The fat and the bad: Mature adipocytes, key actors in tumor progression and resistance." Oncotarget 8(34): 57622-57641.

Durzynska, I., X. Xu, G. Adelmant, S. B. Ficarro, J. A. Marto, P. Sliz, S. Uljon and S. C. Blacklow (2017). "STK40 Is a Pseudokinase that Binds the E3 Ubiquitin Ligase COP1." Structure 25(2): 287-294.

ECIS (2020). "European Cancer Information System " from https://ecis.jrc.ec.europa.eu, accessed on 15.10.2020 © European Union, 2020

Eder, K., H. Guan, H. Y. Sung, J. Ward, A. Angyal, M. Janas, G. Sarmay, E. Duda, M. Turner, S. K. Dower, S. E. Francis, D. C. Crossman and E. Kiss-Toth (2008). "Tribbles-2 is a novel regulator of inflammatory activation of monocytes." International Immunology 20(12): 1543-1550.

Edery, P., S. Lyonnet, L. M. Mulligan, A. Pelet, E. Dow, L. Abel, S. Holder, C. Nihoul-Fékété, B. A. Ponder and A. Munnich (1994). "Mutations of the RET proto-oncogene in Hirschsprung's disease." Nature 367(6461): 378-380.

Ekert, J. E., K. Johnson, B. Strake, J. Pardinas, S. Jarantow, R. Perkinson and D. C. Colter (2014). "Three-dimensional lung tumor microenvironment modulates therapeutic compound responsiveness in vitro--implication for drug development." PloS One 9(3): e92248.

El-Haibi, C. P., R. Singh, P. K. Sharma, S. Singh and J. W. Lillard, Jr. (2011). "CXCL13 mediates prostate cancer cell proliferation through JNK signalling and invasion through ERK activation." Cell Proliferation 44(4): 311-319.

Eller, K., A. Kirsch, A. M. Wolf, S. Sopper, A. Tagwerker, U. Stanzl, D. Wolf, W. Patsch, A. R. Rosenkranz and P. Eller (2011). "Potential role of regulatory T cells in reversing obesity-linked insulin resistance and diabetic nephropathy." Diabetes 60(11): 2954-2962.

Eng, C., D. P. Smith, L. M. Mulligan, M. A. Nagai, C. S. Healey, M. A. Ponder, E. Gardner, G. F. Scheumann, C. E. Jackson, A. Tunnacliffe and et al. (1994). "Point mutation within the tyrosine kinase domain of the RET proto-oncogene in multiple endocrine neoplasia type 2B and related sporadic tumours." Human Molecular Genetics 3(2): 237-241.

Esseghir, S., S. K. Todd, T. Hunt, R. Poulsom, I. Plaza-Menacho, J. S. Reis-Filho and C. M. Isacke (2007). "A role for glial cell derived neurotrophic factor induced expression by inflammatory cytokines and RET/GFR alpha 1 receptor up-regulation in breast cancer." Cancer Research 67(24): 11732-11741.

Esteve, E., W. Ricart and J. M. Fernández-Real (2009). "Adipocytokines and insulin resistance: the possible role of lipocalin-2, retinol binding protein-4, and adiponectin." Diabetes Care 32 Suppl 2(Suppl 2): S362-367.

Eyers, P. A., K. Keeshan and N. Kannan (2017). "Tribbles in the 21st Century: The Evolving Roles of Tribbles Pseudokinases in Biology and Disease." Trends in Cell Biology 27(4): 284-298.

Fasshauer, M. and M. Blüher (2015). "Adipokines in health and disease." Trends in Pharmacological Sciences 36(7): 461-470.

Feldman, B. J. and D. Feldman (2001). "The development of androgen-independent prostate cancer." Nature reviews Cancer 1(1): 34-45.

Fero, M. L., M. Rivkin, M. Tasch, P. Porter, C. E. Carow, E. Firpo, K. Polyak, L. H. Tsai, V. Broudy, R. M. Perlmutter, K. Kaushansky and J. M. Roberts (1996). "A syndrome of multiorgan hyperplasia with features of gigantism, tumorigenesis, and female sterility in p27(Kip1)-deficient mice." Cell 85(5): 733-744.

Ferraro, D. A., J. H. Rüschoff, U. J. Muehlematter, B. Kranzbühler, J. Müller, M. Messerli, L. Husmann, T. Hermanns, D. Eberli, N. J. Rupp and I. A. Burger (2020). "Immunohistochemical PSMA expression patterns of primary prostate cancer tissue are associated with the detection rate of biochemical recurrence with (68)Ga-PSMA-11-PET." Theranostics 10(14): 6082-6094.

Fischbach, C., H. J. Kong, S. X. Hsiong, M. B. Evangelista, W. Yuen and D. J. Mooney (2009). "Cancer cell angiogenic capability is regulated by 3D culture and integrin engagement." Proceedings of the National Academy of Sciences of the United States of America 106(2): 399-404.

Fonseca, M. I., S. H. Chu, M. X. Hernandez, M. J. Fang, L. Modarresi, P. Selvan, G. R. MacGregor and A. J. Tenner (2017). "Cell-specific deletion of C1qa identifies microglia as the dominant source of C1q in mouse brain." Journal of Neuroinflammation 14(1): 48.

Foster, B. A., J. R. Gingrich, E. D. Kwon, C. Madias and N. M. Greenberg (1997). "Characterization of prostatic epithelial cell lines derived from transgenic adenocarcinoma of the mouse prostate (TRAMP) model." Cancer Research 57(16): 3325-3330.

Fritz, A., A. Walch, K. Piotrowska, M. Rosemann, E. Schäffer, K. Weber, A. Timper, G. Wildner, J. Graw, H. Höfler and M. J. Atkinson (2002). "Recessive transmission of a multiple endocrine neoplasia syndrome in the rat." Cancer Research 62(11): 3048-3051.

Fruman, D. A. (2003). Phosphoinositide 3-Kinases. Handbook of Cell Signaling. R. A. Bradshaw and E. A. Dennis. Burlington, Academic Press: 135-141.

Funcke, J. B. and P. E. Scherer (2019). "Beyond adiponectin and leptin: adipose tissue-derived mediators of inter-organ communication." Journal of Lipid Research 60(10): 1648-1684.

Fuster, J. J., N. Ouchi, N. Gokce and K. Walsh (2016). "Obesity-Induced Changes in Adipose Tissue Microenvironment and Their Impact on Cardiovascular Disease." Circulation Research 118(11): 1786-1807.

Gendelman, R., H. Xing, O. K. Mirzoeva, P. Sarde, C. Curtis, H. S. Feiler, P. McDonagh, J. W. Gray, I. Khalil and W. M. Korn (2017). "Bayesian Network Inference Modeling Identifies TRIB1 as a Novel Regulator of Cell-Cycle Progression and Survival in Cancer Cells." Cancer Research 77(7): 1575-1585.

Gonzalez, E. and T. E. McGraw (2009). "The Akt kinases: isoform specificity in metabolism and cancer." Cell Cycle 8(16): 2502-2508.

Graham, F. L., J. Smiley, W. C. Russell and R. Nairn (1977). "Characteristics of a human cell line transformed by DNA from human adenovirus type 5." Journal of General Virology 36(1): 59-74.

Grandinetti, K. B., T. A. Stevens, S. Ha, R. J. Salamone, J. R. Walker, J. Zhang, S. Agarwalla, D. G. Tenen, E. C. Peters and V. A. Reddy (2011). "Overexpression of TRIB2 in human lung cancers contributes to tumorigenesis through downregulation of C/EBPalpha." Oncogene 30(30): 3328-3335.

Grieco, M., M. Santoro, M. T. Berlingieri, R. M. Melillo, R. Donghi, I. Bongarzone, M. A. Pierotti, G. Della Porta, A. Fusco and G. Vecchio (1990). "PTC is a novel rearranged form of the ret proto-oncogene and is frequently detected in vivo in human thyroid papillary carcinomas." Cell 60(4): 557-563.

Guilmette, J. and V. Nosé (2018). "Hereditary and familial thyroid tumours." Histopathology 72(1): 70-81.

Haka, A. S., V. C. Barbosa-Lorenzi, H. J. Lee, D. J. Falcone, C. A. Hudis, A. J. Dannenberg and F. R. Maxfield (2016). "Exocytosis of macrophage lysosomes leads to digestion of apoptotic adipocytes and foam cell formation." Journal of Lipid Research 57(6): 980-992.

Hanahan, D. and R. A. Weinberg (2000). "The hallmarks of cancer." Cell 100(1): 57-70.

Hanahan, D. and R. A. Weinberg (2011). "Hallmarks of cancer: the next generation." Cell 144(5): 646-674.

Hara, T., J. Kouno, K. Nakamura, M. Kusaka and M. Yamaoka (2005). "Possible role of adaptive mutation in resistance to antiandrogen in prostate cancer cells." Prostate 65(3): 268-275.

Härmä, V., J. Virtanen, R. Mäkelä, A. Happonen, J. P. Mpindi, M. Knuuttila, P. Kohonen, J. Lötjönen, O. Kallioniemi and M. Nees (2010). "A comprehensive panel of three-dimensional models for studies of prostate cancer growth, invasion and drug responses." PloS One 5(5): e10431.

Hegedus, Z., A. Czibula and E. Kiss-Toth (2006). "Tribbles: novel regulators of cell function; evolutionary aspects." Cellular and Molecular Life Sciences 63(14): 1632-1641.

Hegedus, Z., A. Czibula and E. Kiss-Toth (2007). "Tribbles: a family of kinase-like proteins with potent signalling regulatory function." Cellular Signalling 19(2): 238-250.

Hill, R., P. A. Madureira, B. Ferreira, I. Baptista, S. Machado, L. Colaco, M. Dos Santos, N. Liu, A. Dopazo, S. Ugurel, A. Adrienn, E. Kiss-Toth, M. Isbilen, A. O. Gure and W. Link (2017). "TRIB2 confers resistance to anti-cancer therapy by activating the serine/threonine protein kinase AKT." Nature communications 8: 14687.

Hofstra, R. M., R. M. Landsvater, I. Ceccherini, R. P. Stulp, T. Stelwagen, Y. Luo, B. Pasini, J. W. Höppener, H. K. van Amstel, G. Romeo and et al. (1994). "A mutation in the RET proto-oncogene associated with multiple endocrine neoplasia type 2B and sporadic medullary thyroid carcinoma." Nature 367(6461): 375-376.

Hopkins, B. D., M. D. Goncalves and L. C. Cantley (2016). "Obesity and Cancer Mechanisms: Cancer Metabolism." Journal of Clinical Oncology 34(35): 4277-4283.

Hou, Z., K. Guo, X. Sun, F. Hu, Q. Chen, X. Luo, G. Wang, J. Hu and L. Sun (2018). "TRIB2 functions as novel oncogene in colorectal cancer by blocking cellular senescence through AP4/p21 signaling." Molecular Cancer 17(1): 172.

Hoy, A. J., S. Balaban and D. N. Saunders (2017). "Adipocyte-Tumor Cell Metabolic Crosstalk in Breast Cancer." Trends in Molecular Medicine 23(5): 381-392.

Hu, R., T. A. Dunn, S. Wei, S. Isharwal, R. W. Veltri, E. Humphreys, M. Han, A. W. Partin, R. L. Vessella, W. B. Isaacs, G. S. Bova and J. Luo (2009). "Ligand-independent androgen receptor variants derived from splicing of cryptic exons signify hormone-refractory prostate cancer." Cancer Research 69(1): 16-22.

Hua, F., R. Mu, J. Liu, J. Xue, Z. Wang, H. Lin, H. Yang, X. Chen and Z. Hu (2011). "TRB3 interacts with SMAD3 promoting tumor cell migration and invasion." Journal of Cell Science 124(Pt 19): 3235-3246.

Huggins, C. and C. V. Hodges (1941). "Studies on prostatic cancer: I. The effect of castration, of estrogen and of androgen injection on serum phosphatases in metastatic carcinoma of the prostate. ." Journal of Urology 168(1): 9-12.

Huh, D., G. A. Hamilton and D. E. Ingber (2011). "From 3D cell culture to organs-on-chips." Trends in Cell Biology 21(12): 745-754.

Ibrahim, M. M. (2010). "Subcutaneous and visceral adipose tissue: structural and functional differences." Obesity Reviews 11(1): 11-18.

Iwamoto, S., S. Boonvisut, S. Makishima, Y. Ishizuka, K. Watanabe and K. Nakayama (2015). "The role of TRIB1 in lipid metabolism; from genetics to pathways." Biochemical Society Transactions 43(5): 1063-1068.

Jain, S., M. A. Watson, M. K. DeBenedetti, Y. Hiraki, J. F. Moley and J. Milbrandt (2004). "Expression profiles provide insights into early malignant potential and skeletal abnormalities in multiple endocrine neoplasia type 2B syndrome tumors." Cancer Research 64(11): 3907-3913.

Jasinski-Bergner, S. and H. Kielstein (2019). "Adipokines Regulate the Expression of Tumor-Relevant MicroRNAs." Obesity Facts 12(2): 211-225.

Johnson, G. L. and R. Lapadat (2002). "Mitogen-activated protein kinase pathways mediated by ERK, JNK, and p38 protein kinases." Science 298(5600): 1911-1912.

Johnston, J., S. Basatvat, Z. Ilyas, S. Francis and E. Kiss-Toth (2015). "Tribbles in inflammation." Biochemical Society Transactions 43(5): 1069-1074.

Johnston, J. M., A. Angyal, R. C. Bauer, S. Hamby, S. K. Suvarna, K. Baidžajevas, Z. Hegedus, T. N. Dear, M. Turner, H. L. Wilson, A. H. Goodall, D. J. Rader, C. C. Shoulders, S. E. Francis and E. Kiss-Toth (2019). "Myeloid Tribbles 1 induces early atherosclerosis via enhanced foam cell expansion." Science advances 5(10): eaax9183.

Juge-Aubry, C. E., E. Henrichot and C. A. Meier (2005). "Adipose tissue: a regulator of inflammation." Best Practice & Research: Clinical Endocrinology & Metabolism 19(4): 547-566.

Kadomatsu, T., M. Tabata and Y. Oike (2011). "Angiopoietin-like proteins: emerging targets for treatment of obesity and related metabolic diseases." FEBS Journal 278(4): 559-564.

Kane, H. and L. Lynch (2019). "Innate Immune Control of Adipose Tissue Homeostasis." Trends in Immunology 40(9): 857-872.

Kathiresan, S., O. Melander, C. Guiducci, A. Surti, N. P. Burtt, M. J. Rieder, G. M. Cooper, C. Roos, B. F. Voight, A. S. Havulinna, B. Wahlstrand, T. Hedner, D. Corella, E. S. Tai, J. M. Ordovas, G. Berglund, E. Vartiainen, P. Jousilahti, B. Hedblad, M. R. Taskinen, C. Newton-Cheh, V. Salomaa, L. Peltonen, L. Groop, D. M. Altshuler and M. Orho-Melander (2008). "Six new loci associated with blood low-density lipoprotein cholesterol, high-density lipoprotein cholesterol or triglycerides in humans." Nature Genetics 40(2): 189-197.

Kato, S., V. Subbiah, E. Marchlik, S. K. Elkin, J. L. Carter and R. Kurzrock (2017). "RET Aberrations in Diverse Cancers: Next-Generation Sequencing of 4,871 Patients." Clinical Cancer Research 23(8): 1988-1997.

Kazanietz, M. G., M. Durando and M. Cooke (2019). "CXCL13 and Its Receptor CXCR5 in Cancer: Inflammation, Immune Response, and Beyond." Frontiers in Endocrinology 10: 471.

Keeley, E. C., B. Mehrad and R. M. Strieter (2010). "CXC chemokines in cancer angiogenesis and metastases." Advances in Cancer Research 106: 91-111.

Keeshan, K., Y. He, B. J. Wouters, O. Shestova, L. Xu, H. Sai, C. G. Rodriguez, I. Maillard, J. W. Tobias, P. Valk, M. Carroll, J. C. Aster, R. Delwel and W. S. Pear (2006). "Tribbles homolog 2 inactivates C/EBPalpha and causes acute myelogenous leukemia." Cancer Cell 10(5): 401-411.

Kiss-Toth, E. (2011). "Tribbles: 'puzzling' regulators of cell signalling." Biochemical Society Transactions 39(2): 684-687.

Kiss-Toth, E., S. M. Bagstaff, H. Y. Sung, V. Jozsa, C. Dempsey, J. C. Caunt, K. M. Oxley, D. H. Wyllie, T. Polgar, M. Harte, A. O'Neill L, E. E. Qwarnstrom and S. K. Dower (2004). "Human tribbles, a protein family controlling mitogen-activated protein kinase cascades." Journal of Biological Chemistry 279(41): 42703-42708.

Kiyokawa, H., R. D. Kineman, K. O. Manova-Todorova, V. C. Soares, E. S. Hoffman, M. Ono, D. Khanam, A. C. Hayday, L. A. Frohman and A. Koff (1996). "Enhanced growth of mice lacking the cyclin-dependent kinase inhibitor function of p27(Kip1)." Cell 85(5): 721-732.

Knuth A., Gabbert H.E., Moll R., Dippold W.G. and M. z. B. K.-H. (1987). "Markers in medullary thyroid cancer established in tissue culture." Proceedings of the American Association for Cancer Research 28: 83-83.

Kohno, T., H. Ichikawa, Y. Totoki, K. Yasuda, M. Hiramoto, T. Nammo, H. Sakamoto, K. Tsuta, K. Furuta, Y. Shimada, R. Iwakawa, H. Ogiwara, T. Oike, M. Enari, A. J. Schetter, H. Okayama, A. Haugen, V. Skaug, S. Chiku, I. Yamanaka, Y. Arai, S. Watanabe, I. Sekine, S. Ogawa, C. C. Harris, H. Tsuda, T. Yoshida, J. Yokota and T. Shibata (2012). "KIF5B-RET fusions in lung adenocarcinoma." Nature Medicine 18(3): 375-377.

Koo, S. H., H. Satoh, S. Herzig, C. H. Lee, S. Hedrick, R. Kulkarni, R. M. Evans, J. Olefsky and M. Montminy (2004). "PGC-1 promotes insulin resistance in liver through PPAR-alpha-dependent induction of TRB-3." Nature Medicine 10(5): 530-534.

Krawczyk, A., K. Hasse-Lazar, A. Pawlaczek, S. Szpak-Ulczok, J. Krajewska, E. Paliczka-Cieślak, B. Jurecka-Lubieniecka, J. Roskosz, E. Chmielik, J. Ziaja, L. Cierpka, M. Peczkowska, A. Preibisz, A. Januszewicz, M. Otto and B. Jarzab (2010). "Germinal mutations of RET, SDHB, SDHD, and VHL genes in patients with apparently sporadic pheochromocytomas and paragangliomas." Endokrynologia Polska 61(1): 43-48.

Kristianto, J., M. G. Johnson, R. K. Zastrow, A. B. Radcliff and R. D. Blank (2017). "Spontaneous recombinase activity of Cre-ERT2 in vivo." Transgenic Research 26(3): 411-417.

Kritsch, D., F. Hoffmann, D. Steinbach, L. Jansen, S. Mary Photini, M. Gajda, A. S. Mosig, J. Sonnemann, S. Peters, M. Melnikova, J. Thomale, M. Dürst, I. B. Runnebaum and N. Häfner (2017). "Tribbles 2 mediates cisplatin sensitivity and DNA damage response in epithelial ovarian cancer." International Journal of Cancer 141(8): 1600-1614.

Kung, J. E. and N. Jura (2016). "Structural Basis for the Non-catalytic Functions of Protein Kinases." Structure 24(1): 7-24.

Kunstman, J. W., C. C. Juhlin, G. Goh, T. C. Brown, A. Stenman, J. M. Healy, J. C. Rubinstein, M. Choi, N. Kiss, C. Nelson-Williams, S. Mane, D. L. Rimm, M. L. Prasad, A. Höög, J. Zedenius, C. Larsson, R. Korah, R. P. Lifton and T. Carling (2015). "Characterization of the mutational landscape of anaplastic thyroid cancer via whole-exome sequencing." Human Molecular Genetics 24(8): 2318-2329.

Kwon, A., S. Scott, R. Taujale, W. Yeung, K. J. Kochut, P. A. Eyers and N. Kannan (2019). "Tracing the origin and evolution of pseudokinases across the tree of life." Science signaling 12(578).

Kypta, R., M. Unda and A. Carracedo (2012). "Is the bench getting closer to the bedside in the war on cancer? A quick look at prostate cancer." Frontiers in Endocrinology 3: 53.

Labrie, F., A. Dupont and A. Belanger (1985). "Complete androgen blockade for the treatment of prostate cancer." Important Advances in Oncology: 193-217.

Labrie, F., A. Dupont, A. Belanger, Y. Lacoursiere, J. P. Raynaud, J. M. Husson, J. Gareau, A. T. Fazekas, J. Sandow, G. Monfette and et al. (1983). "New approach in the treatment of prostate cancer: complete instead of partial withdrawal of androgens." Prostate 4(6): 579-594.

Lago, F., C. Dieguez, J. Gómez-Reino and O. Gualillo (2007). "Adipokines as emerging mediators of immune response and inflammation." Nature Clinical Practice: Rheumatology 3(12): 716-724.

Lago, F., R. Gómez, J. J. Gómez-Reino, C. Dieguez and O. Gualillo (2009). "Adipokines as novel modulators of lipid metabolism." Trends in Biochemical Sciences 34(10): 500-510.

Landa, I., N. Pozdeyev, C. Korch, L. A. Marlow, R. C. Smallridge, J. A. Copland, Y. C. Henderson, S. Y. Lai, G. L. Clayman, N. Onoda, A. C. Tan, M. E. R. Garcia-Rendueles, J. A. Knauf, B. R. Haugen, J. A. Fagin and R. E. Schweppe (2019). "Comprehensive Genetic Characterization of Human Thyroid Cancer Cell Lines: A Validated Panel for Preclinical Studies." Clinical Cancer Research 25(10): 3141-3151.

Langhans, S. A. (2018). "Three-Dimensional in Vitro Cell Culture Models in Drug Discovery and Drug Repositioning." Frontiers in Pharmacology 9: 6.

Langlais, C. S., J. E. Cowan, J. Neuhaus, S. A. Kenfield, E. L. Van Blarigan, J. M. Broering, M. R. Cooperberg, P. Carroll and J. M. Chan (2019). "Obesity at Diagnosis and Prostate Cancer Prognosis and Recurrence Risk Following Primary Treatment by Radical Prostatectomy." Cancer Epidemiology, Biomarkers and Prevention 28(11): 1917-1925.

Lasfargues, E. Y., W. G. Coutinho and E. S. Redfield (1978). "Isolation of two human tumor epithelial cell lines from solid breast carcinomas." Journal of the National Cancer Institute 61(4): 967-978.

Lauby-Secretan, B., C. Scoccianti, D. Loomis, Y. Grosse, F. Bianchini and K. Straif (2016). "Body Fatness and Cancer--Viewpoint of the IARC Working Group." New England Journal of Medicine 375(8): 794-798.

Laurent, V., A. Guerard, C. Mazerolles, S. Le Gonidec, A. Toulet, L. Nieto, F. Zaidi, B. Majed, D. Garandeau, Y. Socrier, M. Golzio, T. Cadoudal, K. Chaoui, C. Dray, B. Monsarrat, O. Schiltz, Y. Y. Wang, B. Couderc, P. Valet, B. Malavaud and C. Muller (2016). "Periprostatic adipocytes act as a driving force for prostate cancer progression in obesity." Nature communications 7: 10230.

Lee Isla Crake, R., E. Phillips, T. Kleffmann and M. J. Currie (2019). "Co-culture With Human Breast Adipocytes Differentially Regulates Protein Abundance in Breast Cancer Cells." Cancer Genomics & Proteomics 16(5): 319-332.

Lefterova, M. I., Y. Zhang, D. J. Steger, M. Schupp, J. Schug, A. Cristancho, D. Feng, D. Zhuo, C. J. Stoeckert, Jr., X. S. Liu and M. A. Lazar (2008). "PPARgamma and C/EBP factors orchestrate adipocyte biology via adjacent binding on a genome-wide scale." Genes and Development 22(21): 2941-2952.

Lengyel, E., L. Makowski, J. DiGiovanni and M. G. Kolonin (2018). "Cancer as a Matter of Fat: The Crosstalk between Adipose Tissue and Tumors." Trends Cancer 4(5): 374-384.

Leong, S. S., R. Zeigel, T. M. Chu, S. Baylin and E. A. Mirand (1981). "A new cell line for study of human medullary thyroid carcinoma." Field Educational Italia, Roma: 95-108.

Leslie, N. R. and M. Foti (2011). "Non-genomic loss of PTEN function in cancer: not in my genes." Trends in Pharmacological Sciences 32(3): 131-140.

Lilja, H., D. Ulmert and A. J. Vickers (2008). "Prostate-specific antigen and prostate cancer: prediction, detection and monitoring." Nature Reviews: Cancer 8(4): 268-278.

Lin, Z. Y., Y. Q. Huang, Y. Q. Zhang, Z. D. Han, H. C. He, X. H. Ling, X. Fu, Q. S. Dai, C. Cai, J. H. Chen, Y. X. Liang, F. N. Jiang, W. D. Zhong, F. Wang and C. L. Wu (2014). "MicroRNA-224 inhibits progression of human prostate cancer by downregulating TRIB1." International Journal of Cancer 135(3): 541-550.

Lipson, D., M. Capelletti, R. Yelensky, G. Otto, A. Parker, M. Jarosz, J. A. Curran, S. Balasubramanian, T. Bloom, K. W. Brennan, A. Donahue, S. R. Downing, G. M. Frampton, L. Garcia, F. Juhn, K. C. Mitchell, E. White, J. White, Z. Zwirko, T. Peretz, H. Nechushtan, L. Soussan-Gutman, J. Kim, H. Sasaki, H. R. Kim, S. I. Park, D. Ercan, C. E. Sheehan, J. S. Ross, M. T. Cronin, P. A. Jänne and P. J. Stephens (2012). "Identification of new ALK and RET gene fusions from colorectal and lung cancer biopsies." Nature Medicine 18(3): 382-384.

Liu, W., C. C. Xie, Y. Zhu, T. Li, J. Sun, Y. Cheng, C. M. Ewing, S. Dalrymple, A. R. Turner, J. Sun, J. T. Isaacs, B. L. Chang, S. L. Zheng, W. B. Isaacs and J. Xu (2008). "Homozygous deletions and recurrent amplifications implicate new genes involved in prostate cancer." Neoplasia 10(8): 897-907.

Lohan, F. and K. Keeshan (2013). "The functionally diverse roles of tribbles." Biochemical Society Transactions 41(4): 1096-1100.

Lopergolo, A., V. Nicolini, E. Favini, L. Dal Bo, M. Tortoreto, D. Cominetti, M. Folini, P. Perego, V. Castiglioni, E. Scanziani, M. G. Borrello, N. Zaffaroni, G. Cassinelli and C. Lanzi (2014). "Synergistic cooperation between sunitinib and cisplatin promotes apoptotic cell death in human medullary thyroid cancer." Journal of Clinical Endocrinology and Metabolism 99(2): 498-509.

Louzada, S., F. Adega and R. Chaves (2012). "Defining the sister rat mammary tumor cell lines HH-16 cl.2/1 and HH-16.cl.4 as an in vitro cell model for Erbb2." PloS One 7(1): e29923.

Lumeng, C. N., S. M. Deyoung, J. L. Bodzin and A. R. Saltiel (2007). "Increased inflammatory properties of adipose tissue macrophages recruited during diet-induced obesity." Diabetes 56(1): 16-23.

Mack, E. A., S. J. Stein, K. S. Rome, L. Xu, G. B. Wertheim, R. C. N. Melo and W. S. Pear (2019). "Trib1 regulates eosinophil lineage commitment and identity by restraining the neutrophil program." Blood 133(22): 2413-2426.

Maliszewska, A., L. J. Leandro-Garcia, E. Castelblanco, A. Macià, A. de Cubas, G. Goméz-López, L. Inglada-Pérez, C. Álvarez-Escolá, L. De la Vega, R. Letón, Á. Gómez-Graña, I. Landa, A. Cascón, C. Rodríguez-Antona, S. Borrego, M. Zane, F. Schiavi, I. Merante-Boschin, M. R. Pelizzo, D. G. Pisano, G. Opocher, X. Matias-Guiu, M. Encinas and M. Robledo (2013). "Differential gene expression of medullary thyroid carcinoma reveals specific markers associated with genetic conditions." American Journal of Pathology 182(2): 350-362.

Manning, B. D. and L. C. Cantley (2007). "AKT/PKB signaling: navigating downstream." Cell 129(7): 1261-1274.

Mashima, T., T. Soma-Nagae, T. Migita, R. Kinoshita, A. Iwamoto, T. Yuasa, J. Yonese, Y. Ishikawa and H. Seimiya (2014). "TRIB1 supports prostate tumorigenesis and tumor-propagating cell survival by regulation of endoplasmic reticulum chaperone expression." Cancer Research 74(17): 4888-4897.

Mata, J., S. Curado, A. Ephrussi and P. Rorth (2000). "Tribbles coordinates mitosis and morphogenesis in Drosophila by regulating string/CDC25 proteolysis." Cell 101(5): 511-522.

Mathur, A., Z. Y. Abd Elmageed, X. Liu, M. L. Kostochka, H. Zhang, A. B. Abdel-Mageed and D. Mondal (2014). "Subverting ER-stress towards apoptosis by nelfinavir and curcumin coexposure augments docetaxel efficacy in castration resistant prostate cancer cells." PloS One 9(8): e103109.

Maughan, B. L. and E. S. Antonarakis (2015). "Androgen pathway resistance in prostate cancer and therapeutic implications." Expert Opinion on Pharmacotherapy 16(10): 1521-1537.

McGregor, L. M., B. K. McCune, J. R. Graff, P. R. McDowell, K. E. Romans, G. D. Yancopoulos, D. W. Ball, S. B. Baylin and B. D. Nelkin (1999). "Roles of trk family neurotrophin receptors in medullary thyroid carcinoma development and progression." Proceedings of the National Academy of Sciences of the United States of America 96(8): 4540-4545.

Miyajima, C., Y. Inoue and H. Hayashi (2015). "Pseudokinase tribbles 1 (TRB1) negatively regulates tumor-suppressor activity of p53 through p53 deacetylation." Biological and Pharmaceutical Bulletin 38(4): 618-624.

Molatore, S., A. Kügler, M. Irmler, T. Wiedemann, F. Neff, A. Feuchtinger, J. Beckers, M. Robledo, F. Roncaroli and N. S. Pellegata (2018). "Characterization of neuroendocrine tumors in heterozygous mutant MENX rats: a novel model of invasive medullary thyroid carcinoma." Endocrine-Related Cancer 25(2): 145-162.

Montironi, R., R. Mazzucchelli, A. Lopez-Beltran, M. Scarpelli and L. Cheng (2011). "Prostatic intraepithelial neoplasia: its morphological and molecular diagnosis and clinical significance." BJU International 108(9): 1394-1401.

Mulligan, L. M., J. B. Kwok, C. S. Healey, M. J. Elsdon, C. Eng, E. Gardner, D. R. Love, S. E. Mole, J. K. Moore, L. Papi and et al. (1993). "Germ-line mutations of the RET proto-oncogene in multiple endocrine neoplasia type 2A." Nature 363(6428): 458-460.

Murphy, J. M., Y. Nakatani, S. A. Jamieson, W. Dai, I. S. Lucet and P. D. Mace (2015). "Molecular Mechanism of CCAAT-Enhancer Binding Protein Recruitment by the TRIB1 Pseudokinase." Structure 23(11): 2111-2121.

Nakayama, K., N. Ishida, M. Shirane, A. Inomata, T. Inoue, N. Shishido, I. Horii, D. Y. Loh and K. Nakayama (1996). "Mice lacking p27(Kip1) display increased body size, multiple organ hyperplasia, retinal dysplasia, and pituitary tumors." Cell 85(5): 707-720.

Nakayama, K. and S. Iwamoto (2017). "An adaptive variant of TRIB2, rs1057001, is associated with higher expression levels of thermogenic genes in human subcutaneous and visceral adipose tissues." Journal of Physiological Anthropology 36(1): 16.

Nieman, K. M., I. L. Romero, B. Van Houten and E. Lengyel (2013). "Adipose tissue and adipocytes support tumorigenesis and metastasis." Biochimica et Biophysica Acta 1831(10): 1533-1541.

Niespolo, C., J. M. Johnston, S. R. Deshmukh, S. Satam, Z. Shologu, O. Villacanas, I. M. Sudbery, H. L. Wilson and E. Kiss-Toth (2020). "Tribbles-1 Expression and Its Function to Control Inflammatory Cytokines, Including Interleukin-8 Levels are Regulated by miRNAs in Macrophages and Prostate Cancer Cells." Frontiers in Immunology 11(3049).

Nilsson, M. and H. Fagman (2017). "Development of the thyroid gland." Development 144(12): 2123-2140.

Novakovic, K., P. Fitchev, C. Brendler, B. Plunkett, P. Dangle, M. McGuire, D. Shevrin, M. Cornwell, M. Quinn, K. Kaul and S. Crawford (2012). "ACTIVE TRIACYLGLYCEROL METABOLISM AND INCREASED INFILTRATING ADIPOCYTE DENSITY IN HIGH GRADE PROSTATE CANCER." The Journal of Urology 187(4, Supplement): e127.

O'Connor, C., K. Yalla, M. Salomé, H. A. Moka, E. G. Castañeda, P. A. Eyers and K. Keeshan (2018). "Trib2 expression in granulocyte-monocyte progenitors drives a highly drug resistant acute myeloid leukaemia linked to elevated Bcl2." Oncotarget 9(19): 14977-14992.

Oczko-Wojciechowska, M., M. Swierniak, J. Krajewska, M. Kowalska, M. Kowal, T. Stokowy, B. Wojtas, D. Rusinek, A. Pawlaczek, A. Czarniecka, S. Szpak-Ulczok, T. Gawlik, E. Chmielik, T. Tyszkiewicz, B. Nikiel, D. Lange, M. Jarzab, M. Wiench and B. Jarzab (2017). "Differences in the transcriptome of medullary thyroid cancer regarding the status and type of RET gene mutations." Scientific Reports 7: 42074.

Ohori, M., T. M. Wheeler and P. T. Scardino (1994). "The New American Joint Committee on Cancer and International Union Against Cancer TNM classification of prostate cancer. Clinicopathologic correlations." Cancer 74(1): 104-114.

Ostertag, A., A. Jones, A. J. Rose, M. Liebert, S. Kleinsorg, A. Reimann, A. Vegiopoulos, M. Berriel Diaz, D. Strzoda, M. Yamamoto, T. Satoh, S. Akira and S. Herzig (2010). "Control of adipose tissue inflammation through TRB1." Diabetes 59(8): 1991-2000.

Ouchi, N., A. Higuchi, K. Ohashi, Y. Oshima, N. Gokce, R. Shibata, Y. Akasaki, A. Shimono and K. Walsh (2010). "Sfrp5 is an anti-inflammatory adipokine that modulates metabolic dysfunction in obesity." Science 329(5990): 454-457.

Ouchi, N., J. L. Parker, J. J. Lugus and K. Walsh (2011). "Adipokines in inflammation and metabolic disease." Nature reviews Immunology 11(2): 85-97.

Pacini, F., M. G. Castagna, C. Cipri and M. Schlumberger (2010). "Medullary thyroid carcinoma." Clinical Oncology (Royal College of Radiologists) 22(6): 475-485.

Paczkowski, M., W. B. Schoolcraft and R. L. Krisher (2014). "Fatty acid metabolism during maturation affects glucose uptake and is essential to oocyte competence." Reproduction 148(4): 429-439.

Park, J., T. S. Morley, M. Kim, D. J. Clegg and P. E. Scherer (2014). "Obesity and cancer--mechanisms underlying tumour progression and recurrence." Nature Reviews: Endocrinology 10(8): 455-465.

Pellegata, N. S., L. Quintanilla-Martinez, H. Siggelkow, E. Samson, K. Bink, H. Höfler, F. Fend, J. Graw and M. J. Atkinson (2006). "Germ-line mutations in p27Kip1 cause a multiple endocrine neoplasia syndrome in rats and humans." Proceedings of the National Academy of Sciences of the United States of America 103(42): 15558-15563.

Pickl, M. and C. H. Ries (2009). "Comparison of 3D and 2D tumor models reveals enhanced HER2 activation in 3D associated with an increased response to trastuzumab." Oncogene 28(3): 461-468.

Pierorazio, P. M., P. C. Walsh, A. W. Partin and J. I. Epstein (2013). "Prognostic Gleason grade grouping: data based on the modified Gleason scoring system." BJU International 111(5): 753-760.

Poulos, S. P., M. V. Dodson and G. J. Hausman (2010). "Cell line models for differentiation: preadipocytes and adipocytes." Experimental Biology and Medicine (Maywood, NJ) 235(10): 1185-1193.

Prudente, S., M. L. Hribal, E. Flex, F. Turchi, E. Morini, S. De Cosmo, S. Bacci, V. Tassi, M. Cardellini, R. Lauro, G. Sesti, B. Dallapiccola and V. Trischitta (2005). "The functional Q84R polymorphism of mammalian Tribbles homolog TRB3 is associated with insulin resistance and related cardiovascular risk in Caucasians from Italy." Diabetes 54(9): 2807-2811.

Puiffe, M. L., C. Le Page, A. Filali-Mouhim, M. Zietarska, V. Ouellet, P. N. Tonin, M. Chevrette, D. M. Provencher and A. M. Mes-Masson (2007). "Characterization of ovarian cancer ascites on cell invasion, proliferation, spheroid formation, and gene expression in an in vitro model of epithelial ovarian cancer." Neoplasia 9(10): 820-829.

Qi, L., J. E. Heredia, J. Y. Altarejos, R. Screaton, N. Goebel, S. Niessen, I. X. Macleod, C. W. Liew, R. N. Kulkarni, J. Bain, C. Newgard, M. Nelson, R. M. Evans, J. Yates and M. Montminy (2006). "TRB3 links the E3 ubiquitin ligase COP1 to lipid metabolism." Science 312(5781): 1763-1766.

Qu, J., B. Liu, B. Li, G. Du, Y. Li, J. Wang, L. He and X. Wan (2019). "TRIB3 suppresses proliferation and invasion and promotes apoptosis of endometrial cancer cells by regulating the AKT signaling pathway." OncoTargets and Therapy 12: 2235-2245.

Quail, D. F. and A. J. Dannenberg (2019). "The obese adipose tissue microenvironment in cancer development and progression." Nature Reviews: Endocrinology 15(3): 139-154.

Ribeiro, R., C. Monteiro, V. Catalan, P. Hu, V. Cunha, A. Rodriguez, J. Gomez-Ambrosi, A. Fraga, P. Principe, C. Lobato, F. Lobo, A. Morais, V. Silva, J. Sanches-Magalhaes, J. Oliveira, F. Pina, C. Lopes, R. Medeiros and G. Fruhbeck (2012). "Obesity and prostate cancer: gene expression signature of human periprostatic adipose tissue." BMC Medicine 10: 108.

Ribeiro, R., C. Monteiro, V. Cunha, A. Azevedo, M. Oliveira, R. Monteiro, A. Fraga, P. Príncipef, C. Lobatog, F. Loboh, A. Moraish, V. Silvah, J. Sanches-Magalhãesh, J. Oliveirah, J. Guimarãese, C. Lopesb and R. Medeirosa (2012). "Tumor Cell-educated Periprostatic Adipose Tissue Acquires an Aggressive Cancer-promoting Secretory Profile." Cellular Physiology and Biochemistry 29: 233-240.

Ribeiro, R., C. Monteiro, V. Cunha, M. J. Oliveira, M. Freitas, A. Fraga, P. Principe, C. Lobato, F. Lobo, A. Morais, V. Silva, J. Sanches-Magalhaes, J. Oliveira, F. Pina, A. Mota-Pinto, C. Lopes and R. Medeiros (2012). "Human periprostatic adipose tissue promotes prostate cancer aggressiveness in vitro." Journal of Experimental and Clinical Cancer Research 31: 32.

Richmond, L. and K. Keeshan (2019). "Pseudokinases: a tribble-edged sword." The FEBS journal.

Rishi, L., M. Hannon, M. Salomè, M. Hasemann, A. K. Frank, J. Campos, J. Timoney, C. O'Connor, M. R. Cahill, B. Porse and K. Keeshan (2014). "Regulation of Trib2 by an E2F1-C/EBPα feedback loop in AML cell proliferation." Blood 123(15): 2389-2400.

Rojas, A., G. Liu, I. Coleman, P. S. Nelson, M. Zhang, R. Dash, P. B. Fisher, S. R. Plymate and J. D. Wu (2011). "IL-6 promotes prostate tumorigenesis and progression through autocrine cross-activation of IGF-IR." Oncogene 30(20): 2345-2355.

Romeo, G., P. Ronchetto, Y. Luo, V. Barone, M. Seri, I. Ceccherini, B. Pasini, R. Bocciardi, M. Lerone, H. Kääriäinen and et al. (1994). "Point mutations affecting the tyrosine kinase domain of the RET proto-oncogene in Hirschsprung's disease." Nature 367(6461): 377-378.

Rosen, E. D., C. J. Walkey, P. Puigserver and B. M. Spiegelman (2000). "Transcriptional regulation of adipogenesis." Genes and Development 14(11): 1293-1307.

Roskoski, R., Jr. and A. Sadeghi-Nejad (2018). "Role of RET protein-tyrosine kinase inhibitors in the treatment RET-driven thyroid and lung cancers." Pharmacological Research 128: 1-17.

Roy, A. K., Y. Lavrovsky, C. S. Song, S. Chen, M. H. Jung, N. K. Velu, B. Y. Bi and B. Chatterjee (1999). "Regulation of androgen action." Vitamins and Hormones 55: 309-352.

Ruiz-Ojeda, F. J., A. I. Rupérez, C. Gomez-Llorente, A. Gil and C. M. Aguilera (2016). "Cell Models and Their Application for Studying Adipogenic Differentiation in Relation to Obesity: A Review." International Journal of Molecular Sciences 17(7).

Sacca, P. A., V. P. Creydt, H. Choi, O. N. Mazza, S. J. Fletcher, V. B. F. Vallone, C. Scorticati, N. A. Chasseing and J. C. Calvo (2012). "Human Periprostatic Adipose Tissue its Influence on Prostate Cancer Cells." Cellular Physiology and Biochemistry 30: 113-122.

Sakai, S., N. Ohoka, K. Onozaki, M. Kitagawa, M. Nakanishi and H. Hayashi (2010). "Dual mode of regulation of cell division cycle 25 A protein by TRB3." Biological and Pharmaceutical Bulletin 33(7): 1112-1116.

Salazar, M., M. Lorente, E. García-Taboada, E. Pérez Gómez, D. Dávila, P. Zúñiga-García, J. María Flores, A. Rodríguez, Z. Hegedus, D. Mosén-Ansorena, A. M. Aransay, S. Hernández-Tiedra, I. López-Valero, M. Quintanilla, C. Sánchez, J. L. Iovanna, N. Dusetti, M. Guzmán, S. E. Francis, A. Carracedo, E. Kiss-Toth and G. Velasco (2015). "Loss of Tribbles pseudokinase-3 promotes Akt-driven tumorigenesis via FOXO inactivation." Cell Death and Differentiation 22(1): 131-144.

Saleem, S. and S. C. Biswas (2017). "Tribbles Pseudokinase 3 Induces Both Apoptosis and Autophagy in Amyloid-β-induced Neuronal Death." Journal of Biological Chemistry 292(7): 2571-2585.

Salomé, M., L. Hopcroft and K. Keeshan (2018). "Inverse and correlative relationships between TRIBBLES genes indicate non-redundant functions during normal and malignant hemopoiesis." Experimental Hematology 66: 63-78.e13.

Salome, M., A. Magee, K. Yalla, S. Chaudhury, E. Sarrou, R. J. Carmody and K. Keeshan (2018). "A Trib2-p38 axis controls myeloid leukaemia cell cycle and stress response signalling." Cell Death & Disease 9(5): 443.

Salomé, M., A. Magee, K. Yalla, S. Chaudhury, E. Sarrou, R. J. Carmody and K. Keeshan (2018). "A Trib2-p38 axis controls myeloid leukaemia cell cycle and stress response signalling." Cell Death & Disease 9(5): 443.

Sarbassov, D. D., D. A. Guertin, S. M. Ali and D. M. Sabatini (2005). "Phosphorylation and regulation of Akt/PKB by the rictor-mTOR complex." Science 307(5712): 1098-1101.

Sassmann, A., S. Offermanns and N. Wettschureck (2010). "Tamoxifen-inducible Cre-mediated recombination in adipocytes." Genesis 48(10): 618-625.

Sathianathen, N. J., B. R. Konety, J. Crook, F. Saad and N. Lawrentschuk (2018). "Landmarks in prostate cancer." Nature reviews Urology 15(10): 627-642.

Satoh, T., H. Kidoya, H. Naito, M. Yamamoto, N. Takemura, K. Nakagawa, Y. Yoshioka, E. Morii, N. Takakura, O. Takeuchi and S. Akira (2013). "Critical role of Trib1 in differentiation of tissue-resident M2-like macrophages." Nature 495(7442): 524-528.

Scherr, M., L. Venturini and M. Eder (2010). "Lentiviral vector-mediated expression of pre-miRNAs and antagomiRs." Methods in Molecular Biology 614: 175-185.

Seo, J. B., M. Riopel, P. Cabrales, J. Y. Huh, G. K. Bandyopadhyay, A. Y. Andreyev, A. N. Murphy, S. C. Beeman, G. I. Smith, S. Klein, Y. S. Lee and J. M. Olefsky (2019). "Knockdown of Ant2 Reduces Adipocyte Hypoxia And Improves Insulin Resistance in Obesity." Nature metabolism 1(1): 86-97.

Sethi, J. K. and A. J. Vidal-Puig (2007). "Thematic review series: adipocyte biology. Adipose tissue function and plasticity orchestrate nutritional adaptation." Journal of Lipid Research 48(6): 1253-1262.

Shafi, A. A., A. E. Yen and N. L. Weigel (2013). "Androgen receptors in hormone-dependent and castration-resistant prostate cancer." Pharmacology & Therapeutics 140(3): 223-238.

Shahrouzi, P., I. Astobiza, A. R. Cortazar, V. Torrano, A. Macchia, J. M. Flores, C. Niespolo, I. Mendizabal, R. Caloto, A. Ercilla, L. Camacho, L. Arreal, M. Bizkarguenaga, M. L. Martinez-Chantar, X. R. Bustelo, E. Berra, E. Kiss-Toth, G. Velasco, A. Zabala-Letona and A. Carracedo (2020). "Genomic and Functional Regulation of TRIB1 Contributes to Prostate Cancer Pathogenesis." Cancers 12(9).

Shen, M. M. and C. Abate-Shen (2010). "Molecular genetics of prostate cancer: new prospects for old challenges." Genes and Development 24(18): 1967-2000.

Shtivelman, E., T. M. Beer and C. P. Evans (2014). "Molecular pathways and targets in prostate cancer." Oncotarget 5(17): 7217-7259.

Silva, H. M., A. Báfica, G. F. Rodrigues-Luiz, J. Chi, P. D. A. Santos, B. S. Reis, D. P. Hoytema van Konijnenburg, A. Crane, R. D. N. Arifa, P. Martin, D. Mendes, D. S. Mansur, V. J. Torres, K. Cadwell, P. Cohen, D. Mucida and J. J. Lafaille (2019). "Vasculature-associated fat macrophages readily adapt to inflammatory and metabolic challenges." Journal of Experimental Medicine 216(4): 786-806.

Soubeyrand, S., A. Martinuk and R. McPherson (2017). "TRIB1 is a positive regulator of hepatocyte nuclear factor 4-alpha." Scientific Reports 7(1): 5574.

Soubeyrand, S., A. Martinuk, T. Naing, P. Lau and R. McPherson (2016). "Role of Tribbles Pseudokinase 1 (TRIB1) in human hepatocyte metabolism." Biochimica et Biophysica Acta 1862(2): 223-232.

Soule, H. D., J. Vazguez, A. Long, S. Albert and M. Brennan (1973). "A human cell line from a pleural effusion derived from a breast carcinoma." Journal of the National Cancer Institute 51(5): 1409-1416.

Starenki, D., S. K. Hong, P. K. Wu and J. I. Park (2017). "Vandetanib and cabozantinib potentiate mitochondria-targeted agents to suppress medullary thyroid carcinoma cells." Cancer Biology & Therapy 18(7): 473-483.

Stein, S. J., E. A. Mack, K. S. Rome and W. S. Pear (2015). "Tribbles in normal and malignant haematopoiesis." Biochemical Society Transactions 43(5): 1112-1115.

Strong, A. L., T. A. Strong, L. V. Rhodes, J. A. Semon, X. Zhang, Z. Shi, S. Zhang, J. M. Gimble, M. E. Burow and B. A. Bunnell (2013). "Obesity associated alterations in the biology of adipose stem cells mediate enhanced tumorigenesis by estrogen dependent pathways." Breast Cancer Research 15(5): R102.

Sung, H. Y., S. E. Francis, D. C. Crossman and E. Kiss-Toth (2006). "Regulation of expression and signalling modulator function of mammalian tribbles is cell-type specific." Immunology Letters 104(1-2): 171-177.

Suzuki, A., J. L. de la Pompa, V. Stambolic, A. J. Elia, T. Sasaki, I. del Barco Barrantes, A. Ho, A. Wakeham, A. Itie, W. Khoo, M. Fukumoto and T. W. Mak (1998). "High cancer susceptibility and embryonic lethality associated with mutation of the PTEN tumor suppressor gene in mice." Current biology : CB 8(21): 1169-1178.

Takagi, A., M. Watanabe, Y. Ishii, J. Morita, Y. Hirokawa, T. Matsuzaki and T. Shiraishi (2007). "Three-dimensional cellular spheroid formation provides human prostate tumor cells with tissue-like features." Anticancer Research 27(1a): 45-53.

Takahashi, M., J. Ritz and G. M. Cooper (1985). "Activation of a novel human transforming gene, ret, by DNA rearrangement." Cell 42(2): 581-588.

Takahashi, Y., N. Ohoka, H. Hayashi and R. Sato (2008). "TRB3 suppresses adipocyte differentiation by negatively regulating PPARgamma transcriptional activity." Journal of Lipid Research 49(4): 880-892.

Tan, W. P., C. Lin, M. Chen and L. A. Deane (2016). "Periprostatic Fat: A Risk Factor for Prostate Cancer?" Urology 98: 107-112.

Taplin, M. E. and S. P. Balk (2004). "Androgen receptor: a key molecule in the progression of prostate cancer to hormone independence." Journal of Cellular Biochemistry 91(3): 483-490.

Taylor, B. S., N. Schultz, H. Hieronymus, A. Gopalan, Y. Xiao, B. S. Carver, V. K. Arora, P. Kaushik, E. Cerami, B. Reva, Y. Antipin, N. Mitsiades, T. Landers, I. Dolgalev, J. E. Major, M. Wilson, N. D. Socci, A. E. Lash, A. Heguy, J. A. Eastham, H. I. Scher, V. E. Reuter, P. T. Scardino, C. Sander, C. L. Sawyers and W. L. Gerald (2010). "Integrative genomic profiling of human prostate cancer." Cancer Cell 18(1): 11-22.

Taylor, R. A., J. Lo, N. Ascui and M. J. Watt (2015). "Linking obesogenic dysregulation to prostate cancer progression." Endocrine Connections 4(4): R68-80.

Templeton, H. (2007). "Prostate cancer – presentation, diagnosis and treatment what does the literature say?" International Journal of Urological Nursing 1(1): 6-17.

The Lancet Diabetes, E. (2020). "The obesity-cancer link: of increasing concern." Lancet Diabetes Endocrinol 8(3): 175.

Thompson, J., F. Saatcioglu, O. A. Jänne and J. J. Palvimo (2001). "Disrupted amino- and carboxyl-terminal interactions of the androgen receptor are linked to androgen insensitivity." Molecular Endocrinology 15(6): 923-935.

Tombal, B. and R. J. van Soest (2017). "Prostate cancer: STAMPEDE, LATITUDE and Fernand Labrie's legacy." Nature reviews Urology 14(10): 588-590.

Toren, P. and V. Venkateswaran (2014). "Periprostatic adipose tissue and prostate cancer progression: new insights into the tumor microenvironment." Clinical Genitourinary Cancer 12(1): 21-26.

Trøseid, M., I. Seljeflot and H. Arnesen (2010). "The role of interleukin-18 in the metabolic syndrome." Cardiovascular Diabetology 9: 11.

Trotman, L. C., M. Niki, Z. A. Dotan, J. A. Koutcher, A. Di Cristofano, A. Xiao, A. S. Khoo, P. Roy-Burman, N. M. Greenberg, T. Van Dyke, C. Cordon-Cardo and P. P. Pandolfi (2003). "Pten dose dictates cancer progression in the prostate." PLoS Biology 1(3): E59.

Uehara, H., T. Kobayashi, M. Matsumoto, S. Watanabe, A. Yoneda and Y. Bando (2018). "Adipose tissue:Critical contributor to the development of prostate cancer." Journal of Medical Investigation 65(1.2): 9-17.

Uljon, S., X. Xu, I. Durzynska, S. Stein, G. Adelmant, J. A. Marto, W. S. Pear and S. C. Blacklow (2016). "Structural Basis for Substrate Selectivity of the E3 Ligase COP1." Structure 24(5): 687-696.

van Staveren, W. C., D. Y. Solís, A. Hébrant, V. Detours, J. E. Dumont and C. Maenhaut (2009). "Human cancer cell lines: Experimental models for cancer cells in situ? For cancer stem cells?" Biochimica et Biophysica Acta 1795(2): 92-103.

Vandanmagsar, B., Y. H. Youm, A. Ravussin, J. E. Galgani, K. Stadler, R. L. Mynatt, E. Ravussin, J. M. Stephens and V. D. Dixit (2011). "The NLRP3 inflammasome instigates obesity-induced inflammation and insulin resistance." Nature Medicine 17(2): 179-188.

Vargo-Gogola, T. and J. M. Rosen (2007). "Modelling breast cancer: one size does not fit all." Nature Reviews: Cancer 7(9): 659-672.

Venkatasubramanian, P. N., C. B. Brendler, B. A. Plunkett, S. E. Crawford, P. S. Fitchev, G. Morgan, M. L. Cornwell, M. S. McGuire, A. M. Wyrwicz and J. A. Doll (2014). "Periprostatic adipose tissue from obese prostate cancer patients promotes tumor and endothelial cell proliferation: A functional and MR imaging pilot study." The Prostate 74(3): 326-335.

Wang, G., D. Zhao, D. J. Spring and R. A. DePinho (2018). "Genetics and biology of prostate cancer." Genes and Development 32(17-18): 1105-1140.

Wang, J., J. S. Park, Y. Wei, M. Rajurkar, J. L. Cotton, Q. Fan, B. C. Lewis, H. Ji and J. Mao (2013). "TRIB2 acts downstream of Wnt/TCF in liver cancer cells to regulate YAP and C/EBPalpha function." Molecular Cell 51(2): 211-225.

Wang, M., J. Zhao, L. Zhang, F. Wei, Y. Lian, Y. Wu, Z. Gong, S. Zhang, J. Zhou, K. Cao, X. Li, W. Xiong, G. Li, Z. Zeng and C. Guo (2017). "Role of tumor microenvironment in tumorigenesis." Journal of Cancer 8(5): 761-773.

Wang, Q., W. Li, Y. Zhang, X. Yuan, K. Xu, J. Yu, Z. Chen, R. Beroukhim, H. Wang, M. Lupien, T. Wu, M. M. Regan, C. A. Meyer, J. S. Carroll, A. K. Manrai, O. A. Jänne, S. P. Balk, R. Mehra, B. Han, A. M. Chinnaiyan, M. A. Rubin, L. True, M. Fiorentino, C. Fiore, M. Loda, P. W. Kantoff, X. S. Liu and M. Brown (2009). "Androgen receptor regulates a distinct transcription program in androgen-independent prostate cancer." Cell 138(2): 245-256.

Wang, S., J. Gao, Q. Lei, N. Rozengurt, C. Pritchard, J. Jiao, G. V. Thomas, G. Li, P. Roy-Burman, P. S. Nelson, X. Liu and H. Wu (2003). "Prostate-specific deletion of the murine Pten tumor suppressor gene leads to metastatic prostate cancer." Cancer Cell 4(3): 209-221.

Wang, Y., N. Wu, B. Pang, D. Tong, D. Sun, H. Sun, C. Zhang, W. Sun, X. Meng, J. Bai, F. Chen, J. Geng, S. Fu and Y. Jin (2017). "TRIB1 promotes colorectal cancer cell migration and invasion through activation MMP-2 via FAK/Src and ERK pathways." Oncotarget 8(29): 47931-47942.

Wang, Y. X., N. Zhu, C. J. Zhang, Y. K. Wang, H. T. Wu, Q. Li, K. Du, D. F. Liao and L. Qin (2019). "Friend or foe: Multiple roles of adipose tissue in cancer formation and progression." Journal of Cellular Physiology 234(12): 21436-21449.

Wang, Z. V., Y. Deng, Q. A. Wang, K. Sun and P. E. Scherer (2010). "Identification and characterization of a promoter cassette conferring adipocyte-specific gene expression." Endocrinology 151(6): 2933-2939.

Webber, M. M., D. Bello and S. Quader (1997). "Immortalized and tumorigenic adult human prostatic epithelial cell lines: characteristics and applications Part 2. Tumorigenic cell lines." Prostate 30(1): 58-64.

Weisberg, S. P., D. McCann, M. Desai, M. Rosenbaum, R. L. Leibel and A. W. Ferrante, Jr. (2003). "Obesity is associated with macrophage accumulation in adipose tissue." Journal of Clinical Investigation 112(12): 1796-1808.

Wennemers, M., J. Bussink, N. Grebenchtchikov, F. C. Sweep and P. N. Span (2011). "TRIB3 protein denotes a good prognosis in breast cancer patients and is associated with hypoxia sensitivity." Radiotherapy and Oncology 101(1): 198-202.

Wennemers, M., J. Bussink, B. Scheijen, I. D. Nagtegaal, H. W. van Laarhoven, J. A. Raleigh, M. A. Varia, J. J. Heuvel, K. M. Rouschop, F. C. Sweep and P. N. Span (2011). "Tribbles homolog 3 denotes a poor prognosis in breast cancer and is involved in hypoxia response." Breast Cancer Research 13(4): R82.

Wilkin, F., N. Suarez-Huerta, B. Robaye, J. Peetermans, F. Libert, J. E. Dumont and C. Maenhaut (1997). "Characterization of a phosphoprotein whose mRNA is regulated by the mitogenic pathways in dog thyroid cells." European Journal of Biochemistry 248(3): 660-668.

Wolin, K. Y., K. Carson and G. A. Colditz (2010). "Obesity and cancer." Oncologist 15(6): 556-565.

Wu, Q., B. Li, Z. Li, J. Li, S. Sun and S. Sun (2019). "Cancer-associated adipocytes: key players in breast cancer progression." Journal of Hematology & Oncology 12(1): 95.

Yan, Y. and H. Huang (2019). "Interplay Among PI3K/AKT, PTEN/FOXO and AR Signaling in Prostate Cancer." Advances in Experimental Medicine and Biology 1210: 319-331.

Ye, R., Q. A. Wang, C. Tao, L. Vishvanath, M. Shao, J. G. McDonald, R. K. Gupta and P. E. Scherer (2015). "Impact of tamoxifen on adipocyte lineage tracing: Inducer of adipogenesis and prolonged nuclear translocation of Cre recombinase." Molecular metabolism 4(11): 771-778.

Ye, Y., G. Wang, G. Wang, J. Zhuang, S. He, Y. Song, J. Ni, W. Xia and J. Wang (2017). "The Oncogenic Role of Tribbles 1 in Hepatocellular Carcinoma Is Mediated by a Feedback Loop Involving microRNA-23a and p53." Frontiers in Physiology 8: 789.

Yokoyama, T., Y. Kanno, Y. Yamazaki, T. Takahara, S. Miyata and T. Nakamura (2010). "Trib1 links the MEK1/ERK pathway in myeloid leukemogenesis." Blood 116(15): 2768-2775.

Yokoyama, T. and T. Nakamura (2011). "Tribbles in disease: Signaling pathways important for cellular function and neoplastic transformation." Cancer Science 102(6): 1115-1122.

Youm, Y. H., T. D. Kanneganti, B. Vandanmagsar, X. Zhu, A. Ravussin, A. Adijiang, J. S. Owen, M. J. Thomas, J. Francis, J. S. Parks and V. D. Dixit (2012). "The Nlrp3 inflammasome promotes age-related thymic demise and immunosenescence." Cell Reports 1(1): 56-68.

Yu, J. M., W. Sun, Z. H. Wang, X. Liang, F. Hua, K. Li, X. X. Lv, X. W. Zhang, Y. Y. Liu, J. J. Yu, S. S. Liu, S. Shang, F. Wang, Z. N. Yang, C. X. Zhao, X. Y. Hou, P. P. Li, B. Huang, B. Cui and Z. W. Hu (2019). "TRIB3 supports breast cancer stemness by suppressing FOXO1 degradation and enhancing SOX2 transcription." Nature communications 10(1): 5720.

Zhou, H., Y. Luo, J. H. Chen, J. Hu, Y. Z. Luo, W. Wang, Y. Zeng and L. Xiao (2013). "Knockdown of TRB3 induces apoptosis in human lung adenocarcinoma cells through regulation of Notch 1 expression." Molecular Medicine Reports 8(1): 47-52.

Zhou, R., A. Tardivel, B. Thorens, I. Choi and J. Tschopp (2010). "Thioredoxin-interacting protein links oxidative stress to inflammasome activation." Nature Immunology 11(2): 136-140.

Appendix

Cytokine Array coordinates

Coordinate	Target/Control	Alternate Nomenclature
A1, A2	Reference Spot	-
A23, A24	Reference Spot	-
B1, B2	BLC	CXCL13/BCA-1
B3, B4	C5/C5a	Complement Component 5a
B5, B6	G-CSF	-
B7, B8	GM-CSF	-
B9, B10	I-309	CCL1/TCA-3
B11, B12	Eotaxin	CCL11
B13, B14	sICAM-1	CD54
B15, B16	IFN-γ	-
B17, B18	IL-1α	IL-1F1
B19, B20	IL-1β	IL-1F2
B21, B22	IL-1ra	IL-1F3
B23, B24	IL-2	-
C1, C2	IL-3	-
C3, C4	IL-4	-
C5, C6	IL-5	-
C7, C8	IL-6	-
C9, C10	IL-7	-
C11, C12	IL-10	-
C13, C14	IL-13	-
C15, C16	IL-12 p70	-
C17, C18	IL-16	-
C19, C20	IL-17	-
C21, C22	IL-23	-
C23, C24	IL-27	-
D1, D2	IP-10	CXCL10/CRG-2
D3, D4	I-TAC	CXCL11
D5, D6	KC	CXCL1
D7, D8	M-CSF	-
D9, D10	JE	CCL2/MCP-1
D11, D12	MCP-5	CCL12
D13, D14	MIG	CXCL9
D15, D16	MIP-1α	CCL3
D17, D18	MIP-1β	CCL4
D19, D20	MIP-2	CXCL2
D21, D22	RANTES	CCL5

D23, D24	SDF-1	CXCL12
E1, E2	TARC	CCL17
E3, E4	TIMP-1	-
E5, E6	TNF-α	-
E7, E8	TREM-1	-
F1, F2	Reference Spot	-
F23, F24	PBS (Negative Control)	Control (-)

Table A.18: Array coordinates for Mouse Cytokine Array Panel A

Plasmid maps

Plasmids were purchased from Origene or obtained from Institute for Diabetes and Cancer plasmid repository. The plasmids maps used in this thesis are as follows:

a.

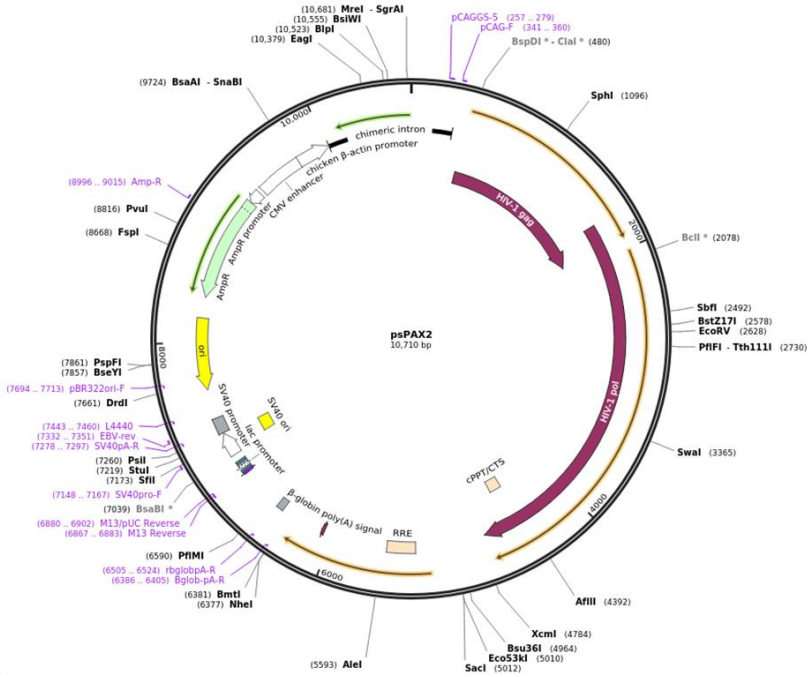

b.

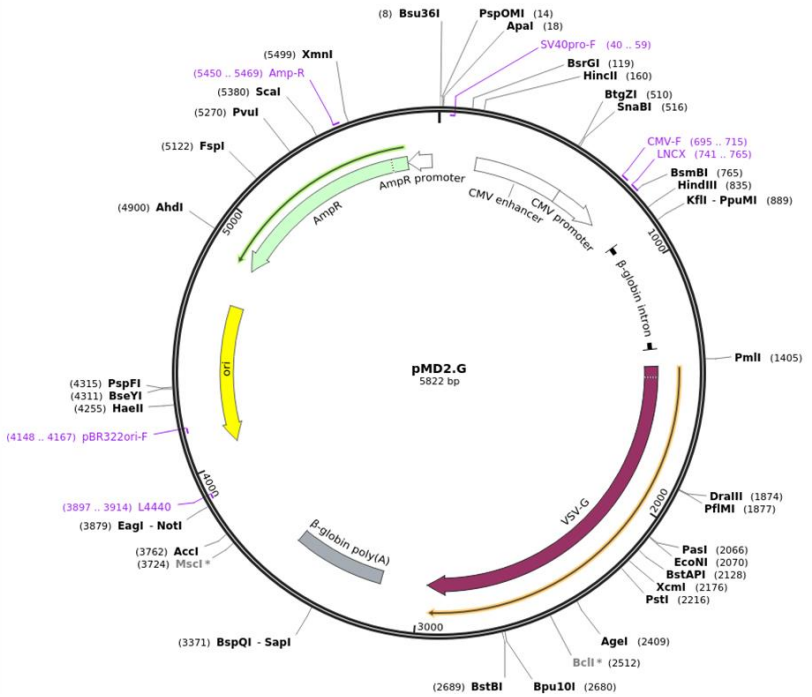

Figure A.1: 2nd generation Lenti-viral packaging plasmids
2nd generation Lenti-viral packaging plasmids used for generation of stable cell lines using Lenti-virus. Map generated using SnapGene 5.2.

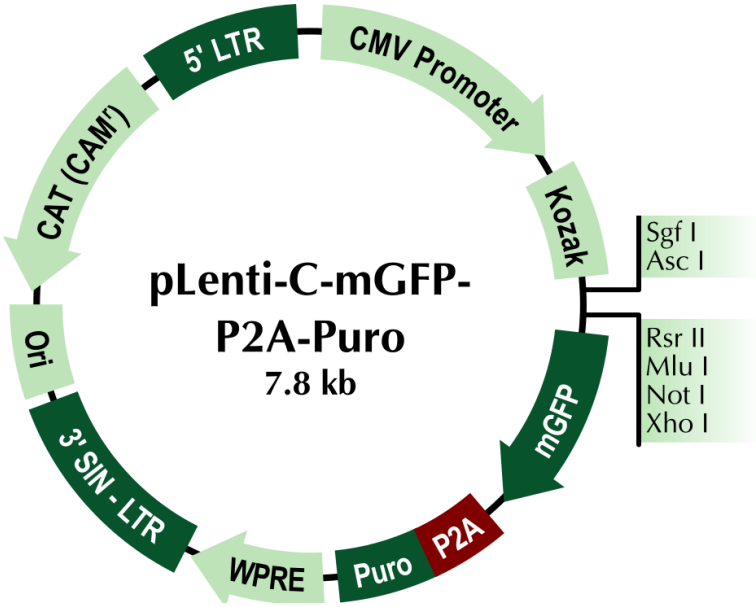

Figure A.2: Overexpression plasmid (pLenti-C-mGFP-P2A-Puro) backbone
pLenti-C-mGFP-P2A-Puro overexpression plasmids were used to overexpress TRIB1 in PCa cells and TRIB2 in MTC cells.

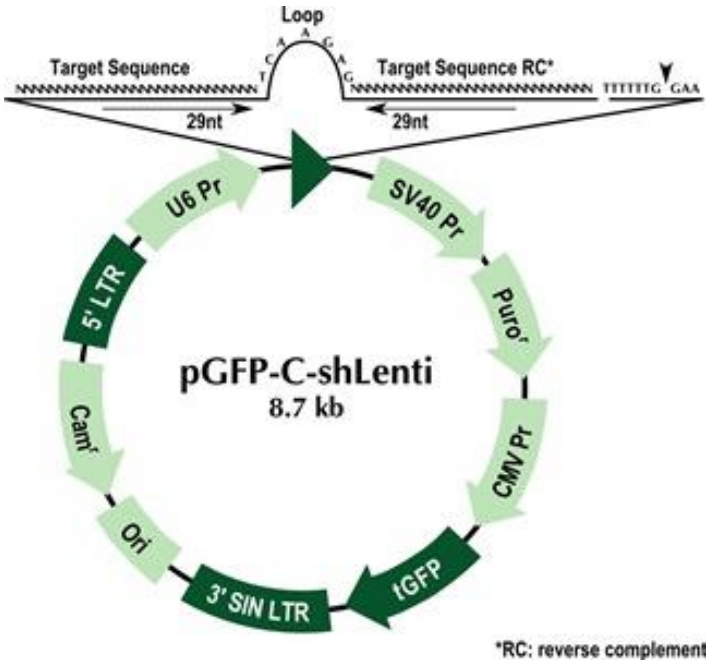

Figure A.3: shRNA plasmid (pGFP-C-shLenti) backbone
pGFP-C-shLenti plasmids were used to downregulate TRIB3 in PCa cells.